

การพัฒนาถังปฏิกรณ์ซูเปอร์ไวเบอร์ชัน-โฟโตแคตาไลติกสำหรับบำบัดลิกนินและ  
2,4-ไดคลอโรฟีนอลในน้ำเสียโรงงานเยื่อและกระดาษ



นางสาว สุชญญา ทองเครือ

ศูนย์วิทยทรัพยากร  
จุฬาลงกรณ์มหาวิทยาลัย

วิทยานิพนธ์นี้เป็นส่วนหนึ่งของการศึกษาตามหลักสูตรปริญญาวิทยาศาสตรดุษฎีบัณฑิต


สาขาวิชาวิทยาศาสตร์สิ่งแวดล้อม (สหสาขาวิชา)

บัณฑิตวิทยาลัย จุฬาลงกรณ์มหาวิทยาลัย

ปีการศึกษา 2553

ลิขสิทธิ์ของจุฬาลงกรณ์มหาวิทยาลัย

DEVELOPMENT OF SUPERVIBRATION-PHOTOCATALYTIC REACTOR FOR  
TREATMENT OF LIGNIN AND 2,4-DICHLOROPHENOL IN  
PULP AND PAPER MILL WASTEWATER



Miss Suchanya Thongkrua

ศูนย์วิทยทรัพยากร  
A Dissertation Submitted in Partial Fulfillment of the Requirements  
for the Degree of Doctor of Philosophy Program in Environmental Science

(Interdisciplinary Program)

Graduate School

Chulalongkorn University


Academic Year 2010

Copyright of Chulalongkorn University

Thesis Title                      DEVELOPMENT OF SUPERVIBRATION-PHOTOCATALYTIC  
REACTOR FOR TREATMENT OF LIGNIN AND 2,4-  
DICHLOROPHENOL IN PULP AND PAPER MILL  
WASTEWATER  
By                                      Miss Suchanya Thongkrua  
Field of Study                      Environmental Science  
Thesis Advisor                      Associate Professor Chavalit Ratanatamskul, Ph.D.

---

Accepted by the Graduate School, Chulalongkorn University in Partial  
Fulfillment of the Requirements for the Doctoral Degree

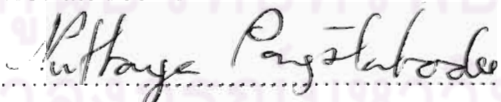
..... Dean of the Graduate School  
(Associate Professor Pornpote Piumsomboon, Ph.D.)


THESIS COMMITTEE

..... Chairman  
(Assistant Professor Chanvit Kositanon, Ph.D.)

..... Thesis Advisor  
(Associate Professor Chavalit Ratanatamskul, Ph.D.)

..... Examiner  
(Associate Professor Amorn Petsom, Ph.D.)

..... Examiner  
(Associate Professor Nuttaya Pongstabodee, Ph.D.)

..... External Examiner  
(Associate Professor Jin Anotai, Ph.D.)

สุชัญญา ทองเครือ: การพัฒนาถังปฏิกรณ์ซูเปอร์ไวเบรชัน-โฟโตแคตาไลติกสำหรับบำบัด  
ลิกนินและ2,4-ไดคลอโรฟีนอลในน้ำเสียโรงงานเยื่อและกระดาษ. (DEVELOPMENT OF  
SUPERVIBRATION-PHOTOCATALYTIC REACTOR FOR TREATMENT OF LIGNIN  
AND 2,4-DICHLOROPHENOL IN PULP AND PAPER MILL WASTEWATER)

อ. ที่ปรึกษาวิทยานิพนธ์หลัก: รศ.ดร.ชวลิต รัตนธรรมสกุล, 193 หน้า.

การสลายตัวของลิกนินและ2,4-ไดคลอโรฟีนอลในน้ำเสียด้วยปฏิกิริยาโฟโตแคตาไลติกถูกศึกษาโดยใช้ถัง  
ปฏิกรณ์ซูเปอร์ไวเบรชัน-โฟโตแคตาไลติกที่มีพื้นฐานมาจากกระบวนการโฟโตแคตาไลติกพร้อมกับเครื่องกวนแบบ  
ซูเปอร์ไวเบรชัน ผลของปัจจัยการเดินระบบ ได้แก่ ค่าพีเอชเริ่มต้นของน้ำเสีย ความเข้มของแสงยูวีความถี่ของการสั่น  
และความเข้มข้นเริ่มต้นของน้ำเสีย ต่อการบำบัดลิกนินและ2,4-ไดคลอโรฟีนอลถูกศึกษาโดยเน้นที่ประสิทธิภาพการ  
กำจัดเพื่อให้ได้มาซึ่งสถานะที่เหมาะสมของการบำบัด งานวิจัยนี้ยังได้ศึกษาจลนพลศาสตร์ของปฏิกิริยาการย่อยสลาย  
ลิกนินและ2,4-ไดคลอโรฟีนอลด้วย รวมทั้งระบุชนิดของสารที่เกิดจากการย่อยสลายลิกนินและ2,4-ไดคลอโรฟีนอล  
ตัวอย่างน้ำเสียที่ใช้ในการทดลองนี้ประกอบด้วย น้ำเสียสังเคราะห์ลิกนิน น้ำเสียสังเคราะห์2,4-ไดคลอโรฟีนอล น้ำเสีย  
สังเคราะห์ผสมที่มีลิกนินและ2,4-ไดคลอโรฟีนอล และน้ำเสียจริงจากโรงงานเยื่อและกระดาษ จากผลการศึกษาที่ได้  
การกำจัดลิกนินและ2,4-ไดคลอโรฟีนอลในการทดลองบำบัดน้ำเสียทุกชนิดมีรูปแบบเหมือนกันคือ เมื่อใช้ความเข้ม  
ของแสงยูวีและความถี่ของการสั่นที่สูงกว่าค่าพีเอชเริ่มต้นและความเข้มข้นเริ่มต้นของน้ำเสียที่ต่ำ จะเพิ่มประสิทธิ  
ภาพการกำจัดลิกนินและ2,4-ไดคลอโรฟีนอล ส่วนสถานะที่เหมาะสมของถังปฏิกรณ์ซูเปอร์ไวเบรชัน-โฟโตแคตาไล  
ติกสำหรับบำบัดลิกนินและ2,4-ไดคลอโรฟีนอล ได้แก่ ค่าพีเอชเริ่มต้นของน้ำเสียที่พีเอช 5 ความเข้มของแสงยูวีที่ 25.2  
mW/cm<sup>2</sup> และความถี่ของการสั่นที่ 50 Hz ภายใต้สถานะที่เหมาะสมของการบำบัด ประสิทธิภาพการกำจัดลิกนินและสี  
ในน้ำเสียสังเคราะห์ลิกนิน (100 mg/l) เท่ากับ 85.12% และ 70.55% ตามลำดับ ภายในเวลา 420 นาที ค่าคงที่ปรากฏ  
ของอัตราการเกิดปฏิกิริยาอันดับที่หนึ่งและอัตราการย่อยสลายเริ่มต้นในการย่อยสลายลิกนินเท่ากับ  $13.9 \times 10^{-3} \text{ min}^{-1}$   
และ  $1.39 \text{ mg/l min}^{-1}$  ตามลำดับ หลังจาก 120 นาที การวิเคราะห์สารที่เกิดจากการย่อยสลายลิกนินโดย GC-MS แสดง  
การมีอยู่ของอนุพันธ์ของลิกนินบางตัว เช่น วานิลลีน ในกรณีของน้ำเสียสังเคราะห์2,4-ไดคลอโรฟีนอล (0.5 mg/l) เกิด  
การย่อยสลาย2,4-ไดคลอโรฟีนอลอย่างสมบูรณ์ภายในเวลา 60 นาที ค่าคงที่ปรากฏของอัตราการเกิดปฏิกิริยาอันดับที่  
หนึ่งและอัตราการย่อยสลายเริ่มต้นในการย่อยสลาย2,4-ไดคลอโรฟีนอลเท่ากับ  $56.3 \times 10^{-3} \text{ min}^{-1}$  และ  $28.2 \times 10^{-3} \text{ mg/l min}^{-1}$   
ตามลำดับ หลังจาก 30 นาที สารที่เกิดจากการย่อยสลาย2,4-ไดคลอโรฟีนอลซึ่งถูกวิเคราะห์ด้วย GC-MS ได้แก่  
ฟีนอล 2-คลอโรฟีนอล และ 4-คลอโรฟีนอล รวมทั้งเส้นทางการย่อยสลาย2,4-ไดคลอโรฟีนอลได้ถูกเสนอขึ้นด้วย  
สำหรับน้ำเสียผสมที่มีลิกนิน 400 mg/l และ2,4-ไดคลอโรฟีนอล 5 mg/l ถังปฏิกรณ์สามารถกำจัดลิกนิน สี และ2,4-ได  
คลอโรฟีนอลด้วยประสิทธิภาพเท่ากับ 76.21%, 60.75% และ 97.13% ตามลำดับ หลังจาก 420 นาที นอกจากนี้  
ประสิทธิภาพการกำจัดลิกนิน สี และ2,4-ไดคลอโรฟีนอลในน้ำเสียโรงงานเยื่อและกระดาษมีค่าเท่ากับ 75.11%,  
52.16% และ 94.14% ตามลำดับ ในเวลาเดียวกัน

สาขาวิชา วิทยาศาสตร์สิ่งแวดล้อม

ปีการศึกษา 2553

ลายมือชื่อนิสิต .....

ลายมือชื่อ อ.ที่ปรึกษาวิทยานิพนธ์หลัก .....

# 4989704920 : MAJOR ENVIRONMENTAL SCIENCE

KEYWORDS : LIGNIN/ 2,4-DICHLOROPHENOL/ SUPERVIBRATION-PHOTOCATALYTIC REACTOR/ PULP AND PAPER MILL WASTEWATER

SUCHIANYA THONGKRUA: DEVELOPMENT OF SUPERVIBRATION-PHOTOCATALYTIC REACTOR FOR TREATMENT OF LIGNIN AND 2,4-DICHLOROPHENOL IN PULP AND PAPER MILL WASTEWATER. THESIS ADVISOR: ASSOC. PROF. CHAVALIT RATANATAMSKUL, Ph.D., 193 pp.

The photocatalytic degradation of lignin and 2,4-DCP in wastewater was studied using a newly developed supervibration-photocatalytic reactor based on photocatalytic process combined with a supervibration agitator. The effects of operating parameters as initial pH, UV intensity, vibration frequency and initial concentration on treatment of lignin and 2,4-DCP were investigated, focusing on removal efficiency to determine the optimum treatment conditions. This work also studied kinetic reaction for degradation of lignin and 2,4-DCP and extended to identify by-products of lignin and 2,4-DCP degradation. Wastewater samples used in the experiments consisted of lignin synthetic wastewater, 2,4-DCP synthetic wastewater, mixed synthetic wastewater containing lignin and 2,4-DCP and real wastewater from pulp and paper mill. From the results obtained, removal efficiencies of lignin and 2,4-DCP in all types of wastewater were similar pattern. High UV intensity and vibration frequency in a low initial pH and initial concentration increased removal efficiencies of lignin and 2,4-DCP. The optimum operating conditions of a supervibration-photocatalytic reactor for treatment of lignin and 2,4-DCP were found to be initial pH 5, UV intensity of  $25.2 \text{ mW/cm}^2$  and vibration frequency of 50 Hz. For lignin synthetic wastewater, under the optimum treatment conditions, removal efficiency of lignin (100 mg/l) and color were 85.12% and 70.55%, respectively within 420 min. The apparent rate constant of first order reaction ( $k_{ap}$ ) and the initial degradation rate ( $r_0$ ) for lignin degradation were  $13.9 \times 10^{-3} \text{ min}^{-1}$  and  $1.39 \text{ mg/l min}^{-1}$ , respectively, after 120 min. The analysis of residue by GC-MS showed the presence of some lignin derivatives such as vanillin. In the case of 2,4-DCP synthetic wastewater, under the optimum operating conditions, 2,4-DCP degradation (0.5 mg/l) was completed within 60 min. The  $k_{ap}$  and  $r_0$  were  $56.3 \times 10^{-3} \text{ min}^{-1}$  and  $28.2 \times 10^{-3} \text{ mg/l min}^{-1}$ , respectively, after 30 min. The by-products detected by GC-MS were phenol, 2-chlorophenol and 4-chlorophenol. The degradation pathway of 2,4-DCP was also proposed. For mixed synthetic wastewater containing lignin of 400 mg/l and 2,4-DCP of 5 mg/l, the reactor could simultaneously remove lignin, color and 2,4-DCP under the optimum conditions with the efficiencies of 76.21%, 60.75% and 97.13%, respectively, after 420 min. Furthermore, removal efficiencies of lignin, color and 2,4-DCP in pulp and paper mill wastewater under the optimum conditions were 75.11%, 52.16% and 94.14%, respectively in the same time.

Field of Study : Environmental Science  
Academic Year : 2010

Student's Signature Suchanya Thongkrua  
Advisor's Signature Chavalit Rattanatskul



## ACKNOWLEDGEMENTS

I would like to express my deep and sincere gratitude to my thesis advisor, Assoc. Prof. Dr. Chavalit Ratanatamskul for the continuous encouragement and guidance of my dissertation. His comments and suggestions provide valuable knowledge and help me in all times of research and writing of this research.

I am deeply grateful to the chairman of the committee, Asst. Prof. Dr. Chanvit Khositanon for invaluable advice. I also wish to thank Assoc. Prof. Dr. Amorn Petsom, Assoc. Prof. Dr. Nuttaya Pongstabodee and Assoc. Prof. Dr. Jin Anotai for their valuable comments and insightful suggestions to this dissertation and for serving as members of the committee.

I owe my most sincere thanks to Assoc. Prof. Dr. Takatoshi Takemoto, who provided a supravibration-photocatalytic reactor from Japan. His understanding, encouraging and personal guidance give me a good basis for the present dissertation.

I also would like to express my appreciation to all staffs and colleagues at Interdisciplinary Programs in Environmental Science, Graduate School, Chulalongkorn University. Special thanks should go to Department of Environmental Engineering, Faculty of Engineering, Chulalongkorn University for assistance and laboratory support.

I am grateful to THE 90<sup>th</sup> ANNIVERSARY of CHULALONGKORN UNIVERSITY FUND (Ratchadaphiseksomphot Endowment Fund) for the research financial support. Without this financial support, this work would not have been completed.

Finally, this dissertation is dedicated to my parents, my sister and my brother for their love, wholehearted understanding, encouragement and patient supports throughout my entire study.

# CONTENTS

	Page
ABSTRACT (THAI).....	iv
ABSTRACT (ENGLISH).....	v
ACKNOWLEDGEMENTS.....	vi
CONTENTS.....	vii
LIST OF TABLES.....	xii
LIST OF FIGURES.....	xiii
CHAPTER I INTRODUCTION.....	1
1.1 Rationale.....	1
1.2 Objectives of Investigation.....	3
1.3 Hypothesis.....	3
1.4 Scope of Research.....	3
1.5 Anticipated Benefits.....	4
CHAPTER II LITERATURE REVIEW.....	5
2.1 Pulp and Paper Making Processes.....	5
2.1.1 Raw materials for pulping process.....	5
2.1.1.1 Wood.....	5
2.1.1.2 Non-wood.....	5
2.1.2 Pulp manufacture.....	6
2.1.2.1 Wood preparation.....	6
2.1.2.2 Pulp disintegration.....	7
2.1.2.2.1 Mechanical pulping.....	7
2.1.2.2.2 Chemical pulping.....	7
2.1.2.2.3 Semicheical pulping.....	9
2.1.2.3 Washing.....	9

	Page
2.1.2.4 Screening.....	9
2.1.2.5 Bleaching.....	10
2.1.3 Paper manufacture.....	10
2.1.3.1 Stock preparation.....	12
2.1.3.2 Paper machines.....	12
2.1.3.2.1 Wet end.....	12
2.1.3.2.2 Dry end.....	13
2.1.3.3 Finishing.....	13
2.2 Pulp and Paper Mill Wastewater.....	14
2.2.1 Dissolved water pollutants.....	14
2.2.2 Slowly biodegradable materials.....	15
2.2.3 Toxic compounds.....	15
2.2.4 The solid materials.....	15
2.2.5 Black liquor.....	16
2.3 Lignin.....	17
2.3.1 General properties of lignin.....	17
2.3.2 Lignin in pulp and paper mill wastewater.....	19
2.3.3 Effects of lignin on the environment.....	21
2.4 2,4-DCP.....	22
2.4.1 General properties of 2,4-DCP.....	22
2.4.2 2,4-DCP in pulp and paper mill wastewater.....	24
2.4.3 Toxicity of 2,4-DCP.....	25
2.5 Principles of Photocatalysis.....	27
2.5.1 The nature of light.....	27
2.5.2 Photocatalyst.....	28
2.5.3 Mechanism of photocatalytic reaction.....	30
2.6 The Langmuir-Hinshelwood Kinetics.....	32
2.7 The Related Research.....	34
2.7.1 Treatment of lignin by photocatalytic process (UV/TiO <sub>2</sub> ).....	34
2.7.2 Treatment of 2,4-DCP by photocatalytic process (UV/TiO <sub>2</sub> )...	38



	Page
CHAPTER III METHODOLOGY.....	41
3.1 Chemicals.....	41
3.2 Experimental Instruments.....	43
3.3 Experimental Set-Up.....	44
3.4 Experimental Procedures.....	46
3.4.1 Experimental run using synthetic wastewater.....	46
3.4.1.1 Synthetic wastewater.....	46
3.4.1.2 Experimental methods for synthetic wastewater.....	47
3.4.2 Experimental run using real wastewater.....	49
3.4.2.1 Real wastewater.....	49
3.4.2.2 Experimental methods for real wastewater.....	50
3.5 Analytical Methods.....	51
3.5.1 Measurement of lignin.....	51
3.5.2 Measurement of color.....	52
3.5.3 Measurement of 2,4-DCP.....	52
3.5.4 Identification of by-products of photocatalytic degradation.....	53
3.5.4.1 Identification of by-products of lignin degradation.....	53
3.5.4.2 Identification of by-products of 2,4-DCP degradation..	53
CHAPTER IV RESULTS AND DISCUSSIONS.....	55
4.1 Treatment of Lignin Synthetic Wastewater.....	55
4.1.1 Effect of initial pH on degradation of lignin in synthetic wastewater.....	55
4.1.2 Effect of UV intensity on degradation of lignin in synthetic wastewater.....	59
4.1.3 Effect of vibration frequency on degradation of lignin in synthetic wastewater.....	62
4.1.4 Effect of initial lignin concentration on degradation of lignin in synthetic wastewater.....	65
4.1.5 Identification of the by-products of lignin degradation.....	72
4.2 Treatment of 2,4-DCP Synthetic Wastewater.....	79

	Page
4.2.1 Effect of initial pH on degradation of 2,4-DCP in synthetic wastewater.....	79
4.2.2 Effect of UV intensity on degradation of 2,4-DCP in synthetic wastewater.....	83
4.2.3 Effect of vibration frequency on degradation of 2,4-DCP in synthetic wastewater.....	86
4.2.4 Effect of initial 2,4-DCP concentration on degradation of 2,4-DCP in synthetic wastewater.....	89
4.2.5 Identification of the by-products of 2,4-DCP degradation.....	93
4.2.6 Proposed reaction pathway of 2,4-DCP degradation.....	96
4.3 Treatment of Mixed Synthetic Wastewater Containing Lignin and 2,4-DCP.....	98
4.3.1 Effect of initial pH on treatment of lignin and 2,4-DCP in mixed synthetic wastewater.....	98
4.3.2 Effect of UV intensity on treatment of lignin and 2,4-DCP in mixed synthetic wastewater.....	102
4.3.3 Effect of vibration frequency on treatment of lignin and 2,4-DCP in mixed synthetic wastewater.....	106
4.4 Treatment of Real Wastewater from Pulp and Paper Mill.....	113
4.4.1 Effect of initial pH on treatment of lignin and 2,4-DCP in real wastewater.....	113
4.4.2 Effect of UV intensity on treatment of lignin and 2,4-DCP in real wastewater.....	117
4.4.3 Effect of vibration frequency on treatment of lignin and 2,4-DCP in real wastewater.....	121
 CHAPTER V CONCLUSIONS AND SUGGESTION FOR FUTURE WORKS.....	 128
5.1 Conclusions.....	128
5.2 Suggestion for Future Works.....	130

	Page
REFERENCES.....	131
APPENDICES.....	143
APPENDIX A Analytical Methods.....	144
APPENDIX B Experimental Figures.....	157
APPENDIX C Experimental Data.....	163
APPENDIX D Journal and Conference Publication Lists.....	191
BIOGRAPHY.....	193



ศูนย์วิทยทรัพยากร  
จุฬาลงกรณ์มหาวิทยาลัย

## LIST OF TABLES

Table		Page
2.1	Qualities of pulp and paper mill effluent.....	14
2.2	Black liquor components.....	16
2.3	The properties of 2,4-DCP.....	23
2.4	Band positions of some common semiconductor photocatalyst.....	29
3.1	The experimental factors of synthetic wastewater.....	47
3.2	Experimental conditions of synthetic wastewater.....	48
3.3	The characteristics of pulp and paper mill wastewater.....	50
3.4	The experimental factors of real wastewater.....	51
3.5	Experimental conditions of real wastewater.....	51
4.1	$k_{ap}$ and $r_0$ of first order kinetic for lignin degradation at various initial pH.....	58
4.2	$k_{ap}$ and $r_0$ of first order kinetic for lignin degradation at various UV intensity.....	61
4.3	$k_{ap}$ and $r_0$ of first order kinetic for lignin degradation at various vibration frequency.....	65
4.4	$k_{ap}$ and $r_0$ of first order kinetic for lignin degradation in various initial concentration.....	69
4.5	Fragmentation pattern of by-products from lignin degradation identified by GC-MS.....	74
4.6	$k_{ap}$ and $r_0$ of first order kinetic for 2,4-DCP degradation at various initial pH.....	82
4.7	$k_{ap}$ and $r_0$ of first order kinetic for 2,4-DCP degradation at various UV intensity.....	85
4.8	$k_{ap}$ and $r_0$ of first order kinetic for 2,4-DCP degradation at various vibration frequency.....	88
4.9	$k_{ap}$ and $r_0$ of first order kinetic for 2,4-DCP degradation in various initial concentration.....	92
4.10	Fragmentation pattern of by-products from 2,4-DCP degradation identified by GC-MS.....	95

## LIST OF FIGURES

Figure		Page
2.1	Simplified flow diagram of a typical paper mill.....	11
2.2	Chemical precursors probably involved in lignin biosynthesis.....	18
2.3	Prominent structure in softwood lignin.....	18
2.4	Structure formula of 2,4-dichlorophenol.....	22
2.5	Spectrum of electromagnetic radiation.....	27
2.6	The schematic diagram of initial charge transfer pathway for TiO <sub>2</sub> photocatalytic degradation of organic pollutants.....	30
3.1	The schematic diagrams of the supervibration-photocatalytic reactor (a) and the supervibration agitator (b).....	45
4.1	The effect of initial pH on degradation of lignin in synthetic wastewater: lignin remaining (a) and removal efficiency (b) (initial lignin concentration = 400 mg/l, UV intensity = 6.3 mW/cm <sup>2</sup> , vibration frequency = 30 Hz).....	56
4.2	Linear transform $\ln(C_0/C)$ vs. time for lignin degradation at various initial pH.....	58
4.3	The effect of UV intensity on degradation of lignin in synthetic wastewater: lignin remaining (a) and removal efficiency (b) (initial lignin concentration = 400 mg/l, initial pH = 5, vibration frequency = 30 Hz).....	60
4.4	Linear transform $\ln(C_0/C)$ vs. time for lignin degradation at various UV intensity.....	61
4.5	The effect of vibration frequency on degradation of lignin in synthetic wastewater: lignin remaining (a) and removal efficiency (b) (initial lignin concentration = 400 mg/l, initial pH = 5, UV intensity = 12.6 mW/cm <sup>2</sup> ).....	64
4.6	Linear transform $\ln(C_0/C)$ vs. time for lignin degradation at various vibration frequency.....	65

Figure	Page	
4.7	The effect of initial concentration on degradation of lignin in synthetic wastewater: lignin remaining (a) and removal efficiency (b) (initial pH = 5, vibration frequency = 50 Hz).....	67
4.8	Linear transform $\ln(C_0/C)$ vs. time for lignin degradation in various initial concentration.....	68
4.9	Linear transform $1/r_0$ vs. $1/C_0$ for lignin degradation.....	69
4.10	Removal of color in lignin synthetic wastewater: color remaining (a) and removal efficiency (b) (initial lignin concentration = 100 mg/l, initial pH = 5, UV intensity = 25.2 mW/cm <sup>2</sup> , vibration frequency = 50 Hz).....	71
4.11	Color of lignin synthetic wastewater at reaction time: 0 min (a) and 420 min (b) (initial lignin concentration = 100 mg/l, initial pH = 5, UV intensity = 25.2 mW/cm <sup>2</sup> , vibration frequency = 50 Hz).....	72
4.12	GC-MS chromatogram of by-products from lignin degradation for reaction time: 0 min (a) and 420 min (b).....	73
4.13	Structure formulas of by-products of lignin degradation.....	77
4.14	The effect of initial pH on degradation of 2,4-DCP in synthetic wastewater: 2,4-DCP remaining (a) and removal efficiency (b) (initial 2,4-DCP concentration = 5 mg/l, UV intensity = 6.3 mW/cm <sup>2</sup> , vibration frequency = 30 Hz).....	80
4.15	Linear transform $\ln(C_0/C)$ vs. time for 2,4-DCP degradation at various initial pH.....	81
4.16	The effect of UV intensity on degradation of 2,4-DCP in synthetic wastewater: 2,4-DCP remaining (a) and removal efficiency (b) (initial 2,4-DCP concentration = 5 mg/l, initial pH = 5, vibration frequency = 30 Hz).....	84
4.17	Linear transform $\ln(C_0/C)$ vs. time for 2,4-DCP degradation at various UV intensity.....	85



Figure	Page
4.18	87
The effect of vibration frequency on degradation of 2,4-DCP in synthetic wastewater: 2,4-DCP remaining (a) and removal efficiency (b) (initial 2,4-DCP concentration = 5 mg/l, initial pH = 5, UV intensity = 12.6 mW/cm <sup>2</sup> ).....	
4.19	88
Linear transform $\ln(C_0/C)$ vs. time for 2,4-DCP degradation at various vibration frequency.....	
4.20	90
The effect of initial concentration on degradation of 2,4-DCP in synthetic wastewater: 2,4-DCP remaining (a) and removal efficiency (b) (initial pH = 5, vibration frequency = 50 Hz).....	
4.21	91
Linear transform $\ln(C_0/C)$ vs. time for 2,4-DCP degradation in various initial concentration.....	
4.22	92
Linear transform $1/r_0$ vs. $1/C_0$ for 2,4-DCP degradation.....	
4.23	94
GC-MS chromatogram of by-products from 2,4-DCP degradation for reaction time: 0 min (a) and 420 min (b).....	
4.24	96
Structure formulas of by-products of 2,4-DCP degradation.....	
4.25	97
Proposed reaction pathway for photocatalytic degradation of 2,4-DCP.....	
4.26	99
The effect of initial pH on degradation of lignin in mixed synthetic wastewater: lignin remaining (a) and removal efficiency (b) (initial lignin concentration = 400 mg/l, initial 2,4-DCP concentration = 5 mg/l, UV intensity = 6.3 mW/cm <sup>2</sup> , vibration frequency = 30 Hz).....	
4.27	101
The effect of initial pH on degradation of 2,4-DCP in mixed synthetic wastewater: 2,4-DCP remaining (a) and removal efficiency (b) (initial lignin concentration = 400 mg/l, initial 2,4-DCP concentration = 5 mg/l, UV intensity = 6.3 mW/cm <sup>2</sup> , vibration frequency = 30 Hz).....	
4.28	102
Lignin and 2,4-DCP removal vs. initial pH for mixed synthetic wastewater (reaction time = 420 min).....	

Figure	Page
4.29	104
The effect of UV intensity on degradation of lignin in mixed synthetic wastewater: lignin remaining (a) and removal efficiency (b) (initial lignin concentration = 400 mg/l, initial 2,4-DCP concentration = 5 mg/l, initial pH = 5, vibration frequency = 30 Hz).....	
4.30	105
The effect of UV intensity on degradation of 2,4-DCP in mixed synthetic wastewater: 2,4-DCP remaining (a) and removal efficiency (b) (initial lignin concentration = 400 mg/l, initial 2,4-DCP concentration = 5 mg/l, initial pH = 5, vibration frequency = 30 Hz).....	
4.31	106
Lignin and 2,4-DCP removal vs. UV intensity for mixed synthetic wastewater (reaction time = 420 min).....	
4.32	107
The effect of vibration frequency on degradation of lignin in mixed synthetic wastewater: lignin remaining (a) and removal efficiency (b) (initial lignin concentration = 400 mg/l, initial 2,4-DCP concentration = 5 mg/l, initial pH = 5).....	
4.33	109
The effect of vibration frequency on degradation of 2,4-DCP in mixed synthetic wastewater: 2,4-DCP remaining (a) and removal efficiency (b) (initial lignin concentration = 400 mg/l, initial 2,4-DCP concentration = 5 mg/l, initial pH = 5).....	
4.34	110
Lignin and 2,4-DCP removal vs. vibration frequency for mixed synthetic wastewater (reaction time = 420 min).....	
4.35	111
Removal of color in mixed synthetic wastewater: color remaining (a) and removal efficiency (b) (initial lignin concentration = 400 mg/l, initial pH = 5, UV intensity = 25.2 mW/cm <sup>2</sup> , vibration frequency = 50 Hz).....	
4.36	112
Color of mixed synthetic wastewater at reaction time: 0 min (a) and 420 min (b) (initial lignin concentration = 400 mg/l, initial pH = 5, UV intensity = 25.2 mW/cm <sup>2</sup> , vibration frequency = 50 Hz).....	

Figure	Page	
4.37	The effect of initial pH on degradation of lignin in real wastewater: lignin remaining (a) and removal efficiency (b) (UV intensity = 6.3 mW/cm <sup>2</sup> , vibration frequency = 30 Hz).....	114
4.38	The effect of initial pH on degradation of 2,4-DCP in real wastewater: 2,4-DCP remaining (a) and removal efficiency (b) (UV intensity = 6.3 mW/cm <sup>2</sup> , vibration frequency = 30 Hz).....	116
4.39	Lignin and 2,4-DCP removal vs. initial pH for real wastewater (reaction time = 420 min).....	117
4.40	The effect of UV intensity on degradation of lignin in real wastewater: lignin remaining (a) and removal efficiency (b) (initial pH = 5, vibration frequency = 30 Hz).....	119
4.41	The effect of UV intensity on degradation of 2,4-DCP in real wastewater: 2,4-DCP remaining (a) and removal efficiency (b) (initial pH = 5, vibration frequency = 30 Hz).....	120
4.42	Lignin and 2,4-DCP removal vs. UV intensity for real wastewater (reaction time = 420 min).....	121
4.43	The effect of vibration frequency on degradation of lignin in real wastewater: lignin remaining (a) and removal efficiency (b) (initial pH = 5).....	122
4.44	The effect of vibration frequency on degradation of 2,4-DCP in real wastewater: 2,4-DCP remaining (a) and removal efficiency (b) (initial pH = 5).....	124
4.45	Lignin and 2,4-DCP removal vs. vibration frequency for real wastewater (reaction time = 420 min).....	125
4.46	Removal of color in real wastewater: color remaining (a) and removal efficiency (b) (initial lignin concentration = 250.79 mg/l, initial pH = 5, UV intensity = 25.2 mW/cm <sup>2</sup> , vibration frequency = 50 Hz).....	126

Figure		
4.47	Color of real wastewater at reaction time: 0 min (a) and 420 min (b) (initial lignin concentration = 250.79 mg/l, initial pH = 5, UV intensity = 25.2 mW/cm <sup>2</sup> , vibration frequency = 50 Hz).....	127



ศูนย์วิทยทรัพยากร  
จุฬาลงกรณ์มหาวิทยาลัย

# CHAPTER I

## INTRODUCTION

### 1.1 Rationale

Pulp and paper industries have continuously expanded to support both domestic demand and export for many years. A number of pulp and paper mills in Thailand were more than 90 plants (Pollution Control, Department, Thailand, 2001). They produce large quantities of wastewater about 29-40 m<sup>3</sup>/ton of pulp (Pollution Control, Department, Thailand, 2000). These liquors are heavily loaded with organic matters such as biochemical oxygen demand (BOD), chemical oxygen demand (COD), chlorinated phenolic compounds, suspended solids, fatty acids, lignin and its derivatives, etc (Ali and Sreekrishnan, 2001). Lignin and chlorinated phenolic compounds from pulp and paper mill wastewater are among the main chemical components of environmental concern (Kringstad and Lindstrom, 1984, cited in Ali and Sreekrishnan, 2001). Lignin, a long-chain phenolic polymer found extensively in all vascular woody plants, is built up by oxidative coupling of three major C<sub>6</sub>-C<sub>3</sub> (phenylpropane) units (syringyl, guaiacyl and p-hydroxyphenyl) linked together through different bonds and which gives the wood structure mechanical strength (Lanzalunga and Bietti, 2000; Leiviskä et al, 2009). Its structure is very complex and amorphous polymer as well as high molecular weight. Hence, lignin is highly resistant to biodegradation (Ksibi et al., 2003). Cooking and pulp bleaching processes discharge lignin as waste contained in black liquor from 10-50% by weight (Ksibi et al., 2003; Ramos et al., 2009). Pulp and paper mill effluent in Finland was found to contain 186-293 mg/l of lignin material (Leiviskä et al, 2009; Pessala et al, 2004). The untreated wastewater causes a loss of aesthetic beauty in the receiving body of water (Pokhrel and Viraraghavan, 2004). For instance, the dark brown color of lignin inhibits the natural process of photosynthesis in streams due to absorbance of sunlight (Sahoo and Gupta, 2005). Furthermore, many authors reported the presence of toxic species on aquatic organisms, such as growth inhibition and genotoxicity (Ali and Sreekrishnan, 2001; Dekker, Barbosa, and Sargent, 2002; Yakovleva, Ostrovskaya, and Novikova, 2004). Whereas, 2,4-dichlorophenol (2,4-DCP) has been produced

from pulp and paper making as a by-product of the chlorine pulp bleaching process (González, Sarria, and Sánchez, 2010; Matafonova et al., 2006; Pera-Titus et al., 2004). It was found in aeration pond, treating pulp and paper mill wastewater in Selenga at 2.38 mg/l (Batoev et al., 2005). Previous studies reported the effects to organisms, such as growth inhibition in microorganism (Matafonova et al., 2006), growth inhibition (Scragg, Spiller, and Morrison, 2003) and physical changes (Sahinkaya and Dilek, 2009) in aquatic organisms and effect on human erythrocytes (Bukowska et al., 2007). Most wastewater treatments of pulp and paper mill are typically carried out using biological treatments but they require long residence time and can only remove small amounts of lignin (Leiviskä et al., 2009; Malaviya and Rathore, 2007; Sahoo and Gupta, 2005) and 2,4-DCP (Bayarri, González et al., 2007; Kaigi, Eker, and Uygur, 2005; Uysal and Türkman, 2005). Therefore, powerful advanced oxidation processes are alternatives for effective treatment.

Photocatalysis is one of Advanced Oxidation Processes (AOPs) that involves the use of titanium dioxide ( $\text{TiO}_2$ ) as a catalyst and ultraviolet light (UV) as an irradiation source. The UV light (wavelengths  $< 385$  nm) absorbed by the photocatalyst with energy higher than band gap energy of  $\text{TiO}_2$  excites an electron from the valence band to the conduction band, producing electron-hole pairs ( $e^-/h^+$ ). During the process, hydroxyl radicals ( $\text{OH}^\bullet$ ) are generated on the surface of  $\text{TiO}_2$ . Due to the high oxidation potential (2.8 V),  $\text{OH}^\bullet$  are the principal agents responsible for the oxidation of numerous aqueous organic contaminants and mineralize them into carbon dioxide ( $\text{CO}_2$ ), water ( $\text{H}_2\text{O}$ ) and other small molecules (Bayarri, González et al., 2007; Chen et al., 2004; Gao et al., 2007; Kaneko and Okura, 2002; Zhou and Smith, 2002). The effects of the form of  $\text{TiO}_2$ ,  $\text{TiO}_2$  dosages, initial pH, UV light, and initial concentration on removal of lignin (Dahm and Lucia, 2004; Kansal, Singh, and Sud 2008; Ksibi et al., 2003; Ma et al., 2008; Portjanskaja and Preis, 2007; Tanaka, Calanag, and Hisanaga, 1999) and 2,4-DCP (Bayarri, Abellán et al., 2007; Bayarri et al., 2005; Chen et al., 2004; Kusvuran et al., 2005; Pandiyan et al., 2002) using UV/ $\text{TiO}_2$  have been continuously studied. González et al. (2010) reported that an increase in suspended  $\text{TiO}_2$  from 0 to 20 mg/L caused an increase in the 2,4-DCP removal initial rate. Effect of UV on 2,4-DCP degradation was studied by Bayarri, Abellán et al. (2007), UV-ABC radiation could be more efficient than UV-A. Furthermore, Dahm and Lucia (2004) found that at the highest light intensity level



(445 mW/cm<sup>2</sup>), lignin removal occurred much faster than that at the lower illumination intensity. However, it is difficult for TiO<sub>2</sub> powder to disperse and be recycled in aqueous solution. TiO<sub>2</sub> should be coated on some carriers before use (Bao-xiu, Xiang-zhong, and Peng, 2007).

In this study, the removal of lignin and 2,4-DCP using a newly developed supervibration-photocatalytic reactor based on the photocatalytic process combined with a supervibration agitator were evaluated as a function of initial pH, UV intensity, vibration frequency and initial concentration, focusing on removal efficiency to determine the optimum treatment conditions. Moreover, this work was extended to identify the intermediates or by-products of lignin and 2,4-DCP degradation.

## **1.2 Objectives of Investigation**

1.2.1 To study the performance of newly developed supervibration-photocatalytic reactor for treatment of lignin and 2,4-DCP in pulp and paper mill wastewater

1.2.2 To determine the optimum operating conditions of supervibration-photocatalytic reactor

1.2.3 To identify the intermediates or by-products of lignin and 2,4-DCP degradation by supervibration-photocatalytic reactor

1.2.4 To study the reaction kinetics of lignin and 2,4-DCP degradation by supervibration-photocatalytic reactor

## **1.3 Hypothesis**

The newly developed supervibration-photocatalytic reactor can be an effective system for lignin and 2,4-DCP removal from pulp and paper mill wastewater.

## **1.4 Scope of Research**

1.4.1 The experiments were conducted in laboratory scale and batch-mode operation using 25 liters of supervibration-photocatalytic reactor at laboratory of Department of Environmental Engineering, Faculty of Engineering, Chulalongkorn University.

1.4.2 Wastewater samples consisted of 4 types as follow

1.4.2.1 Lignin synthetic wastewater

1.4.2.2 2,4-DCP synthetic wastewater

1.4.2.3 Mixed synthetic wastewater containing lignin and 2,4-DCP

1.4.2.4 Real wastewater from pulp and paper mill

1.4.3 The removal of lignin and 2,4-DCP using a supervibration-photocatalytic reactor was evaluated as a function of initial pH, UV intensity, vibration frequency and initial concentration.

## 1.5 Anticipated Benefits

This research is expected to yield the follow benefits

1.5.1 Get new knowledge from new wastewater treatment system as supervibration-photocatalytic reactor for lignin and 2,4-DCP removal in pulp and paper mill wastewater

1.5.2 Acknowledge the effects of operating parameters on the performance of a novel supervibration-photocatalytic reactor for treatment of lignin and 2,4-DCP to determine the optimum treatment conditions

1.5.3 Obtain basic data to apply for real situation

ศูนย์วิทยทรัพยากร  
จุฬาลงกรณ์มหาวิทยาลัย

## CHAPTER II

### LITERATURE REVIEW

#### 2.1 Pulp and Paper Making Processes

2.1.1 Raw materials for pulping process (Eugenia, Gloria, and Elizabeth, 2000)

Fibers, which are in wood, are raw materials for this process. However, only some wood can get good fibers to suitable for pulping process. Moreover, wood cost is also considered to select a suitable type of wood for budget reducing. Wood as raw material in pulping process can be divided of 2 classes:

##### 2.1.1.1 Wood

2.1.1.1.1 Softwood, such as pine spruce, etc., grows in high and cool area. It grows slowly. The leaves are long and small. Fibers are called long fibers, which are rough and strong. These fibers are long about 2-4 mm.

2.1.1.1.2 Hardwood, such as eucalyptus, acacia, birch and aspen, etc., grows quickly in tropical area. The leaves are wide. Fibers are called shot fibers. These fiber characteristics are shot, fine and low strong fibers. Length of fibers is 0.5-1.5 mm.

##### 2.1.1.2 Non-wood

Non-wood, such as cotton and bamboo, etc., gives fibers to suitable for paper making, besides straw and sugar cane, which are residues in agriculture also give good fibers. However, length of fibers does not fix.

Long fibers get a pulp to differ from shot fibers. Long fibers, which are strong fibers, are used for a high impact paper, such as paper for packaging, paper bags and

corrugate boxes, etc. Shot fibers, fined fibers, get a smooth paper. Consequently, they are suitable to produce printing and writing paper. In paper making from non-wood, it has many problems for paper making because it needs a high volume warehouse for storage. Especially, this plant can not feed raw material fibers all season, such as rice straw, etc., but only in harvest period. Hence, it is not suitable for paper industry.

2.1.2 Pulp manufacture (Lavigne, 1979; United Nations Environment Programme [UNEP], 1996)

#### 2.1.2.1 Wood preparation

In the mill woodyards, the unbarked logs are fed into a giant, revolving drum barker in which their bark is stripped as they tumble against each other and the steel channeled wall of the drum. Bark is also removed by moving the logs past streams of high-pressure water in a hydraulic-type barker, or by sets of mechanical knives. Depending on the type of pulping process, they are going to be used in, the debarked logs from the barker and/or the woodlands are either sent directly to the process or to chippers where, by dropping against a revolving disc with heavy, sharp knives set at an angle. They are reduced to small chips approximately one-half to three-quarters of an inch in size. These wood chips and the unscreened wood chips from the woodlands are conveyed to vibrating screens. Oversized chips are removed and sent to a rechipper and returned for another pass through the screens. Usually, the undesirable fine chips and sawdust that are removed at the screens are burned in the power boiler as fuel. The screened chips are then either transported by air conveyors to outside chip storage piles or belt-conveyed to huge tanks or silos for storage according to the type or species. Then they are transported from there to smaller storage bins located in the pulp mill, usually directly over the digesters in which the wood is to be processed.

### 2.1.2.2 Pulp disintegration

These processes remove the majority of lignin and hemicellulose content from the raw material. The conversion of chips into pulp (wood fibers) is usually carried out by one of three general methods, namely: mechanical, chemical and semichemical, depending on the types of wood used and the requirements of the end product.

#### 2.1.2.2.1 Mechanical pulping

The simplest pulping method is generally referred to as mechanical pulping. It differs from other pulping methods in the reduction of wood to fibers and is essentially a physical operation in which the fibers are actually pulled away from each other by the application of some types of mechanical force. In mechanical pulping, the fibers are separated mainly by mechanical force in grinders and/or refiners. The original process was stone groundwood manufacture where the logs are pressed against a rotating grindstone. The process requires wooden logs and, due to treatment, the resulting pulp has relatively low strength and low brightness. This process can produce most pulp of 85-95%. The pulp is used in the manufacture of newsprint and some types of toilet paper. The three most prevalent forms of mechanical pulping are groundwood, refiner groundwood or refiner mechanical and thermomechanical.

#### 2.1.2.2.2 Chemical pulping

In these types of processes, the wood chips are cooked in chemical solutions under temperature and pressure until the fibers are separated from their lignin binder and fall apart without mechanical action. The aim of this treatment is to dissolve and/or soften the main part of lignin material that binds the fibers together in the raw material. There are several chemical pulping processes using one or several solutions, depending on the type of wood used and the kind of pulp desired. All processes use aqueous systems under heat and pressure. Pulp yield is in the range 45-

55% for chemical pulp. There are two main types of chemical pulping processes as the sulfite and the alkaline processes.

### (1) Sulfite process

Conventional sulfite pulping is sensitive to fiber raw materials with high contents of certain types of extractives and uses mainly softwood species, such as spruce, hemlock and fir, etc. The chip cooking liquor consists of sulfurous acid and a salt of this acid produced by burning sulfur to sulfur dioxide. The pulp has weak fibers and shows the highest unbleached brightness, sulfate the lowest, with soda in between. Sulfite pulp is used in the manufacture of bond, writing, high grade books and other fine paper.

### (2) Alkaline processes

#### (2.1) Soda process

Soda pulping is more suited to low lignin raw materials like annual plant, bamboo and hardwood. It is a forerunner to the sulfate process and uses hydroxyl and carbonate as the active components. Soda pulp is weaker than sulfate pulp and is used in the manufacture of printing, writing and soft paper.

#### (2.2) Sulfate or kraft process

The most important chemical process is the sulfate or kraft process. Practically any species of wood can be used. The wood chips are boiled under pressure in a strong solution of sodium hydroxide (NaOH) and sodium sulfide (Na<sub>2</sub>S). Sulfate pulping is the most versatile process and produces the strongest pulp, soda and sulfite pulping give weaker fibers. So, it has grown to be the dominant process in the world. The bleached pulp is used in the manufacture of printing paper and high grade books.



#### 2.1.2.2.3 Semicheical pulping

Another way of making wood pulp combines mechanical and chemical methods and is called the semicheical process. In semicheical pulping, the wood is given only a mild chemical treatment, softening or removing just enough lignin to loosen the fibers, but not enough to separate them. Separation is then effected by mechanical means. The process was developed particularly for the pulping of hardwood and has many variations. Three of the important methods are the neutral sulfite, cold soda and chemigroundwood processes. Pulp yield is in the range 60-75% for semicheical pulp. The pulp produces stiff, resilient products and is used in making corrugated paperboards, egg cartons and similar items.

#### 2.1.2.3 Washing

After being cooked in the digester, the pulp is washed in a countercurrent rotary vacuum washer system using three or four stages. Pulp washing is the removal of washable, spent cooking liquor and intercellular matter dissolved by the cooking liquors during the cooking process. This must be accomplished without diluting the wash liquors any more than is absolutely necessary, as all these liquors must be evaporated later in the process of chemical recovery. Incomplete washing renders subsequent bleaching of the pulp difficult and impairs the value of the pulp. Excessive washing renders recovery of chemicals too costly. Obviously, the maximum amount of wash liquors must be conserved and none should be allowed to escape as waste. Washing has been accomplished in the past by hosing down the pulp in drain tanks, by the use of screw presses, by the use of rotary vacuum washers and lately as well as by the use of continuous diffusion washers. The use of rotary vacuum washers is the most common method.

#### 2.1.2.4 Screening

Screening is essentially the removal of oversized foreign materials, such as knots, uncooked wood particles, large slivers, extraneous dirt and other debris from cooked pulp, etc., either before or after washing, by the use of mechanical separation from the acceptable pulp fibers. This is normally accomplished by coarse or fine

screens located between the blow tank and pulp washing operation or after the washing operation. There are three general types of coarse screens including basket, inclined plate, and cylinder screens. The fine screens are available as a flat, perforated type, or as a rotary type.

#### 2.1.2.5 Bleaching

The aim of chemical pulp bleaching is to remove and/or brighten the residual, colored lignin that remains in the pulp after the cook and to achieve this without undue loss in pulp strength or yield. Lignin removal is achieved using chlorine, hypochlorite, chlorine dioxide, oxygen or ozone. Using oxygen or particularly peroxide under mild conditions brightens pulp without significant lignin dissolution. There is considerable variation in the technique and chemical used between plants in the bleaching operation depending on the fibrous raw materials from which the pulp has been produced (wood species, agriculture residues and grasses, etc.), the pulping process used (sulfite, sulfate and semichemical, etc.) and the final use of the bleached pulp (fine paper, coarse paper, heavy weight, light weight and dissolving pulp, etc.). After the process, the bleaching agents are removed from the pulp. Generally an alkali (caustic soda) is used to extract color and bleaching agents from the pulp.

#### 2.1.3 Paper manufacture (Lavigne, 1979; UNEP, 1996)

Pulp, produced by any of the foregoing or miscellaneous processes, is made into paper in a mill that is at the same location as the pulp mill (referred to as an integrated mill), or it is dried and shipped to a paper mill located remotely from the pulp mill. Paper mill layouts vary somewhat, based on the pulp used and grades of paper produced. Figure 2.1 presents the basic operations carried on in a typical paper mill. They are generally divided into stock preparation, paper machines, and finishing operations. The stock preparations can be further divided into stock proportioning or blending and mechanical treatment. Paper machine operations can also be subdivided into wet end and dry end.

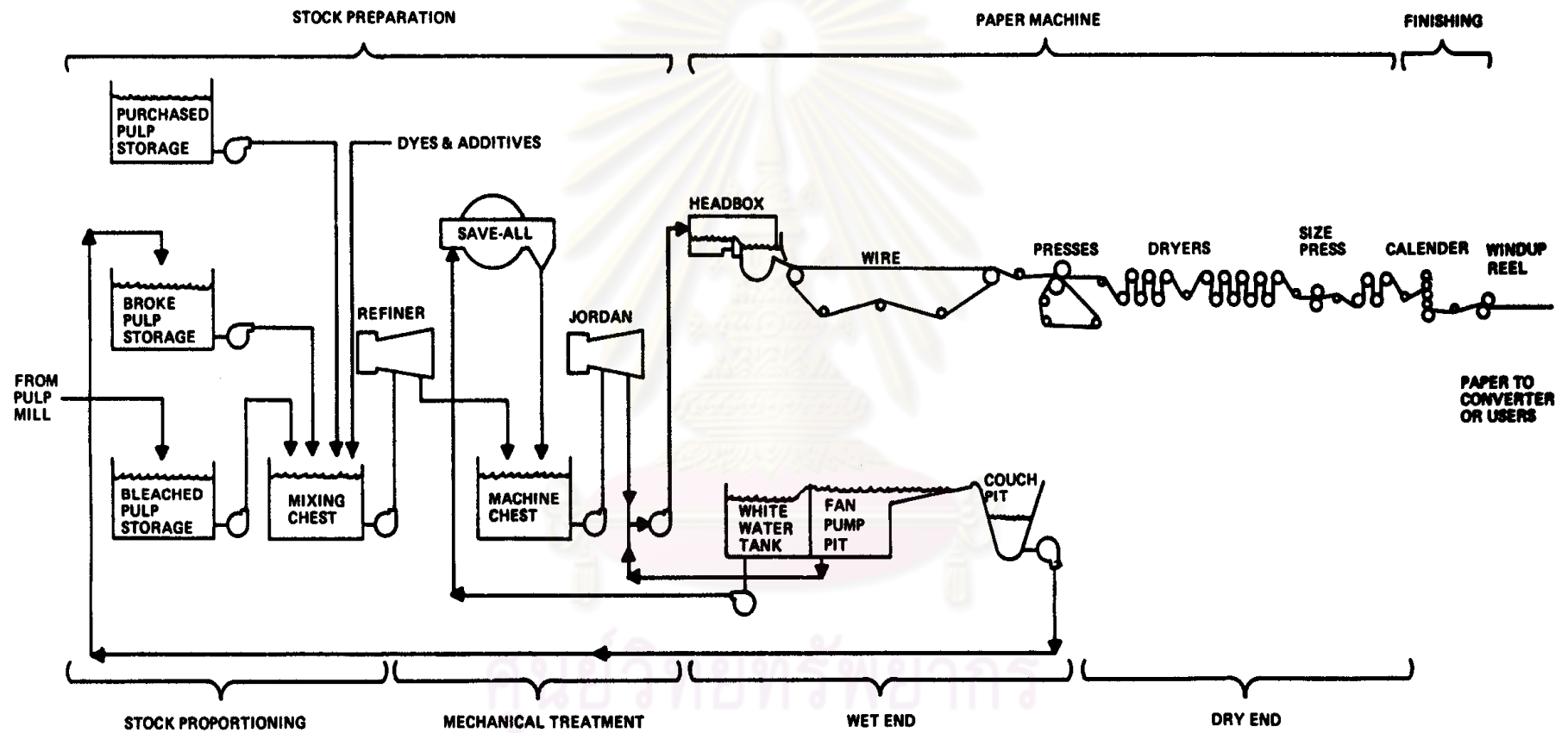


Figure 2.1 Simplified flow diagram of a typical paper mill (Lavigne, 1979)

### 2.1.3.1 Stock preparation

Most of pulp cannot be used for papermaking as it comes from the pulp mill. Therefore, other types of pulp having different characteristics must be purchased from other pulp mills to give the final qualities needed for the paper to be made. Dye and additives are also added to achieve the desired color and physical properties of the sheet. These operations are usually referred to as stock proportioning or stock blending. To impart mechanical strength to the final sheet, the pulp is refined in a variety of machines, typical of which are the refiners, jordans, and beaters. Basically, the operation consists of passing the pulp repeatedly between sharp moving bars that cut and abrade the fibers. The sets of bars can be adjusted to turn out various lengths of fibers with rougher or smoother edges. This improves fiber-to-fiber bonding, making it more uniform, more density, less porous, or more transparent, depending on the kind of paper to be made. Before going to the paper machines, the resulting pulp is screened and, in some cases, cleaned by passing through centrifugal-type cleaners to remove heavy particles of dirt that have not as yet been removed.

### 2.1.3.2 Paper machines

#### 2.1.3.2.1 Wet end

The most common major components of the wet end portion of the paper machines, on which the paper is formed, are a fourdrinier. They consist mainly of a continuous fine screen, called a wire, on which the pulp suspension is spread. The wet end section varies in widths in accordance with the size of the machine and moves at different speeds as determined by the type of paper being produced. Most of water drains at the top end of the wire to form a mat of fibers. The wire then passes over a series of vacuum suction boxes which suck more water from the wet mat through the wire. The wet paper leaves the fourdrinier machine at a consistency of about 20 percent (20% fibers and additives, 80% water).

Paperboard, which consists of several layers of paper, is usually made on a cylinder-type machine instead of a running flat screen. Pulp is pumped to several vats. In each vat, a cylinder covered with a fine wire screen turns at the same speed as the rest of the machine. Water passes from the vat through the screen and is

removed from the center of the cylinder, leaving a mat of paper on the wire screen. A continuous felt blanket in contact with all cylinders picks up layers of paper, forming a laminated, layered board. A good grade of pulp is frequently used on the end cylinders to give the outside of the board a good appearance. The second sheet is often made of a slightly poorer grade, while the inner layers are normally reclaimed paper of poor grade.

#### 2.1.3.2.2 Dry end

After leaving the wet end section of the paper machines, the wet paper is sent to the presses where it is supported by endless woolen or synthetic loops called felts. The paper on top of the felts is then passed between heavy press rolls to press out as much water as possible. The paper leaves the press section at approximately 35% consistency. The rest of the water is then evaporated on steam-heated rolls located in the dryer section. Endless felts again carry the paper though and press it against steam-heated rolls on opposite sides.

#### 2.1.3.3 Finishing

The dried paper passes on to the finishing stage of the process. Most of paper goes through one or more additional processes, one of which is calendering. This process consists of ironing paper between heavy, polished steel rollers, giving it a much smoother surface. Some paper is wound in large rolls as it comes from the calenders. These are later rewound and cut into smaller rolls or sheets as required by the user. Some paper is produced specially for further processing by converter plants which make envelopes, milk containers, grocery bags, paper cups, and many other consumer products. Paperboard is used for corrugated cartons, folding boxes for frozen foods, and many other items. Large quantities of pulp for some types of paperboard are made up of repulped waste paper from which ink and other impurities have been removed.

## 2.2 Pulp and Paper Mill Wastewater

The wastewater of pulp and paper industry is of major concern because large volumes of wastewater are generated for each metric ton of paper produced, depending upon the nature of the raw materials, finished products and extents of water reuse. Pollution Control Department (2000) reported that pulp and paper mills produce large quantities of effluent about 29-40 m<sup>3</sup>/ton of pulp. Pulp and paper making involve five basic steps as debarking, pulping, bleaching, washing and paper and paper products as well as each step can be carried out by a variety of methods. Thus, the final effluent is a combination of wastewater from each of the five different unit processes (Ali and Sreekrishnan, 2001). Qualities of pulp and paper mill effluent are given in Table 2.1.

Table 2.1 Qualities of pulp and paper mill effluent

Processes	Wastewater quantities (m <sup>3</sup> /ton of pulp)	COD (mg/l)	BOD (mg/l)	Color (Pt-Co unit)	SS (mg/l)
Sugar cane semichemical pulping	27.37	5,180	2,060	456	2,190
Kraft pulping	40	2,058	460	958	340
Soda pulping	53.9	1,300	400	535	400

Source : Ministry of Industry, Department of Industrial Work, Environmental  
Technology Office, 1999

### 2.2.1 Dissolved water pollutants

They are produced from the processes can be classified into easily and slowly biodegradable material, colored compounds, toxic material and inorganic salts. The content of easily biodegradable materials is usually measured by the BOD test. The effluents are heavily loaded with organic matter. These effluents cause considerable damage to the receiving water, if discharged untreated since they have a high



biochemical oxygen demand (BOD) and chemical oxygen demand (COD) (Ali and Sreekrishnan, 2001). A considerable parts of the wood components dissolved or formed in the pulping and bleaching operation are easily biodegradable, such as low molecular hemicelluloses, methanol, acetic acid and formic acid, etc. (UNEP, 1983).

### 2.2.2 Slowly biodegradable materials

Slowly biodegradable materials in the mill effluent mainly consist of high molecular weight material of carbohydrate, lignin (dark brown color) and its derivatives from cooking and pulp bleaching processes as well as tannin and fatty acid from wood extractives (Ali and Sreekrishnan, 2001). The relative amount can be estimated by the BOD/COD value ratio. The lower ratio indicates the higher amount of slowly degradable compounds (UNEP, 1983).

### 2.2.3 Toxic compounds

Toxic compound discharges have been studied intensively in recent years. Investigations have shown that the spent liquor and the spent liquor condensate contain the components having most acutely toxic to fish and bacteria. From the bleach plant, the chlorination and alkali stage effluents are the most toxic (UNEP, 1983) containing chlorinated phenolic compounds from chlorine pulp bleaching process (Williams et al., 1996) as well as lignin and its derivative, resin acid, fatty acid and tannin from wood extractives (Ali and Sreekrishnan, 2001).

### 2.2.4 The solid materials

The solid materials in the discharges to receiving water include fibers and fiber fragments, bark and wood particles, solid inorganic salts and mineral fillers. They are measured as suspended solids (SS). The larger particles mainly deposit close to the point of discharge but the fine particles are carried long distance by making turbid water (UNEP, 1983).

### 2.2.5 Black liquor

The separated liquor is very dark and is known as black liquor that had solid content in range of 25-30%. These solids consist of lignin in range of 25-45% by solid weight (Alen, Sari, and McKeough, 1995; Sjoström, 1981; Wallberg, Jonsson, and Wimmerstedt, 2003). The solid components in black liquor are shown in Table 2.2. Black liquor is concentrated in multieffect evaporators to 60-65% of solids. At this concentration, the quantities of dissolved organic compounds from the wood (lignin and carbohydrate) are sufficient to allow the liquor to be burned in recovery furnace. After burning, the inorganic substances are collected on the bottom of furnace as a molten smelt of  $\text{Na}_2\text{CO}_3$  and  $\text{Na}_2\text{S}$ . Sodium sulfate is added to the liquor as make-up and is reduced to  $\text{Na}_2\text{S}$  by carbon. After dissolving in water, this mixture (called green liquor) is reacted with slaked lime. Since  $\text{Na}_2\text{S}$  does not react with the lime, the resultant mixture of  $\text{NaOH}$  and  $\text{Na}_2\text{S}$  (called white liquor) can be reused in pulp digester (Kent and Jame, 1983).

Table 2.2 Black liquor components

Components	Content (% by solid weight)
Organic compounds	
Lignin	25-45%
Aliphatic carboxylic acids	25-35%
Other compounds	3-5%
Inorganic compounds	
Sodium	17-20%
Sulfur	3-5%

Source : Alen et al, 1995; Sjoström and Alen, 1999; Wallberg et al., 2003

This group, along with lignin, its derivatives and chlorinated organic substances from cooking and pulp bleaching processes, are among the main chemical components of environmental concern (Kringstad and Lindström, 1984, cited in Ali

and Sreekrishnan, 2001). The various types of wastewater are produced from different unit processes. As a result, no single specific technology can be applied to the treatment of effluents from all the mills since process diversities may preclude its acceptability (Ali and Sreekrishnan, 2001). Consequently, the knowledge of possible contaminants present in the wastewater, their origins, degree of toxicity and available treatment technologies becomes so essential.

## 2.3 Lignin

### 2.3.1 General properties of lignin

Lignin is a polymer found extensively in all vascular woody plants, mostly between the cells, but also within the cells and in the cell walls, constitutes 1/4 to 1/3 total dry weight of trees. It makes vegetables firm and crunchy. It is a phenolic polymer, which is built up by oxidative coupling of three major C<sub>6</sub>-C<sub>3</sub> (phenylpropane) units as Syringyl (S), Guaiacyl (G) and p-Hydroxyphenyl (H) produced from sinapyl alcohol, coniferyl alcohol and p-coumaryl alcohol, respectively (as shown in Figure 2.2). Three dimensional polymers having in common a phenylpropane structure is a benzene ring with a tail of three carbons, which form a randomized structure in a tridimensional network inside the cell wall. Differential lignin had also difference of S, G and H unit compositions (Hofrichter and Steinbüchel, 2001).

The basic structure of lignin differs to some extent between softwood and hardwood. In structure is known as a guaiacyl unit which contains but a single methoxyl group on the phenylpropane ring; hardwood lignin, on the other hand, is a copolymer or mixture of guaiacyl and syringyl lignin. The latter contains two methoxyl groups per phenylpropane nucleus. The ratio of guaiacyl to syringyl units varies from 4:1 to 1:2 among different hardwood (as shown in Figure 2.2) (Parham, 1983). In their natural unprocessed form, they are so complex that none of them has ever been completely described and have molecular weights that may reach 15,000 or more (McCardy, 2004: online). The example of softwood lignin structure is presented in Figure 2.3.

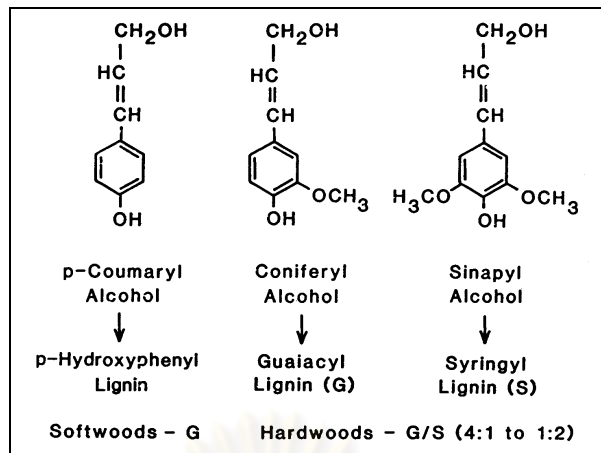


Figure 2.2 Chemical precursors probably involved in lignin biosynthesis (Parham, 1983)

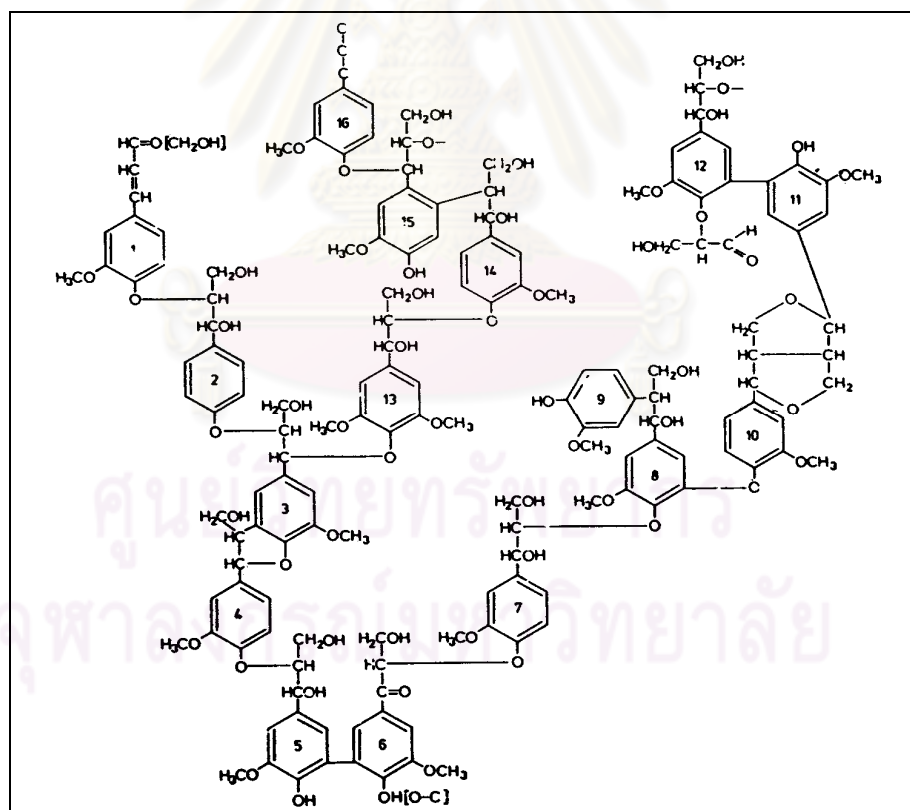


Figure 2.3 Prominent structure in softwood lignin (Adler, 1977)

Lignin quantity in wood, which is different wood types and get differentially a range of quantity. For the example, Eucalyptus has lignin content of 29.5%, whereas Jack pine contains lignin content as 26.7%. However, lignin is amorphous polymer and complex to discover a true structure. Beside aromatic structure, other lignin structures also consisted of hydroxyl, methoxyl and carbonyl groups, so different types of lignin also differ in these functional groups. Moreover, difference of lignin structure depends on many factors, such as source and extraction cause of its difference, etc. Therefore, lignin has many types and also can be nomenclatured by source, such as wheat straw lignin, it can be called by extraction method, such as native lignin (protolignin), milled wood lignin, sulfite lignin and kraft lignin, ect. (Sjostrom, 1981).

### 2.3.2 Lignin in pulp and paper mill wastewater

Lignin is discharged from cooking and pulp bleaching processes and is contained in black liquor as waste from 10-50% by weight (Ksibi et al., 2003). Chanwit Srikaew (2001) reported that concentration of lignin in pulp and paper mill effluents from secondary sedimentation tank were 32-64 mg/l. Pulp and paper mill effluent in Finland was found to contain 186-293 mg/l of lignin material (Leiviskä et al., 2009; Pessala et al., 2004). Lignin is very complex and amorphous polymer as well as high molecular weight. Hence, lignin is highly resistant to biodegradation (Ksibi et al., 2003). Lignin resists attack by most microorganisms, and anaerobic processes tend not to attack the aromatic rings at all. Previous researches have proved that lignin is highly resistant to biodegradation that need long reaction time as follow

Johansson et al. (2000) investigated microbial degradation of lignin (4.4-12.2 mg/l) using white-rot fungus *P. chrysosporium* and chlorine dioxide and found that the fraction of lignin mineralized in the study was small. When used chlorine dioxide of 1 g/l, lignin respired after 7 day of incubation with *P. chrysosporium* was around 3.5%.

Sugiura, Hirai, and Nishida (2003) studied lignin removal using a novel lignin peroxidase (YK-LiP) isolated from white-rot fungus *Phanerochaete sordida* YK-624. 0.1 mM of 4-Ethoxy-3-methoxyphenylglylycerol- $\mu$ -guaiacyl ether (dimer I) and 0.1 mM of guaiacylglycerol- $\beta$ -guaiacyl ether (dimer II) were used as lignin. The results

were found that 1.3 nkat of YK-LiP degraded 93% of dimer I and 1 nkat of YK-LiP degraded all of dimer II within 24 h.

Pimchanok Tengcharoen (2003) investigated lignin (7.5 g/l) removal by Basidiomycota fungus. The carbon source was 0.5% sucrose and the nitrogen source was 0.1% sodium nitrate. After 8 days of cultivation, the maximum reduction of lignin was 75.81%.

Wu, Xiao, and Yu (2005) studied removal of lignin (4.6 g/l) in black liquor from pulp and paper mill in China by white-rot fungi on a porous plastic media. The lignin removal was 54% for S22 and 52% for *P. ostreatus* on 4 day. For *L. edodes*, lignin removal efficiency of 65% was achieved on 10 day and removal efficiency of lignin was 49% with *T. versicolor* on 13 day.

Bohlin, Lundquist, and Jönsson (2008) investigated degradation of a lignin model compound of the arylglycerol  $\beta$ -aryl ether type (0.5 mM) by white-rot fungi and reported that *T. versicolor* could remove lignin at 57-72% after 4 day, whereas *P. chrysosporium* can degrade lignin at 44-92% after 22 day.

Ko et al. (2009) studied biodegradation of lignin under sulfate reducing conditions. The inoculum was obtained under anaerobic condition from a simulated landfill column reactor. Klason lignin decreased slightly, 11.6% of 3.49 mg/l/day, from the 97<sup>th</sup> day to the 156<sup>th</sup> day, and 12% of 3.03 mg/l/day, from the 181<sup>st</sup> day to the 280<sup>th</sup> day.

Most wastewater treatments of pulp and paper mill are typically carried out using biological treatments but they can only remove small amounts of lignin and require long residence time (Leiviskä et al., 2009). Commercial lignin is currently produced as a co-product the paper industry, separated from trees by a chemical pulping process. Sulfite lignin (lignosulfonate) is product of sulfite pulping process. This lignin product is soluble in water. Sulfate lignin (alkaline lignin or kraft lignin) is obtained from kraft pulping process (alkaline pulping process). Sulfate lignin smells slightly like vanillin, is soluble in alkaline aqueous solution (pH > 8). It is insoluble in water and can be precipitated with acids (Wünning, 2001).



### 2.3.3 Effects of lignin on the environment

2.3.3.1 Color in pulp and paper mill wastewater is largely due to lignin and lignin derivatives and polymerized tannins which are mostly discharged from the cooking, pulp bleaching and recovery sections. Lignin and its derivatives have been found to offer resistance to degradation due to the presence of carbon-to-carbon biphenyl linkages. The double bonds conjugated with an aromatic ring, quinone methides and quinone groups are responsible for the color of its solution (Sankaran and Vand Ludwig, 1971). Color is not considered to be a major problem, being classified as a non-conventional pollutant. However, it has now been realized that the discharge of colored effluent from pulp and paper mills is not only a loss of aesthetic beauty or visual pollution but also has other ramifications in receiving body since there is a marked change in the algal and aquatic plant productivity or inhibits the natural processes of photosynthesis in streams caused by the reduced light penetration into water. They may also affect quality of drinking water (Ali and Sreekrishnan, 2001; Sahoo and Gupta, 2005; UNEP, 1983).

2.3.3.2 In the case of toxicity of lignin and its derivatives, living organisms may absorb slowly biodegradable compounds which may cause biological effects (UNEP, 1983). Previous studies have proved that lignin and its derivatives are quite toxic as follow

A study by Roald, 1977 (Ali and Sreekrishnan, 2001) showed that the growth rate of young rainbow trout exposed to a concentration of >160 mg/l of lignosulfonate was lower than that of control fish.

Dekker et al. (2002) reported effect of lignin-related aromatic acid on fungal (*Botryosphaeria* sp.) growth. A trend for inhibition of growth was based upon chemical structural features.

Lignin was proved to be toxic to aquatic organisms (*Daphnia magna* and *Vibrio fischeri*) by Pessala et al. (2004). The calculated EC<sub>50</sub> value for lignin in bleaching effluent would be 34 mg/l and for commercial alkali lignin, its EC<sub>50</sub> value was 11 mg/l.

Yakovleva et al. (2004) found that both toxicity and mutagenic activity of lignin substances on Baikal endemic mollusks and corn depended on the

physicochemical characteristics of lignin, the test organisms and experimental conditions. The results provided evidence that lignin substances discharged into water body created a genetic hazard to Baikal mollusks and corn.

## 2.4 2,4-DCP

### 2.4.1 General properties of 2,4-DCP

2,4-DCP is organic chemical formed from phenol by substitution in the phenol ring with 2 atoms of chlorine. It is a colorless crystals or white solid that has a strong medicinal odor. The molecular formula for 2,4-DCP is  $C_6H_4Cl_2O$  and its molecular weight is 163.0. Boiling point and melting point of 2,4-DCP are 210 and 45 °C, respectively. It can be soluble in ethanol, benzene, carbon tetrachloride and ethyl ether as well as slightly soluble water of 4.5 g/l at 20 °C. In the environment, it is poorly biodegradable substance. The properties of 2,4-DCP are shown in Table 2.3 (Ministry of Economy, Trade and Industry, Chemical Substances Council, 2002) and Figure 2.4 shows structure formula of 2,4-DCP.

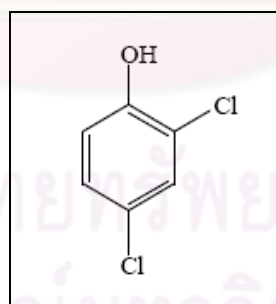


Figure 2.4 Structure formula of 2,4-dichlorophenol (Ministry of Economy, Trade and Industry, Chemical Substances Council, 2002)

Table 2.3 The properties of 2,4-DCP

Parameters	Values/Properties
Product identification	
Chemical name	2,4-Dichlorophenol (2,4-DCP)
Synonyms	4,6-Dichlorophenol, 4-Hydroxy-1,3-dichlorobenzene
CAS number	120-83-2
Molecular formula	C <sub>6</sub> H <sub>4</sub> Cl <sub>2</sub> O
Molecular weight	163.0
Toxicity	Oral rat LD <sub>50</sub> : 47 mg / kg
Physical and chemical properties	
Appearance	Colorless crystals , White or Pale yellow solid
Odor	Strong medicinal
Melting point	45.0 °C
Boiling point	210.0 °C
Flash point	113.0 °C
Specific gravity	1.382
Vapor pressure	16 Pa (25 °C )
Biodegradability	Poorly biodegradable
Stability	Stable under ordinary conditions
Solubility in water	4.5 g/l (20 °C )
Solubility in organic solvents	Soluble in carbon tetrachloride, ethanol, benzene and ethyl ether (aqueous alkali)

Source : Ministry of Economy, Trade and Industry, Chemical Substances Council, 2002

The estimated half-life for the reaction of 2,4-DCP at pH 7 with singlet oxygen in natural water under midday sunlight (assuming a singlet oxygen concentration of  $4 \times 10^{-14}$ ) using experimentally determined rate constants was 62 hours (Scally and Hoigne, 1987). The half-life for 2,4-DCP in sediment was estimated to be approximately 116 days in July and 47 days in November (Mackay, Shiu, and

Ma, 1997, cited in Kieher, Hengraprom, and Knuteson, 1998: online). A study by Liu and Pacepavicius (1990) using a pentachlorophenol-degrading bacterial culture found that half-life of 2,4-DCP in aerobic and anaerobic conditions were 125 and 430 hours, respectively.

#### 2.4.2 2,4-DCP in pulp and paper mill wastewater

2,4-DCP is one of chlorinated phenolic compounds that is among the most abundant recalcitrant wastes produced by the pulp and paper industry. It has been produced from pulp and paper making as a by-product of the chlorine pulp bleaching process to remove colored lignin constituents and to obtain white paper (Pera-Titus et al., 2004; Williams et al., 1996). 2,4-DCP was found in aeration pond, treating pulp and paper mill wastewater in Selenga at 2.38 mg/l (Batoev et al., 2005). Biological treatments can only remove small amounts of 2,4-DCP and require long residence time due to its toxicity (Bayarri, González et al., 2007; Kaigi et al., 2005; Uysal and Türkman, 2005). Previous studies have proved that 2,4-DCP is toxic to biodegradation that need long reaction time as follow

Leuenberger et al. (1985) reported treatment of 2,4-DCP in wastewater effluents of a Swiss pulp mill by activated sludge and found that process could remove 2,4-DCP (7.1 µg/l) at 27% within 12 h.

Atuanya, Purohit, and Chakrabarti (2000) studied treatment of 2,4-DCP synthetic wastewater using up-flow anaerobic sludge blanket (UASB) and aerobic suspended growth (ASG) reactor and found that 2,4-DCP (0.05-0.1 g/l) was degraded to the extent of 52% and 78% in UASB and ASG reactor, respectively, at organic loading rates of 0.18 kg/m<sup>3</sup>/day after retention time of 26.4 h in the presence of glucose (0.35 mg/l).

Yang, Wu, and Kong (2002) investigated biodegradation of 2,4-DCP by marine diatom *Skeletonema costatum*. Exponential phase *S. costatum* cells were inoculated into f/2 medium of 100 ml to a cell density of  $5 \times 10^4$  cells/ml and 2,4-DCP was added to a final concentration of 6 mg/l. The removal of 2,4-DCP over a 10 day period in the control medium and diatom culture was 45.8% and 65%, respectively, whereas the addition of 75 µM of GSH enhanced the removal of 2,4-DCP to 73.7% in 10 days.

Xiangchun et al. (2003) studied biodegradation of 2,4-DCP (6.86-102.38 mg/l) using a novel air-life bioreactor, with a honeycomb-like ceramic column packed in the inner draft tube as the carrier for immobilization of microbial cells (*Achromobacter* sp. isolated from activated sludge). The reactor could remove 2,4-DCP between 84% and 100% after 110 h.

Quan et al. (2004) reported removal of 2,4-DCP in activated sludge through bioaugmentation. Synthetic wastewater contained 2,4-DCP at 24.7-28.3 mg/l. The system could remove 2,4-DCP with a capacity of 95.4% after 24 h.

Uysal and Türkman (2005) investigated biodegradation of 2,4-DCP by JBR 425 rhamnolipid biosurfactant in activated sludge bioreactor. 2,4-DCP removal efficiency was 99.7-99.8% after 40-46 days, when the initial concentration of 2,4-DCP ranged 30 and 100 mg/l. The removal efficiency of 2,4-DCP decreased up to 32.9% after 47-54 days, when the concentration of 2,4-DCP was increased from 100 to 150 mg/l.

Sahinkaya and Dilek (2006) reported that sequencing batch reactor (RBC) could treat 110 mg/l of 2,4-DCP with completed degradation after 22 h and dominant species in the acclimated mixed culture were *Pseudomonas* sp. and *Pseudomonas stutzeri*.

Wang et al. (2007) studied 2,4-DCP biodegradation in a sequencing batch reactor (SBR). Sludge was obtained from activated sludge of municipal wastewater treatment plant in China. The synthetic wastewater was increased stepwise from 50 to 100 mg/l of 2,4-DCP for 25 days to the end of the operation and contained 1,000 mg/l of glucose. The removal efficiency was 94% after 50 days.

#### 2.4.3 Toxicity of 2,4-DCP

In natural environment conditions, toxicity to microorganisms, 1 mg/l of 2,4-DCP was necessary to inhibit bacterial population growth and reduced total biomass and production of marine zooplankton in Dutch coastal water (Kuiper and Hantsveit, 1984). Matafonova et al (2006) reported that higher concentration of 2,4-DCP were inhibitory to cell growth of *Bacillus* sp. Isolated from an aeration pond in the Baikalak pulp and paper mill (Russia).



For toxicity to aquatic organisms, the examples, Gersich and Milazzo (1988) reported that survival, reproduction and growth were all reduced in *Daphnia magna* exposed to 1.48 mg/l of 2,4-DCP in long-term (21 days) static renewal tests. 10-30 mg/l of 2,4-DCP inhibited the initial growth of algae *Chlorella* VT-1 with an LD<sub>50</sub> of 22.5 mg/l (both respiration and photosynthesis) investigated by Scragg, Spiller, and Morrison (2003). Furthermore, Zhang et al (2004) found that the activity of glutathione in freshwater fish (*Carassius auratus*) was inhibited when exposed 0.005-1.0 mg/l of 2,4-DCP for 40 days. Sahinkaya and Dilek (2009) also found that the presence of 2,4-DCP caused some physiological changes in the cell of algae *Chlorella vulgaris*.

In the case of toxicity to animals, a 2-year carcinogenicity study on 2,4-DCP, male rats exposed 250 mg/kg body weight to induce mean body weights were reduced and mean food consumption was also reduced (United State Department of Health and Human Services, National Toxicology Programme [NTP], 1988). Boutwell and Bosch (1959) studied the tumour-promotion action of 2,4-DCP for 24 weeks and found that 2,4-DCP had a tumour-promoting action in mice. Moreover, Amer and Aly (2001) studied genotoxic effect of 2,4-DCP in Swiss mice and found that 180 mg/kg body weight of 2,4-DCP induced a significant percentage of chromosome aberrations and sperm head abnormalities.

In addition, the general population may be exposed to 2,4-DCP through ingestion of food contaminated with the compounds to cause burning sensation, abdominal pain, laboured breathing, convulsions, tremor, weakness and shock or collapse (International Program on Chemical Safety (IPCS) and the Commission of the European Communities (CEC), 2004: online). Furthermore, Bukowska et al. (2007) also studied the effect of 2,4-DCP on human erythrocytes and reported that 2,4-DCP induced an increase in the concentration- and time- dependent 6-carboxy-2',7'-dichlorodihydrofluorescein diacetate (H<sub>2</sub>DCFDA) in erythrocytes and confirmed its toxic effect of 2,4-DCP on human erythrocytes.



## 2.5 Principles of Photocatalysis

Heterogeneous photocatalytic process is one of the Advanced Oxidation Processes (AOPs). This process involves the use of  $\text{TiO}_2$  as a catalyst and ultraviolet light (UV) as irradiation source for degradation of pollutants in water.

### 2.5.1 The nature of light

Usually, light is taken to mean electromagnetic radiation in the visible, near-ultraviolet, and near-infrared spectral range. In the wave model, electromagnetic radiation is characterized by a wavelength ( $\lambda$ ), a frequency ( $\nu$ ) and a velocity ( $c$ ). The three quantities are related by the equation as follow

$$\lambda\nu = c \quad , \quad (1)$$

whereas  $\lambda$  and  $\nu$  may cover a wide range of values and the value of  $c$  is constant ( $2.998 \times 10^8 \text{ ms}^{-1}$  in vacuum). The SI units for  $\lambda$  and  $\nu$  are meter and hertz, respectively. The electromagnetic spectrum encompasses a variety of types of radiation from  $\gamma$ -rays to radio waves, distinguished by their wavelength (or frequency) as shown in Figure 2.5 (Rubin, 2007: online). Ultraviolet light (UV) occurs at wavelength between 100 and 400 nm, whereas visible light occurs between 400 and 700 nm. In photochemistry, we are concerned with the region ranging from 100 to 1000 nm ( $3 \times 10^{15}$  to  $3 \times 10^{14}$  Hz) (Scandola and Balzani, 1989).

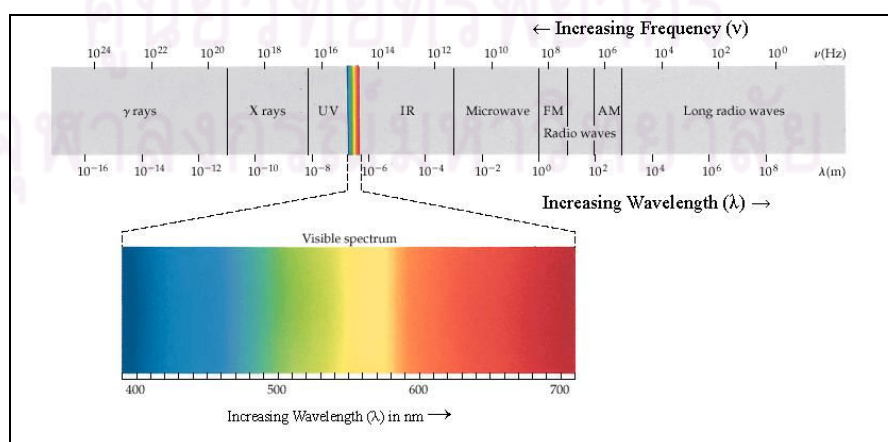


Figure 2.5 Spectrum of electromagnetic radiation (Rubin, 2007)

In the quantum model, a beam of radiation is regarded as a stream of photons or quanta. A photon has no mass but it has a specific energy (E) related to the frequency of the radiation ( $\nu$ ) by the Planck relation as follow

$$E = h\nu \quad , \quad (2)$$

where h is Planck 's constant ( $6.63 \times 10^{-34}$  J.s). From equation (1) and (2), it follows that the photon energy is  $1.99 \times 10^{-18}$  and  $1.99 \times 10^{-19}$  J, respectively, for light of 100 and 1000 nm. This picture of light as made up of individual photons is essential to photochemistry (Scandola and Balzani, 1989).

Ultraviolet light, better known as UV, is one energy region of the electromagnetic spectrum. In this spectrum, UV lies between visible light and X-rays. UV is invisible to humans but may be seen by some animals and insects. The shorter the wavelength, the greater the energy is produced, hence UV has less energy than the X-rays region and more than visible light. The UV region is made up of three major areas including UV A, UV B, and UV C as follow

UV A (long wave or black light): wavelength rang of 400-315 nm

UV B (medium wave): wavelength rang of 315-280 nm

UV C (short wave): wavelength rang of 280-200 nm.

Vacuum UV has wavelength less than 200 nm. It is absorbed strongly by air and is used in a vacuum (Wikipedia, 2008: online). UV light, which has wavelength shorter than 380 nm, is applied in photocatalysis for organic degradation because it has energy more than band gap of  $\text{TiO}_2$ . The solar radiation, that reaches the earth's surface, about 10% is UV light (Cunningham, Cunningham, and Saigo, 2007). Consequently, UV lamps are used as the excitation light source.

### 2.5.2 Photocatalyst

Semiconductors used as a photocatalyst should be an oxide or sulfide of metals, such as  $\text{TiO}_2$ , CdS, ZnO and ZnS, etc., because electron of metal in valence band (VB) can move to conduction band (CB) by appropriated energy of light, which

is higher or equal to the band gap (Robertson, 1996). The common properties of several semiconductors are shown in Table 2.4.

TiO<sub>2</sub> is a popular photocatalyst because the band gap is considerably high around 3.2 eV. It can be activated in the near ultraviolet light (~ 380 nm). Other types of semiconductors that can be used as a photocatalyst, such as ZnO or CdS, etc., may not be applicable because a toxic Zn<sup>2+</sup> is found (De Lasa, Dogu, and Ravella, 1992). CdS also has the toxicity problem because of CdS photocorrosion (Reutergardh and Iangphasuk, 1997), whereas TiO<sub>2</sub> is more stable and insoluble in aqueous solution than ZnO and CdS. It is shown that TiO<sub>2</sub> does not lose its activity, when is reused (De Lasa et al., 1992). Apart from highly corrosive resistance, furthermore it is non toxic substance, relative inexpensiveness and high level of activity (Kaneko and Okura, 2002). There are three crystalline forms of TiO<sub>2</sub> as anatase, rutile and brookite. Anatase is the preferred form used as a catalyst and catalyst support. Moreover, anatase typically has a higher surface area than rutile and is observed to be active and stable over long irradiation time (Cheng, Tsai, and Lee, 1995).

Table 2.4 Band positions of some common semiconductor photocatalyst

Semiconductors	Valence band (eV)	Conductance band (eV)	Band gap (eV)	Band gap wavelength (nm)
TiO <sub>2</sub>	+3.1	+0.1	3.2	380
SnO <sub>2</sub>	+4.1	+0.3	3.9	318
ZnO	+3.0	-0.2	3.2	390
ZnS	+1.4	-2.3	3.7	336
WO <sub>3</sub>	+3.0	+0.2	2.8	443
CdS	+2.1	-0.4	2.5	497
CdSe	+1.6	-0.1	1.7	730
GaAs	+1.0	-0.4	1.4	887
GaP	+1.3	-0.1	2.3	540

Source : Robertson, 1996

### 2.5.3 Mechanism of photocatalytic reaction

The mechanism of photocatalysis is based on the activation of a semiconductor ( $\text{TiO}_2$ ) by light (UV).  $\text{TiO}_2$  can act as sensitizers for light-reduced redox processes because of their electronic structure, which is characterized by a filled valence band and an empty conduction band (Nair, Luo, and Heller, 1993). When a photon with an energy ( $\lambda < 385 \text{ nm}$ ) of  $h\nu$  matches or exceeds the band gap energy ( $E_g$ ) of  $\text{TiO}_2$ , an electron ( $e^-_{\text{CB}}$ ) is excited from the valence band (VB) into the conduction band (CB) leaving a hole ( $h^+_{\text{VB}}$ ) in the valence band (equation (3)) occurring electron-hole pairs on the surface of  $\text{TiO}_2$  (Figure 2.6, (A)) (Chen et al., 2004). These charge carriers can migrate rapidly to the surface of catalyst particles where they are ultimately trapped and poised to undergo redox chemistry with suitable substrates. The valence band hole ( $h^+_{\text{VB}}$ ) is shown to be powerful oxidant (Harvey, Rudham, and Ward, 1983), whereas the conduction band electron ( $e^-_{\text{CB}}$ ) can act as reductants (Bahnemann, Henglein, and Spannel, 1984).

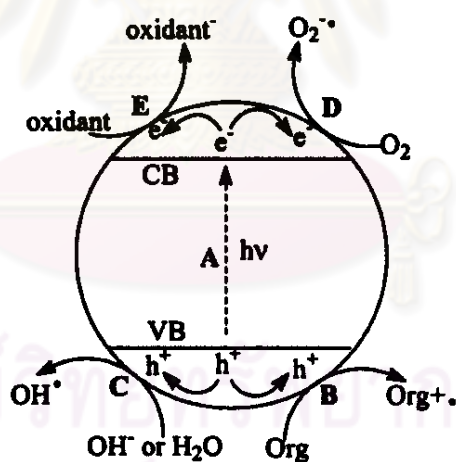
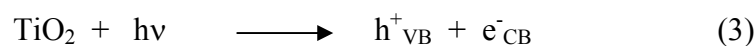


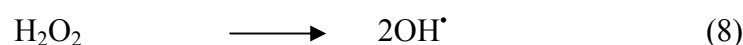
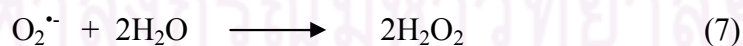
Figure 2.6 The schematic diagram of initial charge transfer pathway for  $\text{TiO}_2$  photocatalytic degradation of organic pollutants (Chen et al., 2004)

The oxidation reaction is more important in photocatalytic degradation because it is the main reaction for organic pollutant degradation. There are two possible mechanisms as direct hole oxidation and hydroxyl radical ( $\text{OH}^\bullet$ ) oxidation (Ilisz and Dombi, 1999). For the direct hole oxidation, the photohole slightly reacts

directly with the adsorbed organic molecules to produce organic radical cation (Figure 2.6, (B)). While, the photohole reacts with adsorbed water or surface hydroxyl group ( $\text{OH}^-$ ) to produce hydroxyl radical species ( $\text{OH}^\bullet$ ) (Figure 2.6, (C)). The hydroxyl radical ( $\text{OH}^\bullet$ ) is formed on the surface of  $\text{TiO}_2$  as follow equation (4)-(5) (De Lasa et al., 1992).



In the absence of suitable electron and hole scavengers, the stored energy is dissipated within a few nanoseconds by recombination (Boer, 1990). If a suitable scavenger or surface defect state is available to trap the electron or hole, recombination is prevented and subsequent redox reaction may occur. The recombination between electron and hole must be avoided because it inhibits the oxidation reaction. Adding some electron scavengers, such as oxygen molecule, etc., can delay the recombination since it can trap the conduction band electron out from the positive hole and transform into superoxide radical anion ( $\text{O}_2^{\bullet-}$ ) (Figure 2.6, (D)) and lead to the additional formation of hydroxyl radical ( $\text{OH}^\bullet$ ) as follow equation (6)-(8) (Litter, 1999). Furthermore, as reported by De Lasa et al. (1992), it has been pointed out that both  $\text{H}_2\text{O}$  and  $\text{O}_2$  are essential species in the photocatalytic process. Other oxidants such as polyoxometalates can also trap conduction band electrons (Figure 2.6, (E)).



This hydroxyl radical ( $\text{OH}^\bullet$ ) has high oxidation potential (2.8 V), so normally hydroxyl radical ( $\text{OH}^\bullet$ ) oxidation tends to be the main mechanism in the photocatalytic oxidation. It can react rapidly and non-selectively with most organic compounds on the catalyzing surface and mineralizes them to carbon dioxide ( $\text{CO}_2$ ), water ( $\text{H}_2\text{O}$ ) and other inorganic compounds (De Lasa et al., 1992).

## 2.6 The Langmuir-Hinshelwood Kinetics

Heterogeneous photocatalysis onto TiO<sub>2</sub>, a reaction occurring on a surface may usually be regarded as involving five consecutive steps following

- (1) Diffusion of reactants to the surface
- (2) Adsorption of the reactants onto the surface
- (3) Reaction at the surface (degradation)
- (4) Desorption of products from the surface
- (5) Diffusion of the products away from the surface

Usually, step (1) and (5) are very fast, thus the rate determining steps in any heterogeneous reaction is likely to involve step (2), (3) or (4) (Pichat and Herrmann, 1989). The Langmuir-Hinshelwood model was initially developed to quantitatively describe gaseous-solid reactions. This model was recently employed to describe solid-liquid reactions for photodegradation of pollutants by UV/TiO<sub>2</sub>. The reactions occur on a surface of TiO<sub>2</sub>. In this model, the reaction rate ( $r$ ) (mg/l min<sup>-1</sup>) is proportional to the fraction of surface covered by the substrate ( $\theta$ ) (mg/mg) as follow

$$r = \frac{-dC}{dt} = k\theta \quad (9)$$

Considering Langmuir's equation

$$\theta = \frac{KC}{(1 + KC)}, \quad (10)$$

$$r = -\frac{dC}{dt} = \frac{kKC}{(1 + KC)}. \quad (11)$$

Since  $k$  is the true rate constant (mg/l min<sup>-1</sup>) which takes into account several parameters, such as the catalyst's mass, efficient photon flow and O<sub>2</sub> layer, etc.  $K$  is the constant of adsorption equilibrium of the substrate onto the TiO<sub>2</sub> particles (l/mg). In photocatalytic studies, the value of  $K$  is obtained empirically through a kinetic



study in the presence of light and is better than that obtained in the darkness, starting from Langmuir's isotherm.  $C$  is the concentration of the organic substrate (mg/l) at any time  $t$ . Integration of equation (11) yields equation (12) as

$$\ln\left(\frac{C_0}{C}\right) + K(C_0 - C) = kKt, \quad (12)$$

where  $C_0$  is the initial concentration of the organic substrate (mg/l) and  $t$  is the irradiation time (min). Equation (11) will be of zero order, when the concentration  $C$  is relatively high,  $KC \gg 1$ , in which case the reaction rate will be maximal as

$$r = k. \quad (13)$$

Equation (12) can also be simplified to a zero order reaction, when the  $C_0$  concentration is very high, in which case one has

$$(C_0 - C) = kt. \quad (14)$$

When the solution is highly diluted, the term  $KC$  becomes  $\ll 1$ , the denominator of equation (11) is neglected and the reaction is essentially an apparent first order reaction as follow

$$r = kKC = k_{ap}C, \quad (15)$$

where  $k_{ap}$  is the apparent rate constant of a pseudo first order reaction ( $\text{min}^{-1}$ ). Thus, equation (12) can be simplified to a first order reaction, when  $C_0$  is very small, in which case one has

$$\ln\left(\frac{C_0}{C}\right) = kKt = k_{ap}t. \quad (16)$$

By plotting  $\ln(C_0/C)$  versus  $t$ , the apparent rate constant ( $k_{ap}$ ) can be determined from the slope of the curve obtained (equation (16)) and the initial degradation rate ( $r_0$ ) ( $\text{mg/l min}^{-1}$ ) can be represented as presented in equation (17) (Konstantinou and Albanis, 2004; Kumar, Porkodi and, Rocha, 2008; Valente, Padilha, and Florentino, 2006).

$$r_0 = k_{ap} C_0 \quad (17)$$

## 2.7 The Related Research

### 2.7.1 Treatment of lignin by photocatalytic process (UV/TiO<sub>2</sub>)

Tanaka et al. (1999) demonstrated using ligninsulfonic acid sodium salt (coniferous wood lignin) as lignin for photocatalyzed degradation in the degradation experiment 0.1 to 2.0 g of TiO<sub>2</sub> (anatase), which was suspended in 300 ml of 0.003 to 0.03% aqueous solution of lignin in a cylindrical reaction vessel. A 100 W ( $\lambda < 310$  nm) super-high pressure mercury lamp was placed in the center of the vessel. The degradation rate decreased as the amount of TiO<sub>2</sub> increased. Whereas, the time required for the complete transformation was shortened by the increase in the amount of TiO<sub>2</sub>. These contradictory results may be due to the large desorption of lignin upon illumination. The result from FTIR and NMR measurement showed that the aromatic ring degrades faster than the aliphatic chain. In GPC, a peak is centered around 2630 of molecular weight. By illumination, the peak shifted toward lower molecular and decreasing in the peak area, indicating that lignin molecule was depolymerized. In the transformation process, lignin was polymerized in the beginning and then converted to smaller molecule successively. Aliphatic intermediates, such as formic acid, acetic acid, glycolic acid and formaldehyde, etc., were formed from the early stage of degradation.

Ksibi et al. (2003) investigated the treatment of lignin from alfalfa black liquor digestion by the photocatalytic degradation (UV/TiO<sub>2</sub> (suspended)) of lignin effluent, which was obtained by the precipitation of black liquor from pulp and paper mill in Tunisia. The degradations were carried out at 293 °K using 1,000 ml of lignin solution and 1 g of TiO<sub>2</sub> (Degussa P-25). Pyrex reactor open to air was utilized for all

experiments with a plunging tube containing a Philips HPK 125 W lamp. The results were found that photolysis reduced lignin at pH 8.2 about 3.3% within 420 min. Whereas, photocatalysis can remove lignin about 56% using 90 mg/l of lignin solution in the same time and can deteriorate chromophors groups of lignin. The COD removal by photocatalytic degradation of lignin solution could be achieved when lignin is used at low concentration. The COD removal reached 81% for the lignin initial concentration of 39.4 mg/l in 420 min. Under the condition of lignin initial concentration of 90 mg/l, initial pH of 8.2 and 1 g of TiO<sub>2</sub>, the reduction in the optical density with time from OD<sub>280</sub> as 0.94 to 0.28 in 420 min with a capacity of 70.%. This gradual reduction of the intensity of the absorption proved that deterioration of chromophors groups of the lignin occurred. The products of lignin photocatalytic degradation were analysed by GC-MS, such as coniferylic alcohol, syringaldehyde, vanillin and palmitic acid, etc.

Chang et al. (2004) explored on applying the photochemical UV/TiO<sub>2</sub> oxidation process to treat the synthetic lignin-containing wastewater for dissolved organic carbon (DOC), color of lignin (ADMI) and reducing A254 (the absorption at the wavelength of 254 nm). The working volume of reactor was 400 cm<sup>3</sup>. The reactor was completely mixed with magnetic stirring and surrounded by 16 vertical UV lamps at out put energy of 35 W. The oxidation process was carried out with addition of 1 g/l of TiO<sub>2</sub> (Degussa P25) at five different pH levels (3, 5, 7, 9 and 11). The process was then repeated at pH 7 using five different TiO<sub>2</sub> dosages (1, 5, 10, 20 and 30 g/l) to obtain the optimal TiO<sub>2</sub> dosage. The combined UV/TiO<sub>2</sub> treatment can achieve better removal of DOC and color than the UV treatment alone. More color removal efficiencies were observed with samples of lower pH levels. The ultimate color removal efficiencies were 99% (pH 3), 92% (pH 5), 64% (pH 7), 42% (pH 9) and 21% (pH 11) with 1 g/l of TiO<sub>2</sub> within 960 min. At the optimum dosage of 10 g/l of TiO<sub>2</sub> at pH 7, the removal efficiency of both color and DOC was close to 88% within 960 min as well as 10 g/l of TiO<sub>2</sub> was the optimum dosage for maximum reduction of A254. Under optimum dosage of 10 g/l of TiO<sub>2</sub>, the first order rate constant for color, DOC and A254 were 0.0018, 0.0016 and 0.0015 min<sup>-1</sup>, respectively.

Dahm and Lucia (2004) studied the photodegradation of dissolved lignin in a water medium resulting from TiO<sub>2</sub> photocatalysis reactions that were conducted in a batch system. Rutile TiO<sub>2</sub> was used in all reactions. Approximately 0.02 g of REPAP

lignin was placed in 15 ml of 0.05 M NaOH for 3 min. The lignin samples were magnetically stirred throughout irradiation with 64-128 W corresponded to a light intensity range of 223-445 mW/cm<sup>2</sup>. However, it was determined that irradiation in the absence of the catalyst allowed for only a 4.6% reduction in the dissolved lignin concentration (0.02 g) after 2 hours. 82% decrease in the total lignin concentration was obtained with a 10 mg/l loading of TiO<sub>2</sub> and UV intensity of 445 mW/cm<sup>2</sup>, after 2 hours. An optimal TiO<sub>2</sub> loading of 10 mg/l was determined, and it was found that higher illumination intensities correlated well with higher initial degradation rates and total lignin degradation. At the highest light illumination power of 445 mW/cm<sup>2</sup>, there was a 40% destruction of lignin in 5 min, while at the lower levels of light intensity, it required up to 1 hour.

Portjanskaja and Preis (2007) examined the photocatalytic oxidation (PCO) of UV-irradiated aqueous solution containing lignin on TiO<sub>2</sub> for the influence of ferrous ions. The UV light source, Philips TLD 15 W/05 low-pressure luminescent mercury UV lamp with the emission maximum at 360 nm and providing irradiation of about 0.7 mW/cm<sup>2</sup>. A mechanically agitated with magnetic stirrers were used in the experiments. The synthetic lignin solution was prepared in concentration of 100 mg/l at around pH 8. TiO<sub>2</sub> as Degussa P-25 was attached to the surface of the glass plate (spraying and submersion). The addition of Fe<sup>2+</sup>, up to 2.8 mg/l, to the acidic lignin solution leads to the drastic, for about 25%, increase in PCO efficiency. A further increase in ferrous ion concentration resulted in a decrease in PCO efficiencies of lignin. The highest photocatalytic oxidation efficiency for lignin, up to 9.2 mg/W.h, was observed in neutral and slightly basic media and the acidic media was most favourable for lignin adsorption although are not the best for photocatalytic oxidation. The lignin solution was PCO-treated for the lignin concentration reduced to 50% after 24 hours in neutral media (pH 8). Also, the difference in the PCO performance with a different attachment mode of titanium dioxide on the catalyst support was observed. Sprayed catalyst exhibited 1.5 times higher efficiency than the one attached by submersion.

Ma et al. (2008) investigated photocatalytic degradation of synthetic lignin using TiO<sub>2</sub> (Degussa P-25) and Pt/TiO<sub>2</sub>. Sixteen near ultra-violet lamps (Rayonet Model RPR-200) with the main emission light wavelength around 253.7 nm were provided as the light source for the UV irradiation experiments. The initial

concentration of dissolved organic carbon (DOC) in lignin solution was 251 mg/l. The influent of pH (3, 7 and 11), catalyst dosage (1, 5, and 10 g/l) and illumination on lignin degradation was studied. The results showed that application of UV irradiation alone has almost no effect on the reduction of DOC and color based on American Dye Manufacture Institute value (ADMI). However, the addition of TiO<sub>2</sub> and Pt/TiO<sub>2</sub> reduced the original DOC by more than 40% within 30 min. Either TiO<sub>2</sub> or Pt/TiO<sub>2</sub> enhanced the reaction constant much more in the acidic region than in the alkali region. In addition, too much catalyst addition has not increased the DOC and ADMI reduction proportionally. The Pt-doped TiO<sub>2</sub> removed 55-69% of ADMI when the dosage of Pt/TiO<sub>2</sub> increased from 1 to 10 g/l. Additional of 1 g/l of TiO<sub>2</sub> was appropriate to achieve maximum ADMI removal, additional increase of TiO<sub>2</sub> dosages to 5 and 10 g/l did not significantly reduced the ADMI. TiO<sub>2</sub> dosages exceeding 2g/l caused a shadow effect that inhibited the formation of more OH<sup>•</sup> hence did not improve ADMI removal. The rate constant of pseudo-first order kinetics increased from  $4.1 \times 10^{-3} \text{ min}^{-1}$  (pH 11) to  $4.0 \times 10^{-2} \text{ min}^{-1}$  (pH 3), if 10 mg/l Pt/TiO<sub>2</sub> was applied. The investigation also indicated that the photocatalytic degradation rates could be enhanced 1-6 times faster after doping TiO<sub>2</sub> with Pt in different pH cases.

Kansal et al. (2008) studied the photocatalytic degradation of lignin obtained from wheat straw kraft digestion by using TiO<sub>2</sub> (Titania P-25) and ZnO semiconductors. The photochemical was carried out in double wall reactor vessels in the UV chamber equipped with five tubes each of 30 W (Philips). Constant stirring of solution was ensured by using magnetic stirrers. TiO<sub>2</sub> and ZnO were fixed on to an inert support (pumice stone). The experiments were carried out by varying the catalyst dose (0.5-2.0 g/l), pH of solution (pH 3-11), oxidant concentration as sodium hypochlorite ( $3.06 \times 10^{-6} \text{ M}$  to  $15.3 \times 10^{-6} \text{ M}$ ) and initial concentration of lignin (10-100 mg/l). The result was found that 18% of lignin was adsorbed to ZnO whereas 10% lignin adsorption was observed with TiO<sub>2</sub> after 15 min. The degradation of lignin was favorable at pH 11. Optimum values of catalyst dose and oxidant concentration were found to be 1 g/l and  $2.2 \times 10^{-6} \text{ M}$ , respectively using lignin initial concentration of 100 mg/l at pH 10. Lignin removal efficiency of UV/TiO<sub>2</sub> was about 30% after 5 hours when using 100 mg/l of lignin initial concentration and 1 g/l of TiO<sub>2</sub> at pH 9.7. Under optimum condition (catalyst dose 1 g/l, pH 11 and oxidant concentration  $12.2 \times 10^{-6} \text{ M}$ ), the effective degradation could be achieved when lower concentration of



lignin was used. The complete destruction of lignin was achieved in 45 min with 10 mg/l initial concentration solution.

### 2.7.2 Treatment of 2,4-DCP by photocatalytic process (UV/TiO<sub>2</sub>)

Pandiyan et al. (2002) investigated destruction of 2,4-DCP using photochemical methods. Three kinds of methods were used as direct UV irradiation, UV irradiation with 4 g/l of TiO<sub>2</sub> and UV light with TiO<sub>2</sub> (catalysts) and 0.03 M of ClO<sub>4</sub><sup>-</sup> (oxidants). A 100 W immersion UV lamp equipped with a quartz well and voltage regulator was employed for UV degradation. 1 mM of initial 2,4-DCP concentration was treated at all experiments. The results were found that the reaction rates in decreasing order were UV/TiO<sub>2</sub>/ClO<sub>4</sub><sup>-</sup>>UV/TiO<sub>2</sub>>UV before the 90 min and UV/TiO<sub>2</sub>>UV/TiO<sub>2</sub>/ClO<sub>4</sub><sup>-</sup>>UV after the 90 min. Initially, degradation of compound was rapid, then steadily declined. Photocatalytic degradation of 2,4-DCP was accelerated in the presence of TiO<sub>2</sub> catalyst as indicated by the first order rate constants calculated from the experimental data were  $2.58 \times 10^{-3} \text{ min}^{-1}$  for direct UV irradiation and  $3.87 \times 10^{-3} \text{ min}^{-1}$  for UV/TiO<sub>2</sub>. The pH value of the irradiation solution decreased from 6.5 to 2.7 and the by-products of 2,4-DCP degradation detected corresponded to chlorophenol and phenol.

Bayarri et al. (2005) explored the photocatalytic treatment of 2,4-DCP by using UV/TiO<sub>2</sub> (suspended anatase, Degussa P25). The source of radiation was a Xenon lamp (PHILIPS XOF-15-OF, 1500 W) with a spectrum very close to the solar one in the UV range. The 2,4-DCP solution was prepared to a concentration of 125 ppm, loaded to the reservoir tank from 0.5 to 1.5 liters. Different amounts of TiO<sub>2</sub> from 0 to 2 g/l were added to the system with different initial pH (2, 5.5, 7.5 and 11). The results were found that the removal efficiency of 2,4-DCP was increase with increasing of TiO<sub>2</sub> loading at pH 5.5, a fast degradation can be observed for initial time and later on it decreased due to for higher times, 2,4-DCP had to compete with intermediates for the TiO<sub>2</sub> sites. After 6 h of irradiation with 0.5 g TiO<sub>2</sub> /l, a 90% of 2,4-DCP had disappeared and for the same time, 2,4-DCP degradation was over 99% using 2 g/l of TiO<sub>2</sub>. The intermediate analyzed were 4-chlorophenol and phenol. In all the case using 0.5 g/l of TiO<sub>2</sub>, the pH decreased along the time. The pH of maximum



removal of 2,4-DCP was 2. For pH greater than 5.5, the final 2,4-DCP removal was decreased.

Kusvuran et al. (2005) examined photocatalytic degradation of 2,4-DCP by UV/TiO<sub>2</sub> (anatase). The light source was the mercury vapour UV lamp (UVP-CPQ-7871) with emitted its maxima radiation at 365 nm. The experiments were carried out in a 250 ml cylindrical glass reactor with magnetic stirrer, which contain 0.5 g/l of TiO<sub>2</sub>. The 2,4-DCP solutions were prepared at 0.1-0.5 mM of initial concentration at pH 3. Degradation rate decreased as a adsorption constant increased. Pseudo-first order kinetic rate constants of 2,4-DCP were decreased from 0.0259 (0.1mM) to 0.0061 min<sup>-1</sup> (0.5 mM) with increasing initial concentration. Furthermore, degradation rate constant (k) and adsorption equilibrium constant (K) were calculated as k 0.0031 mMmin<sup>-1</sup> and K 30.52 mM<sup>-1</sup>.

Bayarri, Abellán et al. (2007) studied the effect of each type of radiation as UV-A (300 nm) and UV-ABC (235 nm) for 2,4-DCP degradation by UV/TiO<sub>2</sub>. The source of radiation was a xenon lamp (PHILIPS XOP-15-OF, 1000 W). Solution of 2,4-DCP were prepared from 100-120 mg/l, loaded in the reservoir tank (1 liters) with 0.5 g/l of TiO<sub>2</sub> (Degussa P25). The results demonstrated that UV-ABC radiation was more effective than UV-A. The 2,4-DCP photocatalysis and the TOC removal was about 20% higher with UV-ABC than with UV-A. For the 2,4-DCP photolysis, the observed degradation was about 60% by using UV-ABC, and about 10% when using UV-A radiation. If both UV-ABC and UV-A processes are compared, photocatalytic process is always much faster than the photolytic degradation of 2,4-DCP.

González et al. (2010) investigated degradation of 2,- CP, 2,4-DCP, 2,4,6-TCP and PCP using UV/TiO<sub>2</sub>. Advanced oxidation process was carried out in a batch process using as catalyst anatase TiO<sub>2</sub> in presence of UV in 100 ml solution of 15 mg/l of each CP. All AOPs were carried out in a Pyrex glass vessel magnetically agitated and irradiated with four UV light lamps (Lexmana, at intensity of 25 mW/cm<sup>2</sup>) placed 10 cm away from the vessel and installed inside of an aluminium box. The effect of TiO<sub>2</sub> amount on CP degradation was determined at 5, 10 and 20 mg/l of TiO<sub>2</sub> (Degussa). The process was carried out during 180 min at room temperature and 150 rpm of magnetic stirrer. During the AOPs, the removal initial rate increased in the following order 2-CP>2,4,6-TCP>2,4-DCP>PCP and the obtained degradation rang from 82% to 24%. For 2,4-DCP, it was observed for all

case that an increase in catalyst (0-20 mg/l) cause an increase in the removal initial rate from 0.0180 to 0.0361 mg/l.h, after 180 min at initial pH 4.5. When using 10 mg/l and 20 mg/l of  $\text{TiO}_2$  at pH 4.5, 2,4-DCP removal efficiency was around 60% and 75%, respectively in the same time.



ศูนย์วิทยทรัพยากร  
จุฬาลงกรณ์มหาวิทยาลัย

## CHAPTER III

### METHODOLOGY

#### 3.1 Chemicals

All chemical substances used in this research were analytical grade. Aqueous solutions were prepared from using ultra pure de-ionized water with a resistivity of  $18.2 \text{ M}\Omega \text{ cm}^{-1}$  from PURELAB Maxima, ELGA.

##### 3.1.1 Supervibration-photocatalytic reactor

Name	Formula	Company
Phosphoric acid (A.R.)	$\text{H}_3\text{PO}_4$	Aldrich
Hydrogen peroxide (A.R.)	$\text{H}_2\text{O}_2$	Aldrich
Hydrofluoric acid (A.R.)	HF	Aldrich
Sulfuric acid (96%)	$\text{H}_2\text{SO}_4$	LAB-SCAN

##### 3.1.2 pH adjustment

Name	Formula	Company
Sulfuric acid (96%)	$\text{H}_2\text{SO}_4$	LAB-SCAN
Sodium hydroxide	NaOH	CARLO ERBA

##### 3.1.3 Lignin measurement

Name	Formula	Company
Lignosulfonic acid sodium salt	-	Aldrich
Folin-Ciocalteu's reagent	-	CARLO ERBA
Sodium carbonate	$\text{Na}_2\text{CO}_3$	Univar
Sodium tartrate	$\text{Na}_2\text{C}_4\text{H}_4\text{O}_6 \cdot 2\text{H}_2\text{O}$	Ajax

## 3.1.4 Identification of by-products of lignin degradation

Name	Formula	Company
Hydrochloric acid (37%)	HCl	LAB-SCAN
Ethyl acetate (A.R.)	CH <sub>3</sub> COOCH <sub>2</sub> CH <sub>3</sub>	LAB-SCAN
<i>N,O</i> -bis(trimethylsilyl) trifluoroacetamide (BSTFA) (≥99%)	CF <sub>3</sub> C[=NSi(CH <sub>3</sub> ) <sub>3</sub> ]OSi(CH <sub>3</sub> ) <sub>3</sub>	Aldrich
Trimethylchlorosilane (TMCS) (≥99%)	(CH <sub>3</sub> ) <sub>3</sub> SiCl	Aldrich
Chloroform (A.R.)	CHCl <sub>3</sub>	LAB-SCAN

## 3.1.5 Color measurement

Name	Formula	Company
Potassium hexachloroplatinate	K <sub>2</sub> PtCl <sub>6</sub>	Panreac
Cobaltous chloride	CoCl <sub>2</sub> ·6H <sub>2</sub> O	Univar
Hydrochloric acid (37%)	HCl	LAB-SCAN
Sodium hydroxide	NaOH	CARLO ERBA

## 3.1.6 2,4-DCP measurement

Name	Formula	Company
2,4-DCP (99%)	C <sub>6</sub> H <sub>4</sub> Cl <sub>2</sub> O	Aldrich
Methanol (HPLC grade)	CH <sub>3</sub> OH	LAB-SCAN
Acetonitrile (HPLC grade)	C <sub>2</sub> H <sub>3</sub> N	LAB-SCAN
Sulfuric acid (96%)	H <sub>2</sub> SO <sub>4</sub>	LAB-SCAN

## 3.1.7 Identification of by-products of 2,4-DCP degradation

Name	Formula	Company
Hydrochloric acid (37%)	HCl	LAB-SCAN
Sodium sulfate	Na <sub>2</sub> SO <sub>4</sub>	CARLO ERBA

### 3.2 Experimental Instruments

- 3.2.1 Supervibration-photocatalytic reactor 25 liters
- 3.2.2 HDPE cylindrical tank with cover 28 liters: Nalgene
- 3.2.3 Clock timer
- 3.2.4 Brown glass bottles 10, 20 and 50 ml
- 3.2.5 pH meter: HORIBA
- 3.2.6 Plastic rectangular tank 20 liters
- 3.2.7 Vacuum pump and microfilter units: SIBATA
- 3.2.8 Ultrasonic cleaners: CREST
- 3.2.9 Analytical balance
- 3.2.10 Spatula
- 3.2.11 Magnetic stirrer and magnetic bar
- 3.2.12 Glass rod
- 3.2.13 Desiccator
- 3.2.14 Volumetric flasks 10, 25, 50, 100, 500 and 1,000 ml
- 3.2.15 Beakers 50, 100, 250, 600 and 1,000 ml
- 3.2.16 Pipettes 5, 10, 25 ml and dropper
- 3.2.17 Dispensing bottle
- 3.2.18 Measuring cylinder 100 ml
- 3.2.19 Nylon membrane filters 0.45  $\mu\text{m}$ , 47 mm: FILTREX
- 3.2.20 PTFE membrane filters 0.45  $\mu\text{m}$ , 47 mm: MUNKTELL
- 3.2.21 Glass microfiber filters GF/C, 47 mm and 110 mm: Whatman
- 3.2.22 Buchner funnel 47 mm, 110 mm and suction flask 250 ml, 1000 ml
- 3.2.23 Forceps
- 3.2.24 Nylon syringe filters 0.45, 13 mm: FILTREX
- 3.2.25 Disposal syringe 3 ml: NIPRO
- 3.2.26 Clear glass vial kit 2 ml: Varian
- 3.2.27 Micropipette 1,000  $\mu\text{l}$ : Nichiryo and pipette tip 1,000  $\mu\text{l}$ : BIOLINE
- 3.2.28 Micropipette 10 ml and pipette tip 10 ml: Rainin
- 3.2.29 An 85  $\mu\text{m}$  polyacrylate (PA) fiber and a SPME fiber holder: Supelco
- 3.2.30 UV-Visible spectrophotometer: Model Helios Alpha, Thermo Electron

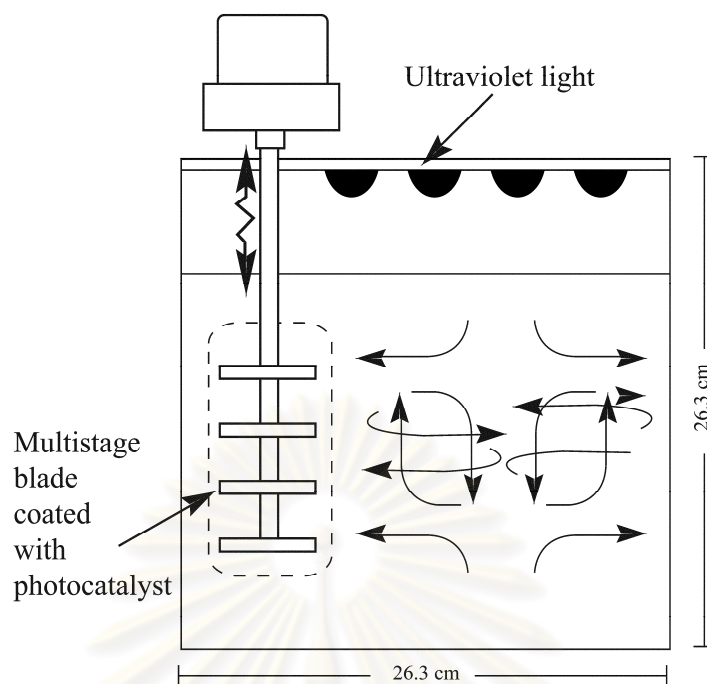
3.2.31 High performance liquid chromatography (HPLC): Varian Prostar with Auto sampler Model 400, pump Model 230, Varian HPLC column C 18 (4.6 mm internal diameter  $\times$  250 mm) holder with guard column and UV-Visible detector Model 325

3.2.32 Gas chromatography-mass spectrometer (GC-MS): Agilent 6890 N Network GC system with ZB-5MS capillary column (30 m  $\times$  0.25 mm internal diameter, 0.25  $\mu$ m film thickness) (Phenomenex) and HP-5 capillary column (30 m  $\times$  0.25 mm internal diameter, 0.25  $\mu$ m film thickness) (J & W Scientific), interfaced with Agilent 5973 N Network Mass Selective detector

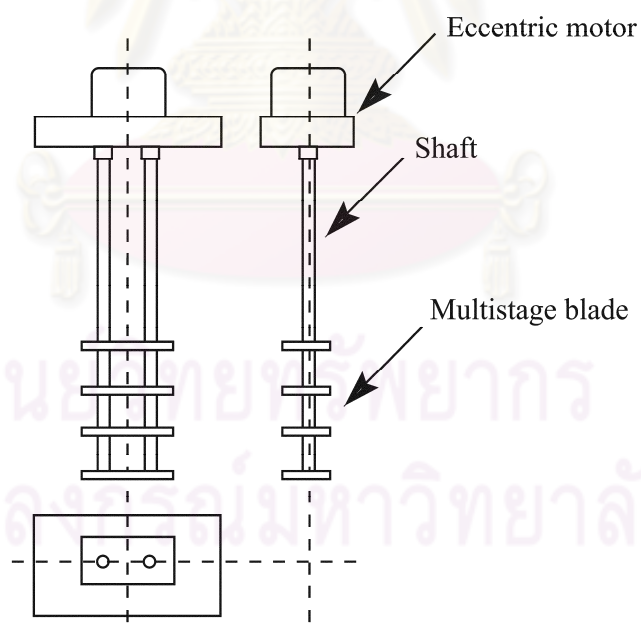
### 3.3 Experimental Set-Up

The experiments were conducted in laboratory scale. The supervibration-photocatalytic reactor, developed in this study, is based on the photocatalytic process combined with a supervibration agitator in order to provide faster reaction and higher efficiency of degradation rate. The schematic diagrams of the supervibration-photocatalytic reactor including an agitated tank, a supervibration agitator and an ultraviolet light source and the supervibration agitator containing an eccentric motor, a shaft and multistage blade are shown in Figure 3.1. All experiments were carried out in batch-mode operation using a rectangular reactor of 26.3  $\times$  36.2  $\times$  26.3 cm<sup>3</sup> with 25 liters capacity, made of stainless steel. The supervibration equipment consists of a set of four multistage blades with each size of 5 cm  $\times$  8 cm  $\times$  1 mm. Micro-structured TiO<sub>2</sub> film with thickness of approximately 1  $\mu$ m as photocatalyst coated on the surface of the multistage blade (titanium plate) was produced by low-voltage electrochemical anodization method of titanium plate, described by Xie and Li. (2006). The plate oxidation was conducted in a dual-electrode reaction chamber, in which the titanium plate was used as the anode and a stainless steel plate of the same size was used as the cathode. Both electrodes were submerged in a mixture of electrolyte solution (H<sub>2</sub>SO<sub>4</sub> (1.0 M)-H<sub>3</sub>PO<sub>4</sub> (0.3 M)-H<sub>2</sub>O<sub>2</sub> (0.6 M)-HF (0.03 M)) and a direct-current source was used to provide electric current (150-200 V) between electrodes.





(a)



(b)

Figure 3.1 The schematic diagrams of the supervibration-photocatalytic reactor (a) and the supervibration agitator (b)

TiO<sub>2</sub> film produced by electrolytic oxidation shows good adhesion to the support (Yerokhin et al., 1999), whereas TiO<sub>2</sub> film, attached mechanically, may be unstable (Portjanskaja and Preis, 2007). The illumination was provided using four low-pressure 6 W mercury lamps (Philip TUV-G6T5, 254 nm), which were attached at the top cover of the agitated vessel. The vertical vibration generated from eccentric motor is transferred to the multistage blade through the shaft and the generated vibrational energy is converted to fluid energy. Consequently, this agitator generates a powerful 3-dimensional agitating flow in the tank and the flow rate produced by the supervibration agitator is higher than that produced by the conventional rotary pump in the same condition of the electrical power source.

### **3.4 Experimental Procedures**

In this study, the experiments were divided into two major sections

#### **3.4.1 Experimental run using synthetic wastewater**

The experiments in this section were carried out with synthetic wastewater, in order to study the performance of supervibration-photocatalytic reactor on treatment of lignin and 2,4-DCP, to obtain the optimum operating conditions and study the reaction kinetics of lignin and 2,4-DCP photocatalytic degradation as well as identify the by-products of lignin and 2,4-DCP degradation. Furthermore, removal efficiency of color under the optimum treatment conditions was also investigated.

##### **3.4.1.1 Synthetic wastewater**

Synthetic wastewater was prepared in laboratory including lignin synthetic wastewater (lignosulfonic acid sodium salt), 2,4-DCP synthetic wastewater and mixed synthetic wastewater containing lignin and 2,4-DCP.

### 3.4.1.2 Experimental methods for synthetic wastewater

The synthetic wastewater at all concentrations was prepared using 15.2 MΩ cm<sup>-1</sup> de-ionized water and then pH was adjusted with NaOH (1 N) and H<sub>2</sub>SO<sub>4</sub> (1 N). The temperature of synthetic wastewater was kept at room temperature (30 °C). Sampling point was set at a center of middle layer in tank. The effluent samples were taken at 15, 30, 60, 90, 120, 180, 300 and 420 min of reaction time for lignin and color analysis on a UV-Visible spectrophotometer and 2,4-DCP analysis on HPLC.

Treatment efficiencies of lignin and 2,4-DCP by supervibration-photocatalytic reactor were studied under different initial pH, UV intensity, vibration frequency and initial concentration as presented in Table 3.1 and experimental conditions are shown in Table 3.2. The reaction kinetics of lignin and 2,4-DCP photocatalytic degradation were studied using Langmuir-Hinshelwood model. The by-products of lignin and 2,4-DCP photodegradation were also identified by analysis of photodegradation products using GC-MS. Furthermore, under the optimum treatment conditions, removal efficiency of color was also investigated.

Table 3.1 The experimental factors of synthetic wastewater

Factors	Values
The effect of initial pH	5, 6, 7, 8, 9
The effect of UV intensity (mW/cm <sup>2</sup> )	0, 6.3, 12.6, 25.2
The effect of vibration frequency (Hz)	0, 20, 30, 40, 50
The effect of initial lignin concentration (mg/l)	100, 200, 300, 400
The effect of initial 2,4-DCP concentration (mg/l)	0.5, 1, 2.5, 5

Table 3.2 Experimental conditions of synthetic wastewater

Synthetic wastewater samples	Experiments	Initial concentration (mg/l)	Initial pH	UV intensity (mW/cm <sup>2</sup> )	Vibration frequency (Hz)	
Lignin synthetic wastewater	1	400	5	6.3	30	
		400	6	6.3	30	
		400	7	6.3	30	
		400	8	6.3	30	
		400	9	6.3	30	
	2	400	Optimum from exp.1	0	30	
		400		12.6	30	
	3	400	Optimum from exp.1	Optimum from exp.2	0	
		400			20	
		400			40	
		400			50	
	4	100	Optimum from exp.1	Optimum from exp.2	Optimum from exp.3	
		200				
		300				
	5	Optimum from exp.4	Optimum from exp.1	25.2	Optimum from exp.3	
	2,4-DCP synthetic wastewater	6	5	5	6.3	30
			5	6	6.3	30
5			7	6.3	30	
5			8	6.3	30	
5			9	6.3	30	
7		5	Optimum from exp.6	0	30	
		5		12.6	30	
8		5	Optimum from exp.6	Optimum from exp.7	0	
		5			20	
		5			40	
		5			50	
9		0.5	Optimum from exp.6	Optimum from exp.7	Optimum from exp.8	
		1				
		2.5				
10		Optimum from exp.9	Optimum from exp.6	25.2	Optimum from exp.8	

Table 3.2 Experimental conditions of synthetic wastewater (continuous)

Synthetic wastewater samples	Experiments	Lignin : 2,4-DCP ratio	Initial pH	UV intensity (mW/cm <sup>2</sup> )	Vibration frequency (Hz)
Mixed synthetic wastewater containing lignin and 2,4-DCP	11	400 : 5	5	6.3	30
		400 : 5	6	6.3	30
		400 : 5	7	6.3	30
		400 : 5	8	6.3	30
		400 : 5	9	6.3	30
	12	400 : 5	Optimum from exp.11	0	30
		400 : 5		12.6	30
	13	400 : 5	Optimum from exp.11	Optimum from exp.12	0
		400 : 5			20
		400 : 5			40
		400 : 5			50
	14	400 : 5	Optimum from exp.11	25.2	Optimum from exp.13

### 3.4.2 Experimental run using real wastewater

The experiments in this part were carried out with real wastewater, in order to study the performance of supervibration-photocatalytic reactor on treatment of lignin and 2,4-DCP, to obtain the optimum operating conditions. Moreover, removal efficiency of color under the optimum treatment conditions was also investigated.

#### 3.4.2.1 Real wastewater

Wastewater samples were supplied from pulp and paper mill located in Kanchanaburi province to be treated wastewater in present research. Table 3.3 shows the characteristics of pulp and paper mill wastewater used in the experiments.

Table 3.3 The characteristics of pulp and paper mill wastewater

Parameters	Values*
pH	5.97-6.38
SS (mg/l)	3,581-3,954
TDS (mg/l)	2,267-2,503
BOD (mg/l)	1,704-1,801
COD (mg/l)	4,936-5,101
Color (Pt-Co unit)	736-957
Lignin (mg/l)	218-290
2,4-DCP ( $\mu\text{g/l}$ )	111-152

Note: \* collected in April-June, 2010

#### 3.4.2.2 Experimental methods for real wastewater

Wastewater samples containing 218-290 mg/l of lignin and 111-152  $\mu\text{g/l}$  of 2,4-DCP were supplied from the pulp and paper mill located at Kanchanaburi province in Thailand and collected at the integrated wastewater pond before treatment system. The samples were collected in April-June, 2010. Before treatment, the wastewater was precipitated with gravity followed by filtration using 0.45  $\mu\text{m}$  glass microfiber filters, 111 mm to remove the suspended solids from the samples, and then pH was adjusted with NaOH (1 N) and H<sub>2</sub>SO<sub>4</sub> (1 N). The temperature of real wastewater was kept at room temperature (30 °C). The effluent samples were taken at 15, 30, 60, 90, 120, 180, 300 and 420 min of reaction time for lignin and color analysis on UV-Visible spectrophotometer and 2,4-DCP analysis on HPLC.

The performances of supervibration-photocatalytic reactor on lignin and 2,4-DCP degradation were studied under various initial pH, UV intensity and vibration frequency which are given in Table 3.4 and experimental conditions are presented in Table 3.5. Furthermore, under the optimum treatment conditions, removal efficiency of color was also investigated.



Table 3.4 The experimental factors of real wastewater

Factors	Values
The effect of initial pH	5, 6, 7, 8, 9
The effect of UV intensity (mW/cm <sup>2</sup> )	0, 6.3, 12.6, 25.2
The effect of vibration frequency (Hz)	0, 20, 30, 40, 50

Table 3.5 Experimental conditions of real wastewater

Wastewater sample	Experiments	Wastewater concentration	Initial pH	UV intensity (mW/cm <sup>2</sup> )	Vibration frequency (Hz)
Pulp and paper mill wastewater	1	Real initial concentration	5	6.3	30
			6	6.3	30
			7	6.3	30
			8	6.3	30
			9	6.3	30
	2	Real initial concentration	Optimum from exp.1	0	30
			12.6	30	
	3	Real initial concentration	Optimum from exp.1	Optimum from exp.2	0
					20
					40
					50
	4	Real initial concentration	Optimum from exp.1	25.2	Optimum from exp.3

### 3.5 Analytical Methods

#### 3.5.1 Measurement of lignin

For synthetic wastewater, lignin concentration was analyzed by UV-Visible spectrophotometer, Model Helios Alpha, with detection wavelength of 280 nm (Ksibi et al., 2003; Pessala et al., 2004; Portjanskaja et al., 2009). Before analysis, the

effluent samples of synthetic wastewater were diluted by distilled water as 2 times for initial concentration of 100 mg/l, 3 times for initial concentration of 200 mg/l, 4 times for initial concentration of 300 mg/l and 5 times for initial concentration of 400 mg/l. Lignin analysis was described in Appendix A.

For real wastewater from pulp and paper mill, lignin concentration was analyzed by UV-Visible spectrophotometer, Model Helios Alpha, with detection wavelength of 700 nm (Eaton et al., 2005) as described in Appendix A. Before analysis, the effluent samples were diluted 4 times by distilled water, and then the solutions were filtered with 0.45  $\mu\text{m}$  nylon membrane filter, 47 mm to remove fine particulates from the samples.

### 3.5.2 Measurement of color

Color of lignin synthetic wastewater and real wastewater were determined by UV-Visible spectrophotometer, Model Helios Alpha, Thermo Electron with detection wavelength of 465 nm (Eaton et al., 2005) as described in Appendix A. Before analysis, the effluent samples of real wastewater from pulp and paper mill were diluted 2 times by distilled water and pH was adjusted to 7.0 with  $\text{H}_2\text{SO}_4$  and  $\text{NaOH}$ , and then the solutions were filtered with glass microfiber filter, GF/C, 47 mm to remove suspended solids from the samples.

### 3.5.3 Measurement of 2,4-DCP

2,4-DCP concentration was detected by HPLC. Firstly, the effluent samples and standard solutions were filtered through 0.45  $\mu\text{m}$  nylon syringe filter, 13 mm. Next, the residual samples and standard solutions were detected by HPLC Varian Prostar with Auto sampler Model 400, pump Model 230, Varian HPLC column C 18 (4.6 mm internal diameter  $\times$  250 mm) holder with guard column and UV-Visible detector Model 325. The wavelength of detector was 280 nm. A mixture of 25% of acetonitrile, 30% of methanol and 45% of ultra pure de-ionized ( $18.2 \text{ M}\Omega \text{ cm}^{-1}$ ) water adjusted at pH 3 with  $\text{H}_2\text{SO}_4$  was used as a mobile phase with flow rate of 1 ml/min (Somshy Kinakul, 2002). Before introduced to HPLC, the mobile phase was filtered through 0.45  $\mu\text{m}$  PTFE membrane filter, 47 mm using vacuum degassing. The

retention time for 2,4-DCP detection is around 7.5 min. 2,4-DCP analysis was described in Appendix A.

### 3.5.4 Identification of by-products of photocatalytic degradation

#### 3.5.4.1 Identification of by-products of lignin degradation

The by-products of lignin degradation in synthetic wastewater by supervibration-photocatalytic reactor were identified using GC-MS. The identification was analyzed as *N,O*-bis(trimethylsilyl)trifluoroacetamide (BSTFA) and Trimethylchlorosilane (TMCS) derivatives by GC-MS analysis. The GC-MS corresponds to the compounds extracted with ethyl acetate from the acidified supernatant. The interpretation of mass spectra was based on the GC-MS library as well as on mass spectra of model compounds.

The samples of lignin synthetic wastewater from irradiated solution (80 ml) were acidified at pH 2 by HCl (1 N) and extracted with ethyl acetate (3 × 40 ml) then dried under nitrogen gas. BSTFA (100 µl) and TMCS (100 µl) were added to the organic extract. The solution was treated at 60 °C under nitrogen current for 5 h. The residue was redissolved in chloroform (1 ml) and analyzed by GC-MS.

GC-MS analysis was performed with an Agilent 6890 N Network GC system, interfaced with an Agilent 5973 N Network Mass Selective detector. The analytical column connecting to the system was ZB-5MS capillary GC column (30 m × 0.25 mm internal diameter, 0.25 µm film thickness) from Phenomenex (Part. No. 7HG-G010-11). The helium gas was used as carrier gas with the flow rate of 1 ml/min. The column temperature program was 80 °C (hold for 1 min); 80-280 °C (7 °C/min, hold for 5 min) (Ksibi et al., 2003).

#### 3.5.4.2 Identification of by-products of 2,4-DCP degradation

The by-products of 2,4-DCP degradation in synthetic wastewater were detected by GC-MS using solid-phase microextraction (SPME) for sample extraction.

The effluent samples of 25 ml were adjusted to pH 2 using hydrochloric acid (HCl) and saturated with sodium sulfate (Na<sub>2</sub>SO<sub>4</sub>) (7.5 mg). An 85 µm

polyacrylate (PA) fiber (Supelco Cat. No. 57304) and a SPME fiber holder (Supelco Cat.No. 57330) were used for sample extraction. The vial capacity was 50 ml, handling 25 ml of samples. The stirring velocity was controlled at 750 rpm at room temperature (30 °C). The optimum extraction conditions were immersion sampling at room temperature for 60 min, with an 85 µm PA coated fiber, saturated salt condition and sample pH 2.

After the extraction, the fiber was introduced in the injection at 250 °C for 3 min with the split valve closed. GC-MS analysis was performed with an Agilent 6890 N Network GC system, interfaced with an Agilent 5973 Network Mass Selective detector. The column was HP-5 (30 m × 0.25 mm internal diameter, 0.25 µm film thickness) from J & W Scientific (Cat.No. 19091J-433). The carrier gas was helium at flow rate of 0.8 ml/min. The oven temperature was initially set at 40 °C hold for 4 min and then programmed at 220 °C with a rate of 10 °C/min (Agilent Technologies, Inc, 2006; Ribeiro et al., 2002).



ศูนย์วิทยทรัพยากร  
จุฬาลงกรณ์มหาวิทยาลัย

## CHAPTER IV

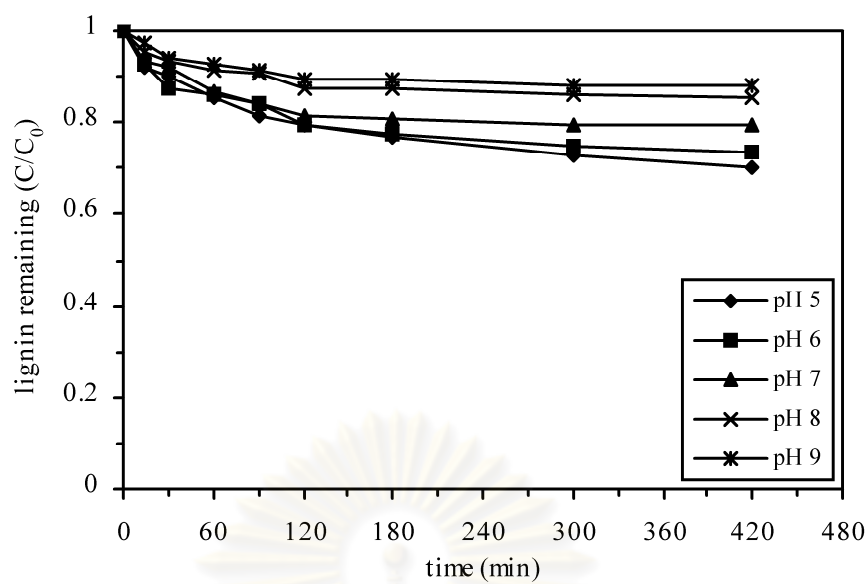
### RESULTS AND DISCUSSIONS

#### 4.1 Treatment of Lignin Synthetic Wastewater

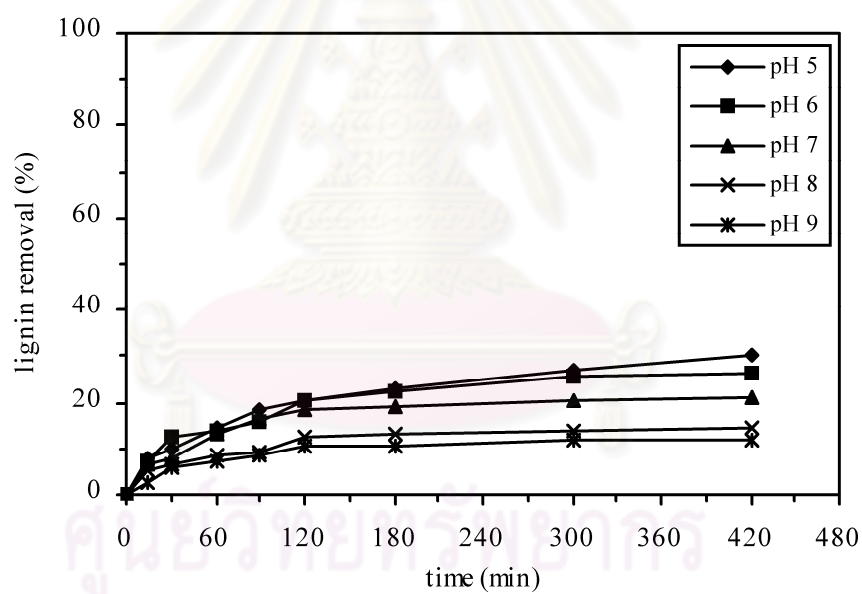
The performance of supervibration-photocatalytic reactor based on the photocatalytic process combined with a supervibration agitator on treatment of lignin in synthetic wastewater was investigated to obtain the optimum operating conditions, study the reaction kinetics of lignin photocatalytic degradation and identify the by-products occurred from lignin degradation. Treatment efficiencies of lignin by supervibration-photocatalytic reactor were studied under different initial pH (5, 6, 7, 8 and 9), UV intensity (0, 6.3, 12.6 and 25.2 mW/cm<sup>2</sup>), vibration frequency (0, 20, 30, 40 and 50 Hz) and initial lignin concentration (100, 200, 300 and 400 mg/l).

##### 4.1.1 Effect of initial pH on degradation of lignin in synthetic wastewater

The effect of initial pH on degradation of lignin in synthetic wastewater was investigated under five different initial pH levels as 5, 6, 7, 8 and 9. Synthetic wastewater prepared in the experiment contained 400 mg/l of lignin solution. The photocatalytic process was carried out with a constant UV intensity of 6.3 mW/cm<sup>2</sup> and vibration frequency of 30 Hz. Figure 4.1 presents the decrease of lignin and removal efficiency by photocatalytic degradation. For the optimum initial pH as pH 5, lignin concentration was decreased from 400 mg/l to 279.86 mg/l ( $C/C_0 = 0.70$ ) after 420 min of reaction time. The ultimate lignin removal efficiencies were 30.03% (pH 5), 26.33% (pH 6), 20.83% (pH 7), 14.66% (pH 8) and 12.17% (pH 9) within 420 min. The results indicate that the lignin removal efficiencies were increased with the decrease in the initial pH.



(a)



(b)

Figure 4.1 The effect of initial pH on degradation of lignin in synthetic wastewater: lignin remaining (a) and removal efficiency (b) (initial lignin concentration = 400 mg/l, UV intensity = 6.3 mW/cm<sup>2</sup>, vibration frequency = 30 Hz)



The kinetic expression in terms of Langmuir-Hinshelwood (Konstantinou and Albanis, 2004; Kumar et al., 2008; Valente et al., 2006) describing photocatalytic degradation of lignin and a first order reaction is induced as

$$\ln\left(\frac{C_0}{C}\right) = kKt = k_{ap}t \quad , \quad (18)$$

where  $C_0$  is the initial lignin concentration (mg/l) and  $C$  is lignin concentration (mg/l) at any time  $t$  (min).  $k$  is the true rate constant (mg/l min<sup>-1</sup>) and  $K$  is the constant of adsorption equilibrium (l/mg).  $k_{ap}$  is the apparent rate constant of first order reaction (min<sup>-1</sup>). By plotting  $\ln(C_0/C)$  versus time, the apparent rate constant ( $k_{ap}$ ) can be determined from the slope of the curve obtained (equation (18)) as shown in Figure 4.2 and the initial degradation rate ( $r_0$ ) (mg/l min<sup>-1</sup>) can be represented as presented in equation (19).

$$r_0 = k_{ap}C_0 \quad . \quad (19)$$

The apparent rate constant of first order reaction ( $k_{ap}$ ) and the initial degradation rate ( $r_0$ ) of Langmuir-Hinshelwood kinetic for lignin degradation at various initial pH obtained from the experimental data show that at the optimum initial pH (pH 5), the highest  $k_{ap}$  as  $2.2 \times 10^{-3}$  min<sup>-1</sup> and the highest  $r_0$  as 0.88 mg/l min<sup>-1</sup> after 120 min were achieved. When initial pH decreased from 9, 8, 7 and 6 to 5, the apparent rate constant of first order reaction ( $k_{ap}$ ) were increased from  $1.1 \times 10^{-3}$ ,  $1.2 \times 10^{-3}$ ,  $1.9 \times 10^{-3}$  and  $2.1 \times 10^{-3}$  to  $2.2 \times 10^{-3}$  min<sup>-1</sup>, respectively and the initial degradation rate ( $r_0$ ) were increased from 0.44, 0.48, 0.76 and 0.84 to 0.88 mg/l min<sup>-1</sup>, respectively after the same time (as shown in Table 4.1). This phenomenon followed the same trend as lignin removal. Several researchers (Chang et al., 2004; Ma et al., 2008; Portjanskaja and Preis, 2007) obtained similar results in which more lignin removal were observed with samples of lower pH level thus, the acidic conditions favor the lignin decomposition. This result was also similar in degradation of other compounds as azo dye acid red 14 (Wang et al., 2008). This increase in lignin removal might be because,

under acidic conditions, a superoxide radical ( $O_2^{\cdot-}$ ) will react with a hydrogen ion ( $H^+$ ) and produce a perhydroxyl radical

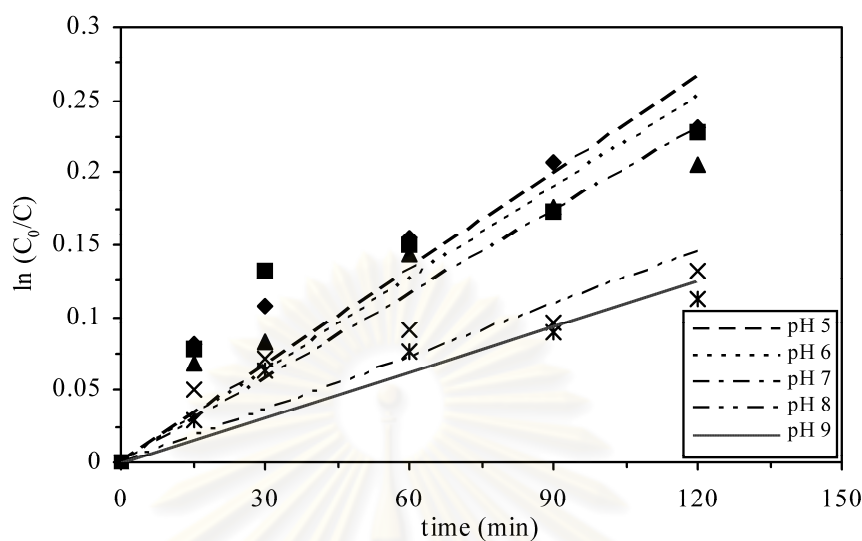


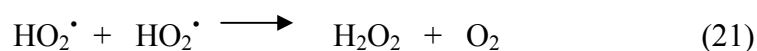
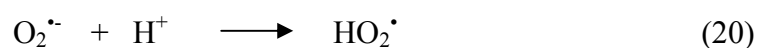
Figure 4.2 Linear transform  $\ln(C_0/C)$  vs. time for lignin degradation at various initial pH

Table 4.1  $k_{ap}$  and  $r_0$  of first order kinetic for lignin degradation at various initial pH

pH	$k_{ap}$ ( $\text{min}^{-1}$ )	$r_0$ ( $\text{mg/l min}^{-1}$ )	Coefficient ( $R^2$ )
5	$2.2 \times 10^{-3}$	0.88	0.8459
6	$2.1 \times 10^{-3}$	0.84	0.7366
7	$1.9 \times 10^{-3}$	0.76	0.874
8	$1.2 \times 10^{-3}$	0.48	0.7024
9	$1.1 \times 10^{-3}$	0.44	0.8152

Note: reaction time = 120 min

( $HO_2^{\cdot}$ ). Consequently, the  $HO_2^{\cdot}$  can form hydrogen peroxide ( $H_2O_2$ ), which in turn gives rise to the  $OH^{\cdot}$  as presented in equation (20)-(23) (De Lasa et al., 1992).

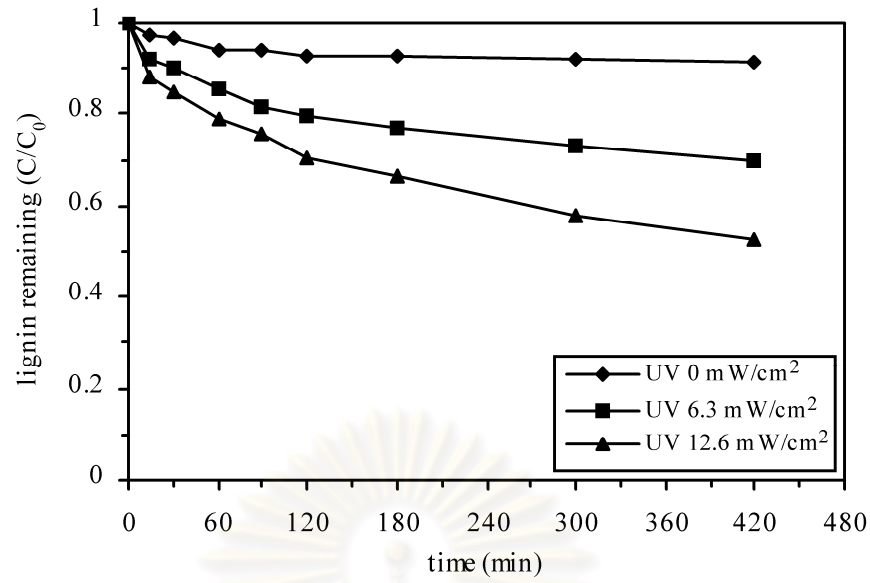




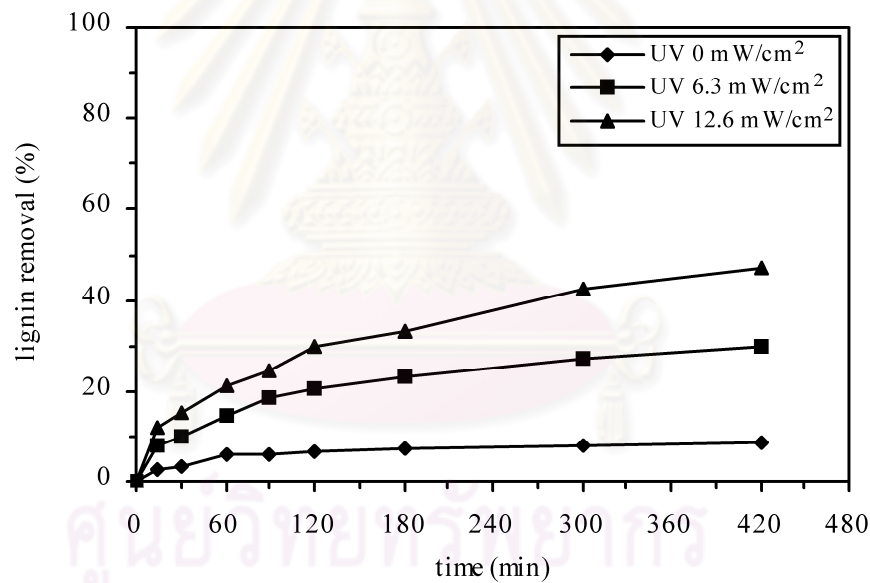
On the other hand, the point of zero charge (pzc) of the TiO<sub>2</sub> is at pH 5.6-6.4 (Bayarri et al., 2005), its surface is positively charged in acidic media (pH < pzc) and negatively charged in alkaline (pH > pzc). Molecules of lignin are negative charge in alkaline solution, being repelled from the TiO<sub>2</sub> surface; which causes to reduce their adsorption. Also the accumulation of carbonate and bicarbonate ions, OH<sup>•</sup> scavenger, could be the reason of decreased efficiency at alkaline pH (Portjanskaja and Preis, 2007).

#### 4.1.2 Effect of UV intensity on degradation of lignin in synthetic wastewater

The process was repeated at a constant of optimum initial pH (pH 5) and vibration frequency of 30 Hz using different UV intensities of 0, 6.3 and 12.6 mW/cm<sup>2</sup> to study effect of UV intensity on degradation of lignin in synthetic wastewater. The experimental data depicted in Figure 4.3 indicate that a higher rate of photocatalytic oxidation could be observed at a higher UV intensity for 420 min. Under UV intensity of 12.6 mW/cm<sup>2</sup> as the best lignin removal, the initial concentration (400 mg/l) of lignin was reduced to 211.79 mg/l ( $C/C_0 = 0.53$ ) with removal efficiency of 47.05% after 420 min. Lignin removal efficiencies of the system with 0, 6.3 and 12.6 mW/cm<sup>2</sup> were 8.33%, 30.03% and 47.05%, respectively, in the same time. The reactor could slightly remove lignin under the absence of UV intensity since some molecules of lignin might be adsorbed on the inner or outer of TiO<sub>2</sub> film surface. Figure 4.4 shows the plotting of  $\ln(C_0/C)$  versus time under various UV intensity to obtain slope of the curve as the apparent rate constant ( $k_{ap}$ ). The apparent rate constant of first order reaction ( $k_{ap}$ ) and the initial degradation rate ( $r_0$ ) of Langmuir-Hinshelwood kinetic for lignin removal after 120 min at different UV intensity show that under UV intensity of 12.6 mW/cm<sup>2</sup>, the highest  $k_{ap}$  as  $3.2 \times 10^{-3} \text{ min}^{-1}$  and the highest  $r_0$  as  $1.28 \text{ mg/l min}^{-1}$  were achieved.



(a)



(b)

Figure 4.3 The effect of UV intensity on degradation of lignin in synthetic wastewater: lignin remaining (a) and removal efficiency (b) (initial lignin concentration = 400 mg/l, initial pH = 5, vibration frequency = 30 Hz)

The apparent rate constant of first order reaction ( $k_{ap}$ ) of lignin degradation were increased from  $0.7 \times 10^{-3}$  and  $2.2 \times 10^{-3}$  to  $3.2 \times 10^{-3} \text{ min}^{-1}$  and the initial degradation rate ( $r_0$ ) were increased from 0.28 and 0.88 to  $1.28 \text{ mg/l min}^{-1}$ , when UV intensity increased from 0 and 6.3 to  $12.6 \text{ mW/cm}^2$ , respectively (as listed in Table 4.2). This phenomenon followed the same trend as lignin removal.

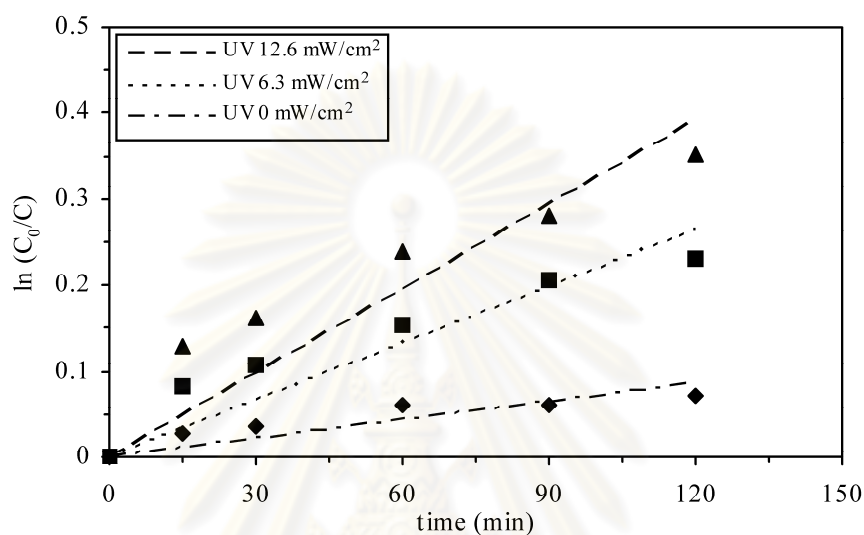


Figure 4.4 Linear transform  $\ln(C_0/C)$  vs. time for lignin degradation at various UV intensity

Table 4.2  $k_{ap}$  and  $r_0$  of first order kinetic for lignin degradation at various UV intensity

UV intensity ( $\text{mW/cm}^2$ )	$k_{ap}$ ( $\text{min}^{-1}$ )	$r_0$ ( $\text{mg/l min}^{-1}$ )	Coefficient ( $R^2$ )
0	$0.7 \times 10^{-3}$	0.28	0.7212
6.3	$2.2 \times 10^{-3}$	0.88	0.8459
12.6	$3.2 \times 10^{-3}$	1.28	0.8147

Note: reaction time = 120 min

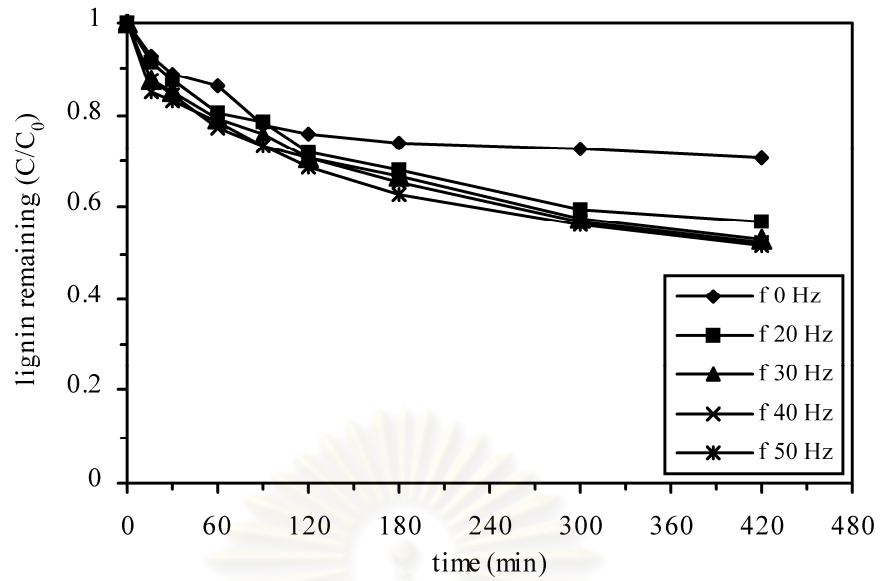
The results indicate that an increase in UV intensity could enhance lignin removal and removal efficiency of lignin was significantly influenced by UV intensity. This is because when UV intensity is higher, the photonic flux irradiation and illumination energy increase and higher rate of electron-hole pair production occurs. Thus, the rate of  $\text{OH}^\bullet$  and the  $\text{O}_2^{\bullet-}$  production increase, which would allow the degradation to be faster. In addition, reaction temperature might increase with increasing in UV intensity. Previous research indicated that increasing the reaction temperature increased the rate of all reactions occurring in the system (Zeltner, Hill, and Anderson, 1993; Hofstadler et al., 1994). Related results were previously observed by Dahm and Lucia (2004). The photodegradation of dissolved lignin in a water medium resulting from  $\text{TiO}_2$  photocatalysis reactions was studied. The lignin samples were magnetically stirred throughout irradiation with 64-128 W corresponded to a light intensity range of 223-445  $\text{mW/cm}^2$ . The results demonstrated that higher illumination intensities correlated well with higher initial degradation rates and total lignin degradation. At the highest light illumination power of 445  $\text{mW/cm}^2$ , there was a 40% destruction of lignin in 5 min, while at the lower levels of light intensity, it required up to 1 hour.

#### 4.1.3 Effect of vibration frequency on degradation of lignin in synthetic wastewater

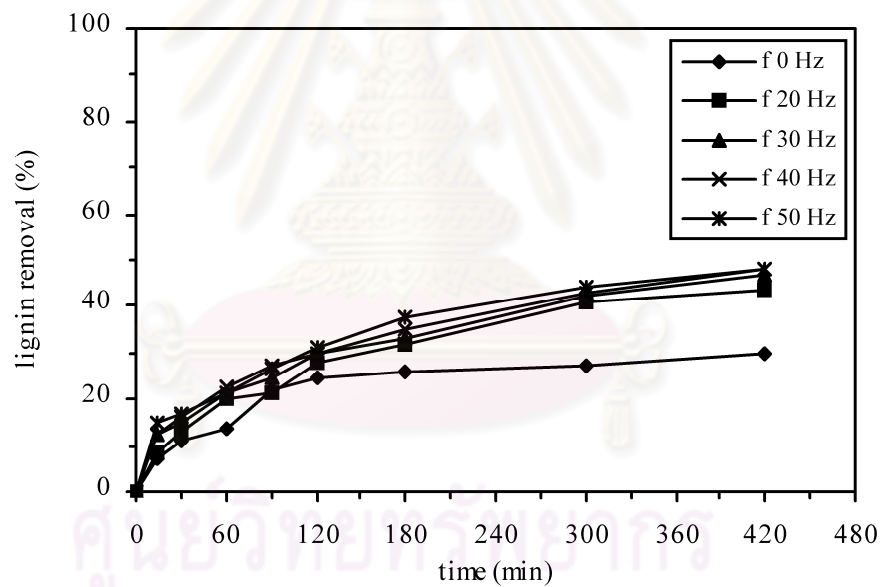
400 mg/l of lignin solutions were prepared for the experiment under different vibration frequencies as 0, 20, 30, 40 and 50 Hz at the optimum initial pH (pH 5) and optimum UV intensity (12.6  $\text{mW/cm}^2$ ) to investigate effect of vibration frequency on degradation of lignin in synthetic wastewater. Figure 4.5 shows the decrease of lignin and removal efficiency, which indicated the influence of vibration frequency on photocatalysis under the conditions used here. Although there was an absence of vibration frequency (0 Hz), the system could remove lignin at 29.66% in 420 min because of photocatalytic degradation (UV/ $\text{TiO}_2$ ). When introducing the vibration frequency into the system, it was able to remove more lignin. The removal efficiencies of lignin were 43.35% (20 Hz), 47.05% (30 Hz) and 47.78% (40 Hz) in the same time. For the optimum vibration frequency as 50 Hz, lignin concentration decreased from 400 mg/l to 206.90 mg/l ( $C/C_0 = 0.52$ ), which corresponds to a



destructive efficiency of 48.28%. Figure 4.6 shows the plotting of  $\ln(C_0/C)$  versus time under various vibration frequency to obtain slope of the curve as the apparent rate constant ( $k_{ap}$ ). The apparent rate constant of first order reaction ( $k_{ap}$ ) and the initial degradation rate ( $r_0$ ) of Langmuir-Hinshelwood kinetic followed the same trend as lignin removal. When vibration frequency increased from 0, 20, 30 and 40 to 50 Hz, the apparent rate constant of first order reaction ( $k_{ap}$ ) of lignin degradation were increased from  $2.6 \times 10^{-3}$ ,  $2.9 \times 10^{-3}$ ,  $3.2 \times 10^{-3}$  and  $3.4 \times 10^{-3}$  to  $3.5 \times 10^{-3} \text{ min}^{-1}$ , respectively and the initial degradation rate ( $r_0$ ) were increased from 1.04, 1.16, 1.28 and 1.36 to  $1.4 \text{ mg/l min}^{-1}$ , respectively after 120 min as presented in Table 4.3. Lignin removal was increased as vibration frequency increased. This is probably because, in the condition of higher vibration frequency, the powerful 3-dimensional agitating flow in the reaction tank is higher. Therefore, the contact between lignin and  $\text{TiO}_2$  was enhanced, then higher adsorption between lignin and  $\text{TiO}_2$  and higher degradation could be occurred. The previous research for treatment of lignin using UV/ $\text{TiO}_2$  process and mechanical agitation were observed. Portjanskaja and Preis (2007) used mechanical agitation with magnetic stirrers in photocatalytic oxidation with 15 W of UV for treatment of lignin. The system could degrade lignin not exceeding 50% after 25 hours when using 100 mg/l of initial lignin concentration at pH around 8.0. Therefore, the supervibration agitator in the present study has higher performance in lignin removal than that of previous research. This may be because the fluid flow rate produced by the supervibration agitator is higher than that produced by magnetic stirrers.



(a)



(b)

Figure 4.5 The effect of vibration frequency on degradation of lignin in synthetic wastewater: lignin remaining (a) and removal efficiency (b) (initial lignin concentration = 400 mg/l, initial pH = 5, UV intensity = 12.6 mW/cm<sup>2</sup>)

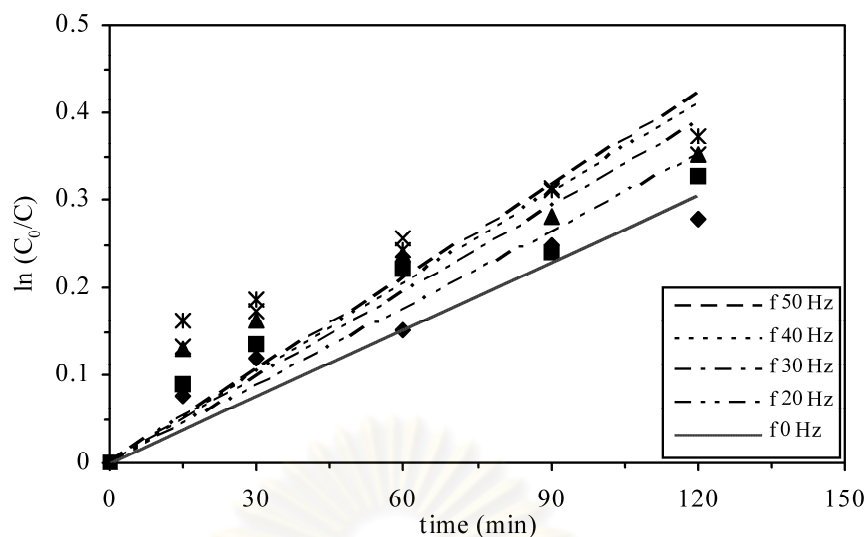


Figure 4.6 Linear transform  $\ln(C_0/C)$  vs. time for lignin degradation at various vibration frequency

Table 4.3  $k_{ap}$  and  $r_0$  of first order kinetic for lignin degradation at various vibration frequency

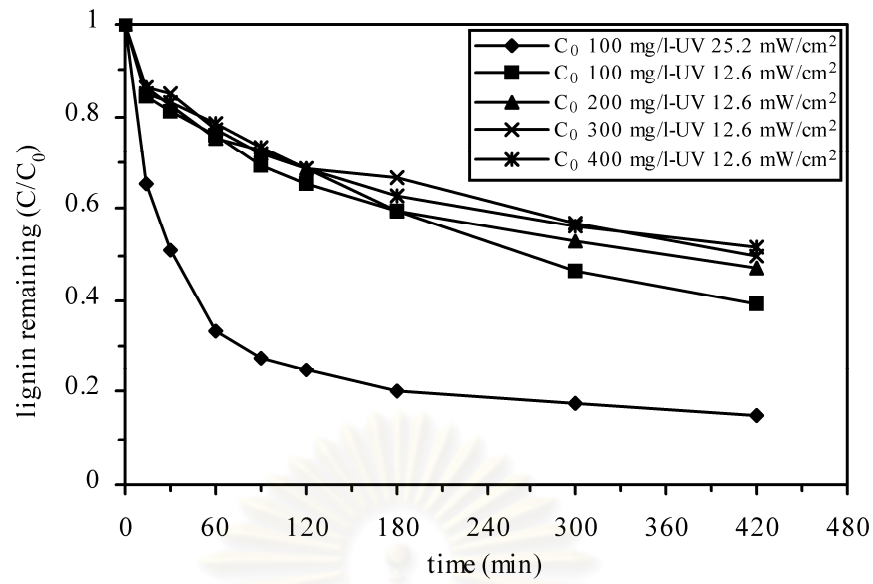
Vibration frequency (Hz)	$k_{ap}$ ( $\text{min}^{-1}$ )	$r_0$ ( $\text{mg/l min}^{-1}$ )	Coefficient ( $R^2$ )
0	$2.6 \times 10^{-3}$	1.04	0.921
20	$2.9 \times 10^{-3}$	1.16	0.8911
30	$3.2 \times 10^{-3}$	1.28	0.8147
40	$3.4 \times 10^{-3}$	1.36	0.7886
50	$3.5 \times 10^{-3}$	1.4	0.7375

Note: reaction time = 120 min

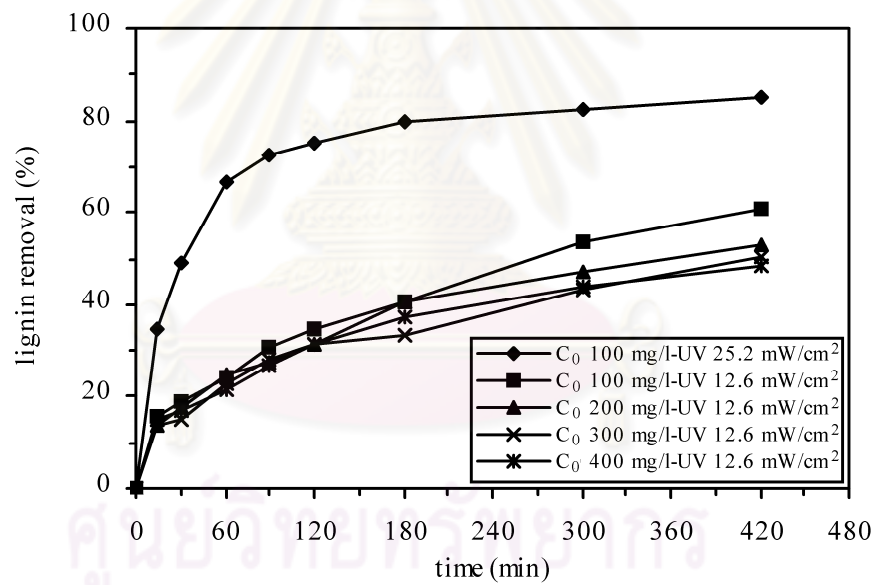
#### 4.1.4 Effect of initial lignin concentration on degradation of lignin in synthetic wastewater

The initial lignin concentration was also a variable parameter to be studied in effluence on degradation of lignin in synthetic wastewater. Figure 4.7 illustrates lignin removal for different initial lignin concentrations of 100, 200, 300 and 400 mg/l.

When optimum initial pH (pH 5), optimum UV intensity ( $12.6 \text{ mW/cm}^2$ ) and optimum vibration frequency (50 Hz) were kept constant, lignin concentration decreased from 100 mg/l initially to 39.36 mg/l ( $C/C_0 = 0.39$ ) with a capacity up to 60.64% after 420 min. The removal efficiencies of lignin for the initial lignin concentration of 200 mg/l, 300 mg/l and 400 mg/l were 53.16%, 50.05% and 48.28%, respectively after the same time. Figure 4.8 shows the plotting of  $\ln(C_0/C)$  versus time under various initial lignin concentration to obtain slope of the curve as the apparent rate constant ( $k_{ap}$ ). When the initial lignin concentration increased from 100, 200 and 300 to 400 mg/l, the apparent rate constant of first order reaction ( $k_{ap}$ ) of Langmuir-Hinshelwood kinetic were decreased from  $4 \times 10^{-3}$ ,  $3.7 \times 10^{-3}$  and  $3.6 \times 10^{-3}$  to  $3.5 \times 10^{-3} \text{ min}^{-1}$ , respectively after 120 min, whereas the initial degradation rate ( $r_0$ ) were increased from 0.4, 0.74 and 1.08 to  $1.4 \text{ mg/l min}^{-1}$ , respectively after the same time as shown in Table 4.4. The only  $k_{ap}$  had the same trend as removal efficiency of lignin. The  $r_0$  increased with  $C_0$  (the initial concentration), since in the product  $k_{ap}C_0$ , the increase in concentration was more significant than the variation in  $k_{ap}$  values. The results indicate that the apparent rate constant ( $k_{ap}$ ) of lignin degradation were decreased with the increase in the initial lignin concentration. Ksibi et al. (2003) obtained similar results. The degradations were carried out 1,000 ml of lignin solution and 1 g of  $\text{TiO}_2$  (Degussa P-25). The COD removal of lignin solution by photocatalytic degradation could be achieved when lignin is used at low concentration. The COD removal reached 81% for the lignin initial concentration of 39.4 mg/l in 420 min. Furthermore, Kansal et al. (2008) also obtained similar result from  $\text{TiO}_2/\text{ZnO}$  photocatalysed degradation of lignin and reported that the percentage degradation of lignin solution depends on the initial concentration of the substrate. The effective degradation could be achieved when lower concentration of lignin was used. When the initial lignin concentration became higher, it had an inhibitory effect on the photodegradation. This phenomena can be explained by the increase of incidental photonic flux irradiating the catalyst in dilute lignin solution, since the photonic flux irradiation on  $\text{TiO}_2$  increases in a diluted lignin solution, thus the rate of hydroxyl radical ( $\text{OH}^\bullet$ ) and superoxide radical ( $\text{O}_2^{\bullet-}$ ) production increases which would allow the degradation to be faster.



(a)



(b)

Figure 4.7 The effect of initial concentration on degradation of lignin in synthetic wastewater: lignin remaining (a) and removal efficiency (b) (initial pH = 5, vibration frequency = 50 Hz)

On the other hand, under a high lignin concentration, saturation coverage of lignin on the surface of TiO<sub>2</sub> occurs (Pandiyan et al., 2002) or a higher initial lignin concentration yields a higher concentration of adsorbed intermediates according to more compete with intermediates for TiO<sub>2</sub> sites (Bayarri et al., 2005).

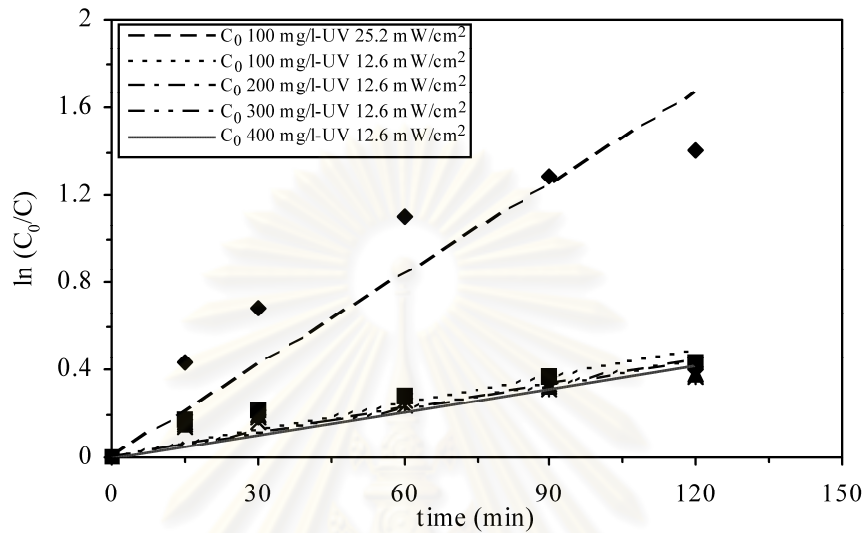


Figure 4.8 Linear transform  $\ln(C_0/C)$  vs. time for lignin degradation in various initial concentration

In this work, the rate constant ( $k$ ) and adsorption constant ( $K$ ) were calculated using the Langmuir-Hinshelwood model, considering the following rate and initial concentrations:

$$r_0 = \frac{-dC}{dt} = \frac{kKC_0}{(1 + KC_0)} \quad (24)$$

This equation can be rearranged into linear form:

$$\frac{1}{r_0} = \frac{1}{kK} \cdot \frac{1}{C_0} + \frac{1}{k} \quad (25)$$

where  $1/r_0$  is the dependent variable and  $1/C_0$  is the independent variable. By plotting  $1/r_0$  versus  $1/C_0$ ,  $1/kK$  can be obtained from the slope of the line and  $1/k$  can be



obtained from the point at which the line crosses the y-axis (Valente et al., 2006). The linearization of the curve in Figure 4.9, plotting  $1/r_0$  versus  $1/C_0$ , from 100 to 400 mg/l of lignin concentration describe a linear behavior with linear coefficient  $R^2 = 0.9994$  and the rate constant ( $k$ ) and adsorption constant ( $K$ ) are shown in Table 4.4.

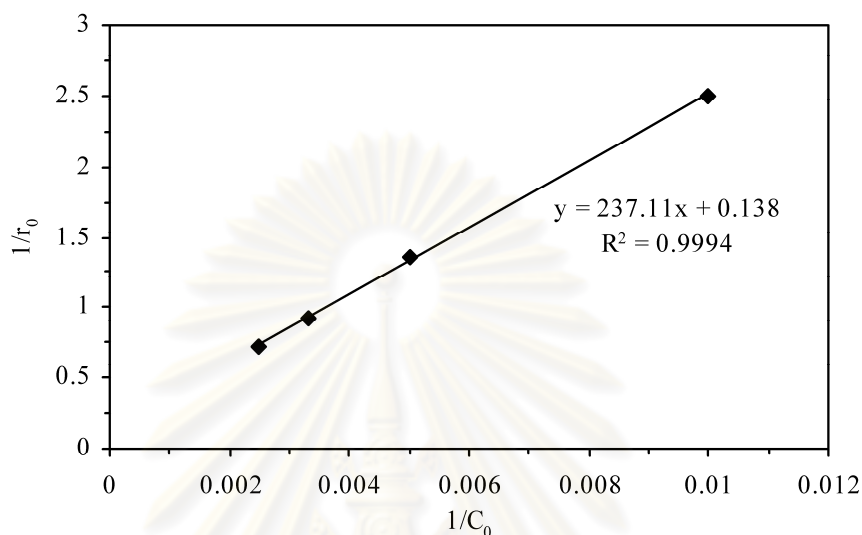


Figure 4.9 Linear transform  $1/r_0$  vs.  $1/C_0$  for lignin degradation

Table 4.4  $k_{ap}$  and  $r_0$  of first order kinetic for lignin degradation in various initial concentration

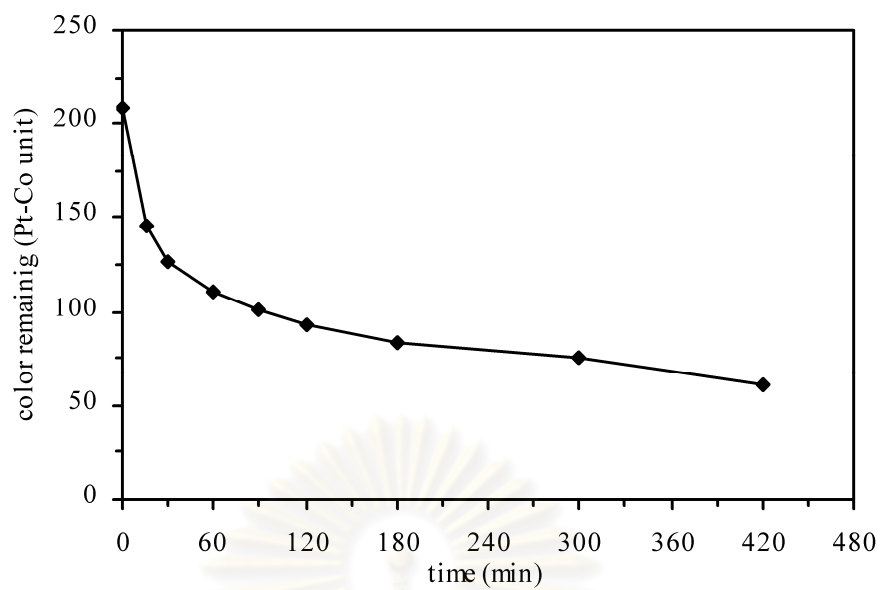
Initial concentration (mg/l)	$k_{ap}$ ( $\text{min}^{-1}$ )	$r_0$ ( $\text{mg/l min}^{-1}$ )	Coefficient ( $R^2$ )	$k$ ( $\text{mg/l min}^{-1}$ )	$K$ (l/mg)
100	$4 \times 10^{-3}$	0.4	0.7892	7.25	$0.58 \times 10^{-3}$
200	$3.7 \times 10^{-3}$	0.74	0.7391		
300	$3.6 \times 10^{-3}$	1.08	0.8209		
400	$3.5 \times 10^{-3}$	1.4	0.7375		
100 mg/l-UV 25.2 mW/cm <sup>2</sup>	$13.9 \times 10^{-3}$	1.39	0.8263	-	-

Note: reaction time = 120 min

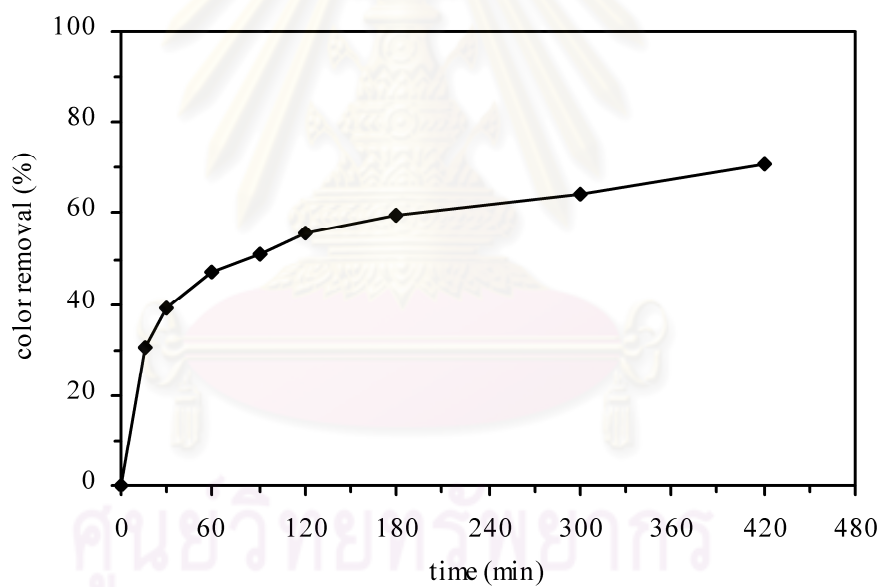
Additional experiment with an increase in UV intensity to 25.2 mW/cm<sup>2</sup>, initial pH 5, vibration frequency of 50 Hz was carried out to improve system performance. The results were found that lignin concentration decreased from 100 mg/l initially to 14.89 mg/l ( $C/C_0 = 0.15$ ) with a removal efficiency up to 85.12% within 420 min as shown in Figure 4.7. The apparent rate constant of first order reaction ( $k_{ap}$ ) and the initial degradation rate ( $r_0$ ) of Langmuir-Hinshelwood kinetic were  $13.9 \times 10^{-3} \text{ min}^{-1}$  and  $1.39 \text{ mg/l min}^{-1}$ , respectively, after 120 min as listed in Table 4.4. The results indicate that an increase in UV intensity as 25.2 mW/cm<sup>2</sup> significantly enhanced lignin removal since the increase in UV intensity can promote the hydroxyl radical (OH<sup>•</sup>) formation in the photocatalytic reaction.

Furthermore, the performance of supervibration-photocatalytic reactor on color removal in lignin synthetic wastewater was also studied under the optimum treatment conditions as initial lignin concentration of 100 mg/l, initial pH 5, UV intensity of 25.2 mW/cm<sup>2</sup> and vibration frequency of 50 Hz. The result was found that color was decreased from 207.96 Pt-Co unit to 61.24 Pt-Co unit after 420 min with removal efficiency of 70.55% as presented in Figure 4.10 and 4.11. For the related research studied by Ksibi et al. (2003), they investigated the treatment of lignin from alfalfa black liquor digestion by the photocatalytic degradation. Under the conditions of lignin initial concentration of 90 mg/l, initial pH of 8.2 and 1 g of TiO<sub>2</sub>, the reduction in the optical density with time from OD<sub>280</sub> as 0.94 to 0.28 in 420 min with a capacity of 70.21%. This gradual reduction of the intensity of the absorption proved that deterioration of chromophors groups of the lignin occurred.

ศูนย์วิทยทรัพยากร  
จุฬาลงกรณ์มหาวิทยาลัย

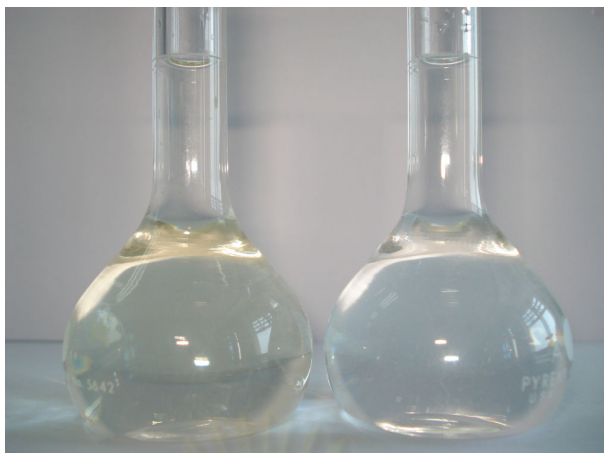


(a)



(b)

Figure 4.10 Removal of color in lignin synthetic wastewater: color remaining (a) and removal efficiency (b) (initial lignin concentration = 100 mg/l, initial pH = 5, UV intensity = 25.2 mW/cm<sup>2</sup>, vibration frequency = 50 Hz)



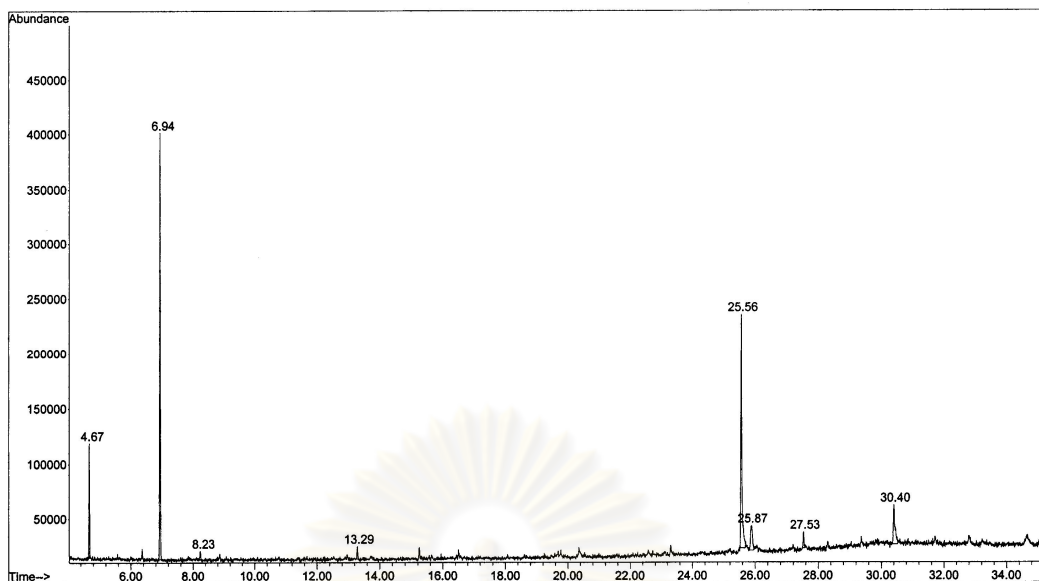
(a)

(b)

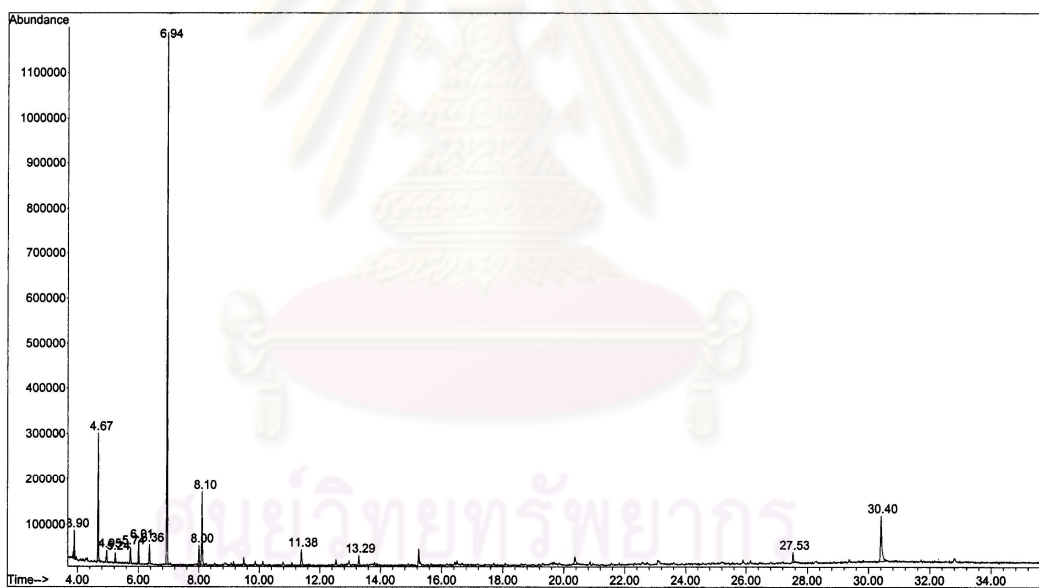
Figure 4.11 Color of lignin synthetic wastewater at reaction time: 0 min (a) and 420 min (b) (initial lignin concentration = 100 mg/l, initial pH = 5, UV intensity = 25.2 mW/cm<sup>2</sup>, vibration frequency = 50 Hz)

#### 4.1.5 Identification of the by-products of lignin degradation

The by-products of lignin degradation by supervibration-photocatalytic reactor were also investigated. The identification was carried out using GC-MS. The photocatalytic degradation of lignin (100 mg/l) was studied for optimum treatment conditions of pH 5, UV intensity of 25.2 mW/cm<sup>2</sup> and vibration frequency of 50 Hz. The chromatographic data in Figure 4.12 shows that the abundance of some initial peaks (initial reaction time) in the sample increased but other peaks disappeared after 420 min. However, new signals were detected in the same time. From total by-products classified by their fragmentation pattern as presented in Table 4.5, we obtained the following results:



(a)



(b)

Figure 4.12 GC-MS chromatogram of by-products from lignin degradation for reaction time: 0 min (a) and 420 min (b)

Table 4.5 Fragmentation pattern of by-products from lignin degradation identified by GC-MS

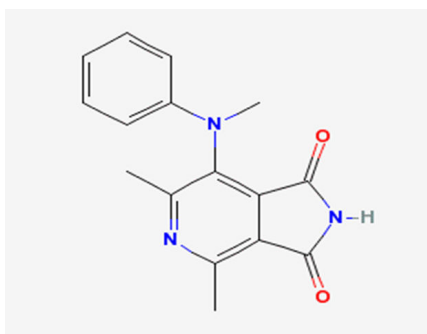
Compounds	Retention time (min)	m/z (% abundance)
2,6-Dimethyl-5-methylphenyl aminopyridine-3,4-dicarboxyimide	3.90	283 (14.6); 282 (30.2); 281 (100); 280 (21.4); 266 (7.9); 249 (6.3); 204 (17.2); 191 (5.1); 120 (8.5); 106 (19.7); 85 (11.1); 84 (12.7); 44 (10.8); 32 (19.8)
1-Methyl-2-phenylindole	4.95	295 (19.2); 209 (11); 208 (23.2); 207 (100); 206 (48); 204 (39.7); 191 (6.8); 178 (21.6); 165 (29.3); 139 (7.2); 102 (20.1); 85 (9.1); 44 (15.8); 32 (36.1)
2-Ethylacridine	5.24	281 (18.9); 237 (17.9); 209 (20.9); 208 (52.4); 207 (100); 193 (25.3); 192 (97.7); 191 (37.5); 166 (31.7); 96 (32.3); 85 (20); 73 (18.7); 44 (22.8); 32 (41.1)
2-Methylbenzaldehyde	5.74	207 (7.6); 121 (9.9); 120 (82.4); 119 (100); 92 (9.3); 91 (77.8); 89 (10); 85 (9.9); 83 (8.7); 65 (14.4); 63 (8.6); 51 (7.7); 44 (21.2); 43 (9.6); 39 (10.9); 32 (44.7)



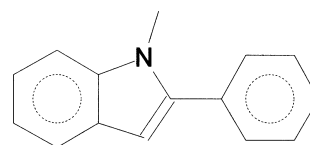
Table 4.5 Fragmentation pattern of by-products from lignin degradation identified by GC-MS (continuous)

Compounds	Retention time (min)	m/z (% abundance)
7H-Dibenzo[b,g]carbazole, 7-methyl-	6.01	325 (16.1); 283 (15.1); 282 (29); 281 (100); 280 (29.1); 266 (25.4); 264 (18.9); 133 (12.8); 73 (8.5); 44 (11.9); 32 (20.7)
Glaucine	6.36	357 (16.5); 356 (20.3); 355 (100); 354 (63.9); 340 (46); 324 (41.7); 312 (38.6); 297 (11.6); 283 (21.4); 281 (31); 265 (14.3); 207 (18.1); 193 (12.2); 73 (17.6); 32 (13.4)
5H-Naphtho[2,3-c]carbazole, 5-methyl-	8.00	283 (18.3); 282 (76.3); 281 (100); 280 (23); 266 (45.4); 264 (33.9); 207 (16.2); 148 (11.6); 141 (12.5); 140 (37.2); 139 (20.4); 73 (16.7); 44 (20.6); 32 (39.8)
2,4-Dimethylbenzaldehyde	8.10	207 (1.8); 135 (8.4); 134 (83); 133 (100); 105 (46.1); 103 (11.3); 91 (13.5); 79 (10.9); 77 (16.1); 63 (4.4); 51 (5.3); 39 (4.5); 32 (8.7)
4-Hydroxy-3-methoxybenzaldehyde (vanillin)	11.38	207 (8.5); 153 (11.7); 152 (98.5); 151 (100); 137 (5); 123 (18.2); 109 (12.8); 108 (8.4); 81 (12.8); 77 (3.7); 65 (6.5); 53 (6.6); 44 (21); 43 (7.4); 32 (36.4)

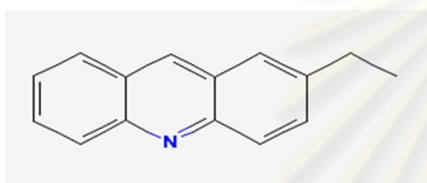
the first peak was detected at retention time 3.90 min as 2,6-dimethyl-5-methylphenylaminopyridine-3,4-dicarboxyimide; the peak at retention time 4.95 min was 1-methyl-2-phenylindole; the peak at 5.24 min was identified as 2-ethylacridine; the peak at retention time 5.74 min could be attributed to 2-methylbenzaldehyde; the peak at retention time 6.01 min was detected as 7H-dibenzo[b,g]carbazole, 7-methyl-; the peak at retention time 6.36 min was glaucine. Furthermore, 5H-naphtho[2,3-c]carbazole, 5-methyl- and 2,4-dimethylbenzaldehyde were detected at 8.00 min and 8.10 min, respectively. The last peak at retention time 11.38 min was assigned to 4-hydroxy-3-methoxybenzaldehyde (vanillin). The mass spectrum of vanillin showed characteristic peaks with fragmentation at  $m/z$  207 (8.5); 153 (11.7); 152 (98.5); 151 (100); 137 (5); 123 (18.2); 109 (12.8); 108 (8.4); 81 (12.8); 77 (3.7); 65 (6.5); 53 (6.6); 44 (21); 43 (7.4) and 32 (36.4). The presence of vanillin from lignin photocatalytic degradation has been reported by Ksibi et al. (2003). Figure 4.13 presents the structure formulas of by-products of lignin degradation. The analysis of residue showed the presence of some lignin derivatives such as 2-methylbenzaldehyde, 2,4-dimethylbenzaldehyde and 4-hydroxy-3-methoxybenzaldehyde (vanillin). Moreover, other by-products detected in the reaction previously had not been observed.



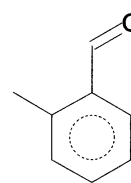
2,6-Dimethyl-5-methylphenyl  
aminopyridine-3,4-dicarboxyimide



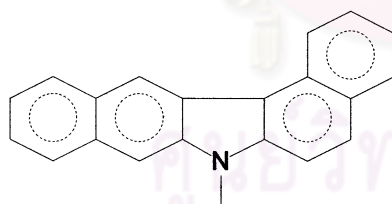
1-Methyl-2-phenylindole



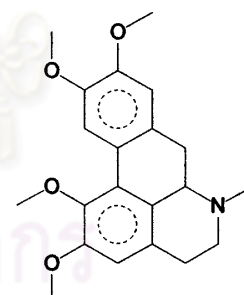
2-Ethylacridine



2-Methylbenzaldehyde

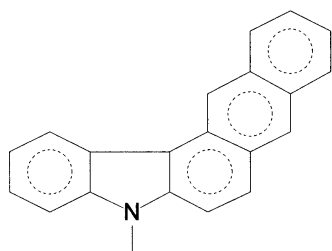


7H-Dibenzo[b,g]carbazole, 7-methyl-

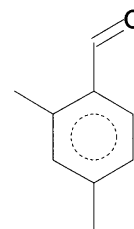


Glaucine

Figure 4.13 Structure formulas of by-products of lignin degradation



5H-Naphtho[2,3-c]carbazole, 5-methyl-



2,4-Dimethylbenzaldehyde

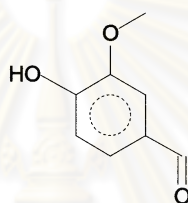
4-Hydroxy-3-methoxybenzaldehyde  
(vanillin)

Figure 4.13 Structure formulas of by-products of lignin degradation (continuous)

ศูนย์วิทยทรัพยากร  
จุฬาลงกรณ์มหาวิทยาลัย

## 4.2 Treatment of 2,4-DCP Synthetic Wastewater

The experiments in this part were carried out with 2,4-DCP synthetic wastewaters in order to study the performance of supervibration-photocatalytic reactor for treatment of 2,4-DCP to obtain the optimum operating conditions, study the reaction kinetics of 2,4-DCP photocatalytic degradation and identify the by-products occurred from 2,4-DCP degradation. Treatment efficiencies of 2,4-DCP by supervibration-photocatalytic reactor were studied under different initial pH (5, 6, 7, 8 and 9), UV intensity (0, 6.3, 12.6 and 25.2 mW/cm<sup>2</sup>), vibration frequency (0, 20, 30, 40 and 50 Hz) and initial 2,4-DCP concentration (0.5, 1, 2.5 and 5 mg/l).

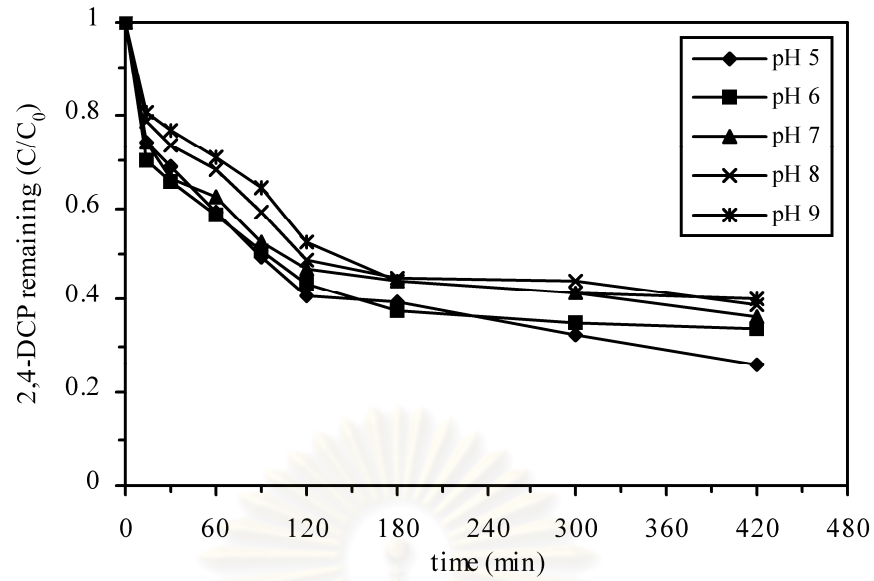
### 4.2.1 Effect of initial pH on degradation of 2,4-DCP in synthetic wastewater

The effect of initial pH on degradation of 2,4-DCP in synthetic wastewater was studied under various initial pH of solution. 2,4-DCP synthetic wastewater of 5 mg/l was prepared in the experiment and treated under five different initial pH levels as 5, 6, 7, 8 and 9. The photocatalytic process was carried out with a constant UV intensity of 6.3 mW/cm<sup>2</sup> and vibration frequency of 30 Hz. Figure 4.14 illustrates effect of initial pH on 2,4-DCP degradation by supervibration-photocatalytic reactor. The ultimate 2,4-DCP removal efficiencies were 66.14% (pH 6), 63.62% (pH 7), 60.87% (pH 8) and 59.71% (pH 9) within 420 min. For the optimum initial pH at 5, 2,4-DCP concentration was reduced from 5 mg/l to 1.30 mg/l ( $C/C_0 = 0.26$ ) with a capacity of 73.99% after the same time. The results indicate that the 2,4-DCP removal efficiencies were increased with the decrease in the initial pH.

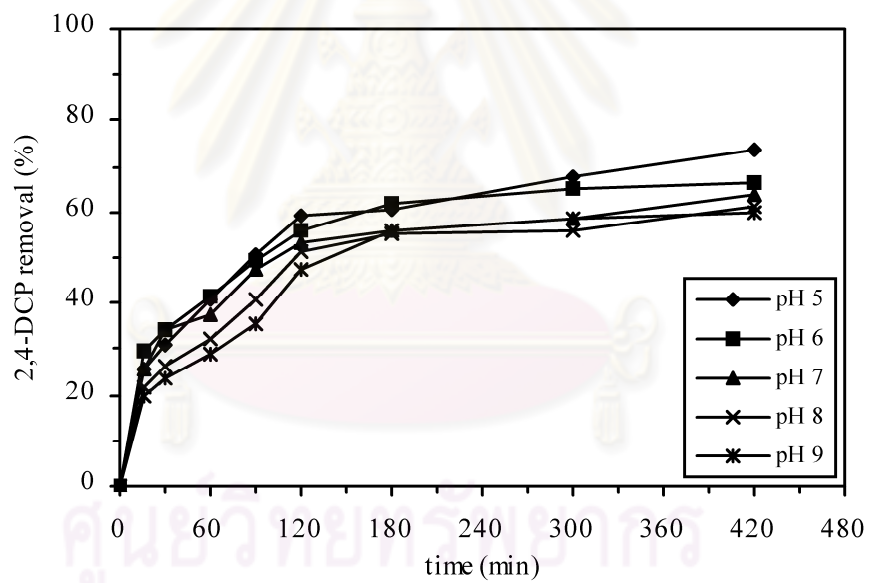
The kinetic expression in terms of Langmuir-Hinshelwood (Konstantinou and Albanis, 2004; Kumar et al., 2008; Valente et al., 2006) describing photocatalytic degradation of 2,4-DCP and a first order reaction is induced as

$$\ln\left(\frac{C_0}{C}\right) = kKt = k_{ap}t \quad , \quad (26)$$

where  $C_0$  is the initial 2,4-DCP concentration (mg/l) and  $C$  is 2,4-DCP concentration (mg/l) at any time  $t$  (min).  $k$  is the true rate constant (mg/l min<sup>-1</sup>) and  $K$  is the constant



(a)



(b)

Figure 4.14 The effect of initial pH on degradation of 2,4-DCP in synthetic wastewater: 2,4-DCP remaining (a) and removal efficiency (b) (initial 2,4-DCP concentration = 5 mg/l, UV intensity = 6.3 mW/cm<sup>2</sup>, vibration frequency = 30 Hz)



of adsorption equilibrium (l/mg).  $k_{ap}$  is the apparent rate constant of first order reaction ( $\text{min}^{-1}$ ). By plotting  $\ln(C_0/C)$  versus time, the apparent rate constant ( $k_{ap}$ ) can be determined from the slope of the curve obtained (equation (24)) as shown in Figure 4.15 and the initial degradation rate ( $r_0$ ) ( $\text{mg/l min}^{-1}$ ) can be represented as presented in equation (25).

$$r_0 = k_{ap} C_0 \quad (27)$$

The apparent rate constant of first order reaction ( $k_{ap}$ ) and the initial degradation rate ( $r_0$ ) of Langmuir-Hinshelwood kinetic of 2,4-DCP photodegradation after 120 min in Table 4.6 shows that at optimum initial pH (pH 5), the highest  $k_{ap}$  as  $8 \times 10^{-3} \text{ min}^{-1}$  and the highest  $r_0$  as  $40 \times 10^{-3} \text{ mg/l min}^{-1}$  were achieved. When initial pH decreased from 9, 8, 7 and 6 to 5, the apparent rate constant of first order reaction ( $k_{ap}$ ) were increased from  $5.5 \times 10^{-3}$ ,  $6.2 \times 10^{-3}$ ,  $7.1 \times 10^{-3}$  and  $7.7 \times 10^{-3}$  to  $8 \times 10^{-3} \text{ min}^{-1}$ , respectively and the initial degradation rate ( $r_0$ ) were increased from  $27.5 \times 10^{-3}$ ,  $31 \times 10^{-3}$ ,  $35.5 \times 10^{-3}$  and  $38.5 \times 10^{-3}$  to  $40 \times 10^{-3} \text{ mg/l min}^{-1}$ , respectively after 120 min (as shown in Table 4.6). This phenomenon followed the same trend as 2,4-DCP removal.

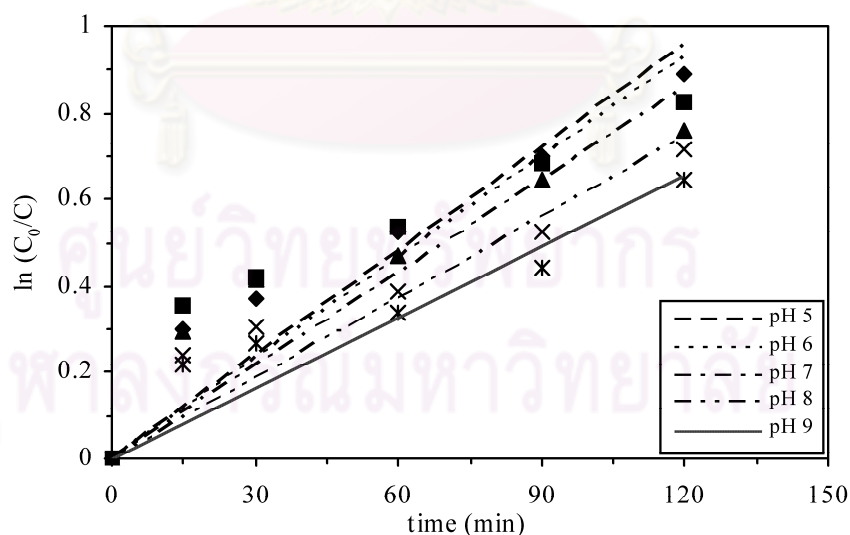


Figure 4.15 Linear transform  $\ln(C_0/C)$  vs. time for 2,4-DCP degradation at various initial pH

Bayarri et al. (2005) and Pandiyan et al. (2002) obtained similar results in which 2,4-DCP removal was higher under acidic conditions. The role of pH as important parameter in the photocatalytic reaction influences the surface charge properties and the adsorption behavior of TiO<sub>2</sub> (Gaya and Abdullah, 2008). The TiO<sub>2</sub> point of zero charge (pzc) is between pH 5.6 and 6.4. Therefore, depending on the pH, the TiO<sub>2</sub> surface is charged positively (pH < pzc) and negatively (pH > pzc) that has a significant effect on the adsorption properties of TiO<sub>2</sub>. It can be assumed that the molecule of 2,4-DCP is mostly in the un-ionized or negative charge form under acidic pH values and then, it can be more easily adsorbed onto the TiO<sub>2</sub> surface, whereas for alkaline conditions, 2,4-DCP and TiO<sub>2</sub> surface are mostly charged negatively so can exist a repulsion between both compounds. On the other hand, under acidic conditions, a superoxide radical (O<sub>2</sub><sup>•-</sup>) reacts with a hydrogen ion (H<sup>+</sup>) and produce a perhydroxyl radical (HO<sub>2</sub><sup>•</sup>). Consequently, the HO<sub>2</sub><sup>•</sup> can form hydrogen peroxide (H<sub>2</sub>O<sub>2</sub>), which in turn gives rise to the OH<sup>•</sup> (De Lasa et al., 1992).

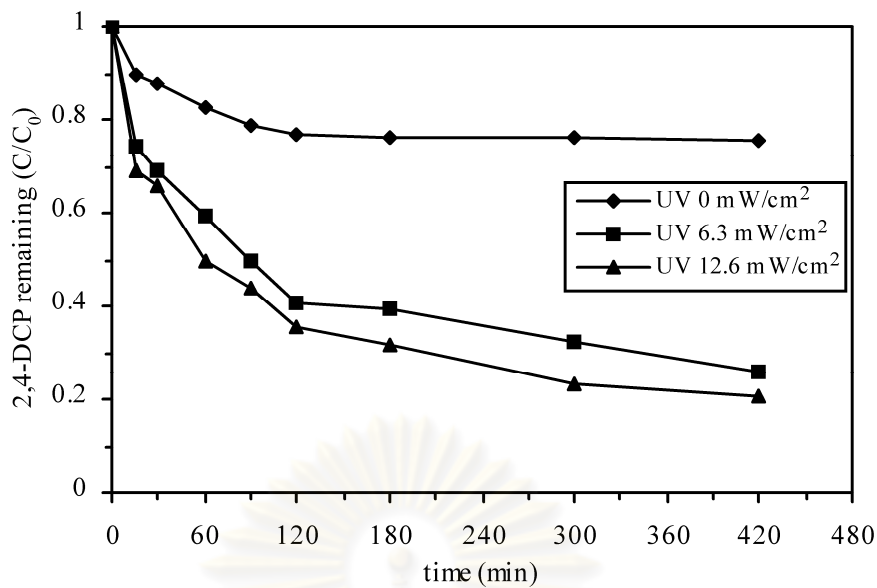
Table 4.6  $k_{ap}$  and  $r_0$  of first order kinetic for 2,4-DCP degradation at various initial pH

pH	$k_{ap}$ (min <sup>-1</sup> )	$r_0$ (mg/l min <sup>-1</sup> )	Coefficient (R <sup>2</sup> )
5	$8 \times 10^{-3}$	$40 \times 10^{-3}$	0.8845
6	$7.7 \times 10^{-3}$	$38.5 \times 10^{-3}$	0.7389
7	$7.1 \times 10^{-3}$	$35.5 \times 10^{-3}$	0.7566
8	$6.2 \times 10^{-3}$	$31 \times 10^{-3}$	0.8685
9	$5.5 \times 10^{-3}$	$27.5 \times 10^{-3}$	0.8661

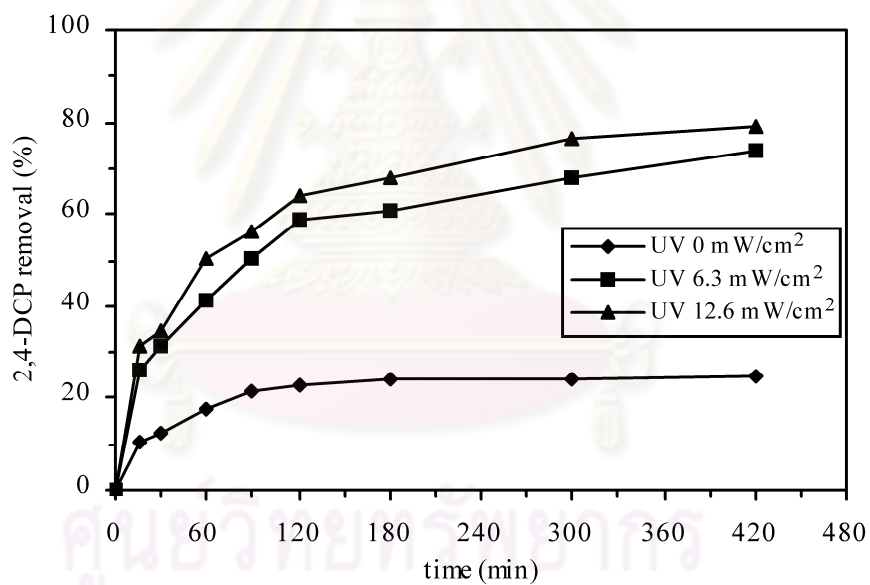
Note : reaction time = 120 min

#### 4.2.2 Effect of UV intensity on degradation of 2,4-DCP in synthetic wastewater

The effect of UV intensity on 2,4-DCP degradation by supervibration-photocatalytic reactor was studied using different UV intensities as 0, 6.3 and 12.6 mW/cm<sup>2</sup>. The experiment was repeated at a constant of optimum initial pH 5 and vibration frequency of 30 Hz. The results depicted in Figure 4.16 indicate that the efficiencies of 2,4-DCP photocatalytic oxidation were higher with a higher UV intensity for 420 min. The initial 2,4-DCP concentration as 5 mg/l was reduced to 1.04 mg/l ( $C/C_0 = 0.21$ ) after 420 min using UV intensity of 12.6 mW/cm<sup>2</sup>. 2,4-DCP removal efficiencies of the reactor with 6.3 and 12.6 mW/cm<sup>2</sup> of UV intensity were 73.99% and 79.14%, respectively, whereas the absence of UV light induced low 2,4-DCP removal as 24.78%. It might be due to the photocatalytic degradation not occurring, but some molecules of 2,4-DCP might be adsorbed on the inner or outer of surface of TiO<sub>2</sub> film. Figure 4.17 shows the plotting of  $\ln(C_0/C)$  versus time under various UV intensity to obtain slope of the curve as the apparent rate constant ( $k_{ap}$ ). The apparent rate constant of first order reaction ( $k_{ap}$ ) and the initial degradation rate ( $r_0$ ) of Langmuir-Hinshelwood kinetic for 2,4-DCP removal after 120 min at different UV intensity show that under UV intensity of 12.6 mW/cm<sup>2</sup>, the highest  $k_{ap}$  as  $9.5 \times 10^{-3} \text{ min}^{-1}$  and the highest  $r_0$  as  $47.5 \times 10^{-3} \text{ mg/l min}^{-1}$  were achieved. The apparent rate constant of first order reaction ( $k_{ap}$ ) of 2,4-DCP degradation were increased from  $2.6 \times 10^{-3}$  and  $8 \times 10^{-3}$  to  $9.5 \times 10^{-3} \text{ min}^{-1}$  and the initial degradation rate ( $r_0$ ) were increased from  $13 \times 10^{-3}$  and  $40 \times 10^{-3}$  to  $47.5 \times 10^{-3} \text{ mg/l min}^{-1}$ , when UV intensity increased from 0 and 6.3 to 12.6 mW/cm<sup>2</sup>, respectively (as listed in Table 4.7). This phenomenon followed the same trend as 2,4-DCP removal. The results indicate that an increase in UV intensity could significantly enhance 2,4-DCP removal. The considerably more effectiveness of 12.6 mW/cm<sup>2</sup> radiation was attributed to the shorter penetration capability of higher energy photon, so there were more electron-hole pairs and OH<sup>•</sup> available for the target compound as 2,4-DCP. In addition, reaction temperature might increase with increasing in UV intensity. Previous research indicated that increasing the reaction temperature increased the rate of all reactions occurring in the system (Zeltner, Hill, and Anderson, 1993; Hofstadler et al., 1994).



(a)



(b)

Figure 4.16 The effect of UV intensity on degradation of 2,4-DCP in synthetic wastewater: 2,4-DCP remaining (a) and removal efficiency (b) (initial 2,4-DCP concentration = 5 mg/l, initial pH = 5, vibration frequency = 30 Hz)

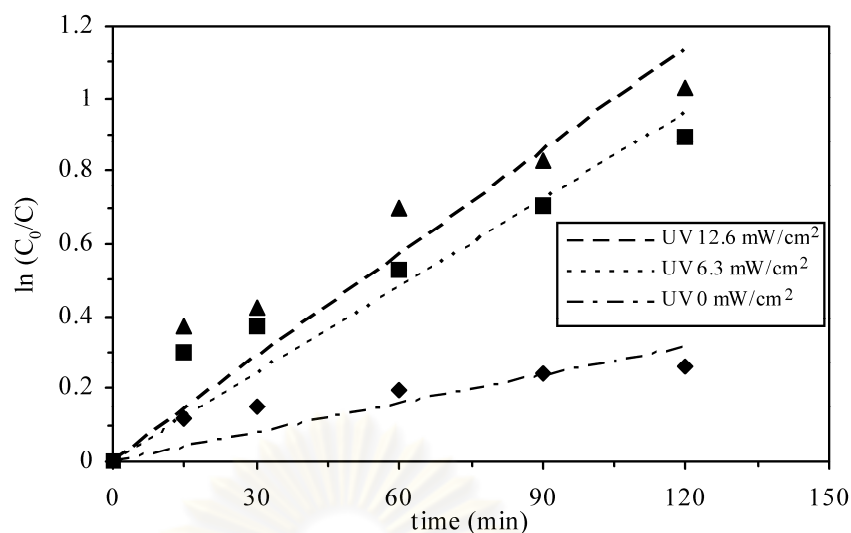


Figure 4.17 Linear transform  $\ln(C_0/C)$  vs. time for 2,4-DCP degradation at various UV intensity

Table 4.7  $k_{ap}$  and  $r_0$  of first order kinetic for 2,4-DCP degradation at various UV intensity

UV intensity (mW/cm <sup>2</sup> )	$k_{ap}$ (min <sup>-1</sup> )	$r_0$ (mg/l min <sup>-1</sup> )	Coefficient ( $R^2$ )
0	$2.6 \times 10^{-3}$	$13 \times 10^{-3}$	0.7606
6.3	$8 \times 10^{-3}$	$40 \times 10^{-3}$	0.8845
12.6	$9.5 \times 10^{-3}$	$47.5 \times 10^{-3}$	0.8485

Note : reaction time = 120 min

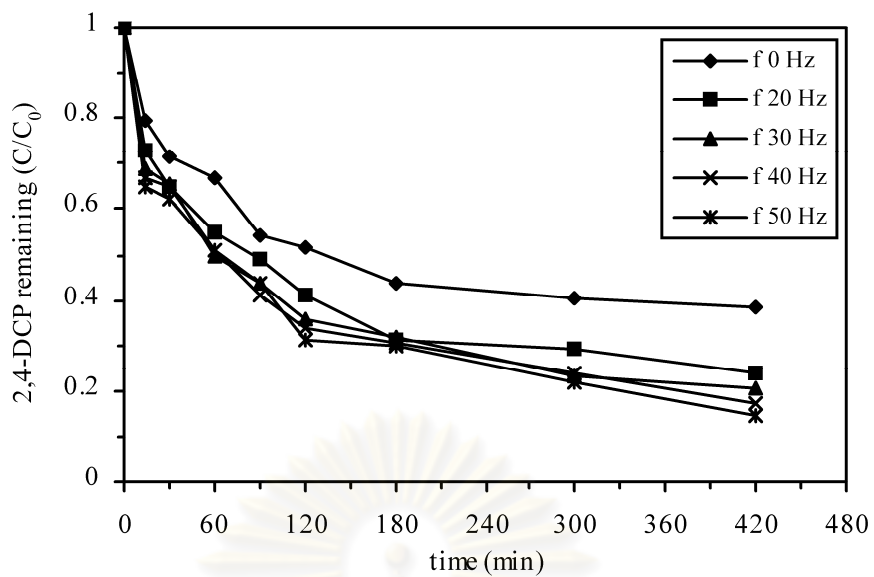
Similar results were previously observed for photocatalytic degradation of endocrine disrupting chemicals by Nakashima et al. (2002), which found that a low intensity light source took a longer time to compose than in cases of a high intensity light source. An increase in UV intensity always increases the reaction rate until the reaction is mass transfer limited (De Lasa et al., 1992). Furthermore, Bayarri, Abellán et al. (2007) studied the effect of each type of radiation as UV-A (300 nm) and UV-ABC (235 nm) for 2,4-DCP degradation by UV/TiO<sub>2</sub>. The source of radiation was a xenon lamp (PHILIPS XOP-15-OF, 1000 W). Solution of 2,4-DCP were prepared

from 100-120 mg/l, loaded in the reservoir tank (1 liters) with 0.5 g/l of TiO<sub>2</sub> (Degussa P25). The results demonstrated that UV-ABC radiation was more effective than UV-A. The 2,4-DCP photocatalysis and the TOC removal was about 20% higher with UV-ABC than with UV-A.

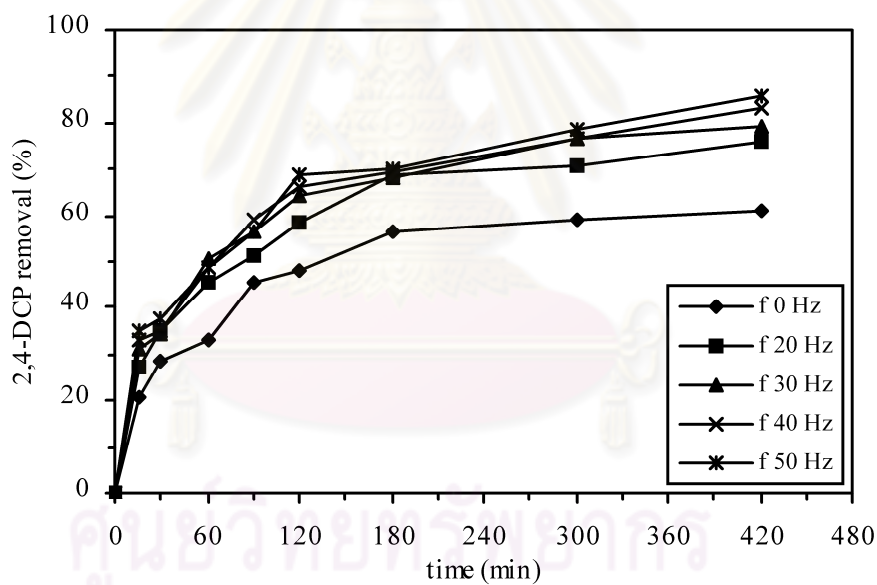
#### 4.2.3 Effect of vibration frequency on degradation of 2,4-DCP in synthetic wastewater

The 2,4-DCP solutions were prepared at the same concentration of 5 mg/l for the study on effect of vibration frequency on degradation of 2,4-DCP in synthetic wastewater under various vibration frequencies as 0, 20, 30, 40 and 50 Hz at a constant of optimum initial pH 5 and optimum UV intensity of 12.6 mW/cm<sup>2</sup>. Figure 4.18 demonstrates the decrease of 2,4-DCP, which indicated the effect of vibration frequency on photocatalysis under the conditions used here. The removal efficiencies of 2,4-DCP were 75.98% (20 Hz), 79.14% (30 Hz) and 83.06% (40 Hz). For the optimum vibration frequency as 50 Hz, 2,4-DCP concentration decreased from 5 mg/l to 0.72 mg/l ( $C/C_0 = 0.14$ ) within 420 min, which corresponds to a destructive efficiency of 85.68%. Although there was an absence of vibration frequency (0 Hz), the reactor could remove 2,4-DCP at 61.30% for the same time because of photocatalytic degradation (UV/TiO<sub>2</sub>). Figure 4.19 shows the plotting of  $\ln(C_0/C)$  versus time under various vibration frequency to obtain slope of the curve as the apparent rate constant ( $k_{ap}$ ). The apparent rate constant of first order reaction ( $k_{ap}$ ) and the initial degradation rate ( $r_0$ ) of Langmuir-Hinshelwood kinetic were followed the same trend as 2,4-DCP removal. When vibration frequency increased from 0, 20, 30 and 40 to 50 Hz, the apparent rate constant of first order reaction ( $k_{ap}$ ) of 2,4-DCP degradation were increased from  $6.3 \times 10^{-3}$ ,  $8.2 \times 10^{-3}$ ,  $9.5 \times 10^{-3}$  and  $9.9 \times 10^{-3}$  to  $10.2 \times 10^{-3} \text{ min}^{-1}$ , respectively and the initial degradation rate ( $r_0$ ) were increased from  $31.5 \times 10^{-3}$ ,  $41 \times 10^{-3}$ ,  $47.5 \times 10^{-3}$  and  $49.5 \times 10^{-3}$  to  $51 \times 10^{-3} \text{ mg/l min}^{-1}$ , respectively after 120 min as presented in Table 4.8. 2,4-DCP removal efficiencies were increased with the increase in vibration frequency. This may be because, in the condition of higher vibration frequency, the powerful 3-dimensional agitating flow in the reaction tank is higher. Therefore, the good contact between 2,4-DCP and TiO<sub>2</sub> can be enhanced, then higher decomposition rate can be obtained.





(a)



(b)

Figure 4.18 The effect of vibration frequency on degradation of 2,4-DCP in synthetic wastewater: 2,4-DCP remaining (a) and removal efficiency (b) (initial 2,4-DCP concentration = 5 mg/l, initial pH = 5, UV intensity = 12.6 mW/cm<sup>2</sup>)

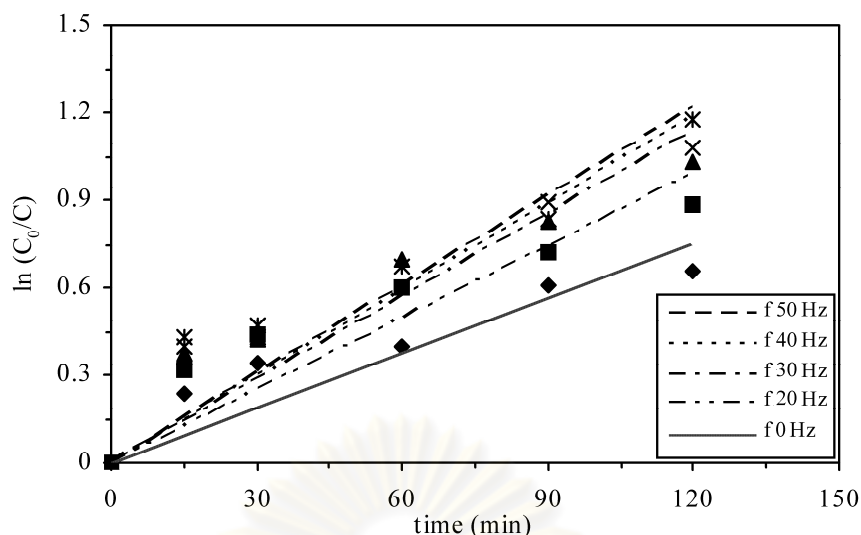


Figure 4.19 Linear transform  $\ln(C_0/C)$  vs. time for 2,4-DCP degradation at various vibration frequency

Table 4.8  $k_{ap}$  and  $r_0$  of first order kinetic for 2,4-DCP degradation at various vibration frequency

Vibration frequency (Hz)	$k_{ap}$ ( $\text{min}^{-1}$ )	$r_0$ ( $\text{mg/l min}^{-1}$ )	Coefficient ( $R^2$ )
0	$6.3 \times 10^{-3}$	$31.5 \times 10^{-3}$	0.8224
20	$8.2 \times 10^{-3}$	$41 \times 10^{-3}$	0.8083
30	$9.5 \times 10^{-3}$	$47.5 \times 10^{-3}$	0.8485
40	$9.9 \times 10^{-3}$	$49.5 \times 10^{-3}$	0.8669
50	$10.2 \times 10^{-3}$	$51 \times 10^{-3}$	0.8520

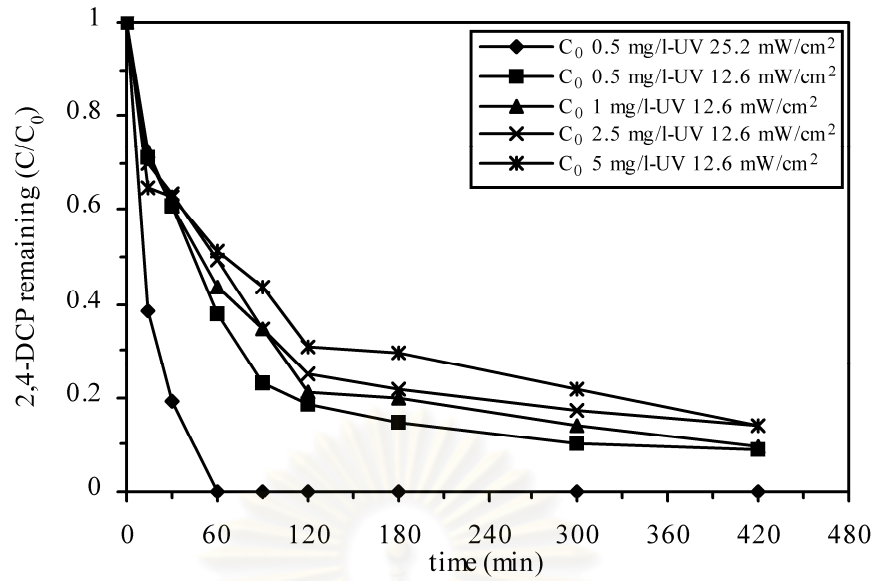
Note : reaction time = 120 min

The previous research for treatment of 2,4-DCP using UV/TiO<sub>2</sub> process and mechanical agitation were observed by González et al. (2010), they investigated 2,4-DCP degradation by UV/TiO<sub>2</sub> and magnetic stirrers under conditions as 25 mW/cm<sup>2</sup> of UV intensity, 10 mg/l of suspended TiO<sub>2</sub> and 15 mg/l of initial concentration at pH 4.5. 2,4-DCP removal efficiency was about 60% after 180 min, whereas the supervibration-photocatalytic reactor in present work using supervibration agitator,

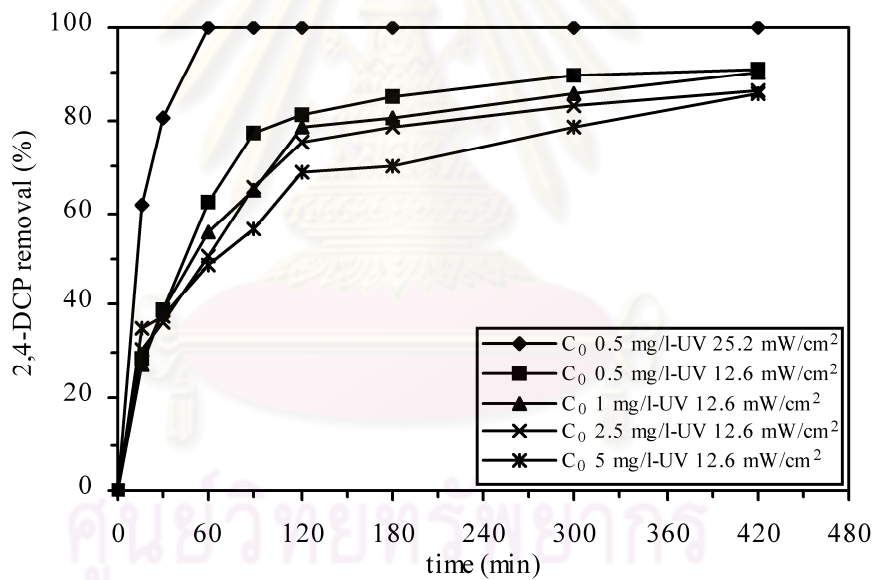
treating 5 mg/l of 2,4-DCP under initial pH 5, UV intensity of 12.6 mW/cm<sup>2</sup> and vibration frequency of 50 Hz, could remove 2,4-DCP up to 70.34% in the same time. Therefore, a supervibration-photocatalytic reactor has higher performance in 2,4-DCP removal and faster reaction rate than that of previous research works. This is because the fluid flow rate produced by the supervibration agitator is superior to that was produced by magnetic stirrers.

#### 4.2.4 Effect of initial 2,4-DCP concentration on degradation of 2,4-DCP in synthetic wastewater

The initial 2,4-DCP concentration was also studied as a variable parameter to investigate the effect of initial 2,4-DCP concentration on degradation of 2,4-DCP in synthetic wastewater. Figure 4.20 presents 2,4-DCP removal under different initial 2,4-DCP concentrations as 0.5, 1, 2.5 and 5 mg/l. When optimum initial pH 5, optimum UV intensity of 12.6 mW/cm<sup>2</sup> and optimum vibration frequency of 50 Hz were kept constant, 2,4-DCP concentration decreased from 0.5 mg/l at initial to 0.04 mg/l ( $C/C_0 = 0.09$ ) with the efficiency up to 91.20% after 420 min. The removal efficiencies of 2,4-DCP for the initial 2,4-DCP concentration of 1 mg/l, 2.5 mg/l and 5 mg/l were 90.20%, 86.12% and 85.68%, respectively in the same time. Figure 4.21 shows the plotting of  $\ln(C_0/C)$  versus time under various initial 2,4-DCP concentration to obtain slope of the curve as the apparent rate constant ( $k_{ap}$ ). Table 4.9 shows that when the initial 2,4-DCP concentration increased from 0.5, 1 and 2.5 to 5 mg/l, the apparent rate constant of first order reaction ( $k_{ap}$ ) of Langmuir-Hinshelwood kinetic were decreased from  $15.1 \times 10^{-3}$ ,  $12.9 \times 10^{-3}$  and  $11.9 \times 10^{-3}$  to  $10.2 \times 10^{-3}$  min<sup>-1</sup>, respectively after 120 min, whereas the initial degradation rate ( $r_0$ ) were increased from  $7.6 \times 10^{-3}$ ,  $12.9 \times 10^{-3}$  and  $29.8 \times 10^{-3}$  to  $51 \times 10^{-3}$  mg/l min<sup>-1</sup>, respectively after the same time. The only  $k_{ap}$  had the same trend as removal efficiency of 2,4-DCP. The  $r_0$  increased with  $C_0$  (the initial concentration), since in the product  $k_{ap}C_0$ , the increase in concentration was more significant than the variation in  $k_{ap}$  values.



(a)



(b)

Figure 4.20 The effect of initial concentration on degradation of 2,4-DCP in synthetic wastewater: 2,4-DCP remaining (a) and removal efficiency (b) (initial pH = 5, vibration frequency = 50 Hz)

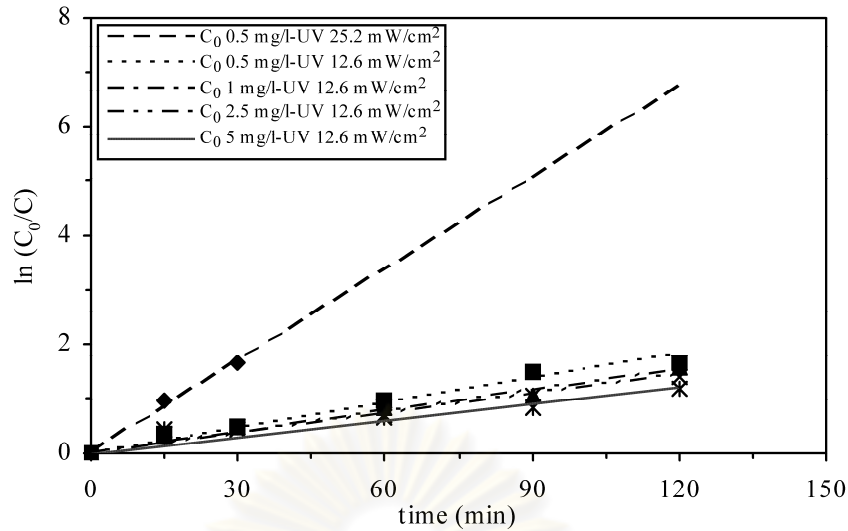


Figure 4.21 Linear transform  $\ln(C_0/C)$  vs. time for 2,4-DCP degradation in various initial concentration

In this work, the rate constant ( $k$ ) and adsorption constant ( $K$ ) were calculated using the Langmuir-Hinshelwood model, considering the following rate and initial concentrations:

$$r_0 = \frac{-dC}{dt} = \frac{kKC_0}{(1 + KC_0)} \quad (28)$$

This equation can be rearranged into linear form:

$$\frac{1}{r_0} = \frac{1}{kK} \cdot \frac{1}{C_0} + \frac{1}{k} \quad (29)$$

where  $1/r_0$  is the dependent variable and  $1/C_0$  is the independent variable. By plotting  $1/r_0$  versus  $1/C_0$ ,  $1/kK$  can be obtained from the slope of the line and  $1/k$  can be obtained from the point at which the line crosses the  $y$ -axis (Valente et al., 2006). The linearization of the curve in Figure 4.22, plotting  $1/r_0$  versus  $1/C_0$ , from 0.5 to 5 mg/l of 2,4-DCP concentration describe a linear behavior with linear coefficient  $R^2 = 0.9947$  and the rate constant ( $k$ ) and adsorption constant ( $K$ ) are shown in Table 4.9.

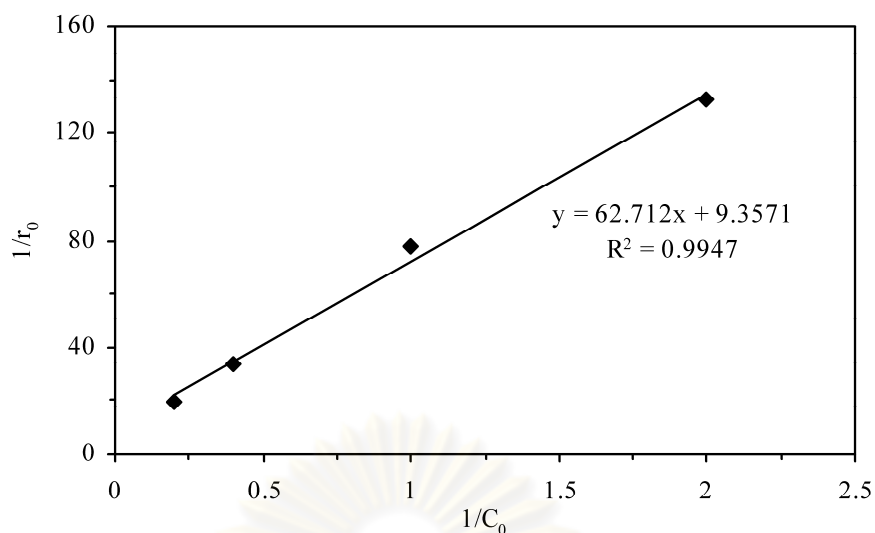


Figure 4.22 Linear transform  $1/r_0$  vs.  $1/C_0$  for 2,4-DCP degradation

Table 4.9  $k_{ap}$  and  $r_0$  of first order kinetic for 2,4-DCP degradation in various initial concentration

Initial concentration (mg/l)	$k_{ap}$ ( $\text{min}^{-1}$ )	$r_0$ ( $\text{mg/l min}^{-1}$ )	Coefficient ( $R^2$ )	k ( $\text{mg/l min}^{-1}$ )	K (l/mg)
0.5	$15.1 \times 10^{-3}$	$7.6 \times 10^{-3}$	0.9766	0.11	$149.21 \times 10^{-3}$
1	$12.9 \times 10^{-3}$	$12.9 \times 10^{-3}$	0.9736		
2.5	$11.9 \times 10^{-3}$	$29.8 \times 10^{-3}$	0.9646		
5	$10.2 \times 10^{-3}$	$51 \times 10^{-3}$	0.8520		
0.5 mg/l-UV 25.2 mW/cm <sup>2</sup>	$56.3 \times 10^{-3} *$	$28.2 \times 10^{-3} *$	0.9890 *	-	-

Note : reaction time = 120 min

: \* reaction time = 30 min

The apparent rate constant ( $k_{ap}$ ) of 2,4-DCP degradation were decreased with the increase in the initial concentration. When the initial 2,4-DCP concentration becomes higher, the adsorption of 2,4-DCP molecules on the surface of  $\text{TiO}_2$  is rate limiting. Photoreactive site on  $\text{TiO}_2$  surface is decreased because of adsorption of both 2,4-

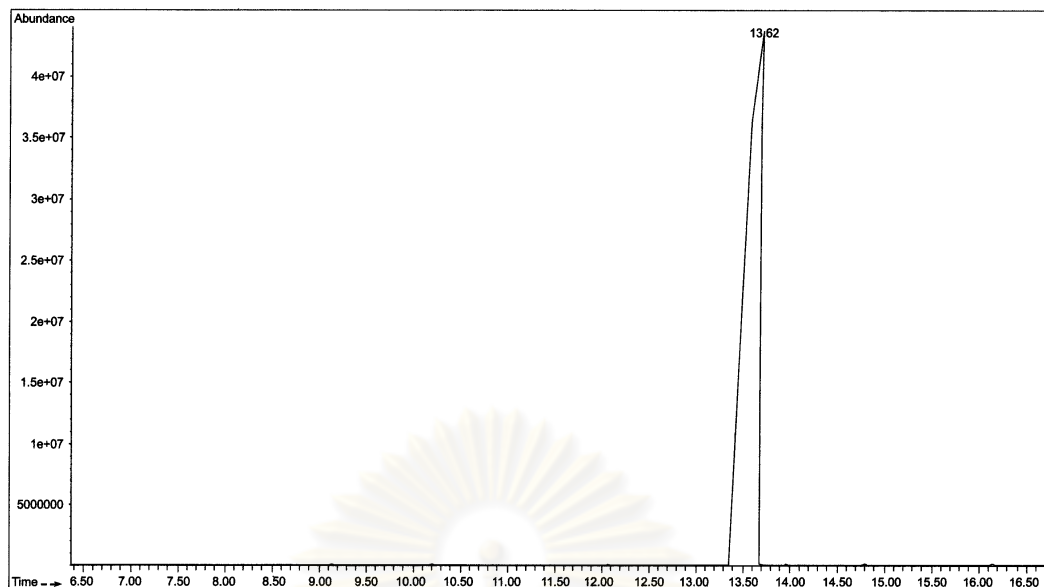


DCP and its intermediates. The similar result was observed by Kusvuran et al. (2005). They examined photocatalytic degradation of 2,4-DCP by UV/TiO<sub>2</sub> (anatase). The experiments were carried out in a 250 ml cylindrical glass reactor with magnetic stirrer, which contain 0.5 g/l of TiO<sub>2</sub> and maxima radiation at 365 nm. The 2,4-DCP solutions were prepared at 0.1-0.5 mM of initial concentration at pH 3. The results was found that pseudo-first-order kinetic rate constants of 2,4-DCP removal were decreased with the increase in the initial concentration. Pseudo-first order kinetic rate constants of 2,4-DCP were decreased from 0.0259 (0.1 mM) to 0.0061 min<sup>-1</sup> (0.5 mM) with increasing initial concentration.

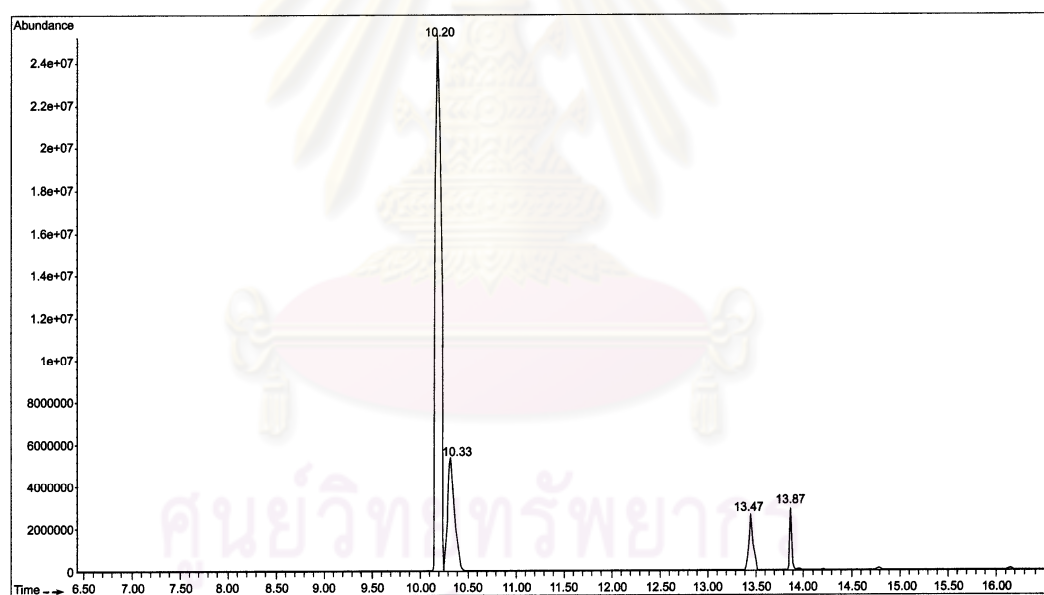
Additional experiment with an increase in UV intensity to 25.2 mW/cm<sup>2</sup>, initial pH 5, vibration frequency of 50 Hz and initial 2,4-DCP concentration of 0.5 mg/l was carried out to improve system performance. The results were found that 2,4-DCP degradation was completed within 60 min as shown in Figure 4.20. The apparent rate constant of first order reaction ( $k_{ap}$ ) and the initial degradation rate ( $r_0$ ) of Langmuir-Hinshelwood kinetic were  $56.3 \times 10^{-3} \text{ min}^{-1}$  and  $28.2 \times 10^{-3} \text{ mg/l min}^{-1}$ , respectively, after 30 min as listed in Table 4.9. The results indicate that an increase in UV intensity as 25.2 mW/cm<sup>2</sup> significantly enhanced 2,4-DCP removal since the increase in UV intensity can promote the hydroxyl radical (OH<sup>•</sup>) formation in the photocatalytic reaction.

#### 4.2.5 Identification of the by-products of 2,4-DCP degradation

The by-products as aromatic compounds of 2,4-DCP degradation by supervibration-photocatalytic reactor were also investigated. The identification was carried out using GC-MS. The photocatalytic degradation of 2,4-DCP was studied under treatment conditions as initial pH 5, UV intensity of 12.6 mW/cm<sup>2</sup> and vibration frequency of 50 Hz. The initial concentration of 2,4-DCP was selected at 5 mg/l for the clear presence of by-product peak height. The GC-MS chromatogram in Figure 4.23 shows that 2,4-DCP peak only appeared at retention time 13.62 min for starting of irradiation time and for reaction time at 420 min, the 2,4-DCP peak height at retention time 13.47 min decreased during the photochemical reaction, while new signals were detected.



(a)



(b)

Figure 4.23 GC-MS chromatogram of by-products from 2,4-DCP degradation for reaction time: 0 min (a) and 420 min (b)

Table 4.10 Fragmentation pattern of by-products from 2,4-DCP degradation identified by GC-MS

Compounds	Retention time (min)	m/z (% abundance)
Phenol	10.20	95 (6.9); 94 (100); 66 (23); 65 (18); 63 (3.9); 55 (5); 50 (2.9)
2-Chlorophenol (2-CP)	10.33	131 (2.2); 130 (32.6); 129 (6.9); 128 (100); 100 (4); 99 (3.3); 92 (11.5); 73 (3.9); 65 (10); 64 (26.9); 63 (14.1); 62 (3.1); 53 (2.2)
4-Chlorophenol (4-CP)	13.87	131 (2.2); 130 (32.9); 129 (7.1); 128 (100); 102 (3.3); 101 (2.2); 100 (9.9); 99 (5.2); 93 (2.9); 75 (2.7); 74 (2.3); 73 (4.8); 65 (22); 64 (9.5); 63 (7.5); 62 (3.3); 61 (2.3); 53 (2.2)

From total by-products classified by their fragmentation pattern as shown in Table 4.10, the peak at retention time 10.20, 10.33 and 13.87 min were detected as phenol, 2-chlorophenol (2-CP) and 4-chlorophenol (4-CP), respectively. The mass spectrum of phenol showed characteristic peaks with fragmentation at m/z 95 (6.9); 94 (100); 66 (23); 65 (18); 63 (3.9); 55 (5) and 50 (2.9), whereas 2-chlorophenol showed peaks with fragmentation at m/z 131 (2.2); 130 (32.6); 129 (6.9); 128 (100); 100 (4); 99 (3.3); 92 (11.5); 73 (3.9); 65 (10); 64 (26.9); 63 (14.1); 62 (3.1) and 53 (2.2). Finally, 4-chlorophenol showed peaks with fragmentation at m/z 131 (2.2); 130 (32.9); 129 (7.1); 128 (100); 102 (3.3); 101 (2.2); 100 (9.9); 99 (5.2); 93 (2.9); 75 (2.7); 74 (2.3); 73 (4.8); 65 (22); 64 (9.5); 63 (7.5); 62 (3.3); 61 (2.3) and 53 (2.2). Figure 4.24 presents the structure formulas of by-products of 2,4-DCP degradation by supervibration-photocatalytic reactor. The similar results were previously found by Bayarri et al. (2005), Liu, Chen, and Yang (2009) and Pandiyan et al. (2002). The results reveal that occurred by-products have toxicity less than the parent compound

due to the toxic effect of chlorophenols are directly proportional to the degree of chlorination (Health Canada, 1987: online).

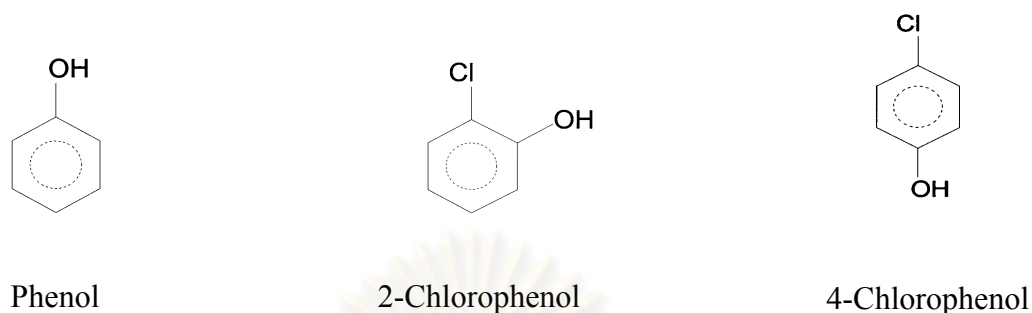


Figure 4.24 Structure formulas of by-products of 2,4-DCP degradation

#### 4.2.6 Proposed reaction pathway of 2,4-DCP degradation

In photocatalytic process, light of suitable energy generated electron-hole pairs. Both species can contribute to the organic substrate degradation since the potentials of the hole and the conduction band electron is sufficient to oxidize or reduce many organic molecules (Serpone and Pelizzetti, 1989). The pathway involving the reduction of the substrate by the conduction band electron can not be excluded, since chlorophenols can be oxidized but can also be reduced. Hydroxylation of chlorophenols through such a reduction pathway has been proposed earlier (Chen et al., 2004; Theurich, Lindner, and Bahnemann, 1996; Yin et al., 2010). In this study, a reaction pathway for photocatalytic degradation of 2,4-DCP based on the GC-MS data is proposed in Figure 4.25, in which the reductive dechlorination was proposed as the major decomposition route. The formation of the 4-chlorophenol (4-CP) and 2-chlorophenol (2-CP) is attributed to the reduction of 2,4-DCP by conduction band electron losing chloride ion at ortho and para position, respectively (Figure 4.25, reaction (a), (b), (e), (f)). A short-lived hydroxyphenyl radical can be formed by a reductive attack of an electron (conduction band) on 4-CP or 2-CP releasing a chloride ion (Figure 4.25, reaction (c), (g)). This radical may combine with a hydrogen atom in the presence of conduction band electron to form phenol (Figure 4.25, reaction (d), (h)). When benzene rings are opened to form aliphatic compounds

such as maleic acids, fumaric acids, formic acids and oxalic acids, eventually all these acids are completely mineralized into  $\text{CO}_2$  and  $\text{H}_2\text{O}$  (Chu et al., 2005; Lu and Gao, 2006).

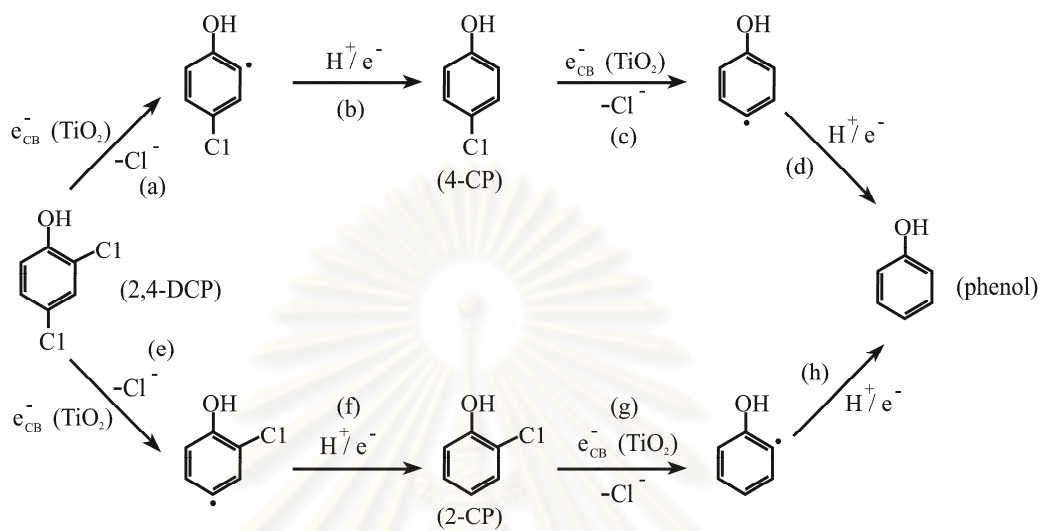


Figure 4.25 Proposed reaction pathway for photocatalytic degradation of 2,4-DCP

ศูนย์วิทยทรัพยากร  
จุฬาลงกรณ์มหาวิทยาลัย

### 4.3 Treatment of Mixed Synthetic Wastewater Containing Lignin and 2,4-DCP

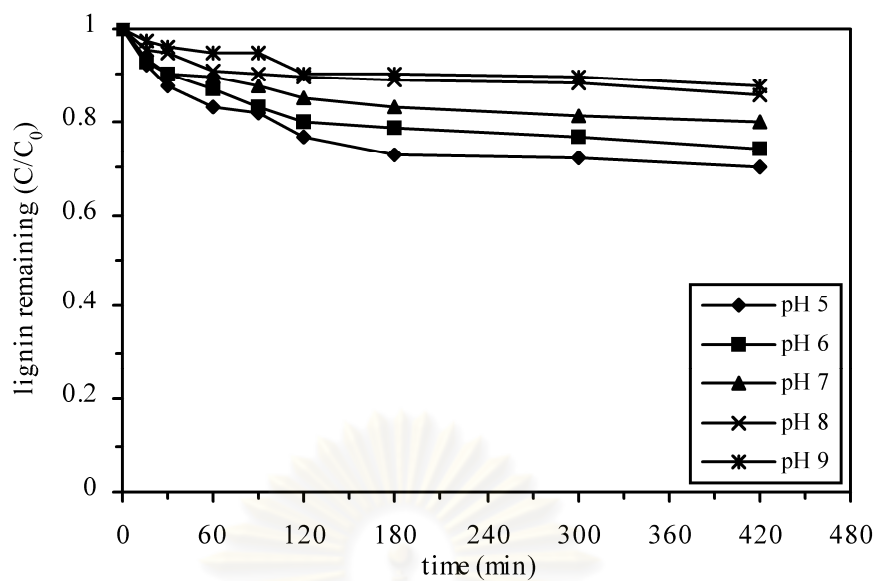
The performance of supervibration-photocatalytic reactor on treatment of lignin and 2,4-DCP in mixed synthetic wastewater were investigated to obtain the optimum operating conditions for lignin and 2,4-DCP removal. Mixed synthetic wastewater contained 400 mg/l of lignin and 5 mg/l of 2,4-DCP. Treatment efficiencies of lignin and 2,4-DCP by supervibration-photocatalytic reactor were studied under different initial pH (5, 6, 7, 8 and 9), UV intensity (0, 6.3, 12.6 and 25.2 mW/cm<sup>2</sup>) and vibration frequency (0, 20, 30, 40 and 50 Hz).

#### 4.3.1 Effect of initial pH on treatment of lignin and 2,4-DCP in mixed synthetic wastewater

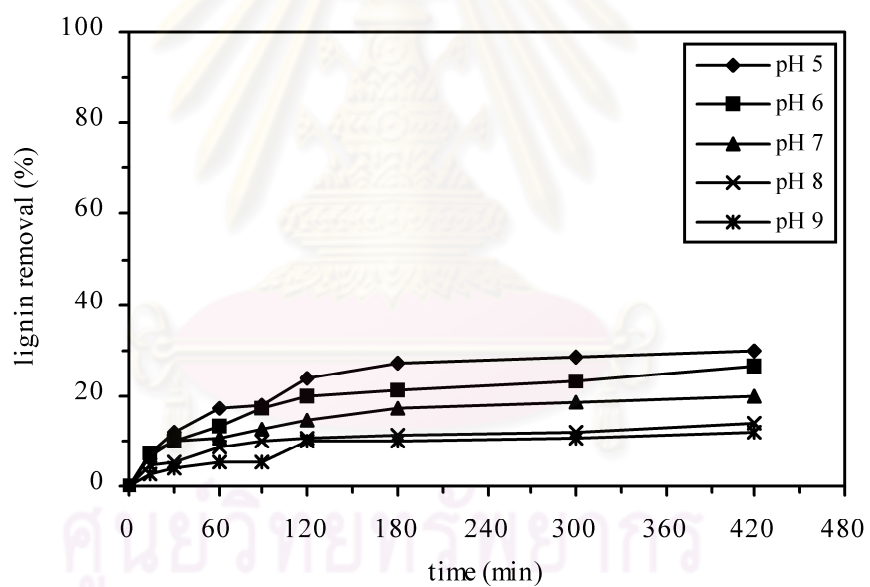
The effect of initial pH on degradation of lignin and 2,4-DCP in mixed synthetic wastewater was studied under five different initial pH levels as 5, 6, 7, 8 and 9. Mixed synthetic wastewater containing lignin and 2,4-DCP was prepared from 400 mg/l of lignin and 5 mg/l of 2,4-DCP solutions. The photocatalytic process was carried out with a constant of UV intensity of 6.3 mW/cm<sup>2</sup> and vibration frequency of 30 Hz.

Figure 4.26 shows the effect of initial pH on lignin degradation within 420 min. When the initial pH was 9, the removal efficiency was 12.02%. The removal efficiency was 14.10% when using pH 8. The degradation of lignin increased as initial pH decreased to initial pH 7 with 20% removal efficiency. When the initial pH was further decreased, the lignin degradation increased as illustrated in Figure 4.26. As initial pH was decreased from 6 to 5, the degradation efficiency increased from 26.27% to 30%, respectively. For the optimum initial pH as pH 5, lignin concentration was dropped from 400 mg/l down to 279.98 mg/l ( $C/C_0 = 0.70$ ) after 420 min. Figure 4.26 indicates that the initial pH that induced the best photocatalytic reaction on treatment of lignin in mixed synthetic wastewater was pH 5 as well as at all pH conditions, a fast degradation could be observed for initial times and later on it decrease. This is probably because for longer time, lignin had to compete with intermediates for the TiO<sub>2</sub> sites.





(a)



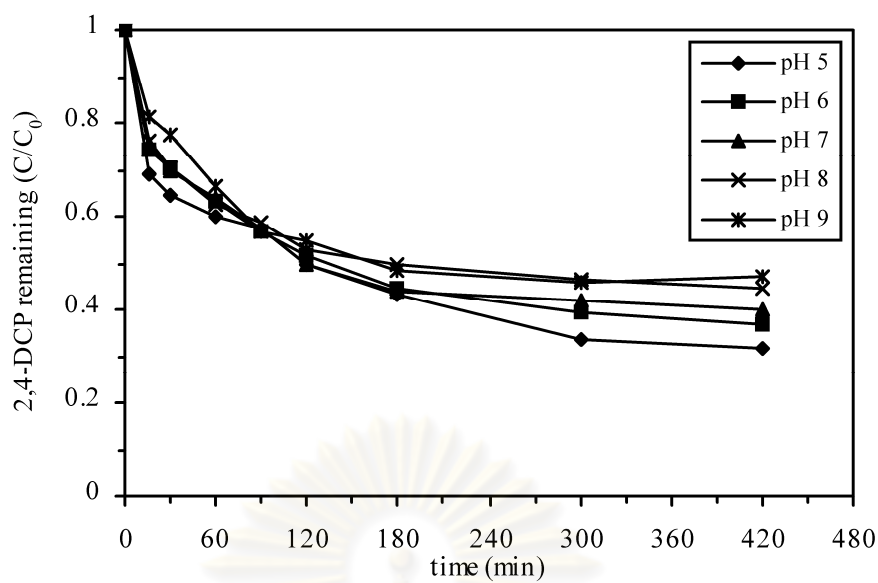
(b)

Figure 4.26 The effect of initial pH on degradation of lignin in mixed synthetic wastewater: lignin remaining (a) and removal efficiency (b) (initial lignin concentration = 400 mg/l, initial 2,4-DCP concentration = 5 mg/l, UV intensity = 6.3 mW/cm<sup>2</sup>, vibration frequency = 30 Hz)

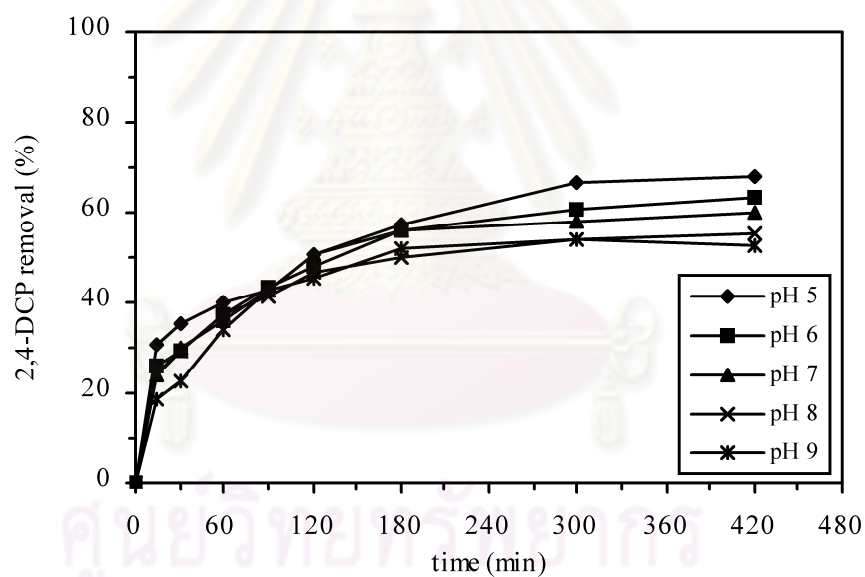
For 2,4-DCP, removal efficiency also followed the same trend as lignin removal. Figure 4.27 illustrates effect of initial pH on 2,4-DCP degradation by supervibration-photocatalytic reactor within 420 min. 2,4-DCP removal were increased from 53%, 55.42%, 60.01% and 63.03% to 68.19% as initial pH decreased, from 9, 8, 7 and 6 to 5, respectively. The highest 2,4-DCP removal as 68.19%, was achieved at initial pH 5, similar to case of lignin removal. For the optimum initial pH at 5, 2,4-DCP concentration was reduced from 5 mg/l to 1.59 mg/l ( $C/C_0 = 0.32$ ) after 420 min.

The summary data depicted in Figure 4.28 show that the effect of initial pH on the removal efficiencies of lignin and 2,4-DCP in mixed synthetic wastewater were similar trend. Since both lignin and 2,4-DCP removal efficiencies were increased with the decrease in the initial pH within 420 min. At every initial pH, removal efficiency of 2,4-DCP was more than that of lignin because the lignin concentration used in the treatment was higher than 2,4-DCP. Furthermore, lignin is very complex polymer and higher molecular weight than that of 2,4-DCP. When removal efficiencies of mixed synthetic wastewater and synthetic wastewater containing single pollutant were compared, lignin had an interference effect on 2,4-DCP removal by the system. For the optimum initial pH, the removal efficiency of 2,4-DCP in mixed synthetic wastewater was approximately 6% less than that in 2,4-DCP synthetic wastewater, whereas removal efficiency of lignin in mixed wastewater was not so different. This might be because yellow color of lignin in mixed synthetic wastewater inhibits UV light penetration into water, whereas 2,4-DCP synthetic wastewater is clear solution. On the other hand, more intermediates occurred of lignin competed in absorption of 2,4-DCP on the surface of  $TiO_2$ .

The pH of the solution can affect the adsorption of pollutants on the photocatalyst surface and the degradation of lignin and 2,4-DCP were increased with decreasing initial pH. This is attributed to the fact that  $TiO_2$  is amphoteric in aqueous solution, the point of zero charge ( $pH_{pzc}$ ) of  $TiO_2$  is between 5.6 and 6.4, thus below this value the  $TiO_2$  surface is positively charged and above it is negatively charged. At higher pH, 2,4-DCP exists as negatively charged species. Moreover, high pH favors the formation of carbonate ions which are effective scavengers of  $OH^-$  ions and can reduce the degradation rate.



(a)



(b)

Figure 4.27 The effect of initial pH on degradation of 2,4-DCP in mixed synthetic wastewater: 2,4-DCP remaining (a) and removal efficiency (b) (initial lignin concentration = 400 mg/l, initial 2,4-DCP concentration = 5 mg/l, UV intensity = 6.3 mW/cm<sup>2</sup>, vibration frequency = 30 Hz)

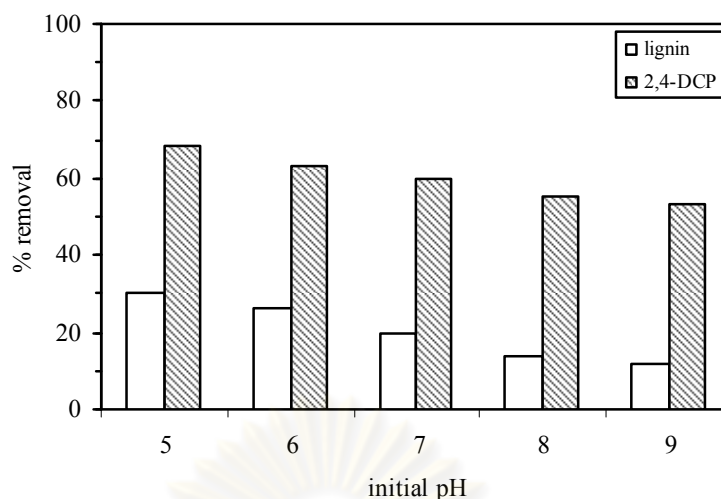


Figure 4.28 Lignin and 2,4-DCP removal vs. initial pH for mixed synthetic wastewater (reaction time = 420 min)

For the related research, the effect of initial pH on photocatalytic degradation of 125 ppm of 2,4-DCP by 1,500 W of UV and 0.5 g/l of anatase TiO<sub>2</sub> were studied by Bayarri et al. (2005) and found that the removal efficiency of 2,4-DCP was highest at initial pH 2 and when initial pH greater than 5.5, the final 2,4-DCP removal was decreased. The similar results were observed for photocatalytic degradation of phenol ( $3.56 \times 10^{-4}$  mol/l) by Naeem and Feng (2009). They reported that when the experiments were carried out with 200 mg/l of TiO<sub>2</sub> and 15 W UV-lamp at 365 nm, the degradation rate decreased with increase in initial pH and the highest degradation efficiency occurred at pH 5 with degradation rate of  $0.676 \times 10^{-6}$  mol/l min<sup>-1</sup>.

#### 4.3.2 Effect of UV intensity on treatment of lignin and 2,4-DCP in mixed synthetic wastewater

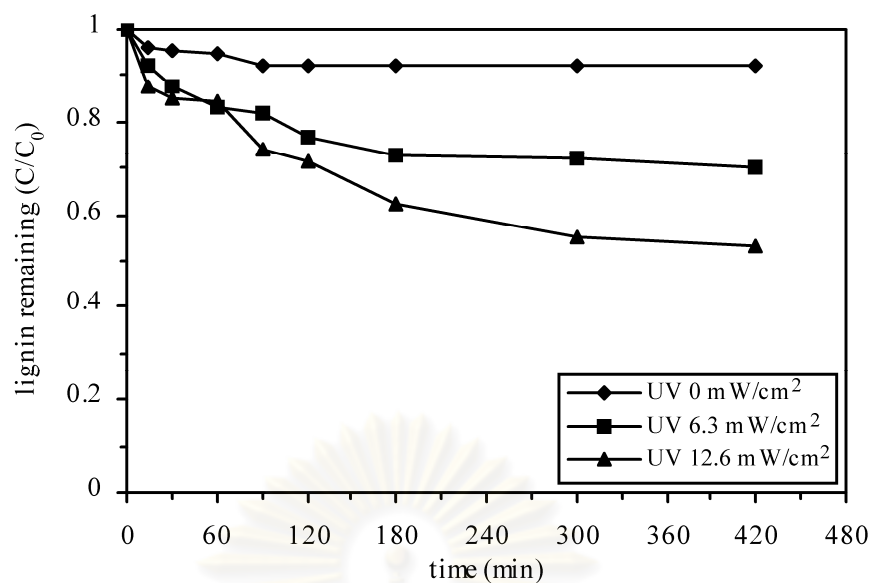
The effect of UV intensity on degradation of lignin and 2,4-DCP in mixed synthetic wastewater by supervibration-photocatalytic reactor was studied using various UV intensities as 0, 6.3 and 12.6 mW/cm<sup>2</sup>. The experiment was repeated at constant optimum initial pH 5 and vibration frequency of 30 Hz using mixed synthetic wastewater containing 400 mg/l of lignin and 5 mg/l of 2,4-DCP.

The results, as shown in Figure 4.29, demonstrated that the increase in UV intensity from 0 to 12.6 mW/cm<sup>2</sup> enhanced the lignin removal efficiency. The removal of lignin increased from 7.98% and 30% to 47.03% within 420 min when UV intensities were applied from 0 and 6.3 to 12.6 mW/cm<sup>2</sup>, respectively. The highest removal efficiency of lignin was achieved when the highest UV intensity was applied. For the optimum UV intensity of 12.6 mW/cm<sup>2</sup>, lignin concentration was decreased from 400 mg/l to 211.88 mg/l ( $C/C_0 = 0.53$ ) after 420 min of reaction time.

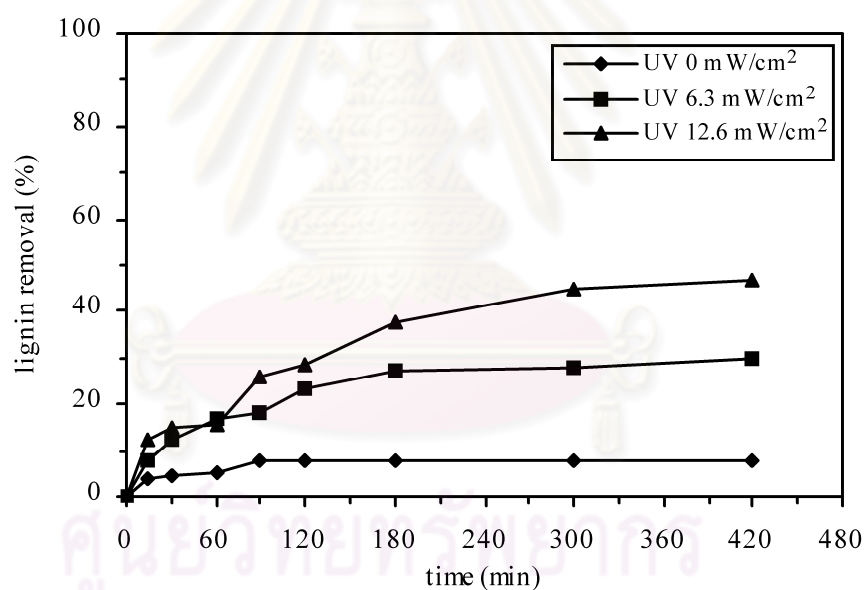
Figure 4.30 shows that the increase in UV intensity from 0 to 12.6 mW/cm<sup>2</sup> enhanced 2,4-DCP removal efficiency which followed the same trend as lignin removal. 2,4-DCP removal was increased from 20.12% and 68.19% to 75.18% in the same reaction time as the UV intensity increased from 0 and 6.3 to 12.6 mW/cm<sup>2</sup>. The highest 2,4-DCP removal of 75.18% was observed when UV intensity of 12.6 mW/cm<sup>2</sup> was used in the experiment and lignin concentration was reduced from 5 mg/l to 1.24 mg/l ( $C/C_0 = 0.25$ ).

The summary results in Figure 4.31 show that the effect of UV intensity on the removal efficiencies of lignin and 2,4-DCP in mixed synthetic wastewater were the same trend. Both lignin and 2,4-DCP removal efficiencies were increased with increasing UV intensity. At all UV intensities, removal efficiency of 2,4-DCP was more than that of lignin. When removal efficiencies of mixed synthetic wastewater and synthetic wastewater containing single pollutant were compared, lignin had an interference effect on 2,4-DCP removal. For the optimum UV intensity, the removal efficiency of 2,4-DCP in mixed synthetic wastewater was about 4% less than that in 2,4-DCP synthetic wastewater, whereas removal efficiency of lignin in mixed wastewater was not so difference and the reasons were the same as explained in part of effect of initial pH. The reactor could slightly remove lignin and 2,4-DCP under the absence of UV light since some molecules of lignin and 2,4-DCP might be adsorbed on the inner or outer of surface of TiO<sub>2</sub> film .

From the results obtained, the photocatalytic activity of lignin and 2,4-DCP degradation significantly increased with increasing UV intensity. The effect of light intensity was explained in terms that at increasing electron-hole generation rate, resulted from higher radiation intensities, then more OH<sup>•</sup> occurred and this OH<sup>•</sup> promoted higher degradation rate. The same results were obtained by Blažková, Csölleová, and Brezová (1998) using 10 mg/g of Pt/TiO<sub>2</sub> immobilized on glass fiber



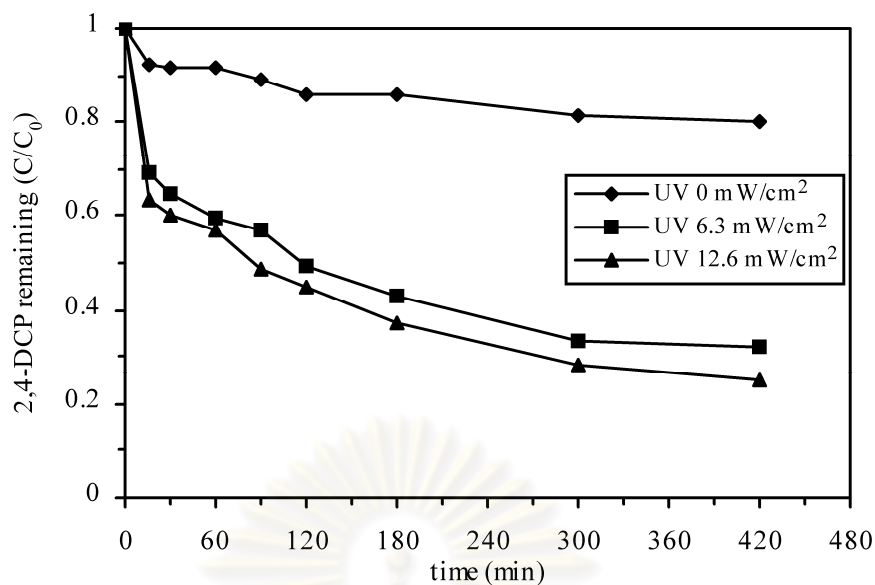
(a)



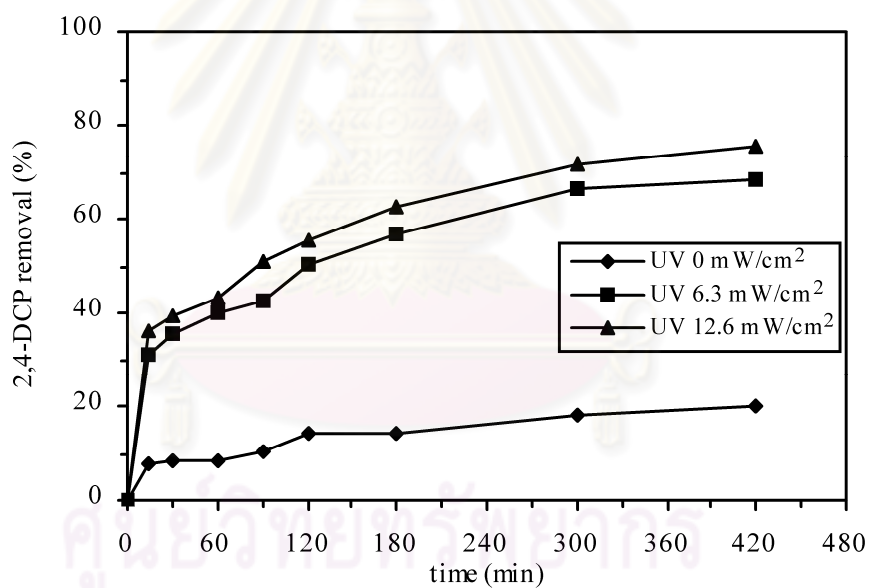
(b)

Figure 4.29 The effect of UV intensity on degradation of lignin in mixed synthetic wastewater: lignin remaining (a) and removal efficiency (b) (initial lignin concentration = 400 mg/l, initial 2,4-DCP concentration = 5 mg/l, initial pH = 5, vibration frequency = 30 Hz)





(a)



(b)

Figure 4.30 The effect of UV intensity on degradation of 2,4-DCP in mixed synthetic wastewater: 2,4-DCP remaining (a) and removal efficiency (b) (initial lignin concentration = 400 mg/l, initial 2,4-DCP concentration = 5 mg/l, initial pH = 5, vibration frequency = 30 Hz)

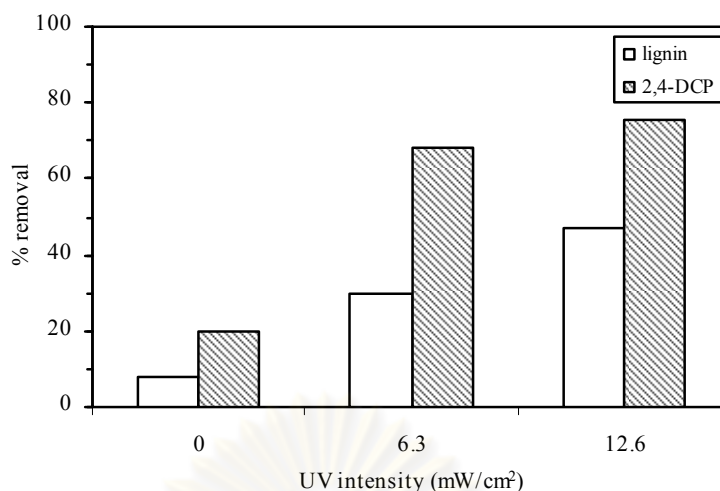


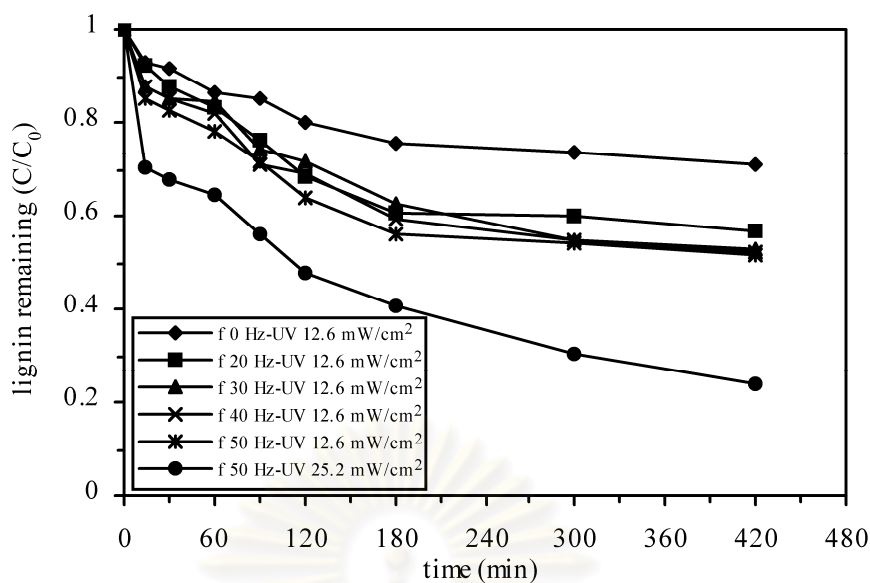
Figure 4.31 Lignin and 2,4-DCP removal vs. UV intensity for mixed synthetic wastewater (reaction time = 420 min)

treating phenol with maximum intensity at 320, 350, 410 nm and white lamp resembling the solar spectrum. The highest photocatalytic activity was found for the source with maximum intensity at 320 nm and the photocatalytic activity increased with the decrease in UV wavelength.

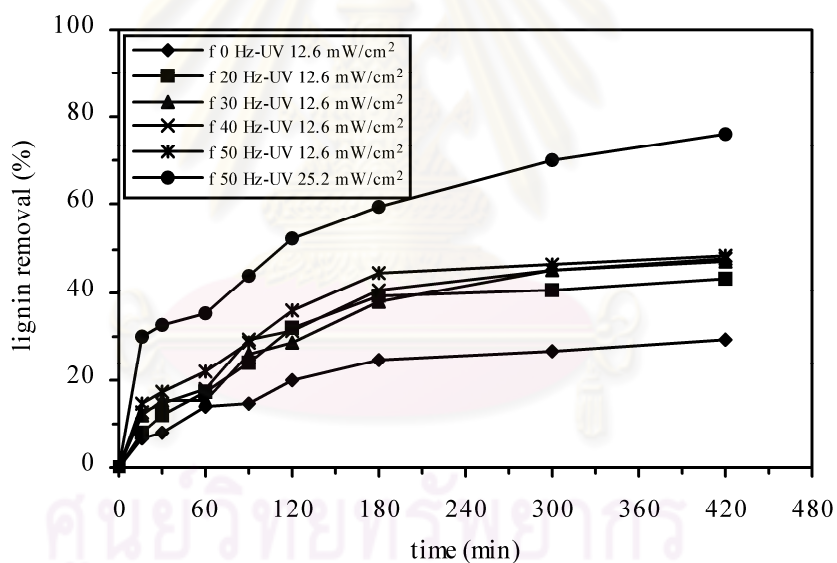
#### 4.3.3 Effect of vibration frequency on treatment of lignin and 2,4-DCP in mixed synthetic wastewater

400 mg/l of lignin and 5 mg/l of 2,4-DCP contained in mixed synthetic wastewater were prepared to study the effect of vibration frequency on treatment of lignin and 2,4-DCP under various vibration frequencies as 0, 20, 30, 40 and 50 Hz at a constant of optimum initial pH (pH 5) and optimum UV intensity (12.6 mW/cm<sup>2</sup>).

The effect of vibration frequency on degradation of lignin by supervibration-photocatalytic reactor is shown in Figure 4.32. The results indicate that an increase in the vibration frequency from 0 to 50 Hz could enhance lignin removal. When vibration frequencies were applied as 0, 20, 30, 40 and 50 Hz, the removal efficiencies of lignin were increased from 29.25%, 42.98%, 47.03% and 47.72% to 48.25%, respectively after 420 min. From the Figure 4.32, the vibration frequency that induced the best photocatalytic process on treatment of lignin in mixed synthetic



(a)



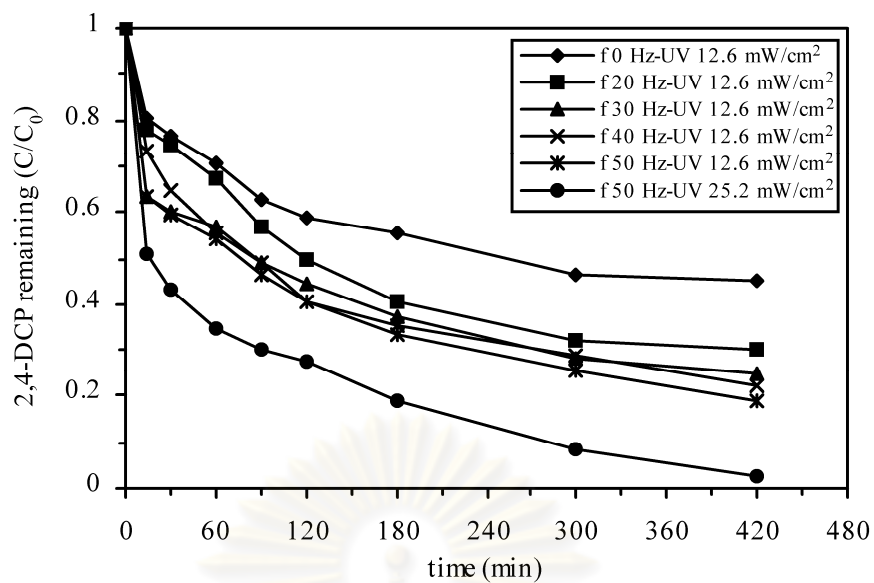
(b)

Figure 4.32 The effect of vibration frequency on degradation of lignin in mixed synthetic wastewater: lignin remaining (a) and removal efficiency (b) (initial lignin concentration = 400 mg/l, initial 2,4-DCP concentration = 5 mg/l, initial pH = 5)

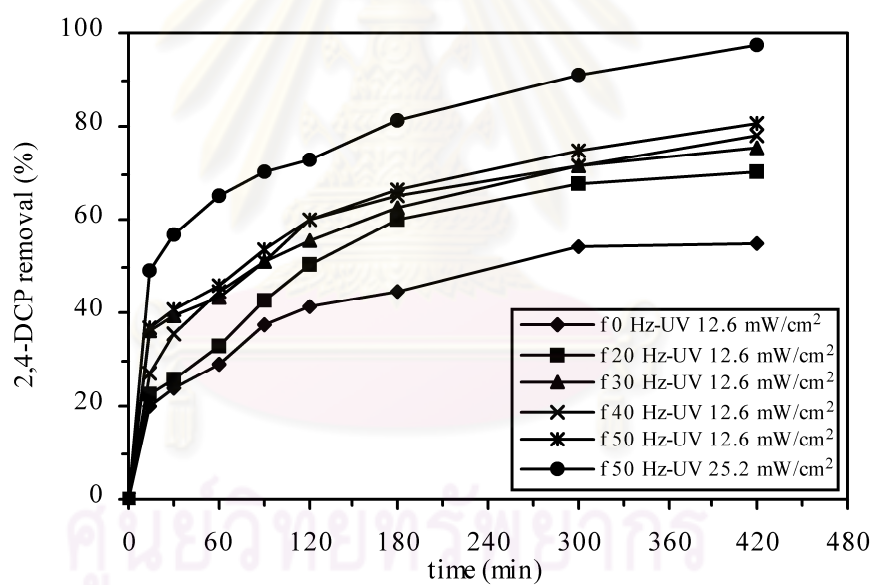
wastewater was 50 Hz. Additional experiment with an increase in UV intensity to  $25.2 \text{ mW/cm}^2$ , initial pH 5, vibration frequency of 50 Hz and initial concentration of mixed synthetic wastewater containing lignin of 400 mg/l and 2,4-DCP of 5 mg/l was carried out to improve system performance. From the result, it was found that the concentration of lignin decreased from 400 mg/l initially to 95.14 mg/l ( $C/C_0 = 0.24$ ) with a capacity of 76.21% after 420 min.

2,4-DCP removal efficiency followed the same trend as lignin removal. Figure 4.33 shows effect of the vibration frequency on 2,4-DCP degradation by supervibration-photocatalytic reactor within 420 min. 2,4-DCP removal were increased from 55.10%, 70.20%, 75.18% and 77.98% to 80.72% as the vibration frequency increased from 0, 20, 30 and 40 to 50 Hz, respectively. The highest 2,4-DCP removal as 80.72%, was achieved at vibration frequency of 50 Hz. Moreover, additional experiment with an increase in UV intensity to  $25.2 \text{ mW/cm}^2$  was carried out to improve system performance under the same conditions as lignin treatment conditions. The result was found that 2,4-DCP concentration decreased from 5 mg/l initially to 0.14 mg/l ( $C/C_0 = 0.03$ ) with a removal efficiency up to 97.13% after the same time. The results indicate that an increase in UV intensity as  $25.2 \text{ mW/cm}^2$  significantly enhanced removal of lignin and 2,4-DCP in mixed synthetic wastewater since an increase in UV intensity can enhance the hydroxyl radical ( $\text{OH}^\bullet$ ) formation in the photocatalytic reaction.

Figure 4.34 shows summary results of the effect of vibration frequency on the removal efficiencies of lignin and 2,4-DCP in mixed synthetic wastewater. Both lignin and 2,4-DCP removal efficiencies were increased as the vibration frequency increased. At all vibration frequencies, removal efficiency of 2,4-DCP was more than that of lignin. When removal efficiencies of mixed synthetic wastewater and synthetic wastewater containing single pollutant were compared, lignin had an interference effect on 2,4-DCP removal. For the optimum treatment conditions, the removal efficiency of 2,4-DCP in mixed synthetic wastewater was much less than that in 2,4-DCP synthetic wastewater, whereas removal efficiency of lignin in mixed wastewater was not different and the reasons were the same as explained in part of effect of initial pH.

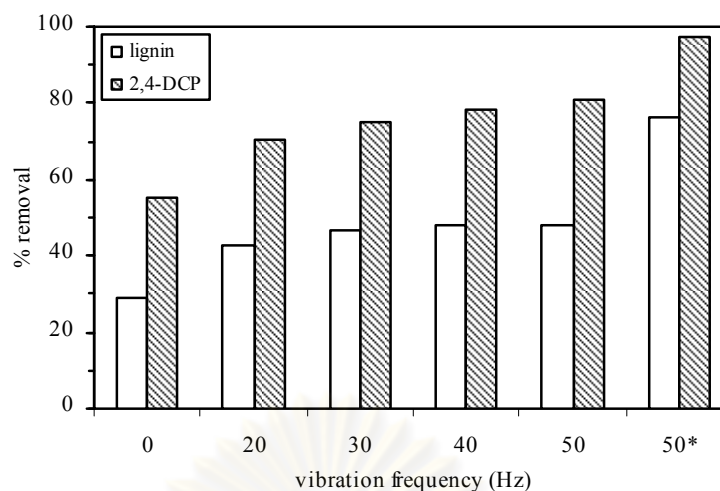


(a)



(b)

Figure 4.33 The effect of vibration frequency on degradation of 2,4-DCP in mixed synthetic wastewater: 2,4-DCP remaining (a) and removal efficiency (b) (initial lignin concentration = 400 mg/l, initial 2,4-DCP concentration = 5 mg/l, initial pH = 5)

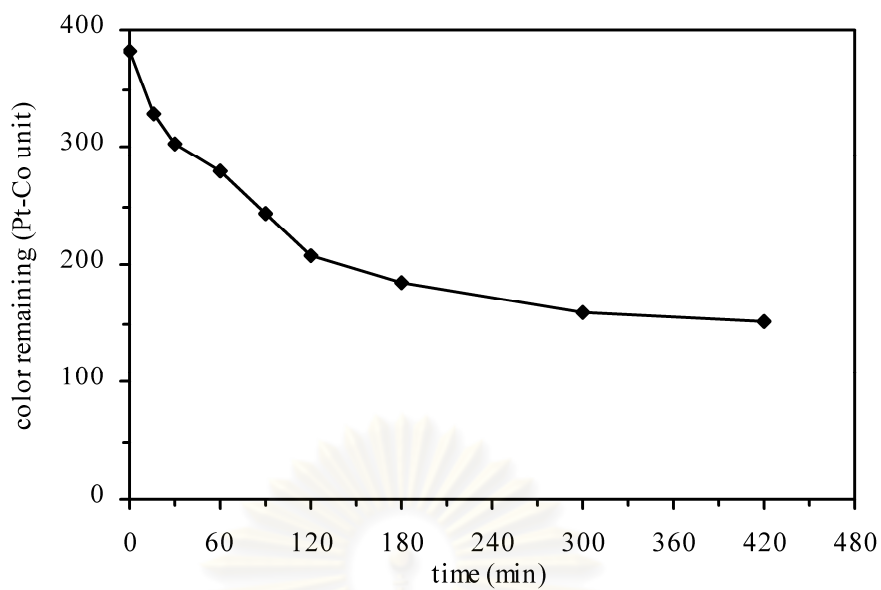


Note : \* UV intensity = 25.2 mW/cm<sup>2</sup>

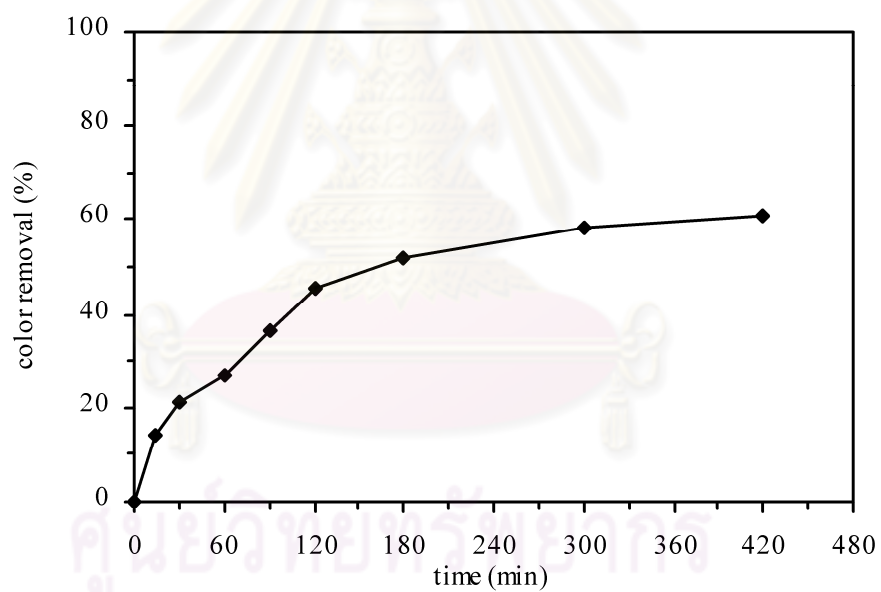
Figure 4.34 Lignin and 2,4-DCP removal vs. vibration frequency for mixed synthetic wastewater (reaction time = 420 min)

Furthermore, the performance of supervibration-photocatalytic reactor on color removal in mixed synthetic wastewater was also investigated under the optimum treatment conditions as initial concentration of mixed synthetic wastewater contained lignin of 400 mg/l and 2,4-DCP of 5 mg/l, initial pH 5, UV intensity of 25.2 mW/cm<sup>2</sup> and vibration frequency of 50 Hz. The result was found that color decreased from 382.64 Pt-Co unit to 150.20 Pt-Co unit after 420 min with removal efficiency of 60.75% as presented in Figure 4.35 and 4.36. The color removal based on ADMI from lignin solution was previously studied by Chang et al. (2004) and Ma et al. (2008). Chang et al. (2004) performed under 35 W of UV and 10 g/l of TiO<sub>2</sub> and found at initial pH 3, color removal was close to 88% in 960 min. Whereas, Ma et al. (2008) reported removal of color in 251 mg/l of lignin solution with TiO<sub>2</sub> and UV at 253.7 nm. The result was found that the Pt-doped TiO<sub>2</sub> removed 55-69% of ADMI after 60 min when the dosage of Pt/TiO<sub>2</sub> increased from 1 to 10 g/l.





(a)



(b)

Figure 4.35 Removal of color in mixed synthetic wastewater: color remaining (a) and removal efficiency (b) (initial lignin concentration = 400 mg/l, initial pH = 5, UV intensity = 25.2 mW/cm<sup>2</sup>, vibration frequency = 50 Hz)



(a)

(b)

Figure 4.36 Color of mixed synthetic wastewater at reaction time: 0 min (a) and 420 min (b) (initial lignin concentration = 400 mg/l, initial pH = 5, UV intensity = 25.2 mW/cm<sup>2</sup>, vibration frequency = 50 Hz)

ศูนย์วิทยทรัพยากร  
จุฬาลงกรณ์มหาวิทยาลัย

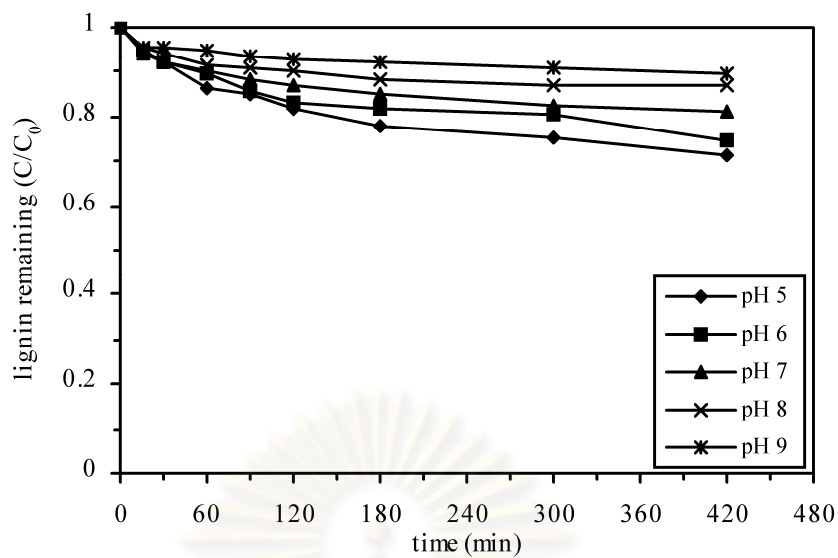
#### 4.4 Treatment of Real Wastewater from Pulp and Paper Mill

The performance of supervibration-photocatalytic reactor on treatment of lignin and 2,4-DCP in real wastewater from pulp and paper mill were investigated to obtain the optimum operating conditions of the reactor for lignin and 2,4-DCP removal. Wastewater samples containing 218-290 mg/l of lignin and 111-152  $\mu\text{g/l}$  of 2,4-DCP were supplied from the pulp and paper mill located at Kanchanaburi province in Thailand. Treatment efficiencies of lignin and 2,4-DCP by supervibration-photocatalytic reactor were studied under different initial pH (5, 6, 7, 8 and 9), UV intensity (0, 6.3, 12.6 and 25.2  $\text{mW/cm}^2$ ) and vibration frequency (0, 20, 30, 40 and 50 Hz).

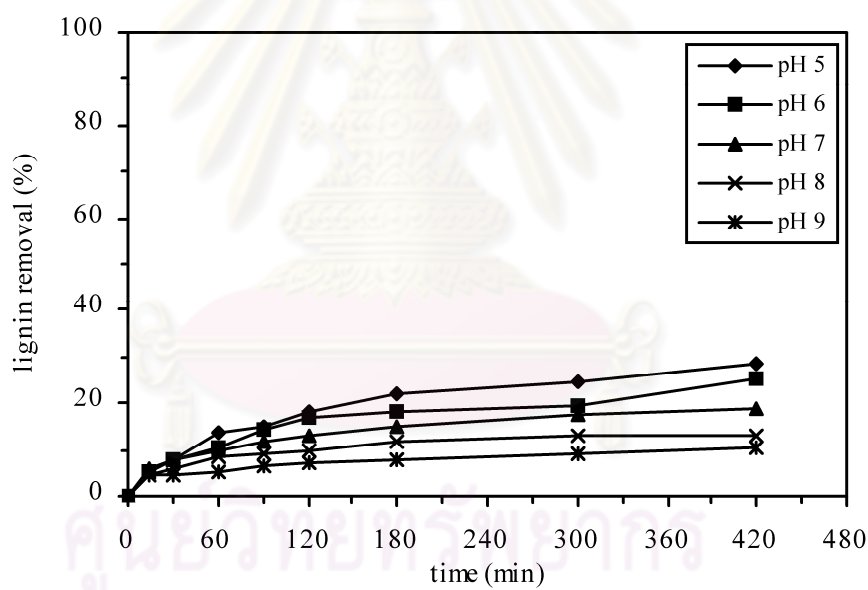
##### 4.4.1 Effect of initial pH on treatment of lignin and 2,4-DCP in real wastewater

The effect of initial pH on removal of lignin and 2,4-DCP in real wastewater from pulp and paper mill was also investigated. Real wastewater samples were treated under five different initial pH levels as 5, 6, 7, 8 and 9. The supervibration-photocatalytic reactor was carried out with UV intensity of 6.3  $\text{mW/cm}^2$  and vibration frequency of 30 Hz.

The results as shown in Figure 4.37 demonstrated that the decrease in initial pH from 9 to 5 could enhance initial lignin removal rate at all pH levels, degradation of lignin was rapid then slightly declined. It might be because for longer time, lignin had to compete with intermediates for the  $\text{TiO}_2$  sites. The removal of lignin were increased from 10.08%, 13.17%, 18.51% and 25.11% to 28.64% within 420 min when initial pH decrease from 9, 8, 7 and 6 to 5, respectively. The highest removal efficiency of lignin was achieved when initial pH 5 was applied. For the optimum initial pH 5, lignin concentration was reduced from 278.24 mg/l to 198.54 mg/l ( $C/C_0 = 0.71$ ) after 420 min of light exposure.



(a)



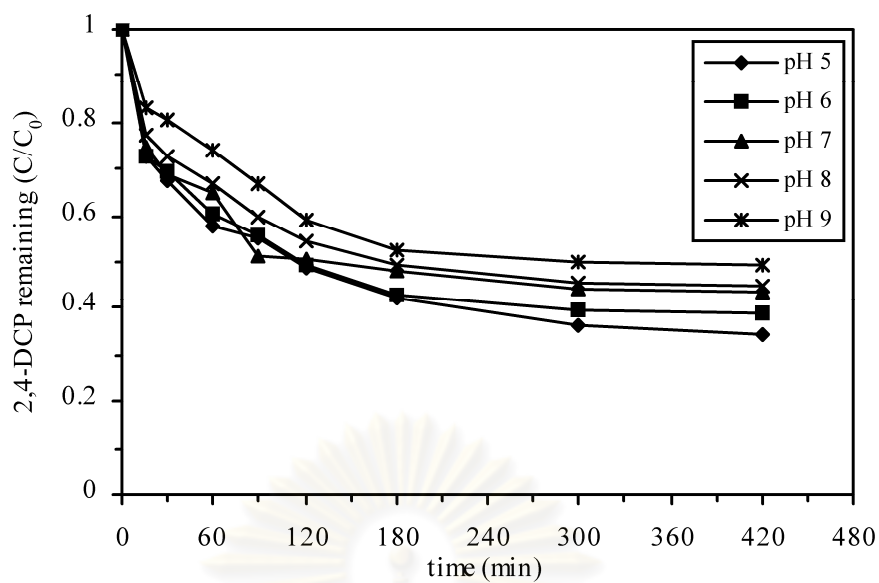
(b)

Figure 4.37 The effect of initial pH on degradation of lignin in real wastewater: lignin remaining (a) and removal efficiency (b) (UV intensity = 6.3 mW/cm<sup>2</sup>, vibration frequency = 30 Hz)

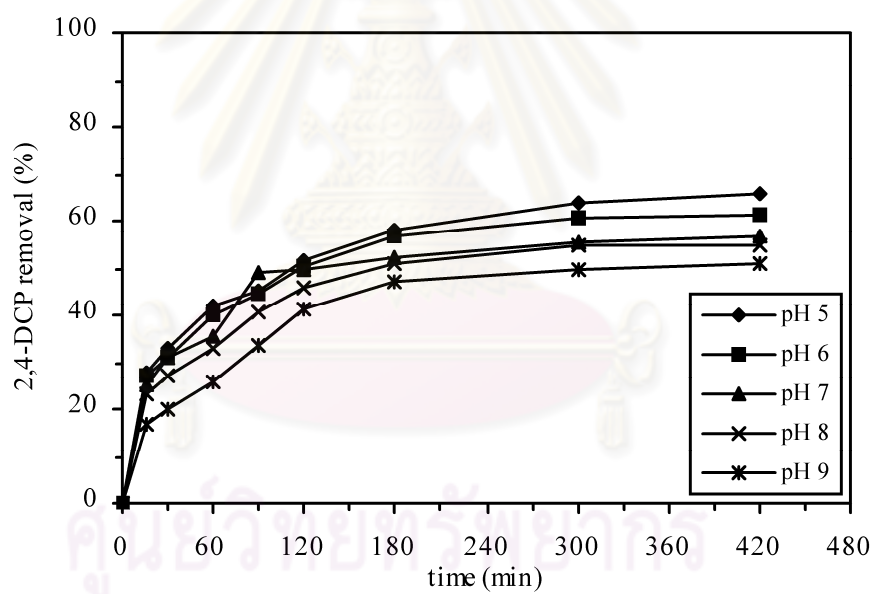
Figure 4.38 illustrates effect of initial pH on 2,4-DCP degradation and indicates that 2,4-DCP removal efficiency followed the same trend as lignin removal. 2,4-DCP removal were increased from 50.76%, 55.15%, 56.81% and 61.17% to 65.60% as initial pH decreased from 9, 8, 7 and 6 to 5, respectively. The highest 2,4-DCP removal as 65.60%, was achieved at initial pH 5. For the optimum initial pH at 5, 2,4-DCP concentration was decreased from 128.52  $\mu\text{g/l}$  to 44.21  $\mu\text{g/l}$  ( $C/C_0 = 0.34$ ) after 420 min.

Figure 4.39 summarizes that effect of initial pH on removal efficiencies of lignin in pulp and paper mill wastewater after 420 min was the same as that of 2,4-DCP. Both lignin and 2,4-DCP removal efficiencies were increased with decrease in initial pH. At all initial pH, removal efficiency of 2,4-DCP was more than that of lignin because the lignin concentration in the pulp and paper mill wastewater was higher than 2,4-DCP concentration. Furthermore, lignin is very complex polymer and higher molecular weight than that of 2,4-DCP. When removal efficiencies of real wastewater and synthetic wastewater containing single pollutant were compared, lignin had an interference effect on 2,4-DCP removal. For the optimum initial pH, the removal efficiency of 2,4-DCP in real wastewater was approximately 8% less than that in 2,4-DCP synthetic wastewater, whereas removal efficiency of lignin in real wastewater was slightly reduced. It is probably because turbid brown color of real wastewater inhibits UV light penetration into water, whereas synthetic wastewater is bright yellow solution. On the other hand, other several constituents in real wastewater and more intermediates occurred of lignin competed in absorption of 2,4-DCP on the surface of  $\text{TiO}_2$ .

The results imply that the degradation of lignin and 2,4-DCP rose slightly when the initial pH value changed from alkaline (pH 11) to weakly acidic (pH 5). The initial pH 5 was the optimum pH for the  $\text{TiO}_2$  photocatalytic degradation of both lignin and 2,4-DCP. The role of pH as important parameter in the photocatalytic reaction influenced the surface charge properties and the adsorption behavior of  $\text{TiO}_2$  (Gaya and Abdullah, 2008). The method widely accepted is the point of zero charge (pzc) of  $\text{TiO}_2$ , which influences the ionization rate of the surface of  $\text{TiO}_2$  as explained in the section of mixed synthetic wastewater. The recently related research studied effect of initial pH on treatment of pulp and paper mill wastewater by photocatalytic degradation and obtained contradictive results. Catalkaya and Kargi (2008) investigated TOC removal in pulp mill located in Turkey with various initial pH (3, 7



(a)



(b)

Figure 4.38 The effect of initial pH on degradation of 2,4-DCP in real wastewater: 2,4-DCP remaining (a) and removal efficiency (b) (UV intensity = 6.3 mW/cm<sup>2</sup>, vibration frequency = 30 Hz)



and 11) using 16 W of UV at 254 nm. However, the TiO<sub>2</sub>-assisted photo-catalysis (UV/TiO<sub>2</sub>) resulted in the highest TOC removal under alkaline conditions, 79.6% TOC removal was obtained with a titanium dioxide concentration of 0.75 g/l at pH 11 within 60 min. Furthermore, Kansal et al. (2008) also investigated the photocatalytic degradation of lignin obtained from wheat straw kraft digestion as black liquor using TiO<sub>2</sub> and ZnO semiconductors. The experiments were carried out with 35 W/m<sup>2</sup> of UV intensity, 10-100 mg/l of initial lignin concentration and 0.5-2 g/l of TiO<sub>2</sub>. The role of pH in the rate of photocatalytic degradation was studied in the pH range 3-11 and found that the maximum lignin degradation was obtained at pH 11. It mainly related to the acid-base equilibrium of the adsorbed hydroxyl group and the formation of hydroxyl radical (OH<sup>•</sup>) from OH<sup>-</sup> was favored at high pH.

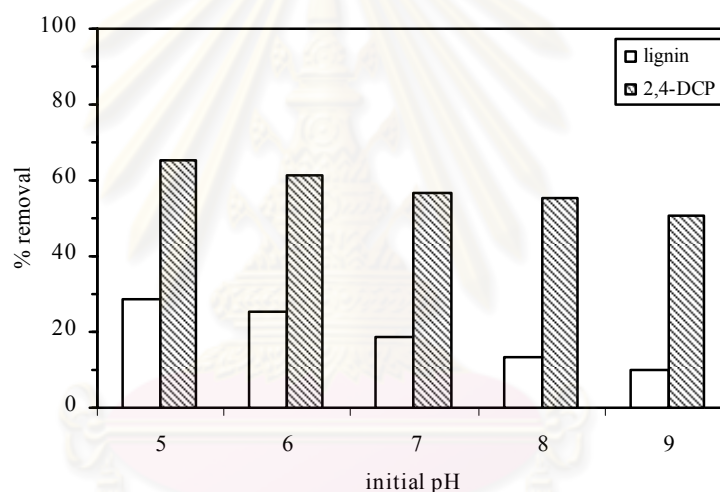


Figure 4.39 Lignin and 2,4-DCP removal vs. initial pH for real wastewater (reaction time = 420 min)

#### 4.4.2 Effect of UV intensity on treatment of lignin and 2,4-DCP in real wastewater

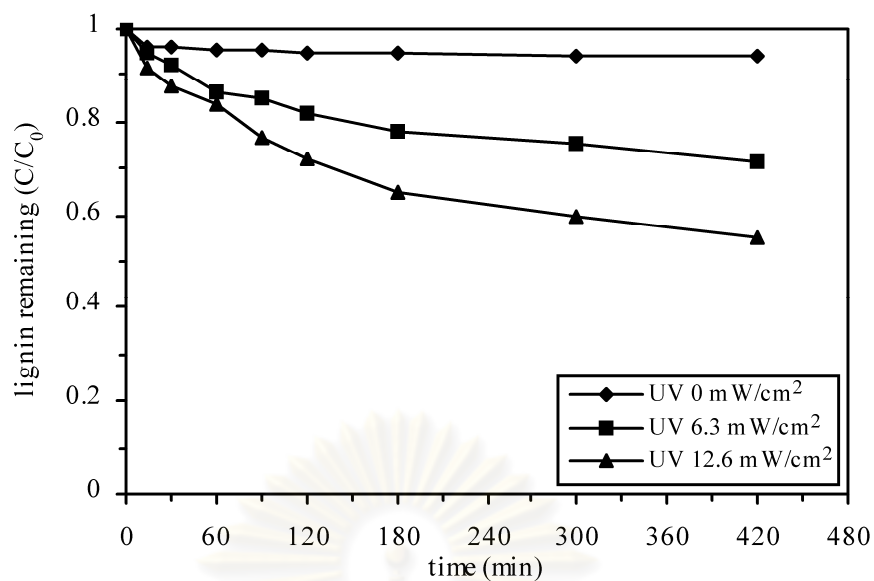
In order to determine effect of UV intensity on treatment of lignin and 2,4-DCP in real wastewater, the experiments were performed by varying UV intensities as 0, 6.3 and 12.6 mW/cm<sup>2</sup> at constant optimum initial pH 5 and vibration frequency of 30 Hz.

Figure 4.40 reveals that lignin removal efficiencies were increased greatly by the increase in UV intensity. The removal efficiencies of lignin were increased from 6.16% and 28.64% to 44.84% within 420 min when UV intensities were applied from 0 and 6.3 to 12.6 mW/cm<sup>2</sup>, respectively. The highest removal efficiency of lignin was achieved when UV intensity of 12.6 mW/cm<sup>2</sup> was applied. For the optimum UV intensity of 12.6 mW/cm<sup>2</sup>, lignin concentration was decreased from 263.44 mg/l to 145.33 mg/l ( $C/C_0 = 0.55$ ) after 420 min of light exposure.

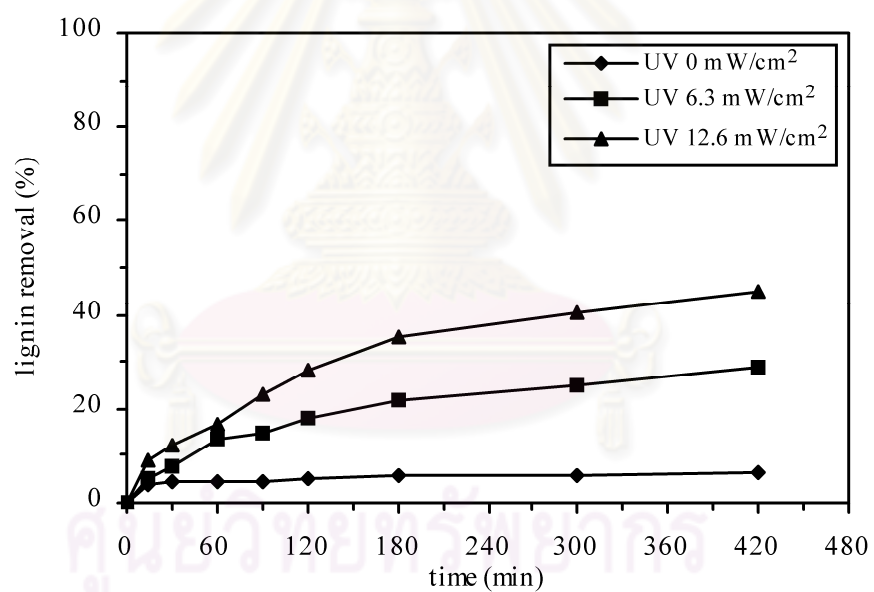
The results present that the increase in UV intensity from 0 to 12.6 mW/cm<sup>2</sup> could enhance 2,4-DCP removal which followed the same trend as lignin removal. 2,4-DCP removal were increased from 15.83% and 65.60% to 73.15% in the same reaction time as the UV intensity increased from 0 and 6.3 to 12.6 mW/cm<sup>2</sup>, respectively as presented in Figure 4.41. The highest 2,4-DCP removal of 73.15% was observed when UV intensity of 12.6 mW/cm<sup>2</sup> was used in the experiment and lignin concentration was reduced from 131.26 µg/l to 35.24 µg/l ( $C/C_0 = 0.27$ ).

Figure 4.42 summarizes that effect of UV intensity on removal efficiencies of lignin and 2,4-DCP in pulp and paper mill wastewater were similar trend. Both lignin and 2,4-DCP removal efficiencies were increased with the increase in UV intensity within 420 min. At all UV intensities, removal efficiency of 2,4-DCP was more than that of lignin. When removal efficiencies of real wastewater and synthetic wastewater containing single pollutant were compared, lignin had an interference effect on 2,4-DCP removal. For the optimum UV intensity, the removal efficiency of 2,4-DCP in real wastewater was around 6% less than that in 2,4-DCP synthetic wastewater, whereas removal efficiency of lignin in real wastewater was slightly reduced and the reasons were the same as explained in part of effect of initial pH. The reactor could slightly remove lignin and 2,4-DCP under the absence of UV light since some molecules of lignin and 2,4-DCP might be adsorbed on the inner or outer of surface of TiO<sub>2</sub> film .

The photocatalytic degradation of lignin and 2,4-DCP in real wastewater significantly increased with increasing UV intensity and had the same trend as in synthetic wastewater. The similar results were studied by Shivaraju, Byrappa, and Ananda (2010). They investigated the effect of UV light source on degradation of pulp and paper industrial effluent using TiO<sub>2</sub> deposited calcium alumino-silicate beads. The experiments were carried out TiO<sub>2</sub> load of 60 mg/50 ml paper and pulp industrial effluent and initial pH 10.

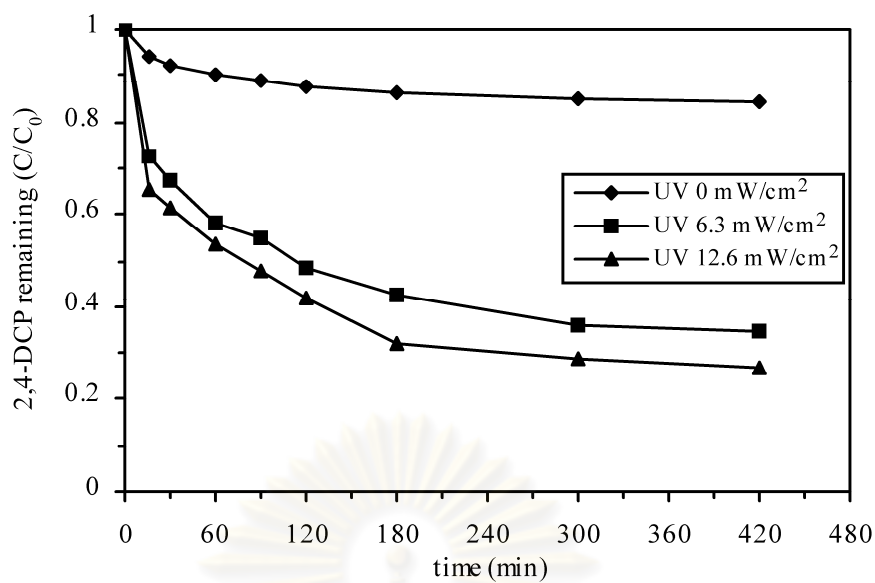


(a)

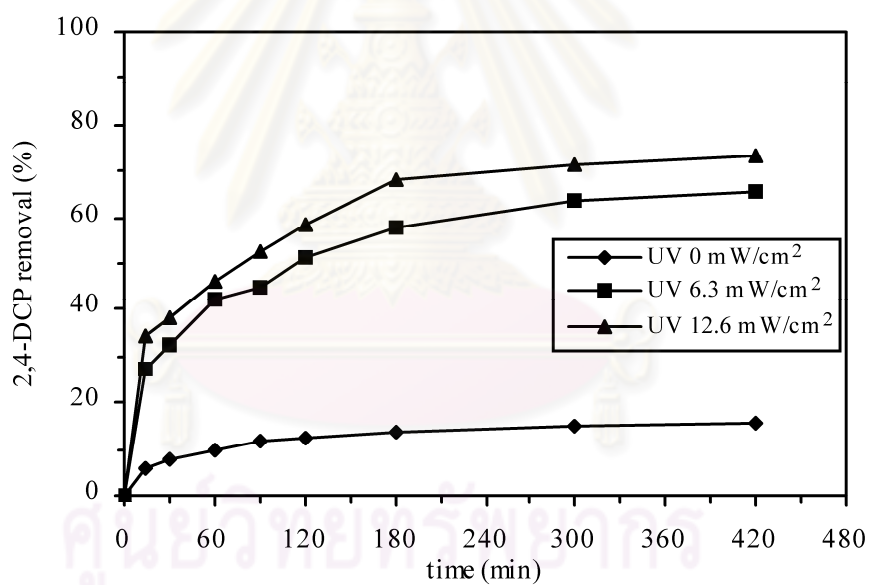


(b)

Figure 4.40 The effect of UV intensity on degradation of lignin in real wastewater: lignin remaining (a) and removal efficiency (b) (initial pH = 5, vibration frequency = 30 Hz)



(a)



(b)

Figure 4.41 The effect of UV intensity on degradation of 2,4-DCP in real wastewater: 2,4-DCP remaining (a) and removal efficiency (b) (initial pH = 5, vibration frequency = 30 Hz)

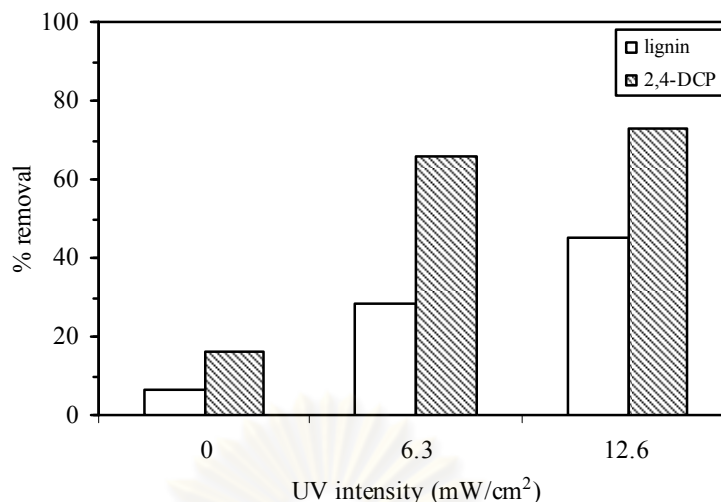


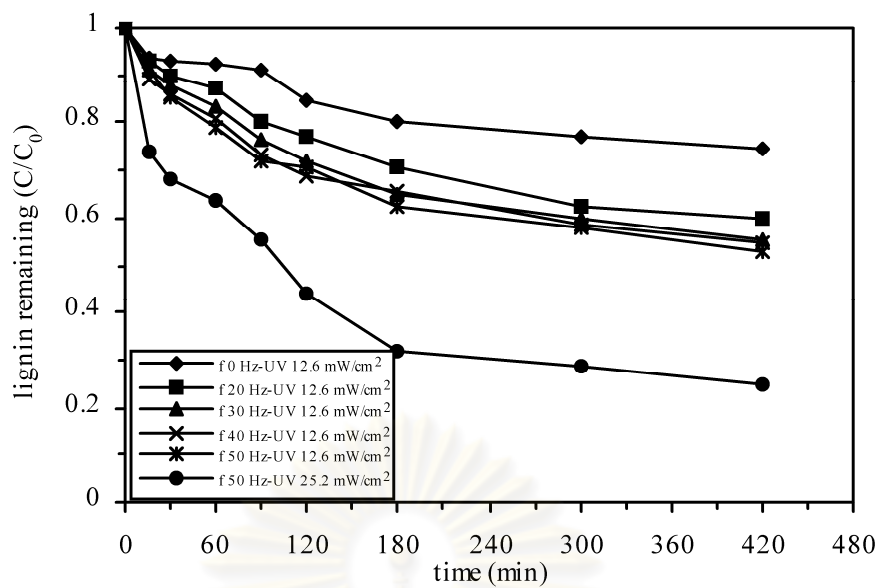
Figure 4.42 Lignin and 2,4-DCP removal vs. UV intensity for real wastewater (reaction time = 420 min)

The results were found that the photocatalytic treatment of effluent under UV light was 87% COD removal efficiency and under the sunlight and visible light, COD removal efficiencies were 83% and 71%, respectively within 300 min.

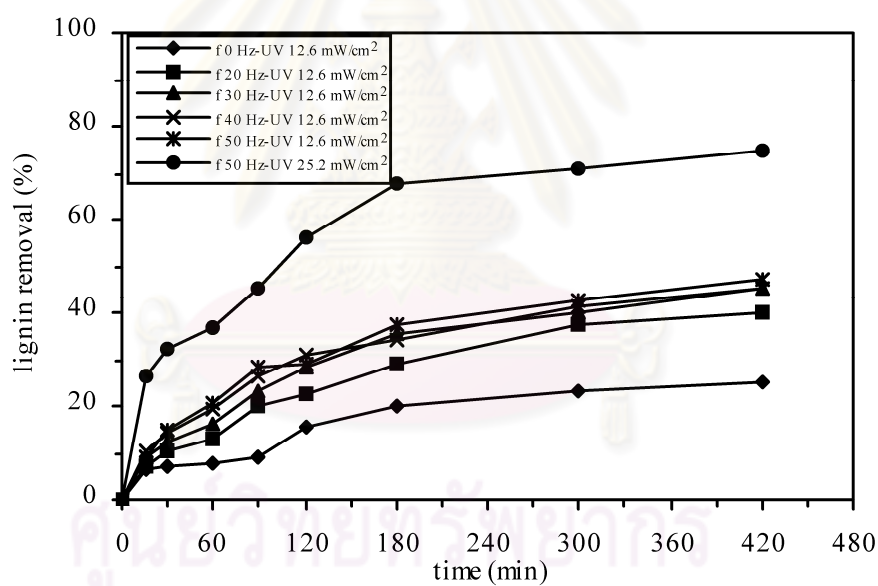
#### 4.4.3 Effect of vibration frequency on treatment of lignin and 2,4-DCP in real wastewater

The influence of vibration frequency on treatment of lignin and 2,4-DCP in real wastewater was also studied using different vibration frequencies as 0, 20, 30, 40 and 50 Hz at a constant optimum initial pH 5 and optimum UV intensity of 12.6 mW/cm<sup>2</sup>.

The results in Figure 4.43 indicate that the increase in the vibration frequency from 0 to 50 Hz could enhance lignin removal. When vibration frequencies were applied as 0, 20, 30, 40 and 50 Hz, the removal efficiencies of lignin were 25.36%, 40.20%, 44.84%, 45.06% and 46.97%, respectively after 420 min. The vibration frequency that induced the best photocatalytic process on treatment of lignin in real wastewater was 50 Hz.



(a)



(b)

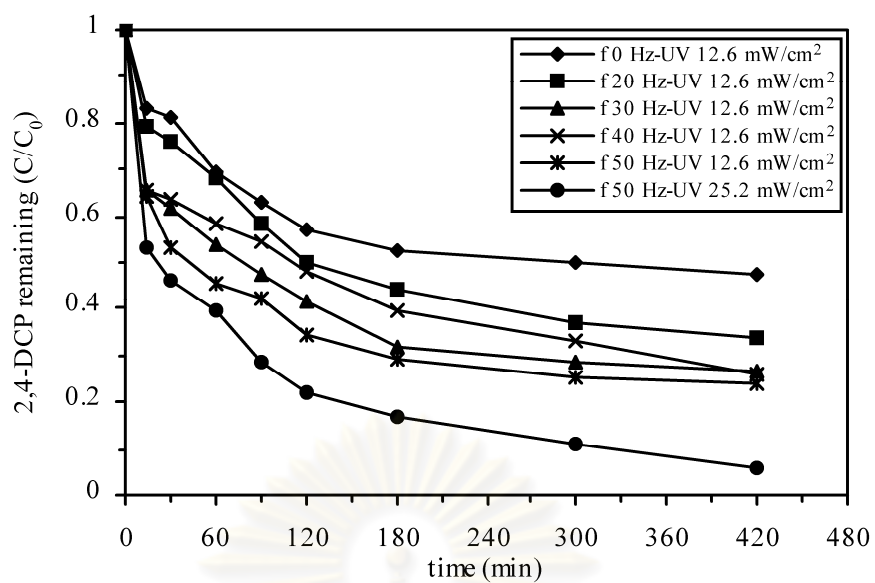
Figure 4.43 The effect of vibration frequency on degradation of lignin in real wastewater: lignin remaining (a) and removal efficiency (b) (initial pH = 5)



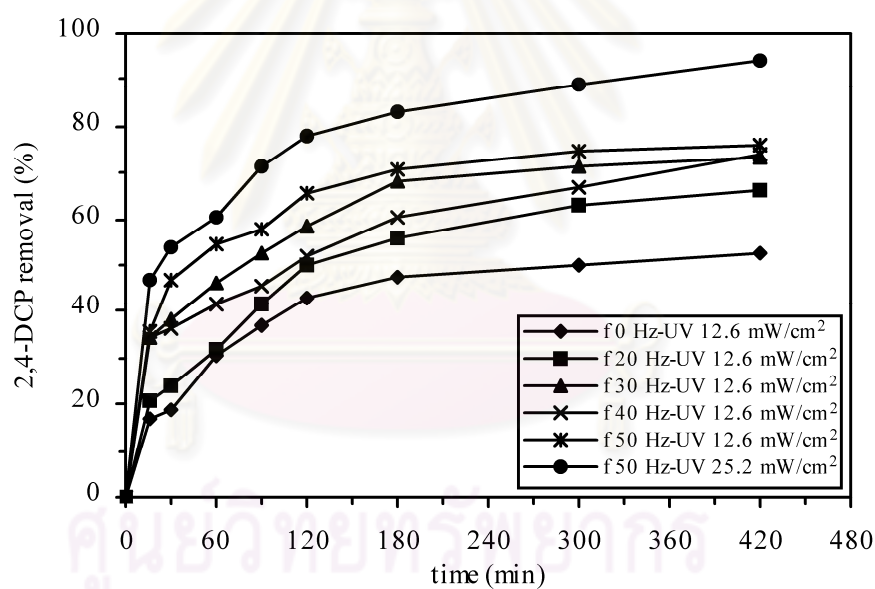
Additional experiment with an increase in UV intensity to  $25.2 \text{ mW/cm}^2$ , initial pH 5, vibration frequency of 50 Hz was carried out to improve system performance. From the result, it was found that lignin concentration decreased from 250.79 mg/l initially to 62.42 mg/l ( $C/C_0 = 0.25$ ) with a capacity of 75.11% after 420 min. The higher removal efficiency of lignin in bleached kraft mill effluent (Turkey) by photocatalytic degradation (30 W of UV and 25 mg/l of  $\text{TiO}_2$ ) in the presence of  $\text{H}_2\text{O}_2$  was reported by Uğurlu and Karaoğlu (2009). The process could degrade lignin from 50 mg/l to 10 mg/l after 50 min with a capacity of 80%.

From the results obtained, 2,4-DCP removal efficiency followed the same trend as lignin removal. Figure 4.44 shows effect of the vibration frequency on 2,4-DCP degradation by supervibration-photocatalytic reactor within 420 min. 2,4-DCP removal were increased from 52.49%, 66.43%, 73.15% and 74.25% to 76.29% as the vibration frequency increased from 0, 20, 30 and 40 to 50 Hz, respectively. The highest 2,4-DCP removal as 76.29% was achieved at vibration frequency of 50 Hz. Moreover, additional experiment with an increase in UV intensity to  $25.2 \text{ mW/cm}^2$  was carried out to improve system performance under the same conditions as lignin treatment conditions. The result was found that 2,4-DCP concentration decreased from 123.96  $\mu\text{g/l}$  initially to 7.26  $\mu\text{g/l}$  ( $C/C_0 = 0.06$ ), which corresponds to a destructive efficiency of 94.14% after the same time. The results indicate that an increase in UV intensity as  $25.2 \text{ mW/cm}^2$  significantly enhanced removal of lignin and 2,4-DCP in pulp and paper mill wastewater since the increase in UV intensity can promote the hydroxyl radical ( $\text{OH}^\cdot$ ) formation in the photocatalytic reaction.

Figure 4.45 summarizes that effect of vibration frequency on removal efficiencies of lignin and 2,4-DCP in pulp and paper mill wastewater had a similar trend. Both lignin and 2,4-DCP removal efficiencies were increased as vibration frequency increased. At every vibration frequencies, removal efficiency of 2,4-DCP was more than that of lignin. When removal efficiencies of real wastewater and synthetic wastewater containing single pollutant were compared, lignin had an interference effect on 2,4-DCP removal. For the optimum operating conditions, the removal efficiency of 2,4-DCP in real wastewater was much less than that in 2,4-DCP synthetic wastewater, whereas removal efficiency of lignin in real wastewater was slightly reduced and the reasons were the same as explained in part of effect of initial pH.

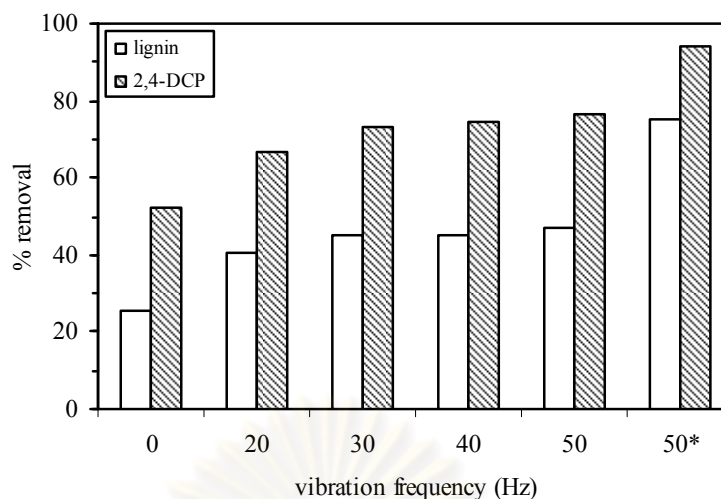


(a)



(b)

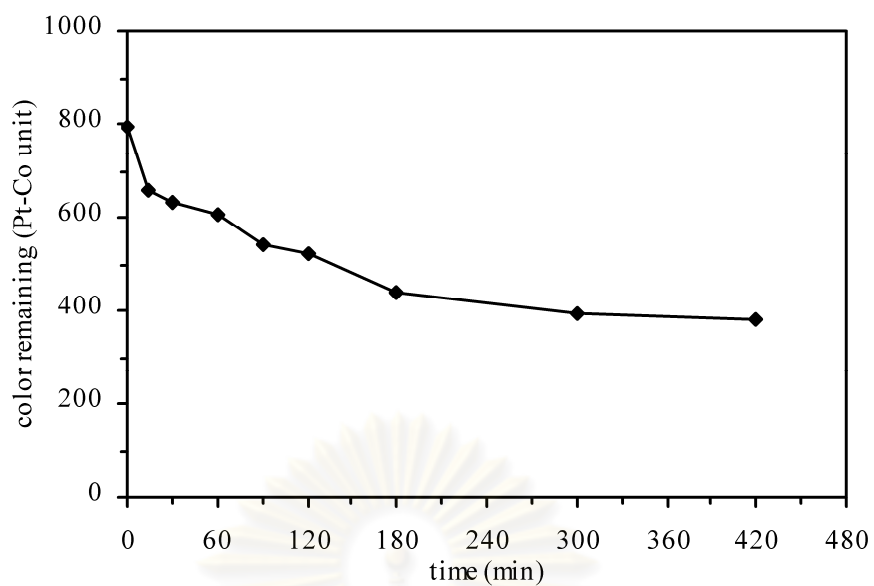
Figure 4.44 The effect of vibration frequency on degradation of 2,4-DCP in real wastewater: 2,4-DCP remaining (a) and removal efficiency (b) (initial pH = 5)



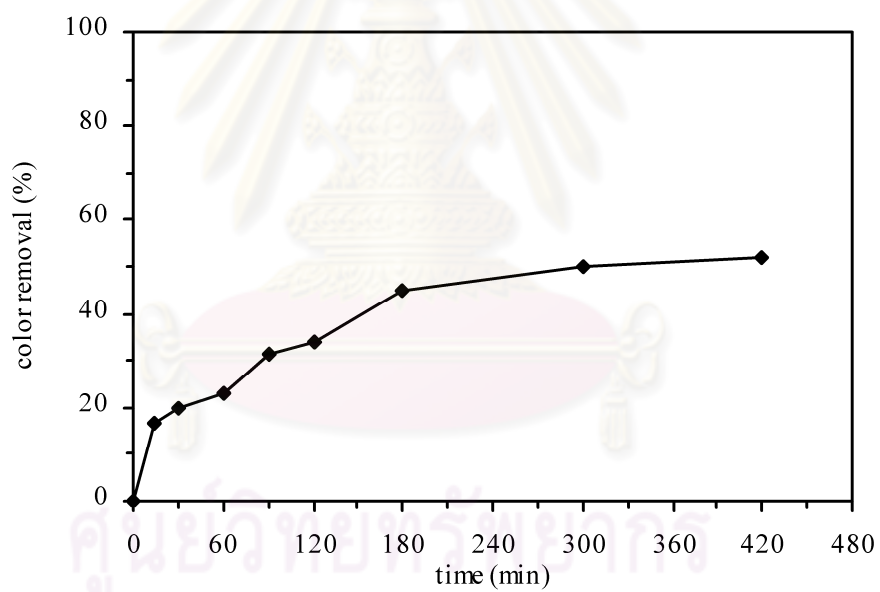
Note : \* UV intensity = 25.2 mW/cm<sup>2</sup>

Figure 4.45 Lignin and 2,4-DCP removal vs. vibration frequency for real wastewater (reaction time = 420 min)

Furthermore, the performance of supervibration-photocatalytic reactor on color removal in real wastewater was also studied under the optimum treatment conditions as initial concentration of pulp and paper mill wastewater contained lignin of 250.79 mg/l, initial pH 5, UV intensity of 25.2 mW/cm<sup>2</sup> and vibration frequency of 50 Hz. The result was found that color decreased from 790.69 Pt-Co unit to 378.24 Pt-Co unit after 420 min with removal efficiency of 52.16% as presented in Figure 4.46 and 4.47. For the related research, Yeber et al. (2000) studied TiO<sub>2</sub>/ZnO photocatalytic degradation of color in cellulose bleaching effluent from Brazilian pulp mill under the conditions of 6.3 mg of TiO<sub>2</sub>, 38 mg of ZnO and 125 W of UV lamp (energy flux 12 mW/cm<sup>2</sup>,  $\lambda < 254$  nm). Both impregnated catalysts presented the same behavior concerning the color reduction, around 50% after 30 min of treatment. After 90 min of reaction, the color was completely eliminated. Color remove efficiencies of previous research were more than that of present study with a short reaction time since ZnO was co-catalyst and promoted photocatalytic activity of TiO<sub>2</sub> for color removal.

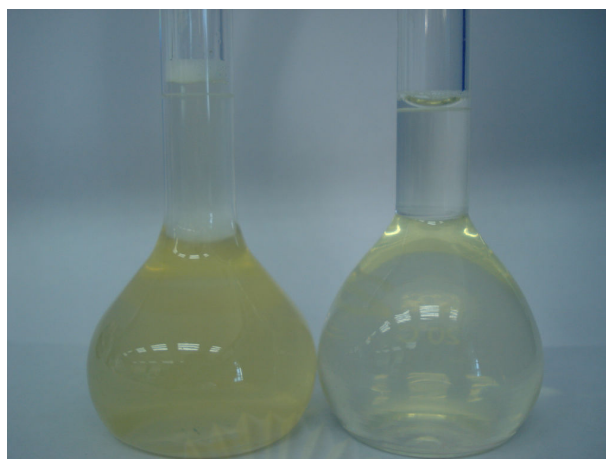


(a)



(b)

Figure 4.46 Removal of color in real wastewater: color remaining (a) and removal efficiency (b) (initial lignin concentration = 250.79 mg/l, initial pH = 5, UV intensity = 25.2 mW/cm<sup>2</sup>, vibration frequency = 50 Hz)



(a)

(b)

Figure 4.47 Color of real wastewater at reaction time: 0 min (a) and 420 min (b) (initial lignin concentration = 250.79 mg/l, initial pH = 5, UV intensity = 25.2 mW/cm<sup>2</sup>, vibration frequency = 50 Hz)

ศูนย์วิทยทรัพยากร  
จุฬาลงกรณ์มหาวิทยาลัย

## CHAPTER V

### CONCLUSIONS AND SUGGESTION FOR FUTURE WORKS

#### 5.1 Conclusions

A supervibration-photocatalytic reactor based on the photocatalytic process combined with a supervibration agitator was applied to remove lignin, color and 2,4-DCP in wastewater. Treatment efficiencies of lignin and 2,4-DCP were studied under different initial pH (5, 6, 7, 8 and 9), UV intensity (0, 6.3, 12.6 and 25.2 mW/cm<sup>2</sup>), vibration frequency (0, 20, 30, 40 and 50 Hz), initial lignin concentration (100, 200, 300 and 400 mg/l) and initial 2,4-DCP concentration (0.5, 1, 2.5 and 5 mg/l) to determine the optimum operating conditions. This work also studied kinetic reaction for degradation of lignin and 2,4-DCP and extended to identify by-products of lignin and 2,4-DCP degradation.

5.1.1 For all types of wastewater samples, the removal efficiencies of lignin and 2,4-DCP using the supervibration-photocatalytic reactor were increased with the increase in UV intensity and vibration frequency. Since an increase in UV intensity could enhance the hydroxyl radical (OH<sup>•</sup>) formation in the photocatalytic reaction and in the condition of higher vibration frequency, a contact or mixing between pollutants and TiO<sub>2</sub> was enhanced, then higher adsorption between pollutants and TiO<sub>2</sub> and higher degradation could be occurred. Whereas, the removal efficiencies of lignin and 2,4-DCP were decreased with increasing initial pH and initial concentration. This might be because the TiO<sub>2</sub> surface and molecules of pollutants are negatively charged in alkaline solution (pH > pzc), being repelled from the TiO<sub>2</sub> surface which causes to reduce their adsorption as well as under high solution concentration, saturation coverage of pollutants on the surface of TiO<sub>2</sub> occurred or yielded a higher concentration of adsorbed intermediates according to more compete with intermediates for TiO<sub>2</sub> sites.

5.1.2 The optimum operating conditions of the supervibration-photocatalytic reactor for treatment of lignin and 2,4-DCP in both synthetic wastewater and real



wastewater from pulp and paper mill were found to be initial pH 5, UV intensity of  $25.2 \text{ mW/cm}^2$  and vibration frequency of 50 Hz. Under the optimum treatment conditions, the supervibration-photocatalytic reactor could remove lignin and color in synthetic wastewater with the efficiencies of 85.12% and 70.55%, respectively after 420 min and 2,4-DCP degradation was completed within 60 min. Whereas, the removal efficiencies of lignin, color and 2,4-DCP in mixed synthetic wastewater were 76.21%, 60.75% and 97.13%, respectively within 420 min. Furthermore, the reactor could remove lignin, color and 2,4-DCP in pulp and paper mill wastewater with the capacities of 75.11%, 52.16% and 94.14%, respectively after the same time. When removal efficiencies of mixed synthetic wastewater, real wastewater from pulp and paper mill and synthetic wastewater containing single pollutant were compared, lignin had an interference effect on 2,4-DCP removal by the system. The removal efficiencies of 2,4-DCP in mixed synthetic wastewater and real wastewater were much less than that in 2,4-DCP synthetic wastewater, whereas removal efficiencies of lignin in mixed synthetic wastewater and real wastewater were slightly reduced. This might be because brown color of lignin in mixed synthetic wastewater and real wastewater inhibits UV light penetration into water, whereas 2,4-DCP synthetic wastewater is clear solution.

5.1.3 The apparent rate constant of first order reaction ( $k_{ap}$ ) and the initial degradation rate ( $r_0$ ) of lignin and 2,4-DCP degradation in synthetic wastewater at various initial pH, UV intensity and vibration frequency followed the same trend as lignin and 2,4-DCP removal. For various initial concentration, only  $k_{ap}$  had the same trend as lignin and 2,4-DCP removal. The  $r_0$  increased with  $C_0$  (the initial concentration), since in the product  $k_{ap}C_0$ , the increase in concentration was more significant than the variation in  $k_{ap}$  values. Under the optimum operating conditions,  $k_{ap}$  and  $r_0$  of lignin degradation were  $13.9 \times 10^{-3} \text{ min}^{-1}$  and  $1.39 \text{ mg/l min}^{-1}$ , respectively after 120 min. Whereas,  $k_{ap}$  and  $r_0$  of 2,4-DCP degradation were  $56.3 \times 10^{-3} \text{ min}^{-1}$  and  $28.2 \times 10^{-3} \text{ mg/l min}^{-1}$ , respectively after 30 min.

5.1.4 The analysis of residue from lignin degradation showed the presence of some lignin derivatives such as 2-methylbenzaldehyde, 2,4-dimethylbenzaldehyde and 4-hydroxy-3-methoxybenzaldehyde (vanillin). Moreover, the by-products of 2,4-DCP degradation were phenol, 2-chlorophenol and 4-chlorophenol. The results reveal that occurred by-products might have toxicity less than the parent compound since the toxic effects of chlorophenols are directly proportional to the degree of chlorination.

## 5.2 Suggestion for Future Works

5.2.1 The photocatalytic activity of lignin, color and 2,4-DCP degradation significantly increased with increasing UV intensity. But for real wastewater from pulp and paper mill, the supervibration-photocatalytic reactor with UV intensity of 25.2 mW/cm<sup>2</sup> could remove color at low capacity as 52.16% within 420 min. Therefore, the higher UV intensity introduced to the reactor is important to enhance the performance of the supervibration-photocatalytic reactor on removal of color in pulp and paper mill wastewater.

5.2.2 Before experimental set up for the photocatalytic degradation using the catalyst as TiO<sub>2</sub> film produced by electrochemical anodization process of titanium plate, the surface morphology, average pore size and pore distribution of the TiO<sub>2</sub> film should be analyzed by scanning electron microscopy (SEM) in order to much understand the photocatalytic oxidation of pollutants in the experiments.

ศูนย์วิทยทรัพยากร  
จุฬาลงกรณ์มหาวิทยาลัย

## REFERENCES

- Adler, E. 1977. Lignin chemistry-past, present and future. Wood Science Technology 11: 169-218.
- Agilent Technologies, Inc. 2006. The essential chromatography and spectroscopy catalog: 2007- 2008 edition. Canada: (n.p.).
- Alen, R., Sari, R., and McKeough, P. 1995. Thermogravimetric behavior of black liquor and their organic constituents. Journal of Analytical and Applied Pyrolysis 31: 1-13.
- Ali, M., and Sreerishnan, T. R. 2001. Aquatic toxicity from pulp and paper mill effluents: a review. Advances in Environmental Research 5: 175-196.
- Amer, S. M., and Aly, F. A. E. 2001. Genotoxic effect of 2,4-dichlorophenoxy acetic acid and its metabolite 2,4-dichlorophenol in mouse. Genetic Toxicology and Environmental Mutagenesis 494: 1-12.
- Atuanya, E. I., Purohit, H. J., and Chakrabarti, T. 2000. Anerobic and aerobic biodegradation of chlorophenols using UASB and ASG bioreactor. World Journal of Microbiology & Biotechnology 16: 95-98.
- Bahnemann, D., Henglein, A., and Spanhel, L. 1984. Detection of the intermediates of colloidal TiO<sub>2</sub>-catalysed photoreactions. Faraday Discussions of the Chemical Society 78: 151-163.
- Bao-xiu, Z., Xiang-zhong, L., and Peng, W. 2007. Degradation of 2,4-dichlorophenol with a novel TiO<sub>2</sub>/Ti-Fe-graphite felt photoelectrocatalytic oxidation process. Journal of Environmental Sciences 19: 1020-1024.
- Batoev, V. B., Nimatsyrenova, G. G., Dabalaeva, G. S., and Palitsyna, S. S. 2005. An assessment of contamination of the Selenga River Basin by chlorinated phenols. Chemistry for Sustainable Development 13: 31-36.
- Bayarri, B., Abellán, M. N., Giménez, J., and Esplugas, S. 2007. Study of the wavelength effect in the photolysis and heterogeneous photocatalysis. Catalysis Today 129: 231-239.

- Bayarri, B., Giménez, J., Curcó, D., and Esplugas, S. 2005. Photocatalytic degradation of 2,4-dichlorophenol by TiO<sub>2</sub>/UV: kinetics, actinometries and models. Catalysis Today 101: 227-236.
- Bayarri, B., González, O., Maldonado, M. I., Giménez, J., and Esplugas, S. 2007. Comparative study of 2,4-dichlorophenol degradation with different advanced oxidation processes. Journal of Solar Energy Engineering 129: 60-67.
- Blažková, A., Csölleová, I., and Brezová, V. 1998. Effect of light sources on the phenol degradation using Pt/TiO<sub>2</sub> photocatalysis immobilized on glass fibres. Journal of Photochemistry and Photobiology A: Chemistry 113: 251-256.
- Boer, K. W. 1990. Survey of semiconductor physics. New York: Van Nostrand Reinhold.
- Bohlin, C., Lundquist, K., and Jönsson, L. J. 2008. Diastereomer selectivity in the degradation of a lignin model compound of the arylglycerol β-aryl ether type by white-rot fungi. Enzyme and Microbial Technology 43: 199-204.
- Boutwell, R. K., and Bosch, D. K. 1959. The tumour-promoting action of phenol and related compounds for mouse skin. Cancer Research 19: 413-424.
- Browning, B., ed. 1975. The chemistry of wood. Huntington, New York: Robert E. Krieger.
- Bukowska, B., Michalowicz, J., Krokosz, A., and Sicińska, P. 2007. Comparison of the effect of phenol and its derivatives on protein and free radical formation in human erythrocytes (*in vitro*). Blood Cells, Molecules, and Diseases 39: 238-244.
- Catalkaya, E. C., and Kargi, F. 2008. Advanced oxidation treatment of pulp mill effluent for TOC and toxicity removals. Journal of Environmental Management 87: 396-404.
- Chang, C.-N., et al. 2004. Decolorizing of lignin wastewater using the photochemical UV/TiO<sub>2</sub> process. Chemosphere 56: 1011-1017.
- Chanwit Srikaew. 2001. Lignin removal from pulp and paper mill wastewater by chitosan. Master's Thesis. Department of Environmental Engineering, Faculty of Engineering, Khon Kaen University.
- Chen, C., Lei, P., Ji, H., Ma, W., and Zhao, J. 2004. Photocatalysis by titanium dioxide and polyoxometalate/TiO<sub>2</sub> cocatalysts: intermediates and mechanistic study. Environmental Science & Technology 38: 329-337.

- Cheng, S., Tsai, S. J., and Lee, Y. F. 1995. Photocatalytic decomposition of phenol over titanium oxide of various structure. Catalysis Today 26: 87-96.
- Chu, W., Kwan, C. Y., Chan, K. H., and Kam, S. K. 2005. A study of kinetic modeling and reaction pathway of 2,4-dichlorophenol transformation by photo-fenton-like oxidation. Journal of Hazardous Materials B121: 119-126.
- Cunningham, W. P., Cunningham, M. A., and Saigo, B. W. 2007. Environmental science: a global concern. 9<sup>th</sup>ed. New York: McGraw-Hill.
- Dahm, A., and Lucia, L. A. 2004. Titanium dioxide catalyzed photodegradation of lignin in industrial effluents. Industrial & Engineering Chemistry Research 43: 7996-8000.
- Dekker, R. F. H., Barbosa, A. M., and Sargent, K. 2002. The effect of lignin-related compounds on the growth and production of laccases by the ascomycete, *Botryosphaeria* sp. Enzyme and Microbial Technology 30: 374-380.
- De Lasa, H. I., Dogu, G., and Ravella, A., eds. 1992. Chemical reactor technology for environmentally safe reactors and product. London: Kluwer Academic.
- Eaton, A. D., Clesceri, L. S., Rice, E. W., and Greenberg, A. E. 2005. Standard methods for the examination of water and wastewater. 21<sup>st</sup>ed. Washington, DC: American Public Health Association.
- Economy, Trade and Industry, Ministry. Chemical Substances Council. 2002. Hazard assessment of some chemical substances which have been suspected to be endocrine disrupters. Japan: (n.p.).
- Eugenia, J. O., Gloria, S., and Elizabeth, H. 2000. Environmental biotechnology and cleaner bioprocesses. London: Taylor and Francis.
- Gao, Z., Yang, S., Sun, C., and Hong, J. 2007. Microwave assisted photocatalytic degradation of pentachlorophenol in aqueous TiO<sub>2</sub> nanotubes suspension. Separation and Purification Technology 58: 24-31.
- Gaya, U. I., and Abdullah, A. H. 2008. Heterogeneous photocatalytic degradation of organic contaminants over titanium dioxide: a review of fundamentals, progress and problems. Journal of Photochemistry and Photobiology C: Photochemistry Reviews 9: 1-12.
- Gersich, F. M., and Milazzo, D. P. 1988. Chronic toxicity of aniline and 2,4-dichlorophenol to *Daphnia magna* Straus. Bullentin of Environmental Contamination and Toxicology 40: 1-7.



- González, L. F., Sarria, V., and Sánchez, O. F. 2010. Degradation of chlorophenols by sequential biological-advanced oxidative process using *Trametes pubescens* and TiO<sub>2</sub>/UV. Bioresource Technology 101: 3493-3499.
- Harvey, P. R., Rudham, R., and Ward, S. 1983. Photocatalytic oxidation of liquid propan-2-ol by TiO<sub>2</sub>. Journal of the Chemical Society, Faraday Transaction 1 79: 1381-1390.
- Health and Human Services, United State Department. National Toxicology Programme (NTP). 1988. NTP technical report on the toxicology and carcinogenesis studies of 2,4-dichlorophenols in F344/N rats and B6C3F1 mice (feed studies). Research Triangle Park. North Carolina: (n.p.).
- Health Canada. 1987. Chlorophenols [Online]. Ottawa, Canada. Available from: <http://www.hc-sc.gc.ca/ewh-semt/alt-formats/hecs-sesc/pdf/pubs/water-eau/chlorophenols/chlorophenols-eng.pdf> [2011, January 10]
- Hofrichter, M., and Steinbüchel, A., eds. 2001. Biopolymers: lignin, humic substances and coal. Vol.1. Germany: WILEY-VCH.
- Hofstadler, K., Bauer, R., Novalic, S., and Heiser, G. 1994. New reaction design for photocatalytic wastewater treatment with TiO<sub>2</sub> immobilized on fused-silica glass fibers: photomineralization of 4-chlorophenol. Environmental Science & Technology 28: 670-674.
- Ilisz, I., and Dombi, A. 1999. Investigation of the photodecomposition of phenol in near UV irradiated aqueous TiO<sub>2</sub> suspensions II: effects of charge trapping species on product distribution. Applied Catalysis A: General 180: 35-45.
- Industry, Ministry. Department of Industrial Work, Environmental Technology Office. 1999. Environmental management in the pulp and paper industry. Thailand: (n.p.).
- International Program on Chemical Safety (IPCS) and the Commission of the European Communities (CEC). 2004. 2,4-Dichlorophenol [Online]. (n.p.). Available from: <http://www.inchem.org/documents/icsc/eics/0438.htm> [2008, July 12]
- Johansson, E., Krantz-Rülcker, C., Zhang, B. X., and Öberg, G. 2000. Chlorination and biodegradation of lignin. Soil Biology & Biochemistry 32: 1029-1032.



- Kaigi, F., Eker, S., and Uygur, A. 2005. Biological treatment of synthetic wastewater containing 2,4-dichlorophenol (DCP) in an activated sludge unit. Journal of Environmental Management 76: 191-196.
- Kaneko, M., and Okura, I., eds. 2002. Photocatalysis: science and technology. Tokyo: Kodansha.
- Kansal, S. K., Singh, M., and Sud, D. 2008. Studies on TiO<sub>2</sub>/ZnO photocatalysed degradation of lignin. Journal of Hazardous Materials 153: 412-417.
- Kent, A., and Jame, A. 1983. Riegel's handbook of industrial chemistry. 8<sup>th</sup>ed. New York: Van Nostrand Reinhold.
- Ko J.-J. et al. 2009. Biodegradation of high molecular weight lignin under sulfate reducing conditions: lignin degradability and degradation by-products. Bioresource Technology 100: 1622-1627.
- Konstantinou, I. K., and Albanis, T. A. 2004. TiO<sub>2</sub>-assisted photocatalytic degradation of azo dyes in aqueous solution: kinetic and mechanistic investigations a review. Applied Catalysis B: Environmental 49: 1-14.
- Kringstad, K. P., and Lindstrom, K. 1984. Spent liquors from pulp bleaching. Environmental Science & Technology 18: 236A-248A. Cited in Ali, M., and Sreekrishnan, T. R. 2001. Aquatic toxicity from pulp and paper mill effluents: a review. Advances in Environmental Research 5: 175-196.
- Ksibi, M., et al. 2003. Photodegradation of lignin from black liquor using a UV/TiO<sub>2</sub> system. Journal of Photochemistry and Photobiology A: Chemistry 154: 211-218.
- Kuiper, J., and Hantsveit, A. O. 1984. Fate and effects of 4-chlorophenol and 2,4-dichlorophenol in marine plankton communities in experimental enclosures. Ecotoxicology and Environmental Safety 8: 15-33.
- Kumar, K. V., Porkodi, K., and Rocha, F. 2008. Langmuir-Hinshelwood kinetics-a theoretical study. Catalysis Communications 9: 82-84.
- Kusvuran, E., Samil, A., Atanur, O. M., and Eebatur, O. 2005. Photocatalytic degradation kinetics of di- and tri-substituted phenolic compounds in aqueous solution by TiO<sub>2</sub>/UV. Applied Catalysis B: Environmental 58: 211-216.

- Lanzalunga, O., and Bietti, M. 2000. Photo-and radiation chemical induced degradation of lignin model compounds. Journal of Photochemistry and Photobiology B: Biology 56: 85-108.
- Lavigne, J. R. 1979. Instrumentation applications for the pulp and paper industry. 1<sup>st</sup>ed. USA: Miller Freeman.
- Leiviskä, T., Rämö, J., Nurmesniemi, H., Pöykiö, R., and Kuokkanen, T. 2009. Size fractionation of wood extractives, lignin and trace elements in pulp and paper mill wastewater before and after biological treatment. Water Research 43: 3199-3206.
- Leuenberger, C., Giger, W., Coney, R., Graydon, J. W., and Molnar-Kubica, E. 1985. Persistent chemicals in pulp mill effluents: occurrence and behaviour in an activated sludge treatment plant. Water Research 19: 885-894.
- Litter, M. I. 1999. Heterogeneous photocatalysis transition metal ions in photocatalytic systems. Applied Catalysis B: Environmental 23: 89-114.
- Liu, D., and Pacepavicius, G. 1990. A systematic of the aerobic and anaerobic biodegradation of 18 chlorophenols and 3 cresols. Toxicity Assessment 5: 367-388.
- Liu, L., Chen, F., and Yang, F. 2009. Stable photocatalytic activity of immobilized Fe<sup>0</sup>/TiO<sub>2</sub>/ACF on composite membrane in degradation of 2,4-dichlorophenol. Separation and Purification Technology 70: 173-178.
- Lu, Q., and Gao, J. 2006. Degradation of 2,4-dichlorophenol by using glow discharge electrolysis. Journal of Hazardous Materials B136: 526-531.
- Ma, Y-S., Chang, C-N., Chiang, Y-P., Sung, H-F., and Chao, A. C. 2008. Photocatalytic degradation of lignin using Pt/TiO<sub>2</sub> as the catalyst. Chemosphere 71: 998-1004.
- Malaviya, P., and Rathore, V. S. 2007. Bioremediation of pulp and paper mill effluent by a novel fungal consortium isolated from polluted soil. Bioresource Technology 98: 3647-3651.
- Matafonova, G., et al. 2006. Degradation of 2,4-dichlorophenol by *Bacillus* sp. Isolated from an aeration pond in the Baikalsk pulp and paper mill (Russia). International Biodeterioration & Biodegradation 58: 209-212.

- McCarthy, E. 2004. The nature of lignin [Online]. (n.p.). Available from: <http://www.palimpsest.stanford.edu/byorg/abbey/ap/ap04/ap04-4/ap04-042.html> [2007, April 6]
- Mackay, D., Shiu, W. Y., and Ma, K.C. 1997. Illustrated handbook of physical-chemical properties and environmental fate of organic chemicals. (n.p.): Lewis Publishers 351 and 374. Cited in Kieher, M. C., Hengraprom, S., and Knuteson, S. 1998. Organochlorines: analysis of the chlorophenol group [Online]. (n.p.): Clemson University. Available from: <http://www.entweb.cleson.edu/pesticide/document/leeorg1/leeorg1.htm> [2008, July 13]
- Naeem, K., and Feng, O. 2009. Parameters effect on heterogeneous photocatalysed degradation of phenol in aqueous dispersion of TiO<sub>2</sub>. Journal of Environmental Sciences 21: 527-533.
- Nair, M., Luo, Z. H., and Heller, A. 1993. Rate of photocatalytic oxidation of crude oil on salt water on buoyant, cenosphere-attached titanium dioxide. Industrial & Engineering Chemistry Research 32: 2318-2323.
- Nakashima, T., Ohko, Y., Tryk, D. A., and Fujishima, A. 2002. Decomposition of endocrine-disrupting chemicals in water by use of TiO<sub>2</sub> photocatalysts immobilized on polytetrafluorethylene mesh sheets. Journal of Photochemistry and Photobiology A: Chemistry 151: 207-212.
- Pandiyan, T., Rivas, O. M., Martínez, J. O., Amezcua, G. B., and Martínez-Carrillo, M. A. 2002. Comparison of methods for the photochemical degradation of chlorophenols. Journal of Photochemistry and Photobiology A: Chemistry 146: 149-155.
- Parham, R. A. 1983. Ultra-structure and chemistry. In M. J. Kocurek, and F. Stevens (eds.), Pulp and paper manufacture: properties of fibrous raw materials and their preparation for pulping, pp. 40-42. Vol. 1, 3<sup>rd</sup>ed. Canada: The joint textbook committee of the paper industry.
- Pera-Titus, M., García-Molina, V., Baños, M. A., Giménez, J., and Esplugas, S. 2004. Degradation of chlorophenols by means of advanced oxidation processes: a general review. Applied Catalysis B: Environmental 47: 219-256.
- Pessala, P., et al. 2004. Lignin as the cause of acute toxicity in pulp and paper mill effluents. In D. L. Borton, T. J. Hall, R. P. Fisher, and J. F. Thomas (eds.),

- Pulp & paper mill effluent environmental fate & effects, pp. 319-330. Lancaster Philadelphia: DEStech Publications.
- Pichat, P., and Herrmann, J-M. 1989. Adsorption-desorption, related mobility and reactivity in photocatalysis. In N. Serpone, and E. Pelizzetti (eds.), Photocatalysis, pp. 217-250. New York: John Wiley & Sons.
- Pimchanok Tengcharoen. 2003. Decolorization of wastewater from lignin production by white rot fungi. Master's Thesis. Inter-Department of Environmental Science, Graduate School, Chulalongkorn University.
- Pokhrel, D., and Viraraghavan, T. 2004. Treatment of pulp and paper mill wastewater-a review. Science of the Total Environment 333: 37-58.
- Pollution Control, Department. 2000. The project of industrial environment index making. Bangkok: (n.p.).
- Pollution Control, Department. 2001. The completed report: the project of demonstration of waste reduction technology in pulp and paper industry. Bangkok: (n.p.).
- Portjanskaja, E., and Preis, S. 2007. Aqueous photocatalytic oxidation of lignin: the influence of mineral admixtures. International Journal of Photoenergy 1-7.
- Portjanskaja, E., Stepanova, K., Klauson, D., and Preis, S. 2009. The influence of titanium dioxide modifications on photocatalytic oxidation of lignin and humic acids. Catalysis Today 144: 26-30.
- Quan, X., Shi, H., Liu, H., Wang, J., and Qian, Y. 2004. Removal of 2,4-dichlorophenol in a conventional activated sludge system through bioaugmentation. Process Biochemistry 39: 1701-1707.
- Ramos, W. D. S., Poznyak, T., Chairez, I., and Córdova, I. R. 2009. Remediation of lignin and its derivatives from pulp and paper industry wastewater by the combination of chemical precipitation and ozonation. Journal of Hazardous Materials 169: 428-434.
- Reutergardh, L. B., and Iangphasuk, M. 1997. Photocatalytic decolourization of reactive azo dye: a comparative between TiO<sub>2</sub> and CdS photocatalysis. Chemosphere 35: 585-596.
- Ribeiro, A., Neves, M. H., Almeida, M. F., Alves, A., and Santos, L. 2002. Direct determination of chlorophenols in landfill leachates by solid-phase micro-

- extraction-gas chromatography-mass spectrometry. Journal of Chromatography A 975: 267-274.
- Robertson, P. K. J. 1996. Semiconductor photocatalysis: an environmentally acceptable alternative production technique and effluent treatment process. Journal of Cleaner Production 4: 203-212.
- Rubin, J. 2007. Electromagnetic radiation [Online]. Australia: Queensland University of Technology. Available from: [http://www.juliantrubin.com/encyclopedia/electricity/electromagnetic\\_radiation.html](http://www.juliantrubin.com/encyclopedia/electricity/electromagnetic_radiation.html) [2008, September 19]
- Sahinkaya, E., and Dilek, F. B. 2006. Effect of biogenic substrate concentration on the performance of sequencing batch reactor treating 4-CP and 2,4-DCP mixtures. Journal of Hazardous Materials B128: 258-264.
- Sahinkaya, E., and Dilek, F. B. 2009. The growth behavior of *Chlorella vulgaris* in the presence of 4-chlorophenol and 2,4-dichlorophenol. Ecotoxicology and Environmental Safety 72: 781-786.
- Sahoo, D., and Gupta, R. 2005. Evaluation of ligninolytic microorganisms for efficient decolorization of a small pulp and paper mill effluent. Process Biochemistry 40:1573-1578
- Sankaran, K., and Vand Lundwig, C. H. 1971. Lignin: occurrence, formation, structure and reactions. New York: John Wiley & Sons.
- Scally, F. E. J., and Hoigne, J. 1987. Rate constants for reaction of singlet oxygen with phenols and other compounds in water. Chemosphere 16: 681-694.
- Scandola, F., and Balzani, V. 1989. Interaction between light and matter. In N. Serpone, and E. Pelizzetti (eds.), Photocatalysis. fundamentals and applications, pp. 9-44. New York: John Wiley & Sons.
- Scragg, A. H., Spiller, L., and Morrison, J. 2003. The effect of 2,4-dichlorophenol on the microalga *Chlorella* VT-1. Enzyme and Microbial Technology 32: 616-622.
- Serpone, N., and Pelizzetti, E., eds. 1989. Photocatalysis. fundamentals and applications. New York: John Wiley & Sons.
- Shivaraju, H. P., Byrappa, K., and Ananda, S. 2010. Photocatalytic treatment of paper and pulp industrial effluents using TiO<sub>2</sub> deposited calcium aluminosilicate beads. International Journal of Chemical Engineering Research 2: 219-230.



- Sjostrom, E. 1981. Wood chemistry fundamentals and applications. Finland: Harcourt Brace Jovanovich.
- Sjostrom, E., and Alen, R. 1999. Analytical methods in wood chemistry, pulping and papermaking. New York: Springer-Verlag Berlin Heidelberg.
- Somshy Kinakul. 2002. High performance liquid chromatographic analysis of phenolic compounds and photooxidation of chlorophenols using titanium dioxide as photosensitizer. Master's Thesis. Department of Environmental Engineering, Faculty of Engineering, Khon Kaen University.
- Sugiura, M., Hirai, H., and Nishida, T. 2003. Purification and characterization of a novel lignin peroxidase from white-rot fungus *Phanerochaete sordida* YK-624. FEMS Microbiology Letters 224: 285-290.
- Tanaka, K., Calanag, R. C. R., and Hisanaga, T. 1999. Photocatalyzed degradation of lignin on TiO<sub>2</sub>. Journal of Molecular Catalysis A: Chemical 138: 287-294.
- Theurich, U., Lindner, M., and Bahnemann, D. W. 1996. Photocatalytic degradation of 4-chlorophenol in aerated aqueous titanium dioxide suspensions: a kinetic and mechanistic study. Langmuir 12: 6368-6376.
- Uğurlu, M., and Karaoğlu, M. H. 2009. Removal of AOX, total nitrogen and chlorinated lignin from bleached Kraft mill effluents by UV oxidation in the presence of hydrogen peroxide utilizing TiO<sub>2</sub> as photocatalyst. Environmental Science and Pollution Research 16: 265-273.
- United Nations Environment Programme (UNEP). 1996. Cleaner production at pulp and paper mills: a guidance manual. (n.p.).
- United Nations Environment Programme (UNEP), Industry and Environment Office. 1983. Environmental management in the pulp and paper industry-executive summary. 1<sup>st</sup>ed. (n.p.).
- Uysal, A., and Türkman, A. 2005. Effect of biosurfactant on 2,4-dichlorophenol biodegradation in an activated sludge bioreactor. Process Biochemistry 40: 2745-2749.
- Valente, J. P. S., Padilha, P. M., and Florentino, A. O. 2006. Studies on the adsorption and kinetics of photodegradation of a model compound for heterogeneous photocatalysis onto TiO<sub>2</sub>. Chemosphere 64: 1128-1133.



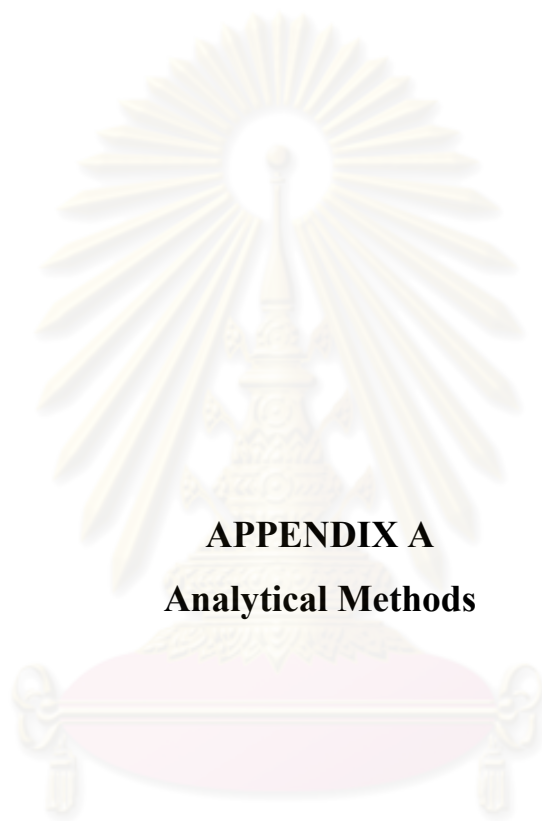
- Wallberg, O., Jonsson, A. S., and Wimmerstedt, R. 2003. Fractionation and concentration of kraft black liquor lignin with ultrafiltration. Desalination 154: 187-199.
- Wang, G., Wang, X., Yu, R., and Deng, N. 2008. Photocatalytic degradation of azo dye acid red 14 based on molecular recognition interaction. Fresenius Environmental Bulletin 17: 1054-1060.
- Wang, S.-G. et al. 2007. Aerobic granulation for 2,4-dichlorophenol biodegradation in a sequencing batch reactor. Chemosphere 69: 769-775.
- Wikipedia. 2008. Ultraviolet [Online]. United State: Wikipedia Foundation. Available from: [http://www .en.wikipedia.org/wiki/Ultraviolet](http://www.en.wikipedia.org/wiki/Ultraviolet) [2008, August 9]
- Williams, T. G., Carey, J. H., Burnison, B. K., Dixon, D. G., and Lee, H. B. 1996. Rainbow trout (*Oncorhynchus mykiss*) mixed function oxygenase responses by unbleached and bleached pulp mill effluents: a laboratory-based study. In M. R. Servos, K. R. Munkittrick, J. H. Carey, and G. J. Vander kraak (eds.), Environmental fate and effects of pulp and paper mill effluents, pp. 379-389. Florida: St. Lucie.
- Wu, J., Xiao, Y.-Z., and Yu, H.-Q. 2005. Degradation of lignin in pulp mill wastewaters by white-rot fungi on biofilm. Bioresource Technology 96: 1357-1363.
- Wünning, P. 2001. Applications and use of lignin as raw material. In M. Hofrichter, and A. Steinbüchel (eds.), Biopolymers: lignin, humic substance, and coal, Vol. 1, pp. 117-127. Germany: Wiley-VCH.
- Xiangchun, Q., Hanchang, S., Yongming, Z., Jianlong, W., and Yi, Q. 2003. Biodegradation of 2,4-dichlorophenol in an air-life honeycomb-like ceramic reactor. Process Biochemistry 38: 1545-1551.
- Xie, Y. B., and Li, X. Z. 2006. Interactive oxidation of photoelectrocatalysis and electro-Fenton for azo dye degradation using TiO<sub>2</sub>-Ti mesh and reticulated vitreous carbon electrodes. Materials Chemistry and Physics 95: 39-50.
- Yakovleva, Y. N., Ostrovskaya, R. M., and Novikova, L. N. 2004. Assessment of genotoxicity of lignin substances as risk factors for aquatic ecosystems. Russian Journal of Ecology 35: 242-246.

- Yang, S., Wu, R. S. S., and Kong, R. Y. C. 2002. Biodegradation and enzymatic responses in the marine diatom *Skeletonema costatum* upon exposure to 2,4-dichlorophenol. *Aquatic Toxicology* 59: 191-200.
- Yeber, M. C., Rodríguez, J., Freer, J., Durán, N., and Mansilla, H. D. 2000. Photocatalytic degradation of cellulose bleaching effluent by supported TiO<sub>2</sub> and ZnO. *Chemosphere* 41: 1193-1197.
- Yerokhin, A. L., Nie, X., Leyland, A., Matthews, A., and Dowey, S. J. 1999. Plasma electrolysis for surface engineering. *Surface and Coatings Technology* 122: 73-93.
- Yin, L., Shen, Z., Niu, J., Chen, J., and Duan, Y. 2010. Degradation of pentachlorophenol and 2,4-dichlorophenol by sequential visible-light driven photocatalysis and laccase catalysis. *Environmental Science & Technology* 44: 9117-9122.
- Zeltner, W. A., Hill, C. G. J., and Anderson, M. A. 1993. Supported titania for photodegradation. *Chemtech* 23: 21-28.
- Zhang, J., Shen, H., Wang, X., Wu, J., and Xue, Y. 2004. Effects of chronic exposure of 2,4-dichlorophenol on the antioxidant system in liver of freshwater fish *Carassius auratus*. *Chemosphere* 55: 167-174.
- Zhou, H., and Smith, D. W. 2002. Advanced technologies in water and wastewater treatment. *Journal of Environmental Engineering and Science* 1: 247-264.



**APPENDICES**

ศูนย์วิทยทรัพยากร  
จุฬาลงกรณ์มหาวิทยาลัย



**APPENDIX A**  
**Analytical Methods**

ศูนย์วิทยทรัพยากร  
จุฬาลงกรณ์มหาวิทยาลัย

## Analytical Method of Lignin

### 1. Synthetic wastewater

(Ksibi et al., 2003; Pessala et al., 2004; Portjanskaja et al., 2009)

#### 1.1 Apparatus

UV-Visible spectrophotometer, Model Helios Alpha.

#### 1.2 Reagents

Stock solution: Dissolved 0.1 g lignosulfonic acid sodium salt in distilled water and diluted to 1,000 ml. This stock solution has a lignin of 100 mg/l.

#### 1.3 Procedures

1.3.1 Standard preparation for calibration curve: Standard lignin solutions were prepared in the concentration of 10, 20, 30, 40, 50, 60, 70 and 80 mg/l by diluting 10, 20, 30, 40, 50, 60, 70 and 80 ml stock solution with distilled water in 100 ml volumetric flasks. After that, the standard lignin solutions were analyzed as light absorbance using UV-Visible spectrophotometer with detection wavelength of 280 nm and obtained standard curve as shown in Table A.1 and Figure A.1.

1.3.2 Sample analysis: The effluent samples of synthetic wastewater were diluted by distilled water as 2 times for initial concentration of 100 mg/l (12.5 ml samples in 25 ml distilled water), 3 times for initial concentration of 200 mg/l (8.33 ml samples in 25 ml distilled water), 4 times for initial concentration of 300 mg/l (6.25 ml samples in 25 ml distilled water) and 5 times for initial concentration of 400 mg/l (5 ml samples in 25 ml distilled water). After that, measured light absorbance of samples by UV-Visible spectrophotometer at a wavelength of 280 nm and calculated lignin concentration using standard curve.

Table A.1 Light absorbance of lignin standards detected by  
UV-Visible spectrophotometer at 280 nm

Lignin concentration (mg/l)	Absorbance at 280 nm
10	0.113
20	0.222
30	0.335
40	0.457
50	0.581
60	0.706
70	0.811
80	0.914

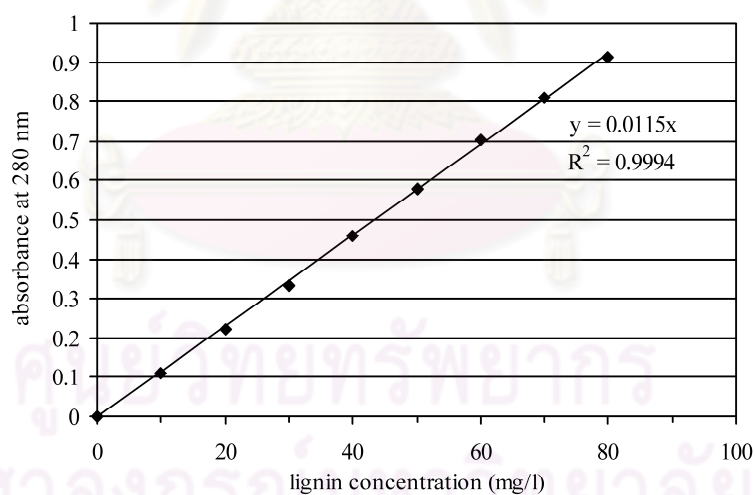


Figure A.1 Standard curve of lignin standards detected by  
UV-Visible spectrophotometer at 280 nm



## 2. Real wastewater from pulp and paper mill

(Eaton et al., 2005, Standard methods)

### 2.1 General discussion

Lignin is a plant that often is discharged as a waste during the manufacture of paper pulp. Both lignin and tannin contain aromatic hydroxyl groups that react with Folin phenol reagent (tungstophosphoric and molybdophosphoric acids) to form a blue color suitable for estimation of concentrations up to at least 9 mg/l.

### 2.2 Apparatus

2.2.1 UV-Visible spectrophotometer, Model Helios Alpha.

2.2.2 Nylon membrane filters 0.45  $\mu\text{m}$ , 47 mm: FILTREX

### 2.3 Reagents

2.3.1 Folin phenol reagent: Purchased commercially prepared Folin phenol reagent as Folin-Ciocalteu's reagent.

2.3.2 Carbonate-tartrate reagent: Dissolved 200 g sodium carbonate ( $\text{Na}_2\text{CO}_3$ ) and 12 g sodium tartrate ( $\text{Na}_2\text{C}_4\text{H}_4\text{O}_6 \cdot 2\text{H}_2\text{O}$ ) in 750 ml hot distilled water, cool to 20 °C, and diluted to 1,000 ml.

2.3.3 Stock solution: Dissolved 0.1 g liginosulfonic acid sodium salt in distilled water and diluted to 1,000 ml. This stock solution has a lignin of 100 mg/l.

### 2.4 Procedures

2.4.1 Standard preparation for calibration curve: Standard lignin solutions were prepared in the concentration of 10, 20, 30, 40, 50, 60, 70 and 80 mg/l by diluting 10, 20, 30, 40, 50, 60, 70 and 80 ml stock solution with distilled water in 100 ml volumetric flasks. Brought 25 ml portion clear standards to a temperature above 20 °C and maintained within a  $\pm 2$  °C rang. Added in rapid succession 0.5 ml

Folin-Ciocalteu's reagent and 5 ml carbonate-tartrate reagent. Allowed 30 min for color development. After that, the standard lignin solutions were analyzed as light absorbance using UV-Visible spectrophotometer with detection wavelength of 700 nm and obtained standard curve as shown in Table A.2 and Figure A.2.

Table A.2 Light absorbance of standard lignin solutions detected by UV-Visible spectrophotometer at 700 nm

Lignin concentration (mg/l)	Absorbance at 700 nm
10	0.082
20	0.191
30	0.273
40	0.375
50	0.446
60	0.529
70	0.621
80	0.688

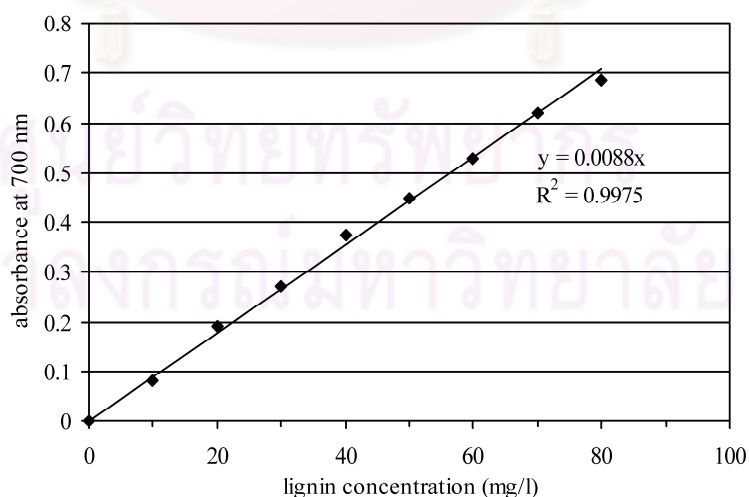


Figure A.2 Standard curve of standard lignin solutions detected by UV-Visible spectrophotometer at 700

2.4.2 Sample analysis: 12.5 ml of the effluent samples of real wastewater were diluted to 50 ml with distilled water (4 times) and the samples were filtered using 0.45  $\mu\text{m}$  nylon membrane filter, 47 mm to remove fine particulates. Then, brought 25 ml portion clear samples to a temperature above 20 °C and maintained within a  $\pm 2$  °C rang. Added in rapid succession 0.5 ml Folin-Ciocalteu's reagent and 5 ml carbonate-tartrate reagent. Allowed 30 min for color development. After that, measured light absorbance of samples by UV-Visible spectrophotometer at a wavelength of 700 nm and calculated lignin concentration using standard curve.



ศูนย์วิทยทรัพยากร  
จุฬาลงกรณ์มหาวิทยาลัย

## **Analytical Method of Color**

(Eaton et al., 2005, Standard methods)

### **1. Introduction**

Industrial wastewaters can contain lignin, tannin, dyes and other organic and inorganic chemicals that cause color. The term “color” is used here to mean true color, that is, the color of water from which turbidity has removed. The term “apparent color” includes not only color due to substances in solution, but also that due to suspended matter. Apparent color is determined on the original sample without filtration. Suspended particles, especially colloidal-size particles such as clays, algae, iron and manganese oxides, give water an appearance of color; they should be removed before measurement.

### **2. General discussion**

Color is determined spectrophotometrically at a wavelength between 450 and 465 nm, with platinum-cobalt solutions as standards. True color of real samples and platinum-cobalt standards follows Beer’s Law. The spectrophotometric platinum-cobalt method is applicable to natural waters, potable waters and wastewaters, both domestic and industrial.

### **3. Apparatus**

3.1 UV-Visible spectrophotometer, Model Helios Alpha

3.2 Glass microfiber filters GF/C, 47 mm, Whatman

3.3 pH meter, HORIBA

#### 4. Reagents

- 4.1 Potassium hexachloroplatinate ( $K_2PtCl_6$ ), analytical grade
- 4.2 Cobaltous chloride ( $CoCl_2 \cdot 6H_2O$ ), analytical grade
- 4.3 Hydrochloric acid (HCl), analytical grade
- 4.4 Sodium hydroxide (NaOH), analytical grade

#### 5. Procedures

5.1 Standard preparation for calibration curve: Dissolved 1.246 g potassium hexachloroplatinate ( $K_2PtCl_6$ ) and 1.00 g crystallized cobaltous chloride ( $CoCl_2 \cdot 6H_2O$ ) in distilled water with 100 ml Conc. Hydrochloric acid (HCl) and diluted to 1,000 ml. This stock solution has a color of 500 Pt-Co unit. Prepared standards having Pt-Co unit of 50, 100, 150, 200, 250, 300 and 400 by diluting 10, 20, 30, 40, 50, 60 and 80 ml stock color standard with distilled water in 100 ml volumetric flasks. The standards were analyzed as light absorbance using UV-Visible spectrophotometer with detection wavelength of 465 nm and obtained standard curve as shown in Table A.3 and Figure A.3.

Table A.3 Light absorbance of standard color solutions detected by UV-Visible spectrophotometer

Color (Pt-Co unit)	Absorbance at 465 nm
50	0.014
100	0.027
150	0.038
200	0.051
250	0.064
300	0.076
400	0.104
500	0.129

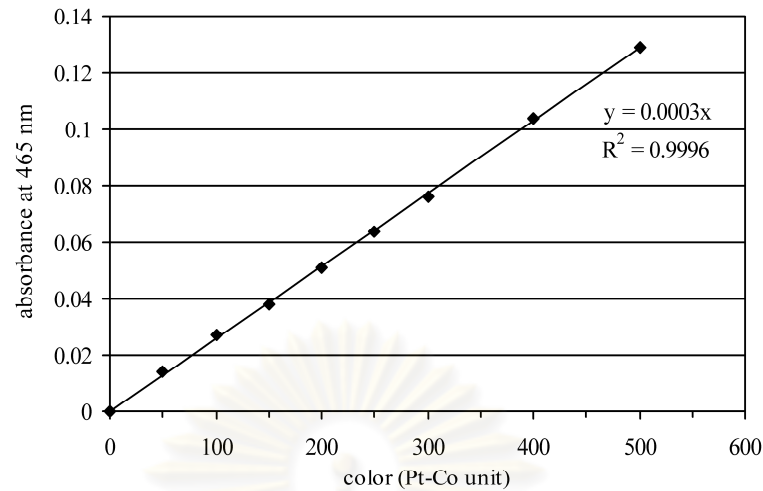


Figure A.3 Standard curve of standard color solutions detected by UV-Visible spectrophotometer at 465 nm

5.2 Sample analysis: Brought 15 ml effluent samples of synthetic wastewater to room temperature and adjusted pH to 7.0 by using  $H_2SO_4$  and NaOH. Then, filtered the samples with glass microfiber filter, GF/C, 47 mm to remove suspended solids from the samples. For real wastewater from pulp and paper mill, 12.5 ml effluent samples were diluted to 25 ml with distilled water (2 times). After that, measured light absorbance of samples by using UV-Visible spectrophotometer with detection wavelength of 465 nm and calculated color concentration using standard curve.



## Analytical Method of 2,4-DCP

(Somshy Kinakul, 2002)

### 1. Apparatus

1.1 HPLC Varian Prostar with Auto sampler Model 400, pump Model 230, Varian HPLC column C 18 (4.6 mm internal diameter  $\times$  250 mm) holder with guard column and UV-Visible detector Model 325.

1.2 Nylon syringe filters 0.45, 13 mm, FILTREX

1.3 PTFE membrane filters 0.45  $\mu\text{m}$ , 47 mm, MUNKTELL

### 2. Reagents

2.1 Ultra pure de-ionized water: 18.2  $\text{M}\Omega\ \text{cm}^{-1}$ , ELGA.

2.2 Mobile phase: mixture of 25% of acetonitrile, 30% of methanol and 45% of ultra pure de-ionized water adjusted at pH 3 with  $\text{H}_2\text{SO}_4$

### 3. Procedures

3.1 Standard preparation for calibration curve: For 2,4-DCP synthetic wastewater, dissolved 0.005 g 2,4-DCP in 18.2  $\text{M}\Omega\ \text{cm}^{-1}$  ultra pure de-ionized water and diluted to 500 ml. This stock solution has a 2,4-DCP concentration of 10 mg/l. Prepare standard having 2,4-DCP of 1, 2, 3, 4, 5 and 6 mg/l by diluting 1, 2, 3, 4, 5 and 6 ml stock 2,4-DCP standard with ultra pure de-ionized water in 10 ml volumetric flasks. For real wastewater from pulp and paper mill, dissolved 0.001 g 2,4-DCP in 18.2  $\text{M}\Omega\ \text{cm}^{-1}$  ultra pure de-ionized water and diluted to 1000 ml. This stock solution has a 2,4-DCP concentration of 1,000  $\mu\text{g}/\text{l}$ . Prepare standard having 2,4-DCP of 100, 200, 300, 400, 500 and 600  $\mu\text{g}/\text{l}$  by diluting 1, 2, 3, 4, 5 and 6 ml stock 2,4-DCP standard with ultra pure de-ionized water in 10 ml volumetric flasks. The standard solutions were filtered through 0.45  $\mu\text{m}$  nylon syringe filter, 13 mm. Next, the residual standard solutions were detected by HPLC with column C 18 (4.6 mm internal diameter  $\times$  250 mm) holder with guard column and UV-Visible detector

Model 325. A mixture of 25% of acetonitrile, 30% of methanol and 45% of ultra pure de-ionized water adjusted at pH 3 with H<sub>2</sub>SO<sub>4</sub> was used as a mobile phase with flow rate of 1 ml/min. The wavelength of detector was 280 nm. Before introduced to HPLC, the mobile phase was filtered through 0.45 µm PTFE membrane filter, 47 mm using vacuum degassing. The retention time for 2,4-DCP detection is around 7.5 min as presented in Figure A.4. Table A.4 and Figure A.5 show peak area and standard curve for 2,4-DCP synthetic wastewater. Table A.5 and Figure A.6 show peak area and standard curve for real wastewater.

3.2 Sample analysis: The effluent samples were filtered through 0.45 µm nylon syringe filter, 13 mm. Next, the residual solutions were detected by HPLC and used HPLC conditions as same as conditions of standard analysis. Then, calculated 2,4-DCP concentration in 2,4-DCP synthetic wastewater and real wastewater using standard curve in Figure A.5 and Figure A.6, respectively.

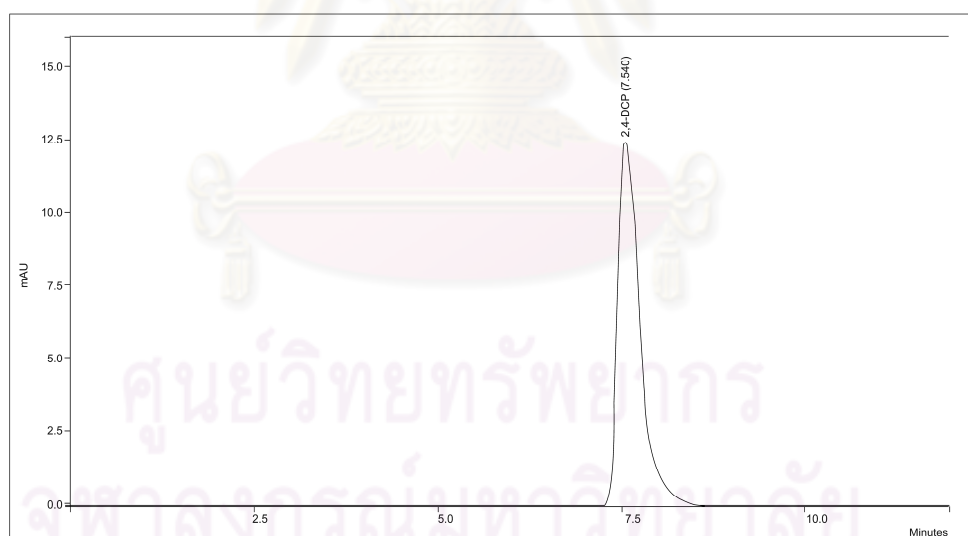


Figure A.4 2,4-DCP chromatogram detected by HPLC

Table A.4 Peak area of 2,4-DCP standard solutions for 2,4-DCP synthetic wastewater detected by HPLC

2,4-DCP concentration (mg/l)	Peak area
1	551748
2	1219129
3	1868091
4	2664677
5	3406984
6	3958680

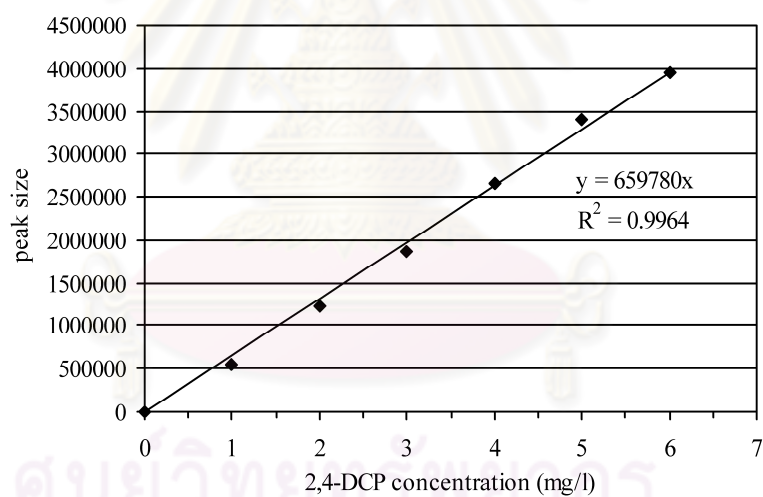


Figure A.5 Calibration curve of 2,4-DCP standard solutions for 2,4-DCP synthetic wastewater detected by HPLC

Table A.5 Peak area of 2,4-DCP standard solutions for real wastewater detected by HPLC

2,4-DCP concentration ( $\mu\text{g/l}$ )	Peak area
100	56124
200	120454
300	166324
400	241204
500	286452
600	329514

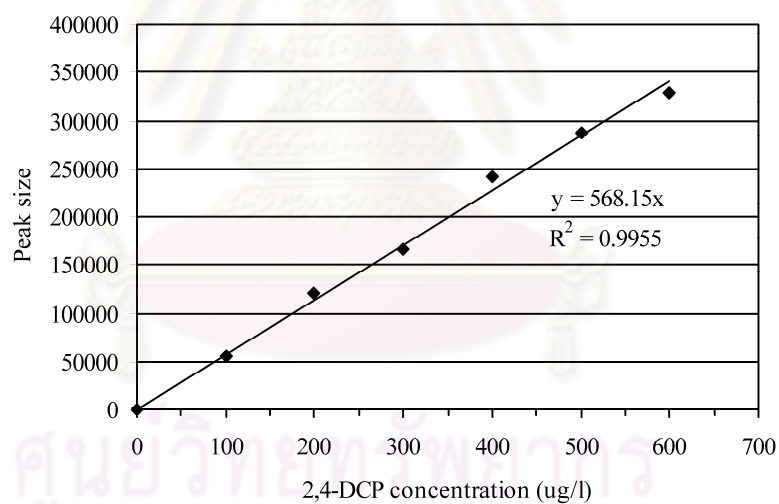
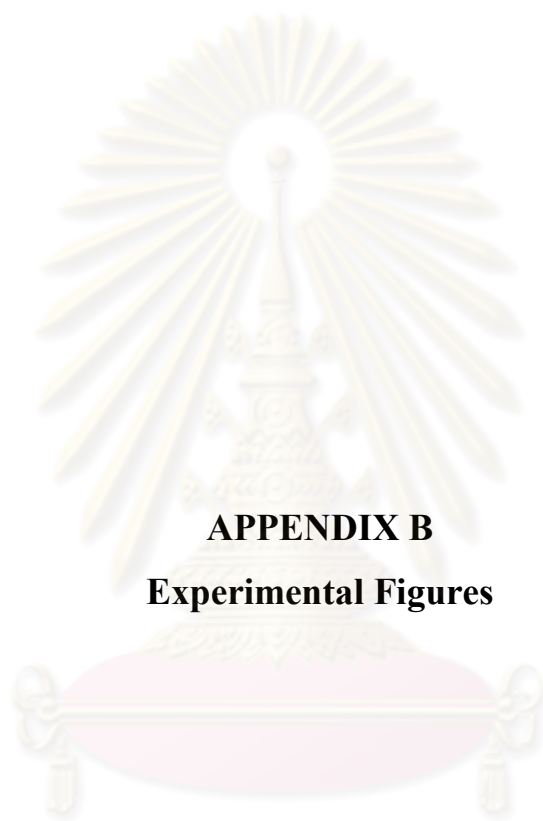


Figure A.6 Calibration curve of 2,4-DCP standard solutions for real wastewater detected by HPLC



**APPENDIX B**  
**Experimental Figures**

ศูนย์วิทยทรัพยากร  
จุฬาลงกรณ์มหาวิทยาลัย



Figure B.1 Supervibration-photocatalytic reactor

ศูนย์วิทยทรัพยากร  
จุฬาลงกรณ์มหาวิทยาลัย





Figure B.2 System control switch

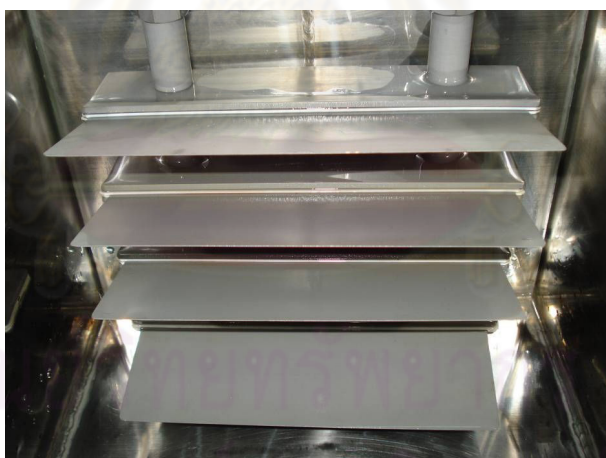


Figure B.3 Multistage blade



Figure B.4 UV lamps



Figure B.5 Controller of vibration frequency



Figure B.6 High performance liquid chromatography (HPLC)



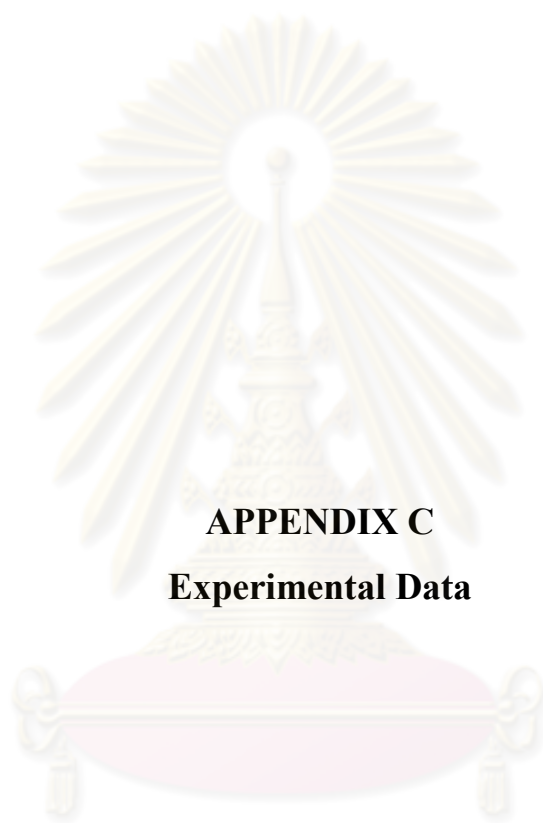
Figure B.7 UV-Visible spectrophotometer



Figure B.8 Gas chromatography-mass spectrometer (GC-MS)



Figure B.9 Solid-phase microextraction (SPME) fiber and holder



**APPENDIX C**

**Experimental Data**

ศูนย์วิทยทรัพยากร  
จุฬาลงกรณ์มหาวิทยาลัย

### Treatment of Lignin Synthetic Wastewater

Table C.1 Effect of initial pH on lignin degradation in lignin synthetic wastewater by supervibration-photocatalytic reactor

Time (min)	Lignin concentration (mg/l)				
	pH 5	pH 6	pH 7	pH 8	pH 9
0	400	400	400	400	400
15	368.843	370.134	373.259	380.249	388.648
30	359.257	350.368	368.125	372.381	375.293
60	342.648	344.125	346.791	365.134	370.512
90	325.429	336.287	335.493	363.462	365.482
120	317.205	318.236	325.642	350.736	357.259
180	308.614	310.851	322.965	348.621	357.015
300	291.825	298.476	318.429	344.014	353.249
420	279.861	294.672	316.672	341.352	351.315

Note: Experimental conditions: UV intensity = 6.3 mW/cm<sup>2</sup>,  
vibration frequency = 30 Hz

ศูนย์วิทยทรัพยากร  
จุฬาลงกรณ์มหาวิทยาลัย



Table C.2 Effect of UV intensity on lignin degradation in lignin synthetic wastewater by supervibration-photocatalytic reactor

Time (min)	Lignin concentration (mg/l)		
	UV intensity of 0 mW/cm <sup>2</sup>	UV intensity of 6.3 mW/cm <sup>2</sup>	UV intensity of 12.6 mW/cm <sup>2</sup>
0	400	400	400
15	389.543	368.843	351.359
30	385.642	359.257	340.235
60	376.154	342.648	315.298
90	376.032	325.429	302.369
120	372.324	317.205	281.624
180	370.234	308.614	266.287
300	369.264	291.825	230.358
420	366.693	279.861	211.794

Note: Experimental conditions: initial pH = 5, vibration frequency = 30 Hz

ศูนย์วิทยทรัพยากร  
จุฬาลงกรณ์มหาวิทยาลัย

Table C.3 Effect of vibration frequency on lignin degradation in lignin synthetic wastewater by supervibration-photocatalytic reactor

Time (min)	Lignin concentration (mg/l)				
	Vibration frequency of 0 Hz	Vibration frequency of 20 Hz	Vibration frequency of 30 Hz	Vibration frequency of 40 Hz	Vibration frequency of 50 Hz
0	400	400	400	400	400
15	370.359	366.249	351.359	350.040	339.965
30	355.246	349.245	340.235	336.254	331.689
60	344.259	320.365	315.298	309.698	313.675
90	312.268	314.356	302.369	292.136	293.059
120	302.578	288.567	281.624	281.326	275.495
180	295.687	273.214	266.287	260.245	250.354
300	290.015	237.256	230.358	228.236	224.289
420	281.358	226.614	211.794	208.894	206.896

Note: Experimental conditions: initial pH = 5, UV intensity = 12.6 mW/cm<sup>2</sup>

ศูนย์วิทยทรัพยากร  
จุฬาลงกรณ์มหาวิทยาลัย

Table C.4 Effect of initial concentration on lignin degradation in lignin synthetic wastewater by supervibration-photocatalytic reactor

Time (min)	Lignin concentration (mg/l)				
	Initial concentration of 100 mg/l	Initial concentration of 200 mg/l	Initial concentration of 300 mg/l	Initial concentration of 400 mg/l	Initial concentration of 100 mg/l*
0	100	200	300	400	100
15	84.489	172.593	259.268	339.965	65.231
30	80.943	164.289	254.469	331.689	50.689
60	75.598	150.369	231.358	313.675	33.241
90	69.245	144.486	215.231	293.059	27.569
120	65.235	137.359	206.314	275.495	24.522
180	59.579	119.258	199.159	250.354	20.277
300	46.268	105.458	169.647	224.289	17.694
420	39.359	93.672	149.842	206.896	14.885

Note: Experimental conditions: initial pH = 5, UV intensity = 12.6 mW/cm<sup>2</sup>,  
vibration frequency = 50 Hz

: \* Experimental conditions: initial pH = 5, UV intensity = 25.2 mW/cm<sup>2</sup>,  
vibration frequency = 50 Hz

ศูนย์วิจัยทรัพยากร  
จุฬาลงกรณ์มหาวิทยาลัย

Table C.5 Color removal in lignin synthetic wastewater by  
supervibration-photocatalytic reactor

Time (min)	Color (Pt-Co unit)
0	207.961
15	145.235
30	126.267
60	110.354
90	101.527
120	92.322
180	83.545
300	74.628
420	61.244

Note: Experimental conditions: initial lignin concentration = 100 mg/l,  
initial pH = 5, UV intensity = 25.2 mW/cm<sup>2</sup>, vibration frequency = 50 Hz

ศูนย์วิทยทรัพยากร  
จุฬาลงกรณ์มหาวิทยาลัย

### Treatment of 2,4-DCP Synthetic Wastewater

Table C.6 Effect of initial pH on 2,4-DCP degradation in 2,4-DCP synthetic wastewater by supervibration-photocatalytic reactor

Time (min)	2,4-DCP concentration (mg/l)				
	pH 5	pH 6	pH 7	pH 8	pH 9
0	5	5	5	5	5
15	3.701	3.515	3.715	3.930	4.027
30	3.445	3.275	3.303	3.673	3.825
60	2.954	2.934	3.121	3.393	3.554
90	2.480	2.522	2.624	2.966	3.211
120	2.047	2.190	2.339	2.448	2.626
180	1.965	1.895	2.209	2.232	2.214
300	1.607	1.754	2.088	2.198	2.086
420	1.301	1.693	1.819	1.957	2.015

Note: Experimental conditions: UV intensity =  $6.3 \text{ mW/cm}^2$ ,  
vibration frequency = 30 Hz

ศูนย์วิทยทรัพยากร  
จุฬาลงกรณ์มหาวิทยาลัย

Table C.7 Effect of UV intensity on 2,4-DCP degradation in 2,4-DCP synthetic wastewater by supervibration-photocatalytic reactor

Time (min)	2,4-DCP concentration (mg/l)		
	UV intensity of 0 mW/cm <sup>2</sup>	UV intensity of 6.3 mW/cm <sup>2</sup>	UV intensity of 12.6 mW/cm <sup>2</sup>
0	5	5	5
15	4.493	3.701	3.442
30	4.390	3.445	3.276
60	4.121	2.954	2.482
90	3.935	2.480	2.185
120	3.848	2.047	1.789
180	3.805	1.965	1.593
300	3.794	1.607	1.164
420	3.761	1.301	1.043

Note: Experimental conditions: initial pH = 5, vibration frequency = 30 Hz

ศูนย์วิทยทรัพยากร  
จุฬาลงกรณ์มหาวิทยาลัย



Table C.8 Effect of vibration frequency on 2,4-DCP degradation in 2,4-DCP synthetic wastewater by supervibration-photocatalytic reactor

Time (min)	2,4-DCP concentration (mg/l)				
	Vibration frequency of 0 Hz	Vibration frequency of 20 Hz	Vibration frequency of 30 Hz	Vibration frequency of 40 Hz	Vibration frequency of 50 Hz
0	5	5	5	5	5
15	3.962	3.652	3.442	3.351	3.248
30	3.568	3.238	3.276	3.248	3.127
60	3.357	2.742	2.482	2.555	2.554
90	2.716	2.438	2.185	2.057	2.169
120	2.589	2.068	1.789	1.698	1.549
180	2.187	1.565	1.593	1.532	1.483
300	2.034	1.468	1.164	1.184	1.084
420	1.935	1.201	1.043	0.847	0.716

Note: Experimental conditions: initial pH = 5, UV intensity = 12.6 mW/cm<sup>2</sup>

ศูนย์วิทยทรัพยากร  
จุฬาลงกรณ์มหาวิทยาลัย

Table C.9 Effect of initial concentration on 2,4-DCP degradation in 2,4-DCP synthetic wastewater by supervibration-photocatalytic reactor

Time (min)	2,4-DCP concentration (mg/l)				
	Initial concentration of 0.5 mg/l	Initial concentration of 1 mg/l	Initial concentration of 2.5 mg/l	Initial concentration of 5 mg/l	Initial concentration of 0.5 mg/l*
0	0.5	1	2.5	5	0.5
15	0.357	0.725	1.739	3.248	0.193
30	0.306	0.612	1.589	3.127	0.098
60	0.189	0.439	1.238	2.554	0.000
90	0.114	0.348	0.865	2.169	0.000
120	0.094	0.212	0.621	1.549	0.000
180	0.074	0.198	0.541	1.483	0.000
300	0.051	0.143	0.428	1.084	0.000
420	0.044	0.098	0.347	0.716	0.000

Note: Experimental conditions: initial pH = 5, UV intensity = 12.6 mW/cm<sup>2</sup>, vibration frequency = 50 Hz

: \* Experimental conditions: initial pH = 5, UV intensity = 25.2 mW/cm<sup>2</sup>, vibration frequency = 50 Hz

ศูนย์วิทยทรัพยากร  
จุฬาลงกรณ์มหาวิทยาลัย

### Treatment of Mixed Synthetic Wastewater containing Lignin and 2,4-DCP

Table C.10 Effect of initial pH on lignin degradation in mixed synthetic wastewater by supervibration-photocatalytic reactor

Time (min)	Lignin concentration (mg/l)				
	pH 5	pH 6	pH 7	pH 8	pH 9
0	400	400	400	400	400
15	369.825	371.046	373.945	380.591	389.590
30	351.027	361.258	360.125	378.235	385.123
60	332.452	347.256	358.133	364.235	380.102
90	328.465	331.241	350.235	360.012	379.022
120	305.235	320.458	341.246	357.413	360.215
180	291.328	314.579	332.316	355.964	359.987
300	287.126	307.132	325.235	351.985	358.911
420	279.981	294.913	320.012	343.596	351.921

Note: Experimental conditions: UV intensity =  $6.3 \text{ mW/cm}^2$ ,  
vibration frequency = 30 Hz

ศูนย์วิทยทรัพยากร  
จุฬาลงกรณ์มหาวิทยาลัย

Table C.11 Effect of initial pH on 2,4-DCP degradation in mixed synthetic wastewater by supervibration-photocatalytic reactor

Time (min)	2,4-DCP concentration (mg/l)				
	pH 5	pH 6	pH 7	pH 8	pH 9
0	5	5	5	5	5
15	3.461	3.698	3.785	3.796	4.079
30	3.235	3.524	3.498	3.521	3.869
60	2.996	3.150	3.199	3.126	3.311
90	2.869	2.835	2.869	2.946	2.853
120	2.475	2.595	2.469	2.653	2.746
180	2.147	2.215	2.205	2.499	2.412
300	1.667	1.975	2.098	2.309	2.302
420	1.591	1.848	2.000	2.229	2.350

Note: Experimental conditions: UV intensity =  $6.3 \text{ mW/cm}^2$ ,  
vibration frequency = 30 Hz

ศูนย์วิทยทรัพยากร  
จุฬาลงกรณ์มหาวิทยาลัย

Table C.12 Effect of UV intensity on lignin degradation in mixed synthetic wastewater by supervibration-photocatalytic reactor

Time (min)	Lignin concentration (mg/l)		
	UV intensity of 0 mW/cm <sup>2</sup>	UV intensity of 6.3 mW/cm <sup>2</sup>	UV intensity of 12.6 mW/cm <sup>2</sup>
0	400	400	400
15	383.294	369.825	351.381
30	382.620	351.027	340.145
60	378.662	332.452	338.642
90	370.012	328.465	297.246
120	369.946	305.235	286.424
180	369.021	291.328	250.123
300	368.982	287.126	220.246
420	368.072	279.981	211.881

Note: Experimental conditions: initial pH = 5, vibration frequency = 30 Hz

ศูนย์วิทยทรัพยากร  
จุฬาลงกรณ์มหาวิทยาลัย

Table C.13 Effect of UV intensity on 2,4-DCP degradation in mixed synthetic wastewater by supervibration-photocatalytic reactor

Time (min)	2,4-DCP concentration (mg/l)		
	UV intensity of 0 mW/cm <sup>2</sup>	UV intensity of 6.3 mW/cm <sup>2</sup>	UV intensity of 12.6 mW/cm <sup>2</sup>
0	5	5	5
15	4.602	3.461	3.186
30	4.594	3.235	3.021
60	4.586	2.996	2.846
90	4.469	2.869	2.452
120	4.302	2.475	2.236
180	4.299	2.147	1.864
300	4.085	1.667	1.406
420	3.994	1.591	1.241

Note: Experimental conditions: initial pH = 5, vibration frequency = 30 Hz

ศูนย์วิทยทรัพยากร  
จุฬาลงกรณ์มหาวิทยาลัย



Table C.14 Effect of vibration frequency on lignin degradation in mixed synthetic wastewater by supervibration-photocatalytic reactor

Time (min)	Lignin concentration (mg/l)					
	Vibration frequency of 0 Hz	Vibration frequency of 20 Hz	Vibration frequency of 30 Hz	Vibration frequency of 40 Hz	Vibration frequency of 50 Hz	Vibration frequency of 50 Hz*
0	400	400	400	400	400	400
15	372.246	368.049	351.381	350.140	340.525	281.654
30	367.021	351.246	340.145	341.025	330.145	271.365
60	345.235	332.015	338.642	328.346	312.645	258.356
90	340.954	304.126	297.246	284.675	286.345	223.921
120	320.159	273.547	286.424	276.341	256.724	190.365
180	302.459	243.578	250.123	238.456	223.548	161.648
300	295.247	238.786	220.246	219.876	215.567	120.358
420	283.014	228.088	211.881	209.120	206.996	95.142

Note: Experimental conditions: initial pH = 5, UV intensity = 12.6 mW/cm<sup>2</sup>

: \* Experimental conditions: initial pH = 5, UV intensity = 25.2 mW/cm<sup>2</sup>

ศูนย์วิทยทรัพยากร  
จุฬาลงกรณ์มหาวิทยาลัย

Table C.15 Effect of vibration frequency on 2,4-DCP degradation in mixed synthetic wastewater by supervibration-photocatalytic reactor

Time (min)	2,4-DCP concentration (mg/l)					
	Vibration frequency of 0 Hz	Vibration frequency of 20 Hz	Vibration frequency of 30 Hz	Vibration frequency of 40 Hz	Vibration frequency of 50 Hz	Vibration frequency of 50 Hz*
0	5	5	5	5	5	5
15	4.013	3.875	3.186	3.648	3.154	2.533
30	3.821	3.722	3.021	3.229	2.967	2.166
60	3.533	3.358	2.846	2.768	2.703	1.727
90	3.143	2.856	2.452	2.436	2.313	1.497
120	2.942	2.468	2.236	2.016	2.012	1.365
180	2.769	2.014	1.864	1.751	1.664	0.943
300	2.305	1.613	1.406	1.426	1.260	0.436
420	2.245	1.490	1.241	1.101	0.964	0.144

Note: Experimental conditions: initial pH = 5, UV intensity = 12.6 mW/cm<sup>2</sup>

: \* Experimental conditions: initial pH = 5, UV intensity = 25.2 mW/cm<sup>2</sup>

ศูนย์วิทยทรัพยากร  
จุฬาลงกรณ์มหาวิทยาลัย

Table C.16 Color removal in mixed synthetic wastewater by supervibration-  
photocatalytic reactor

Time (min)	Color (Pt-Co unit)
0	382.643
15	328.365
30	302.441
60	279.658
90	243.622
120	208.754
180	183.587
300	159.869
420	150.203

Note: Experimental conditions: initial lignin concentration = 400 mg/l,  
initial pH = 5, UV intensity = 25.2 mW/cm<sup>2</sup>, vibration frequency = 50 Hz

ศูนย์วิทยทรัพยากร  
จุฬาลงกรณ์มหาวิทยาลัย

### Treatment of Real Wastewater from Pulp and Paper Mill

Table C.17 Effect of initial pH on lignin degradation in pulp and paper mill wastewater by supervibration-photocatalytic reactor

Time (min)	Lignin concentration (mg/l)				
	pH 5	pH 6	pH 7	pH 8	pH 9
0	278.235	261.255	271.225	252.173	290.244
15	263.891	248.112	255.312	240.285	277.954
30	257.245	240.457	250.033	237.124	276.867
60	240.245	234.221	245.641	230.224	274.661
90	237.012	223.553	240.178	229.004	272.245
120	228.245	217.544	236.452	227.421	270.010
180	217.351	214.113	230.056	223.147	267.121
300	209.547	210.245	224.344	219.008	264.336
420	198.541	195.642	221.025	218.954	260.994

Note: Experimental conditions: UV intensity =  $6.3 \text{ mW/cm}^2$ ,  
vibration frequency = 30 Hz

ศูนย์วิทยทรัพยากร  
จุฬาลงกรณ์มหาวิทยาลัย

Table C.18 Effect of initial pH on 2,4-DCP degradation in pulp and paper mill wastewater by supervibration-photocatalytic reactor

Time (min)	2,4-DCP concentration ( $\mu\text{g/l}$ )				
	pH 5	pH 6	pH 7	pH 8	pH 9
0	128.515	121.346	147.245	110.521	152.356
15	93.123	88.345	110.236	85.041	126.589
30	86.576	84.012	101.621	80.246	122.345
60	74.357	73.015	95.314	74.268	113.245
90	70.594	67.546	75.452	65.694	101.548
120	62.276	60.124	74.246	60.128	89.647
180	54.228	52.247	70.694	54.316	80.246
300	46.358	48.034	65.454	50.024	76.642
420	44.214	47.124	63.598	49.574	75.026

Note: Experimental conditions: UV intensity =  $6.3 \text{ mW/cm}^2$ ,  
vibration frequency = 30 Hz

ศูนย์วิทยทรัพยากร  
จุฬาลงกรณ์มหาวิทยาลัย

Table C.19 Effect of UV intensity on lignin degradation in pulp and paper mill wastewater by supervibration-photocatalytic reactor

Time (min)	Lignin concentration (mg/l)		
	UV intensity of 0 mW/cm <sup>2</sup>	UV intensity of 6.3 mW/cm <sup>2</sup>	UV intensity of 12.6 mW/cm <sup>2</sup>
0	281.352	278.235	263.442
15	270.045	263.891	240.366
30	269.520	257.245	231.112
60	269.074	240.245	220.154
90	267.864	237.012	201.841
120	266.541	228.245	189.478
180	265.989	217.351	170.655
300	264.788	209.547	157.358
420	264.032	198.541	145.326

Note: Experimental conditions: initial pH = 5, vibration frequency = 30 Hz

ศูนย์วิทยทรัพยากร  
จุฬาลงกรณ์มหาวิทยาลัย



Table C.20 Effect of UV intensity on 2,4-DCP degradation in pulp and paper mill wastewater by supervibration-photocatalytic reactor

Time (min)	2,4-DCP concentration ( $\mu\text{g/l}$ )		
	UV intensity of $0 \text{ mW/cm}^2$	UV intensity of $6.3 \text{ mW/cm}^2$	UV intensity of $12.6 \text{ mW/cm}^2$
0	115.264	128.515	131.256
15	108.845	93.123	85.654
30	106.321	86.576	80.564
60	104.231	74.357	70.456
90	102.153	70.594	62.498
120	100.875	62.276	54.642
180	99.457	54.228	41.689
300	97.978	46.358	37.495
420	97.023	44.214	35.241

Note: Experimental conditions: initial pH = 5, vibration frequency = 30 Hz

ศูนย์วิทยทรัพยากร  
จุฬาลงกรณ์มหาวิทยาลัย

Table C.21 Effect of vibration frequency on lignin degradation in pulp and paper mill wastewater by supervibration-photocatalytic reactor

Time (min)	Lignin concentration (mg/l)					
	Vibration frequency of 0 Hz	Vibration frequency of 20 Hz	Vibration frequency of 30 Hz	Vibration frequency of 40 Hz	Vibration frequency of 50 Hz	Vibration frequency of 50 Hz*
0	257.244	224.511	263.442	218.424	240.138	250.786
15	240.924	208.221	240.366	195.268	218.058	185.005
30	239.589	201.325	231.112	187.254	205.245	170.245
60	237.451	195.214	220.154	176.521	190.265	159.328
90	234.456	180.336	201.841	160.124	172.324	138.247
120	217.589	173.225	189.478	150.078	170.015	110.358
180	206.589	159.348	170.655	143.841	150.225	80.647
300	198.214	140.245	157.358	128.522	138.599	72.654
420	192.015	134.258	145.326	120.011	127.355	62.424

Note: Experimental conditions: initial pH = 5, UV intensity = 12.6 mW/cm<sup>2</sup>

: \* Experimental conditions: initial pH = 5, UV intensity = 25.2 mW/cm<sup>2</sup>

ศูนย์วิทยทรัพยากร  
จุฬาลงกรณ์มหาวิทยาลัย

Table C.22 Effect of vibration frequency on 2,4-DCP degradation in pulp and paper mill wastewater by supervibration-photocatalytic reactor

Time (min)	2,4-DCP concentration ( $\mu\text{g/l}$ )					
	Vibration frequency of 0 Hz	Vibration frequency of 20 Hz	Vibration frequency of 30 Hz	Vibration frequency of 40 Hz	Vibration frequency of 50 Hz	Vibration frequency of 50 Hz*
0	118.549	145.852	131.256	128.642	120.598	123.958
15	98.347	115.642	85.654	84.021	77.598	65.617
30	96.234	111.058	80.564	82.014	64.268	57.321
60	82.345	99.246	70.456	75.234	54.951	49.325
90	74.568	85.324	62.498	70.124	50.912	35.214
120	67.459	72.596	54.642	61.541	41.356	27.364
180	62.145	64.569	41.689	50.869	34.952	21.021
300	58.921	54.016	37.495	42.579	30.865	13.564
420	56.324	48.965	35.241	33.124	28.597	7.262

Note: Experimental conditions: initial pH = 5, UV intensity =  $12.6 \text{ mW/cm}^2$

: \* Experimental conditions: initial pH = 5, UV intensity =  $25.2 \text{ mW/cm}^2$

ศูนย์วิทยทรัพยากร  
จุฬาลงกรณ์มหาวิทยาลัย

Table C.23 Color removal in pulp and paper mill wastewater by supervibration-photocatalytic reactor

Time (min)	Color (Pt-Co unit)
0	790.689
15	659.653
30	634.152
60	607.598
90	543.654
120	521.065
180	436.521
300	394.401
420	378.241

Note: Experimental conditions: initial lignin concentration = 250.79 mg/l,  
initial pH = 5, UV intensity = 25.2 mW/cm<sup>2</sup>, vibration frequency = 50 Hz

### Mass Spectrum of By-Products of Lignin Degradation

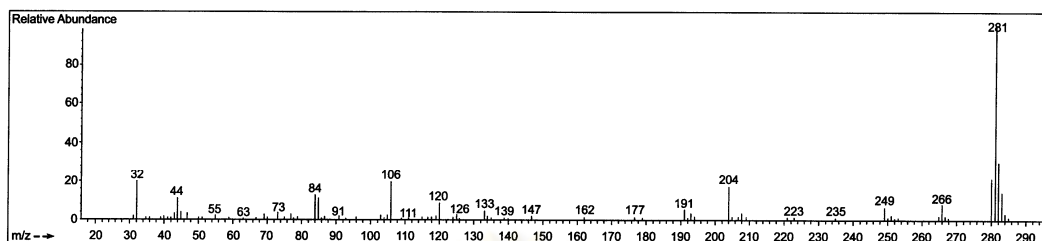


Figure C.1 Mass spectrum of 2,6-dimethyl-5-methylphenylaminopyridine-3,4-dicarboxyimide at retention time of 3.90 min

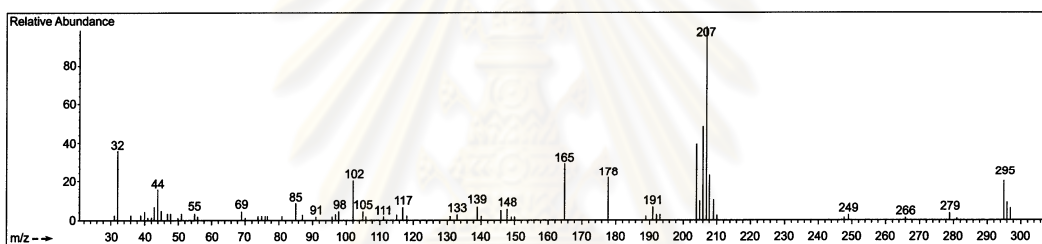


Figure C.2 Mass spectrum of 1-methyl-2-phenylindole at retention time of 4.95 min

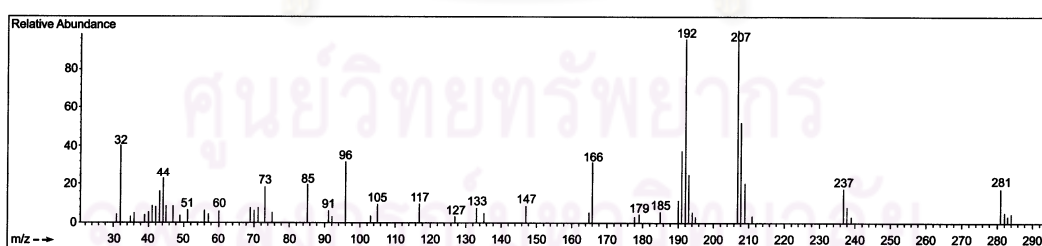


Figure C.3 Mass spectrum of 2-ethylacridine at retention time of 5.24 min

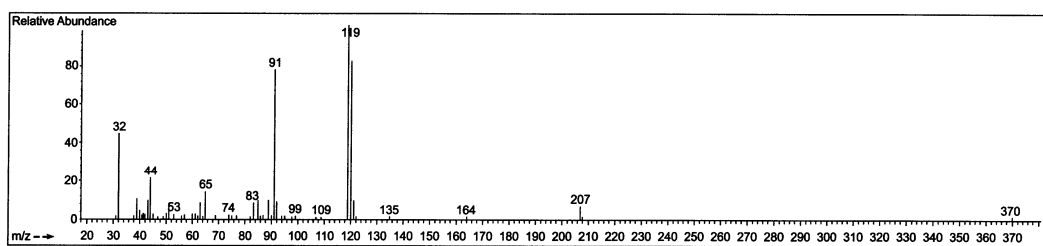


Figure C.4 Mass spectrum of 2-methylbenzaldehyde at retention time of 5.74 min

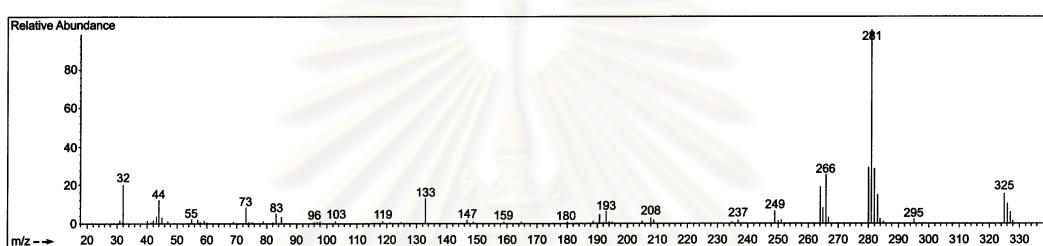


Figure C.5 Mass spectrum of 7H-dibenzo[b,g]carbazole, 7-methyl- at retention time of 6.01 min

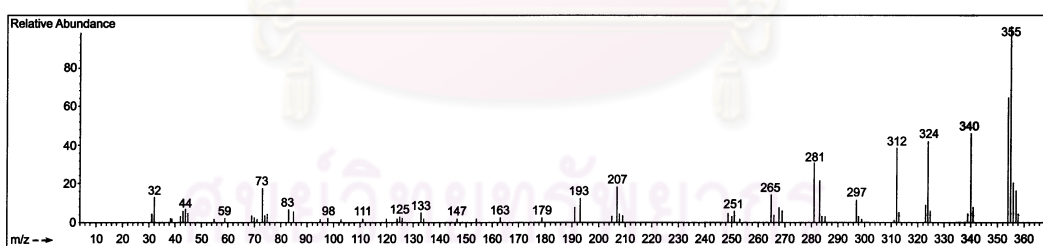


Figure C.6 Mass spectrum of glucine at retention time of 6.36 min



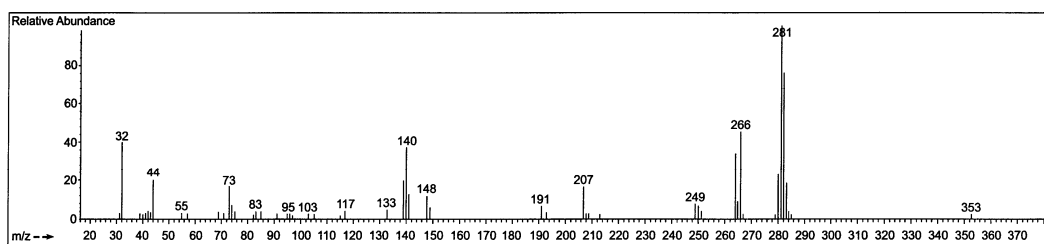


Figure C.7 Mass spectrum of 5H-naphtho[2,3-c]carbazole, 5-methyl- at retention time of 8.00 min

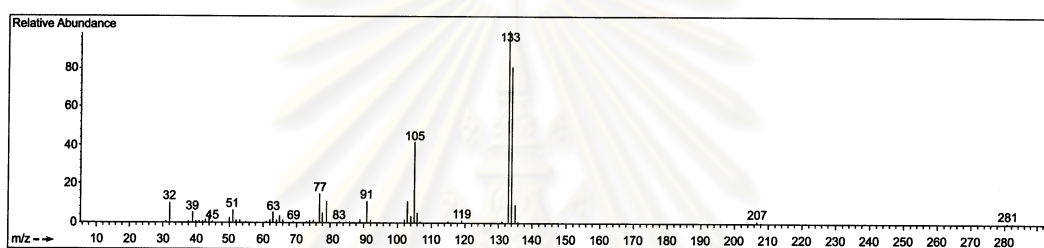


Figure C.8 Mass spectrum of 2,4-dimethylbenzaldehyde at retention time of 8.10 min

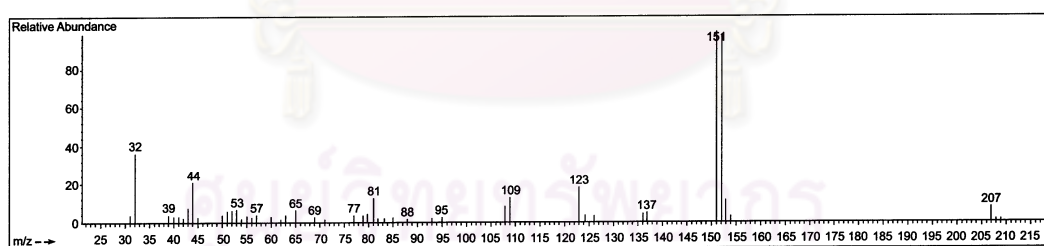


Figure C.9 Mass spectrum of 4-hydroxy-3-methoxybenzaldehyde (vanillin) at retention time of 11.38 min

### Mass Spectrum of By-Products of 2,4-DCP Degradation

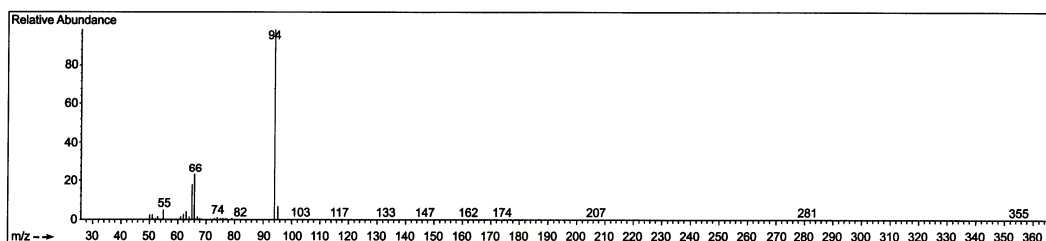


Figure C.11 Mass spectrum of phenol at retention time of 10.20 min

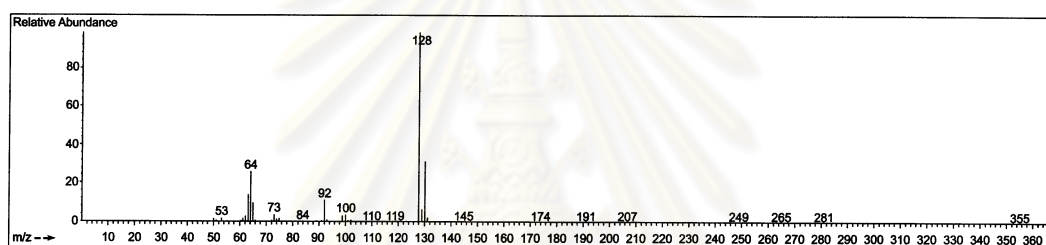


Figure C.12 Mass spectrum of 2-chlorophenol at retention time of 10.33 min

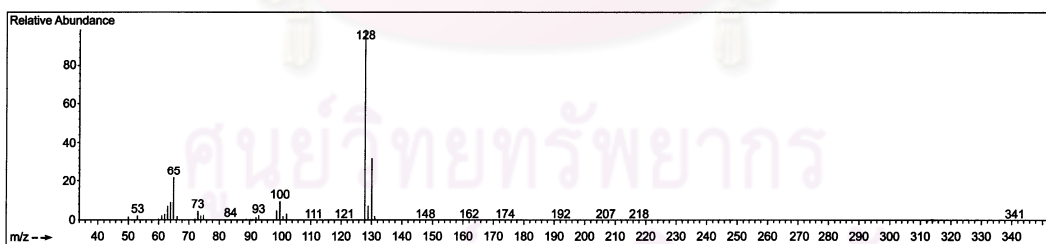


Figure C.13 Mass spectrum of 4-chlorophenol at retention time of 13.87 min



**APPENDIX D**  
**Journal and Conference Publication Lists**

ศูนย์วิทยทรัพยากร  
จุฬาลงกรณ์มหาวิทยาลัย

**Journal Publication**

1. Thongkrua, S. and Ratanatamskul, C. 2011. Simultaneous removal of lignin and 2,4-dichlorophenol in pulp and paper mill wastewater using a supervibration-photocatalytic reactor. Modern Applied Science 5: 92-100.
2. Thongkrua, S. and Ratanatamskul, C. 2011. Treatment of lignin using a supervibration-photocatalytic reactor. Fresenius Environmental Bulletin 20: 704-710.

**Conference Paper Publication**

Thongkrua, S. and Ratanatamskul, C. 2011. Treatment of 2,4-dichlorophenol in pulp and paper mill wastewater using a supervibration-photocatalytic reactor. The 10<sup>th</sup> National Conference on Environment, Songkhla, Thailand.

ศูนย์วิทยทรัพยากร  
จุฬาลงกรณ์มหาวิทยาลัย

## BIOGRAPHY

Miss Suchanya Thongkrua was born on August 31, 1979 in Kanchanaburi province, Thailand. She received her Bachelor's Degree in Environmental Health Science, Faculty of Public Health, Mahidol University in 2001 and Master's Degree in Inter-department of Environmental Science, Graduate School, Chulalongkorn University in 2004. She pursued her Degree of Doctor of Philosophy studies in Inter-department of Environmental Science, Graduate School, Chulalongkorn University, Bangkok, Thailand in June, 2006. She finished her Degree of Doctor of Philosophy in May 2011.



ศูนย์วิทยทรัพยากร  
จุฬาลงกรณ์มหาวิทยาลัย